

ERID#:

31492

LOS ALAMOS NATIONAL LABORATORY  
ENVIRONMENTAL RESTORATION (RRES-R)  
Records Processing Facility  
ER Records Index Form

Date Received: 2/28/1994 Processor: DIC Page Count: 373

Privileged: (Y/N) N Record Category: R Administrative Record: (Y/N) R

FileFolder: N/A

Miscellaneous Comments: N/A

Record Documents:

Start Pg	Doc Type	Doc Date	Title	Box	Package
1	REPORT	9/1/1989	PATHWAY ANALYSIS AT MATERIAL DISPOSAL AREA T, LOS ALAMOS NATIONAL LABORATORY (LANL), LOS ALAMOS, NEW MEXICO	55	



14316



Los Alamos Environmental Restoration  
Records Processing Facility

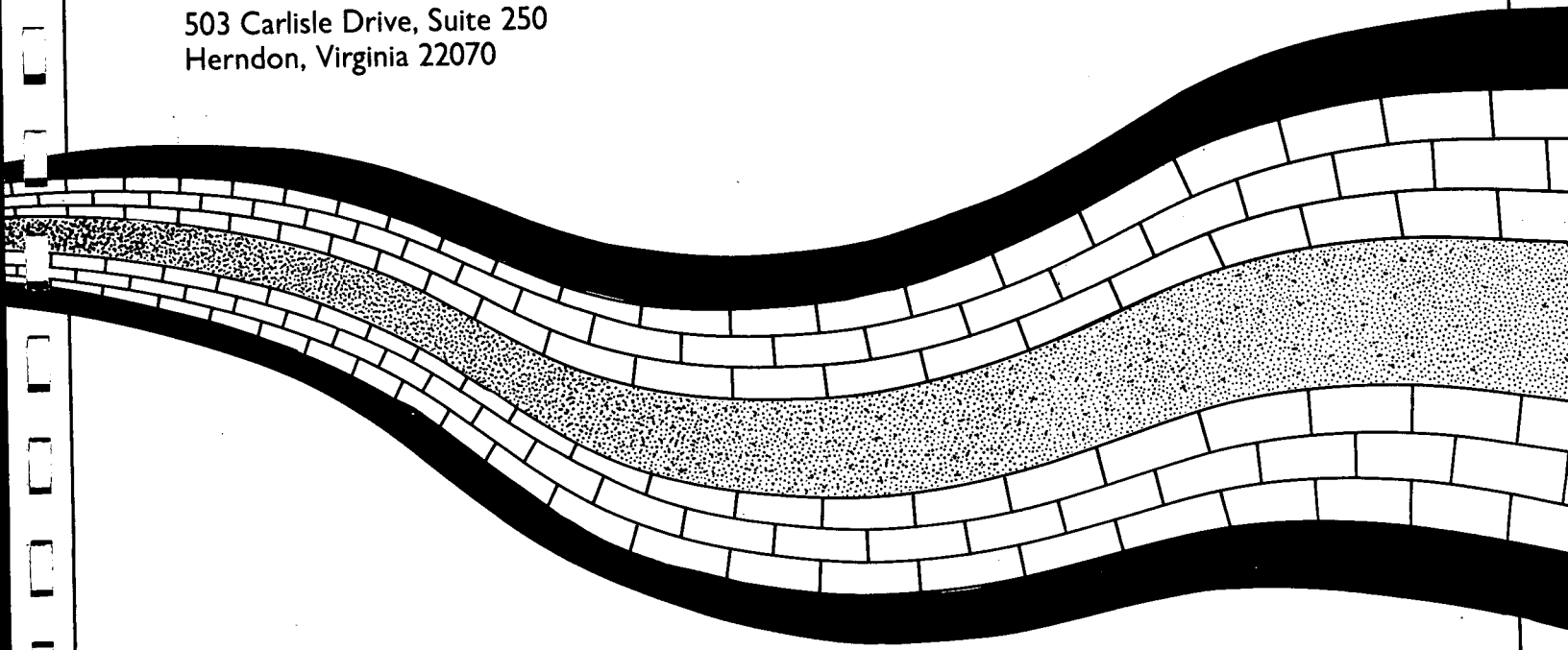


ER Record I.D.# 31492

**Pathway Analysis at Material Disposal Area T  
Los Alamos National Laboratory (LANL)  
Los Alamos, New Mexico**

September 1989

503 Carlisle Drive, Suite 250  
Herndon, Virginia 22070



## PREFACE

This study was conducted and prepared by Peter Huyakorn, John Robertson, Jan Kool, and David Back of HydroGeologic, Inc. under subcontract to Roy F. Weston, Inc. Technical oversight was provided by Richard Kilbury (Roy F. Weston) and Micheline Devaurs, the LANL Principal Investigator.

## TABLE OF CONTENTS

	<u>Page</u>
1.0 INTRODUCTION .....	1-1
1.1 General .....	1-1
1.2 Purpose and Scope of Work .....	1-1
1.3 Site Description and Waste Disposal History .....	1-2
1.4 Current Site Conditions .....	1-5
1.5 Report Description and Organization .....	1-5
1.6 Previous Investigations .....	1-9
2.0 SITE CONDITIONS .....	2-1
2.1 Hydrogeological Setting .....	2-1
2.2 Primary Aquifer System .....	2-4
2.3 Vadose Zone Conditions .....	2-6
2.3.1 General .....	2-6
2.3.2 Hydrologic and Transport Properties .....	2-10
2.3.3 Climatology .....	2-10
2.4 Waste Characteristics .....	2-10
2.4.1 General .....	2-10
2.4.2 Radionuclide Releases to Material Disposal Area T .....	2-10
2.4.2.1 Method of Disposal .....	2-12
2.4.2.2 Contamination Volumes .....	2-12
3.0 PATHWAY ANALYSIS MODELS .....	3-1
3.1 Initial Conceptual Model .....	3-1
3.2 Rationale for Code Selection .....	3-1
3.2.1 HYDRUS (one dimensional) .....	3-2
3.2.1.1 Assumptions of HYDRUS .....	3-4
3.2.1.2 Limitations of HYDRUS .....	3-4
3.2.2 SOILSIM (two dimensional) .....	3-5
3.2.2.1 Assumptions in SOILSIM .....	3-6
3.2.2.2 Limitations of SOILSIM .....	3-7

## TABLE OF CONTENTS (continued)

	<u>Page</u>
3.3 Numerical Accuracy .....	3-7
3.4 Regulatory Acceptance .....	3-8
3.4.1 HYDRUS .....	3-8
3.4.2 SOILSIM .....	3-8
4.0 MODEL APPLICATION .....	4-1
4.1 General .....	4-1
4.2 Data Preparation .....	4-2
4.2.1 Input Parameters .....	4-2
4.2.1.1 Rock Matrix Properties .....	4-2
4.2.1.2 Physical and Chemical Properties .....	4-4
4.2.2 Uncertainty of Input Data .....	4-4
4.2.3 Boundary Conditions .....	4-4
4.2.3.1 HYDRUS .....	4-8
4.2.3.2 SOILSIM .....	4-8
4.2.4 Initial Conditions .....	4-8
4.2.4.1 HYDRUS .....	4-8
4.2.4.2 SOILSIM .....	4-9
4.2.5 Time Dependent Input Data .....	4-9
4.2.5.1 Waste Discharge .....	4-9
4.2.5.1.1 HYDRUS .....	4-9
4.2.5.1.2 SOILSIM .....	4-11
4.2.5.2 Radionuclide Loading .....	4-11
4.2.5.2.1 HYDRUS .....	4-11
4.2.5.2.2 SOILSIM .....	4-15
4.2.6 Mesh Design .....	4-15
4.2.6.1 HYDRUS (1-D Mesh) .....	4-15
4.2.6.2 SOILSIM (2-D Mesh) .....	4-18

## TABLE OF CONTENTS (continued)

	<u>Page</u>
4.2.7 Convergence Criteria and Time Discretization .....	4-18
4.2.7.1 HYDRUS .....	4-21
4.2.7.2 SOILSIM .....	4-21
5.0 PATHWAY ANALYSIS .....	5-1
5.1 General .....	5-1
5.2 Sensitivity Analysis .....	5-4
5.2.1 Distribution Coefficients .....	5-4
5.2.2 Mesh Spacing .....	5-9
5.2.3 Shape of Moisture Release Curves .....	5-9
5.2.3.1 Power Index (n) of the Relative Permeability Versus Saturation Relationship .....	5-9
5.2.3.2 Leading Coefficient $\alpha$ of the Relative Permeability Versus Saturation Relationship .....	5-20
5.2.3.3 Leading Coefficient $\beta$ of the Relative Permeability Versus Saturation Relationship .....	5-20
5.2.4 Saturated Hydraulic Conductivity .....	5-20
5.2.5 Dispersivity .....	5-29
5.2.6 Volume of Water Added to Bed 1 .....	5-29
5.3 Historical Data Comparisons .....	5-35
5.3.1 Distribution Coefficients .....	5-41
5.3.2 Saturated Hydraulic Conductivity .....	5-41
5.4 Mass Comparison .....	5-65
5.5 Case Simulations .....	5-67
5.5.1 Case I - Ambient Flow Simulations .....	5-67
5.5.1.1 Scenario I.1 - Natural Recharge .....	5-67
5.5.1.1.1 Procedures and Input Parameters .....	5-67
5.5.1.1.2 Saturation Distributions .....	5-68
5.5.1.1.3 Discussion .....	5-68

TABLE OF CONTENTS (continued)

	<u>Page</u>
5.5.2 Case II - Flow Simulations . . . . .	5-68
5.5.2.1 Scenario II.1 - Liquid Radionuclide Waste Addition . . . . .	5-71
5.5.2.1.1 Procedures and Input Parameters . . . . .	5-71
5.5.2.1.2 Saturation Distributions . . . . .	5-71
5.5.2.1.3 Discussion . . . . .	5-71
5.5.2.2 Scenario II.2 - Moisture Pulse in 1960 and 1961 . . . . .	5-76
5.5.2.2.1 Procedures and Input Parameters . . . . .	5-76
5.5.2.2.2 Saturation Distributions . . . . .	5-76
5.5.2.2.3 Discussion . . . . .	5-76
5.5.2.3 Scenario II.3 - Pipe Leak . . . . .	5-83
5.5.2.3.1 Procedures and Input Parameters . . . . .	5-83
5.5.2.3.2 Velocity Field . . . . .	5-86
5.5.2.3.3 Discussion . . . . .	5-86
5.5.3 Case III - Transport Simulations . . . . .	5-86
5.5.3.1 Scenario III.1 . . . . .	5-88
5.5.3.1.1 Procedures and Input Parameters . . . . .	5-88
5.5.3.1.2 Concentration Distributions . . . . .	5-88
5.5.3.1.3 Discussion . . . . .	5-88
5.5.3.2 Scenario III.2 . . . . .	5-88
5.5.3.2.1 Procedures and Input Parameters . . . . .	5-88
5.5.3.2.2 Concentration Distributions . . . . .	5-92
5.5.3.2.3 Discussion . . . . .	5-92
5.5.3.3 Scenario III.3 . . . . .	5-92
5.5.3.3.1 Procedures and Input Parameters . . . . .	5-96
5.5.3.3.2 Concentration Distributions . . . . .	5-96
5.5.3.3.3 Discussion . . . . .	5-96

## TABLE OF CONTENTS (continued)

	<u>Page</u>
6.0 PATHWAY ANALYSIS RESULTS AND CONCLUSIONS .....	6-1
6.1 Fluid Movement .....	6-1
6.1.1 Lateral Fluid Movement .....	6-2
6.2 Radionuclide Movement .....	6-3
6.3 Role of Fractures .....	6-4
6.4 Interpretation of Moisture and Radionuclide Profiles .....	6-5
6.5 Implications on the Remedial Investigation .....	6-6
7.0 CONCEPTUAL MODEL .....	7-1
8.0 RECOMMENDED CHARACTERIZATION ACTIVITIES AND DATA REQUIREMENTS .....	8-1
8.1 Background Research .....	8-1
8.2 Bench-Scale Laboratory Studies .....	8-6
8.2.1 Chemical Characteristics .....	8-6
8.2.2 Physical Characteristics .....	8-8
8.3 Field Investigation .....	8-8
8.3.1 Location of Proposed Boreholes .....	8-9
8.3.1.1 Proposed Borehole Investigation Area 1 .....	8-9
8.3.1.2 Proposed Borehole Investigation Area 2 .....	8-9
8.3.1.3 Proposed Borehole Investigation Area 3 .....	8-11
8.3.1.4 Proposed Borehole Investigation Area 4 .....	8-11
8.3.1.5 Proposed Borehole Investigation Area 5 .....	8-12
8.3.2 Sampling .....	8-12
8.3.3 Testing .....	8-13
8.3.4 Permanent Instrumentation .....	8-15
8.4 Confirmatory Modeling .....	8-16

TABLE OF CONTENTS (continued)

	<u>Page</u>
9.0 POTENTIAL REMEDIAL ALTERNATIVES .....	9-1
9.1 No Action Alternative .....	9-1
9.2 Waste Disposal .....	9-1
9.3 Capping .....	9-2
9.4 Vapor Extraction .....	9-2
9.4.1 Description of Technique .....	9-2
9.4.1.1 General Principle .....	9-2
9.4.1.2 Theory and Operating Principles .....	9-6
9.4.1.3 Design Parameters .....	9-6
9.4.2 Stage of Development .....	9-9
9.4.3 Background .....	9-10
9.4.4 Benefits .....	9-10
9.4.5 Constraints .....	9-11
9.4.5.1 Environmental/Climate .....	9-11
9.4.5.2 Accessibility .....	9-11
9.4.5.3 By-Products .....	9-11
9.4.5.4 Schedule/Duration .....	9-11
9.4.5.5 Support Systems .....	9-12
9.4.5.6 Equipment Size .....	9-12
9.4.5.7 Operational Factors .....	9-12
9.4.5.8 Safety .....	9-13
9.4.5.9 Regulatory Issues .....	9-13
9.4.5.10 Efficiencies .....	9-13
9.5 Alteration of Recharge Flow Paths .....	9-13
9.5.1 Application .....	9-13
9.5.2 Description of Technique .....	9-13
9.5.2.1 General Principle .....	9-13
9.5.3 State of Development .....	9-16
9.5.4 Background .....	9-16
9.5.5 Benefits .....	9-16

## TABLE OF CONTENTS (continued)

	<u>Page</u>
9.5.5.1 Pressure Control by Air Injection/Withdrawal . . . . .	9-17
9.5.5.2 Mechanical Alteration of Permeability Capillary/ Fracturing . . . . .	9-17
9.5.6 Constraints . . . . .	9-17
9.5.6.1 Pressure Control by Air Injection/Withdrawal . . . . .	9-17
9.5.6.2 Mechanical Alteration of Permeability by Capillary, by Hydrofracturing, or by Construction of Capillary Barrier . . . . .	9-17
9.6 Freezing of the Unsaturated Zone . . . . .	9-18
9.6.1 Application . . . . .	9-18
9.6.2 Description of Technique . . . . .	9-18
9.6.2.1 General Principle . . . . .	9-18
9.6.2.2 Design Parameters . . . . .	9-19
9.6.2.3 Design, Procure, Construct, Fabricate Information . .	9-20
9.6.3 Stage of Development . . . . .	9-20
9.6.3.1 Initial LANL Action and Subsequent Actions . . . . .	9-21
9.6.4 Benefits . . . . .	9-21
9.6.5 Constraints . . . . .	9-22
9.7 Microbial Products Utilized as a Grout . . . . .	9-22
9.7.1 Application . . . . .	9-22
9.7.2 Description of Technique . . . . .	9-22
9.7.3 Stage of Development . . . . .	9-23
9.7.4 Background . . . . .	9-23
9.7.5 Advantages/Disadvantages . . . . .	9-24
9.8 In-Situ Coating with Inorganics/Clay . . . . .	9-24
9.8.1 Application . . . . .	9-24
9.8.2 Description of Technique . . . . .	9-25
9.8.3 Stage of Development/Background . . . . .	9-25

## TABLE OF CONTENTS (continued)

	<u>Page</u>
9.8.4 Action Plan .....	9-26
9.8.5 Benefits .....	9-27
9.8.6 Constraints .....	9-27
9.9 Grout Fissures and Pores .....	9-28
9.9.1 Application .....	9-28
9.9.2 Description of Technique .....	9-28
9.9.3 Stage of Development/Background .....	9-29
9.9.3.1 Action Plan .....	9-29
9.9.4 Benefits .....	9-31
9.9.5 Constraints .....	9-31
9.10 In-Situ Treatment .....	9-31
9.10.1 Application .....	9-31
9.10.2 Description of Technique .....	9-31
9.10.2.1 General Principle .....	9-31
9.10.2.2 Theory/Operating Principles .....	9-32
9.10.2.2.1 In-Situ Sintering .....	9-32
9.10.2.2.2 Design Parameters .....	9-32
9.10.2.2.3 Design/Procure/Construct/Fabricate .....	9-33
9.10.2.2.4 Stage of Development .....	9-33
9.10.2.2.5 Background .....	9-33
9.10.2.2.6 Benefits .....	9-34
9.10.2.2.6.1 Advantages .....	9-34
9.10.2.2.6.2 Disadvantages .....	9-34
9.10.2.2.7 Constraints .....	9-34
9.10.3 Description of Technique .....	9-35
9.10.3.1 In-Situ Vitrification .....	9-35
9.10.3.1.1 Design Parameters .....	9-35
9.10.3.1.2 Design/Procure/Construct/Fabricate .....	9-35

## TABLE OF CONTENTS (continued)

	<u>Page</u>
9.10.3.2 Stage of Development .....	9-36
9.10.3.3 Background .....	9-36
9.10.3.3.1 History .....	9-36
9.10.3.3.2 Past Use/Applications .....	9-36
9.10.3.4 Benefits .....	9-37
9.10.3.4.1 Advantages .....	9-37
9.10.3.4.2 Disadvantages .....	9-37
9.10.3.5 Constraints .....	9-37
9.11 Bioaccumulation of Pu .....	9-38
9.11.1 Application .....	9-38
9.11.2 Description of Technique .....	9-38
9.11.2.1 Surface Treatment of Contaminated Aquifer or Interbed Sediments Brought to the Surface .....	9-38
9.11.2.2 In-Situ Biosorption of Pu from Aquifer .....	9-38
9.11.3 State of Development .....	9-39
9.11.3.1 Action Plan .....	9-39
9.11.4 Background .....	9-39
9.11.5 Benefits .....	9-40
9.11.6 Constraints .....	9-40
9.12 Leach and Collect .....	9-40
9.12.1 Application .....	9-40
9.12.2 Description of Technique .....	9-40
9.12.3 Stage of Development .....	9-41
9.12.4 Background .....	9-41
9.12.5 Benefits .....	9-41
9.12.6 Constraints .....	9-42

References

Appendices

## LIST OF FIGURES

<u>Figure</u>		<u>Page</u>
1.1	Technical areas (TAs) of Los Alamos National Laboratory . . . . .	1-3
1.2	Location of corrugated metal pipes removed in 1984 . . . . .	1-4
1.3	Pathway analysis approach . . . . .	1-7
2.1	Physiographic features of the Jemez Mountains . . . . .	2-2
2.2	Geological cross section from the Jemez Mountains on the west, through the Pajarito Plateau, to the Rio Grande River on the east .	2-3
2.3	Illustration of geologic-hydrologic relationships in the Los Alamos area . . . . .	2-5
2.4	Location of supply wells, test wells, stock wells, springs in the Main Aquifer in the Los Alamos area . . . . .	2-7
2.5	Rate of movement of water in the main aquifer in the Los Alamos area . . . . .	2-8
2.6	Design of absorption beds at Area T . . . . .	2-14
4.1	Relationships for water saturation versus pressure head, and relative permeability versus saturation . . . . .	4-5
4.2	Yearly mass averaged flux rates for 2-D SOILSIM simulations (including pulse in 1960-61) . . . . .	4-12
4.3	Yearly mass averaged flux rates for 2-D SOILSIM simulations (excluding pulse in 1960-61) . . . . .	4-13
4.4	Pu-239 input concentrations for 2-D SOILSIM simulations . . . . .	4-16
4.5	Fine and coarse mesh utilized for 1-D HYDRUS simulations . . . . .	4-17
4.6	Coarse mesh utilized for SOILSIM 2-D flow simulations . . . . .	4-19
4.7	Fine mesh utilized for SOILSIM 2-D transport simulations . . . . .	4-20
5.1	Strategy to identify RI data requirements . . . . .	5-3

## LIST OF FIGURES (continued)

<u>Figure</u>		<u>Page</u>
5.2	Simulated americium concentrations versus depth assuming $K_d$ values in the lower range of Yucca Mountain tuffs . . . . .	5-6
5.3	Simulated americium concentrations versus depth assuming $K_d$ values in the moderate range of Yucca Mountain tuffs . . . . .	5-7
5.4	Simulated americium concentrations versus depth assuming $K_d$ values in the high range of Yucca Mountain tuffs . . . . .	5-8
5.5	Sensitivity simulation of Pu transport to $K_d$ , run 1 . . . . .	5-10
5.6	Sensitivity simulation of Pu transport to $K_d$ , run 2 . . . . .	5-11
5.7	Sensitivity simulation of Pu transport to $K_d$ , run 3 . . . . .	5-12
5.8	Sensitivity simulation of Pu transport to $K_d$ , run 4 . . . . .	5-13
5.9	Sensitivity of Pu transport to $K_d$ , run 5 . . . . .	5-14
5.10	Sensitivity of Pu transport to $K_d$ , run 6 . . . . .	5-15
5.11	Sensitivity of Pu transport to mesh spacing (fine mesh) . . . . .	5-16
5.12	Sensitivity of Pu transport to mesh spacing (coarse mesh) . . . . .	5-17
5.13	Sensitivity of saturation distributions to mesh design (fine mesh) . . . . .	5-18
5.14	Sensitivity of saturation distributions to mesh design (coarse mesh) . . . . .	5-19
5.15	Sensitivity of transport to power index (n) of the relative permeability versus saturation relationship . . . . .	5-21
5.16	Sensitivity of transport to power index (n) of the relative permeability versus saturation relationship . . . . .	5-22
5.17	Sensitivity of transport to power index (n) of the relative permeability versus saturation relationship . . . . .	5-23
5.18	Sensitivity of transport to power index (n) of the relative permeability versus saturation relationship . . . . .	5-24

## LIST OF FIGURES (continued)

<u>Figure</u>		<u>Page</u>
5.19	Sensitivity of transport to the leading coefficient ( $\alpha$ ) of the saturation versus capillary head relationship . . . . .	5-25
5.20	Sensitivity of transport to the leading coefficient ( $\alpha$ ) of the saturation versus capillary head relationship . . . . .	5-26
5.21	Sensitivity of transport to the power index ( $\beta$ ) of the saturation versus capillary head relationship . . . . .	5-27
5.22	Sensitivity of transport to the power index ( $\beta$ ) of the saturation versus capillary head relationship . . . . .	5-28
5.23	Sensitivity of saturation distributions to saturated hydraulic conductivity . . . . .	5-30
5.24	Sensitivity of saturation distributions to saturated hydraulic conductivity . . . . .	5-31
5.25	Sensitivity of Pu transport to saturated hydraulic conductivity . . . . .	5-32
5.26	Sensitivity of Pu transport to saturated hydraulic conductivity and dispersivity . . . . .	5-33
5.27	Sensitivity of Pu transport to dispersivity . . . . .	5-34
5.28	Sensitivity of saturation distribution to volume of water added to absorption bed . . . . .	5-36
5.29	Sensitivity of saturation to volume of water added to absorption bed in conjunction with a lower hydraulic conductivity . . . . .	5-37
5.30	Gravimetric soil water content as a function of sampling depth for absorption beds 1 and 2 in 1978 . . . . .	5-39
5.31	Concentration of plutonium as a function of sampling depth for absorption beds 1 and 2 in 1978 . . . . .	5-40
5.32	Simulated rock concentration of Pu in five layer system (Run 1) . . . . .	5-42
5.33	Simulated rock concentration of Pu in five layer system (Run 2) . . . . .	5-43

## LIST OF FIGURES (continued)

<u>Figure</u>		<u>Page</u>
5.34	Simulated rock concentration of Pu in five layer system (Run 3) . .	5-44
5.35	Simulated rock concentration of Pu in five layer system (Run 4) . .	5-45
5.36	Simulated rock concentration of Pu in five layer system (Run 5) . .	5-46
5.37	Simulated water concentration of Pu in five layer system (Run 1) .	5-47
5.38	Simulated water concentration of Pu in five layer system (Run 2) .	5-48
5.39	Simulated water concentration of Pu in five layer system (Run 3) .	5-49
5.40	Simulated water concentration of Pu in five layer system (Run 4) .	5-50
5.41	Simulated water concentration of Pu in five layer system (Run 5) .	5-51
5.42	Simulated saturation distributions of five-layer system (Run 6) . . . .	5-53
5.43	Simulated saturation distributions of five-layer system (Run 7) . . . .	5-54
5.44	Simulated saturation distributions of five-layer system (Run 8) . . . .	5-55
5.45	Simulated saturation distributions of five-layer system (Run 9) . . . .	5-56
5.46	Simulated rock concentrations of Pu in five-layer system (Run 6) . . .	5-57
5.47	Simulated rock concentrations of Pu in five-layer system (Run 7) . .	5-58
5.48	Simulated rock concentrations of Pu in five-layer system (Run 8) . .	5-59
5.49	Simulated rock concentrations of Pu in five-layer system (Run 9) . .	5-60
5.50	Simulated water concentrations of Pu in five-layer system (Run 6) .	5-61
5.51	Simulated water concentrations of Pu in five-layer system (Run 7) .	5-62
5.52	Simulated water concentrations of Pu in five-layer system (Run 8) .	5-63
5.53	Simulated water concentrations of Pu in five-layer system (Run 9) .	5-64
5.54	Steady state moisture distribution . . . . .	5-70

## LIST OF FIGURES (continued)

<u>Figure</u>		<u>Page</u>
5.55	Saturation profile of Scenario II.1 (coarse mesh) . . . . .	5-74
5.56	Saturation profile of Scenario II.1 (fine mesh) . . . . .	5-75
5.57	Hydrograph for flux input into SOILSIM and HYDRUS . . . . .	5-79
5.58	Saturation distribution for Scenario II.2 (with pulse in 1960-61) (coarse mesh) . . . . .	5-80
5.59	Saturation distribution for Scenario II.2 (with pulse in 1960-61) (fine mesh) . . . . .	5-81
5.60	2-D Scenario II.2 saturation distribution obtained from SOILSIM (pulse in 1960-61 applied/no pipe) . . . . .	5-82
5.61	Location of buried pipe . . . . .	5-84
5.62	Velocity field of Scenario II.3 (pipe leak and pulse in 1960-61) . . .	5-87
5.63	Concentration input for 1- and 2-D Scenarios . . . . .	5-90
5.64	Simulated plutonium concentration profiles of Scenario III.1 . . . . .	5-91
5.65	Simulated plutonium concentration profiles of Scenario III.2 . . . . .	5-94
5.66	Simulated normalized concentration profiles for two-dimensional simulation involving a conservative species including 1960-61 pulses but without the pipe leak) . . . . .	5-95
5.67	Simulated normalized concentration profiles for two-dimensional simulations involving a conservative species with pipe leak and 1961 pulses . . . . .	5-98
5.68	Simulated concentration profiles for two-dimensional simulations of Plutonium in 1978 with and without the pipe . . . . .	5-99
5.69	Simulated concentration (dpm) profiles for two-dimensional simulations of Plutonium in 1990 with and without the pipe . . . . .	5-100
7.1	Site conceptual model . . . . .	7-2

LIST OF FIGURES (continued)

<u>Figure</u>		<u>Page</u>
8.1	Site characterization process . . . . .	8-2
8.2	Map of proposed boreholes . . . . .	8-10
9.1	Simple vapor extraction system . . . . .	9-3
9.2	Air pump activated vapor extraction system . . . . .	9-4
9.3	Dual well vapor extraction system . . . . .	9-5
9.4	Barometrically driven dual well vapor extraction system . . . . .	9-7
9.5	Water flow path changed through pressurization . . . . .	9-15
9.6	Potential grouting methods for remediation . . . . .	9-30

## LIST OF TABLES

<u>Table</u>		<u>Page</u>
2.1	On-site estimates of radioactivity to absorption beds (covered seepage pits, Area T and Area V) . . . . .	2-11
2.2	Reported volumes of wastes discharged to Area T absorption beds .	2-13
2.3	Historical Pu-239 releases to MDA T . . . . .	2-15
4.1	Source and range of model input parameters . . . . .	4-3
4.2	Input parameter relative uncertainties . . . . .	4-6
4.3	Flux input to absorption bed 1 . . . . .	4-10
4.4	Reported Pu-239 concentrations released to absorption beds at MDA T . . . . .	4-14
5.1	Typical distribution coefficients and approximate retardation factors for welded and nonwelded Yucca Mountain hydrogeologic units . . .	5-5
5.2	Parameter input for historical comparisons . . . . .	5-39
5.3	Mass comparison between field measurements and simulations . . . .	5-66
5.4	Parameter input for scenario I.1 (1-D) . . . . .	5-69
5.5	Parameter input for scenario II.1 (1-D) . . . . .	5-72
5.6	Flux input to absorption beds at MDA T without 1960-1961 pulse . .	5-73
5.7	Parameter input for Scenario II.2 . . . . .	5-77
5.8	Flux input to absorption beds at MDA T including 1960-61 pulse . .	5-78
5.9	Parameter input for Scenario II.3 2-D . . . . .	5-85
5.10	Parameter input for Scenario III.1 . . . . .	5-89
5.11	Parameter input for Scenario III.2 . . . . .	5-93
5.12	Parameter input for Scenario III.3 . . . . .	5-97
8.1	Fulfillment of information needs . . . . .	8-3

---

Pathway Analysis at Material Disposal Area T  
Los Alamos National Laboratory (LANL)  
Los Alamos, New Mexico

EXECUTIVE SUMMARY

The primary objectives of this pathway analysis are to (1) estimate unsaturated flow conditions and contaminant transport using available data, and (2) define data requirements necessary for completing a remedial investigation at Material Disposal Area T (MDA T). This pathway analysis has been instrumental in developing a conceptual model for MDA T that may be tested and refined during the remedial investigation. This model, with minor refinements, may be applied to other sites at LANL that are characterized by similar hydrogeologic properties and settings. Furthermore, remedial investigation activities and technologies developed for MDA T may also be transferred to other LANL sites.

The conceptual model for MDA T describes a heterogeneous system where the addition of both liquid waste and waste-free water provides a contaminant source and a driving force for at least limited downward migration of radionuclides. Fracture systems in the Bandelier tuff are considered to play an important role in moisture migration. The rate and depth of contaminant migration is largely controlled by the rate of water movement and retardation caused by adsorption of radionuclides within the vadose zone matrix. It is estimated that the volume of water discharged to adsorption bed number 1 during the period between 1945 and 1967 has already passed through vadose zone system. The relatively high adsorptive capacity of the Bandelier tuff, as reflected in estimated distribution coefficient values, would have severely retarded the migration of radionuclides. In the case of fracture-dominated flow, matrix diffusion may have acted to significantly retard the movement of dissolved constituents.

It is recognized that some of the parameters controlling flow and transport today and into the future may be quite different compared to conditions that governed flow and transport during the application of water and liquid waste in the past. Natural recharge is presently the primary force for migration. Its magnitude is not considered sufficient to induce measurable transport of radionuclides through fractures or the rock matrix. Other processes, such as lateral migration, canyon recharge, or groundwater flow, may affect the distribution of any contaminants that may have passed through the vadose zone with moisture pulses associated with past input. Fractures were probably the predominant avenue for flow and transport during the application of large volumes of water and liquid waste in the past. Under ambient recharge conditions the same fractures are thought to behave as natural barriers to flow and migration.

Distinguishing whether the flow and transport processes are primarily controlled by rock and fracture permeabilities or by other chemical or physical properties is critical to the design of a characterization program at MDA T. If observed subsurface peaks in moisture content and radionuclide concentration reflect downward migration of pulses

---

---

from past waste discharges, then water flux and travel times can be computed on that basis. If subsurface peaks reflect instead remnants of water and solutes retained by higher retention and adsorption capacity, then entirely different interpretations result. Migration pathway analysis results indicate that the bulk of the moisture applied to bed number 1 has migrated through the vadose zone within an estimated 10-year period, and subsurface peaks in moisture content and radionuclide concentration are thought to represent remnants of past applications of water and liquid waste that have been retained by the adsorption capacity of the tuff.

Pathway analysis results also indicate uncertainty in some input parameters compared to previous estimates, particularly hydraulic conductivities and distribution coefficients. To explain available data and modeling results, either the matrix saturated hydraulic conductivity is substantially greater than previously estimated by Abeele and others (1983), or fractures add considerably to secondary permeabilities and play a significant role in flow processes occurring at the time of liquid waste application in the past.

In order to match subsurface radionuclide concentrations measured by Nyhan and others in 1984, distribution coefficients ( $K_d$ ) must be considerably lower than those measured for other tuffs to allow for faster transport. One of two conclusions may be drawn; either the sorptive characteristics of the Bandelier tuff are considerably different than those reported for other tuffs, or other factors involving physical or chemical characteristics of the wastes cause a reduced  $K_d$ .

Two-dimensional simulation results suggest that increases in saturation could occur in the vadose zone at substantial lateral distances from adsorption beds at MDA T. The possibility of lateral flow and migration to points of release along the wall of Los Alamos Canyon to the north is addressed as a remedial investigation data requirement.

Other data requirements for a remedial investigation at MDA T are listed and remedial investigation activities are recommended. The relationship between lithology, water saturation, contaminant concentrations, and geographic setting is emphasized. Four recommended phases consist of further background research to obtain a more-detailed waste inventory, bench-scale studies to observe waste chemistry behavior in tuff samples, field investigation activities designed to obtain moisture and contaminant profiles at depth, and confirmatory modeling to integrate collected data into the migration pathway analysis and refine the current conceptual model. Potential remedial measures are presented that address both source removal and plume stabilization. A description of each technology includes benefits and constraints.

---

---

## 1.0 INTRODUCTION

### 1.1 General

This study is a part of the remedial investigation scoping and feasibility study process under the Environmental Restoration Program. The Environmental Restoration Program is a Department of Energy (DOE) program designed to bring DOE facilities into compliance with Comprehensive Environmental Response, Compensation, and Liability Act (CERCLA) requirements. The ER Program Technical Support Office (TSO) is responsible for conducting several phases of the CERCLA investigations, including the completion of the Preliminary Assessment/Site Investigation (PA/SI), the Remedial Investigation/Feasibility study (RI/FS), and verification sampling. In addition to responsibility for these site-specific investigations, the TSO is also responsible for providing integrated technical direction and program management for the ER Program.

### 1.2 Purpose and Scope of Work

This study is designed to estimate subsurface migration rates, distances and directions of moisture and associated dissolved waste constituents of radionuclide waste materials disposed between 1945 and 1967 at Material Disposal Area (MDA T). Study results will be used to help define remedial investigation (RI) data requirements and to design RI activities.

The primary goal is to provide a sound technical basis from which to develop the remedial investigation. The planning and implementation of a remedial investigation based on defensible technical rationale will help assure acceptance of the remedial investigation program by regulatory agencies. Specific technical objectives of the study are to:

- develop a working conceptual model of MDA T to formulate, test and evaluate hypotheses, plan site characterization activities, and assess the relative feasibility and effectiveness of potential remedial actions;
- estimate the present lateral and vertical subsurface distribution of key radioactive and non-radioactive waste constituents;
- identify those physical and chemical parameters that control the migration of waste-products;
- prioritize field measurement criteria pertaining to sampling frequencies and sampling or measurement sensitivity requirements;

- estimate the future potential for vertical and lateral movement of fluid and waste radionuclides in the site vicinity;
- identify existing data deficiencies that should be addressed as part of future RI activities or confirmatory modeling.

### 1.3 Site Description and Waste Disposal History

Liquid and solid wastes containing plutonium and other radionuclides have been disposed at Los Alamos National Laboratory (LANL) since the beginning of Laboratory operations in the early 1940's. Open pits or trenches have provided the principal disposal facilities. For special waste forms vertical shafts and covered seepage pits have been used (Abeelee and others, 1981). All shafts, pits, and trenches are excavated into the Bandelier tuff. The Bandelier tuff is the principal rock type exposed in the Los Alamos area. The tuff is a nonwelded to welded volcanic ash that comprises an upland area called the Pajarito Plateau. Numerous east-west trending canyons dissect the Plateau draining east to the Rio Grande River. Most of the LANL facilities, including the waste disposal sites, are located on top of the finger-like mesas (Abeelee and others, 1981).

At Los Alamos a wide variety of disposal operations are performed. Disposal activities range from shaft disposal of cylinders containing millicurie quantities of tritium to demolition and burial of entire contaminated buildings. During the LANL's early years, liquid wastes were discharged directly into seepage pits. Since 1952, the sludges resulting from liquid waste treatment are placed in drums or mixed with cement and poured into shafts (Abeelee and others, 1981).

From 1945 through 1968 liquid radioactive wastes at TA-21 DP West were discharged into a series of four seepage beds excavated into porous tuff underlying Material Disposal Area T (Figure 1.1). A previous site investigation (Nyhan and others, 1984) indicated that the vadose zone beneath Material Disposal Area T (MDA T) may act as a contaminant migration pathway.

MDA T consists of four absorption beds, Building 257, a Retrievable Waste Storage Area and cement paste shafts. The scope of this study is limited to the four absorption beds.

Waste treatment operations shifted to a new treatment plant (TA-21-257) in 1968, replacing Building 35. The raw and treated waste storage tanks and cement silo from Building 35 were incorporated into the operation of Building 257. The Building 257 plant generated sludge residue contaminated with plutonium and americium. In 1968, a pug mill operation was started to mix the sludge with cement. The resulting cement paste was pumped directly into asphalt coated vertical shafts augered between absorption beds 2 and 4 (Figure 1.2). This procedure continued through 1974.

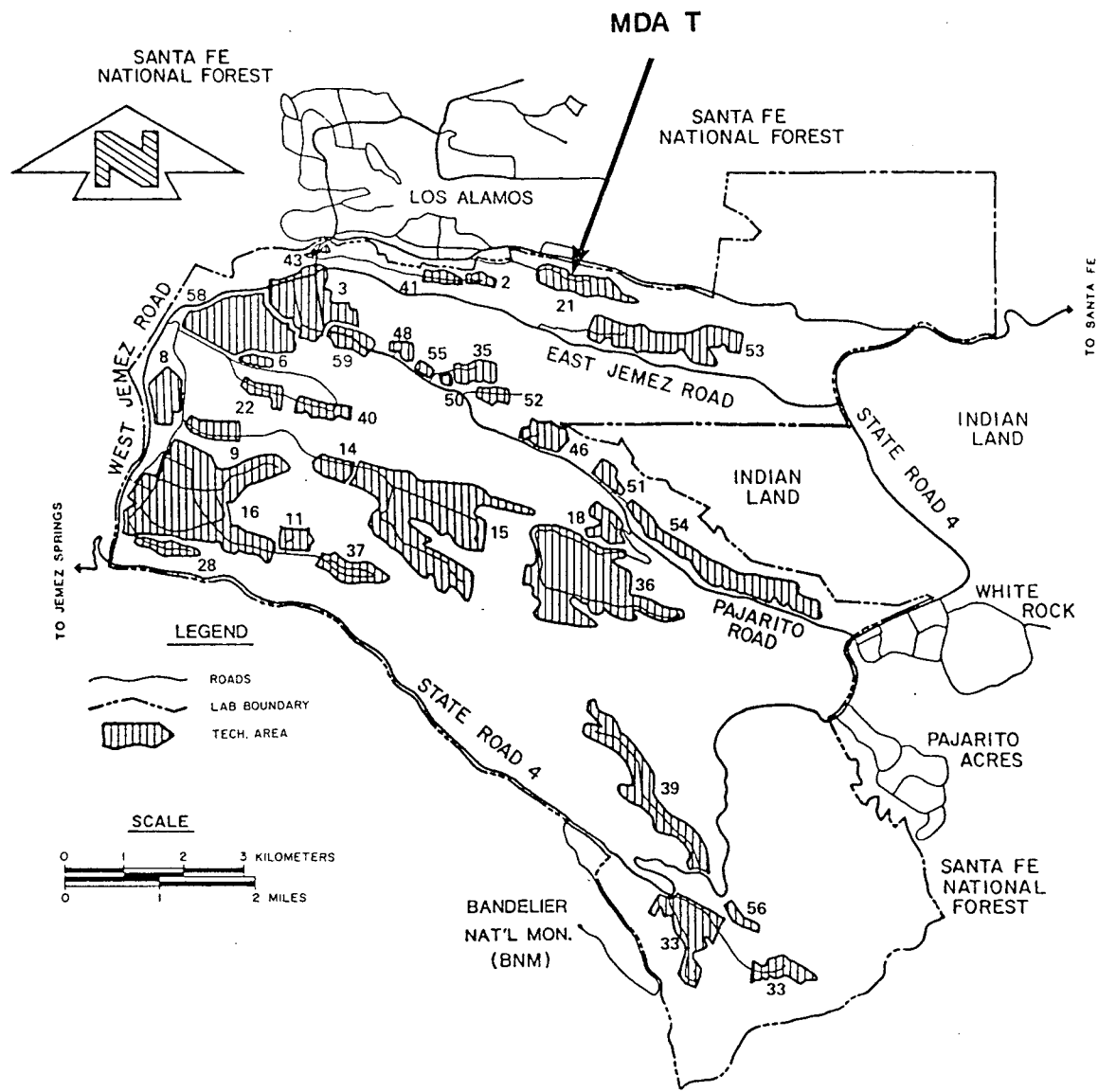


Figure 1.1. Technical areas (TAs) of Los Alamos National Laboratory.

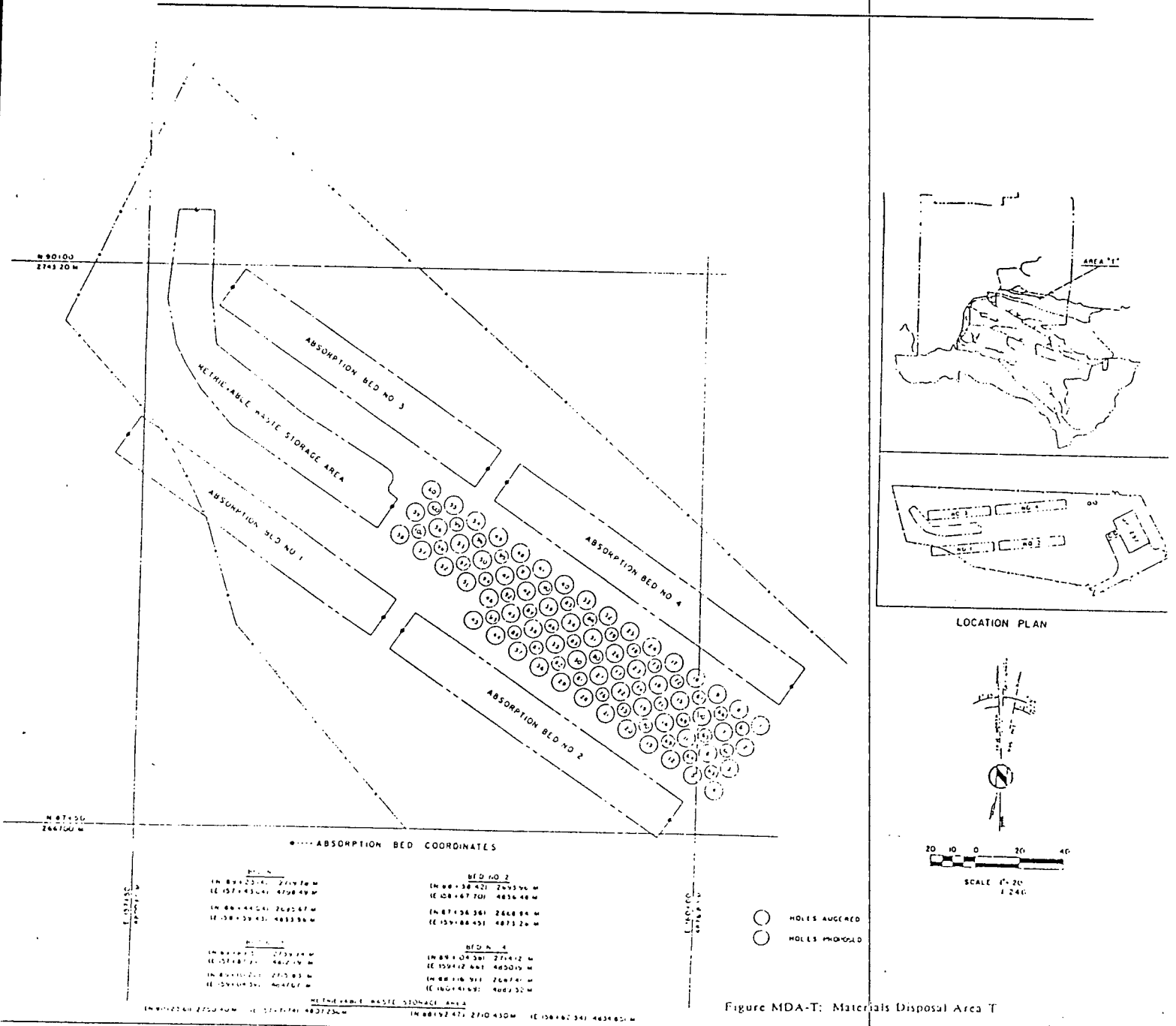


Figure 1.2. Location of corrugated metal pipes removed in 1984.

---

In late 1974, a new disposal technique was implemented at MDA T. A Retrievable Waste Storage Area was excavated between beds 1 and 3. This storage area was composed of a pit 36.6 m long, 7.3 m wide, and 5.8 m deep. Corrugated metal pipes (CMP) were filled with transuranic cement pastes and placed in the pit. Low-level cement paste was pumped into shafts at the site through April 1983. In August 1984, the 70 CMP's were relocated from MDA T to MDA G. They contained transuranic wastes with concentrations below 100 nCi/g.

An inventory of recorded radionuclide content and composition of solid wastes disposed at LANL since the beginning of Laboratory operations was conducted by Rogers (1977). Waste disposal records were highly variable in quality and incomplete until the mid-1950's (Abeele and others, 1981). Detailed records of waste content and composition were started in 1959. The quality of recording has apparently improved steadily since that time (Abeele and others, 1981). Waste disposal records specifically pertaining to the MDA T site have limitations and uncertainties similar to those associated with Laboratory-wide data.

#### 1.4 Current Site Conditions

Environmental surveillance of Material Disposal Area T is part of LANL's program of routine environmental surveillance of low-level radioactive waste management areas, as required for compliance with appropriate standards. Objectives of this surveillance program are to (1) identify undesirable trends that may require remedial actions, and (2) monitor the performance of waste confinement.

Radioactive concentrations in air (particulate and moisture), water, soil, and sediment samples are measured regularly along with the levels of external penetrating radiation. These monitoring data are available in the current edition of the environmental surveillance report (Environmental Surveillance Group, 1988).

Surface stabilization at the four absorption beds was completed in 1987. Stabilization included measures to control runoff from paved portions around MDA T (i.e., reroute parking lot drainage around MDA T into a paved ditch instead of through Area T). After grading, the site was contoured to less than a 5 percent slope, and covered with approximately forty inches of fill material. The site was revegetated with a native seed mix typically used on LANL waste sites. Long-term stabilization of the steep bank on the north perimeter of the disposal area is difficult because of erosion. Routine surveillance activities are conducted to monitor and maintain site stability and integrity.

#### 1.5 Report Description and Organization

To present the information provided in this study as succinctly as possible, this report is divided into four general areas: (1) background literature search and evaluation of data

---

---

needs; (2) model selection and description; (3) pathway analysis and results; (4) characterization activities and remedial alternatives. The approach for this study is briefly discussed below and outlined in Figure 1.3.

The input and output of the pathway analysis are reported in metric units. The dimensional units referenced from other authors are not generally converted to a consistent standard convention. For convenience a standard conversion table is included as Appendix A.

#### Background Literature Search and Evaluation of Data Needs

To formulate a preliminary conceptual model and to obtain data necessary for the pathway analysis, a review of previous investigators work and conclusions pertaining to the hydrogeological conditions at Los Alamos was performed. This information review also aided in the identification of data deficiencies and enabled parameter uncertainties to be estimated.

#### Formulation of Initial Conceptual Model

The initial conceptual model was formulated to facilitate the selection of appropriate numerical models, develop the modeling approach and to assign boundary and initial conditions to the problem domain. During the pathway analysis the initial conceptual model was further tested and refined.

#### Model Selection and Description

The numerical codes SOILSIM (Huyakorn, 1989) and HYDRUS (Kool, 1987) were selected to perform the pathway analysis because few (if any) other codes are available that will simulate sharp wetting fronts caused by the addition of large volumes of fluid moving through very dry conditions. Complete descriptions of the models, together with the assumptions and limitations associated with each, are included in Section 3.0.

#### Pathway Analysis

The pathway analysis involved several integrated tasks which are discussed below.

Testing and refinement of the preliminary conceptual model. The development of a well formulated conceptual model was one of the primary goals of the pathway analysis. A sound conceptual model should include known gross characteristics of the system and should account for known major system responses to stresses.

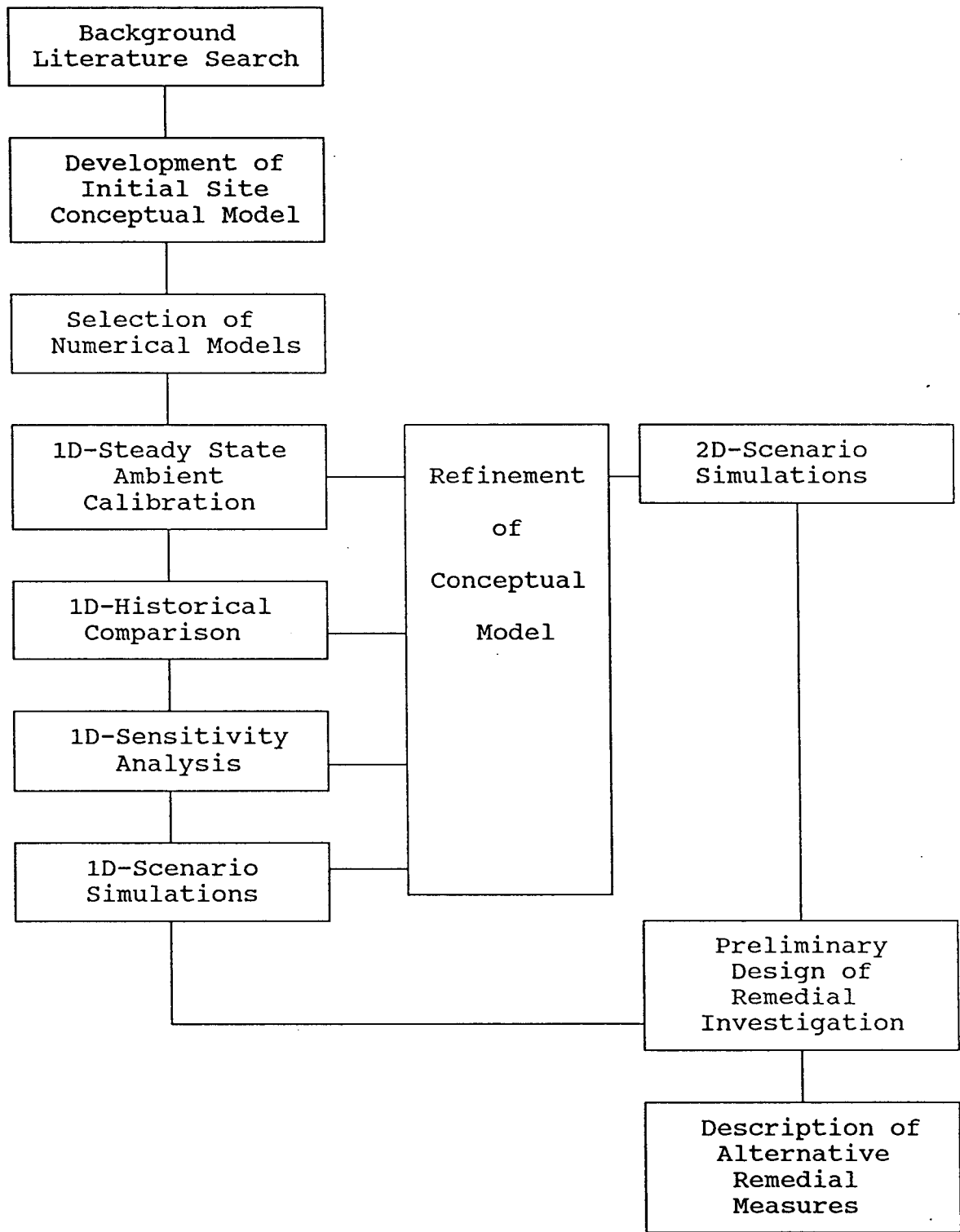


Figure 1.3. Pathway analysis approach.

---

The conceptual model serves as the basis to guide the formulation and refinement of the numerical models, sensitivity analyses, the testing of various alternatives, and establishing priorities for collecting or estimating additional needed parameters.

Model calibration. The calibration of the model involved the adjustment of ambient recharge rates, rock properties and distribution coefficients within reasonable ranges of expected or known values to approximate measured data from the field.

Sensitivity analysis. The sensitivity analysis was designed to test the relative sensitivity of the system to various key parameters which may influence flow and transport.

Historical comparison. A series of moisture and radionuclide profiles that were constructed from data collected during several previous field investigations are used as the focus of the historical comparison. Saturation and radionuclide output from the pathway analysis are compared against the measured values.

#### Site Specific Model Simulations

The numerical simulations designed to reproduce conditions at MDA T are divided into three cases, which are described below.

##### Case I- Ambient Flow Simulations

In Case I simulations, the steady-state flow regime was simulated under estimated ambient conditions to establish a baseline for other simulations. Using this baseline, effects of various man-induced stresses were then simulated and compared (Cases II and III).

##### Case II - Man-induced Flow Simulations

Three unsaturated flow scenarios simulated known or estimated man-induced stresses on the system. These include: (1) the intermittent addition of liquid wastes applied from 1945-1967; (2) two discrete moisture pulses applied in 1960-61 during infiltration studies; and (3) a simulated pipe leak of 0.03 gpm.

Each of the flow scenarios used the input from the calibrated flow analysis in Case I as the initial condition. During Case II the documented or estimated man-induced stresses placed on the system since 1945 were superimposed on the natural hydrologic system calibrated during Case I.

---

### Case III - Contaminant Transport Simulations

The transport simulations performed in Case III of this analysis coupled the flow simulations used in Case II with contaminant transport simulations.

#### Characterization Activities and Remedial Alternatives

Pathway analysis results were used to help select components of a proposed characterization program and will be useful in selecting appropriate remedial measures.

#### 1.6 Previous Investigations

Currently, archive searches and interviews are being conducted to better define the composition and quantity of waste stream input into the four absorption beds at MDA T.

Some of the earliest environmental monitoring surveys at LANL that include data on MDA T, are presented in "Survey of Los Alamos and Pueblo Canyon for Radioactive Contamination and Radioassay Tests Run on Sewer-Water Samples and Water and Soil Samples Taken from Los Alamos and Pueblo Canyons," (Kingsley and others, 1947).

The collection of effluent samples from the DP-Site chemical sewer outlets began at two month intervals in April 1947. Samples were assayed for plutonium, polonium, and uranium. The first report was issued October 20, 1947 (Tribby, 1947).

The fluorine concentration for DP West seepage, main drain, MDA T, was 4.2 mg/l. The monthly report for October 21 to November 20, 1947, gives a radioassay in c/m/l (counts/min/liter) as 29,836 for plutonium and 5.8 for polonium (Cox and Schnap, 1948). Samples collected September 20-30, 1947, were reported January 2, 1948, with the following comment: "As expected the highest activity due to plutonium was found at DP-W Seepage Pit Main Drain ("B") with 65,639 d/m/l (disintegrations/min/liter). Records on studies and monitoring at MDA T from 1948 to 1953 were either not kept or were not available.

In 1953 the United States Geological Survey (USGS) conducted a study at MDA T to determine "the fate of plutonium contained in liquid wastes discharged onto or just below the surface of the earth" (Herman, 1954). Five test borings were drilled in and around the absorption beds. Samples were collected at 0.3-m intervals. All samples were analyzed for plutonium, and ion-exchange capacity was measured on three samples. Results appear to be fairly representative of each test boring (Appendix B). According to Rogers (1977) the observations pertaining to the travel of plutonium through the earth, sand, gravel, and rock media are:

1. No appreciable horizontal movement of the plutonium occurs in the first 20 feet of depth.
2. The plutonium is readily retained by the various earth media (sand, clay, gravel and rock).
3. Apparently retention of the plutonium is greater in finer materials.
4. Penetration of the plutonium into the underlying strata is not to be expected.

Initial laboratory studies of the interaction of radionuclides in the liquid wastes with local soils and geologic materials were performed at LANL. Cores of Bandelier tuff, exposed to waste solutions of plutonium, retained essentially all of the radionuclides in the top few millimeters of the core. Subsequent attempts to leach the sorbed plutonium failed (Christenson and others, 1958).

In 1959, a field study was initiated to determine the distribution of plutonium previously discharged into an absorption bed at MDA T (Christenson and Thomas, 1962). Unlike the previous laboratory study, the 1959 field study showed that plutonium species penetrated as far as 8.5 m into the Bandelier tuff and that this penetration may have taken place along fissures in the tuff. Clays occurring non-uniformly in the tuff by local weathering, were speculated to have adsorbed plutonium species. This preferential adsorption resulted in localized areas of high plutonium concentrations.

In the summer of 1960, DP waste flows were discharged to seepage bed 1 for one month at an average rate of 8,700 gpd. The following month tap water was applied at a rate of 6,600 gpd. Moisture profiles were collected during and after these runs (Christenson and Thomas, 1962) (Appendix C).

In 1961, DP raw waste was again diverted to seepage bed 1. An average rate of 6,400 gpd was maintained from June 30 to August 1. From August 2 to August 26, approximately 7,100 gpd of tap water was applied. Moisture, radionuclide, pH and total dissolved solid profiles from that experiment are reported in Christenson and Thomas (1962), and are presented in Appendix B.

LANL and USGS conclusions from the 1960-61 addition of water, summarized in Christenson and Thomas (1962) and Abrahams (1963), include:

1. The waste-water movement through the tuff may have changed some of the physical properties of the tuff, such as pore and particle sizes by chemical alteration (Abrahams, 1963).

- 
2. Some of the wastes discharged in the east end of the disposal pit may have moved laterally through the sandy material along the sloping top of the tuff and then vertically into the tuff (Abrahams, 1963).
  3. The lower moisture values seem to coincide with areas of tuff in which the greatest amount of staining has occurred. The stained areas may indicate a different stage of weathering than that at the clay layer due to alternate wetting and drying cycles (Abrahams, 1963).
  4. The moisture content and gross alpha activity of the cores collected in the study area decreased significantly from east to west and with depth. This decrease in activity indicated that much of the liquid discharged into the pit moved only a short distance laterally through the sandy material before infiltration into the tuff (Abrahams, 1963).
  5. The tuff is extensively jointed and the tendency for liquid to move through the joints is indicated by higher gross alpha activity in local areas. This observation is supported by the gross alpha count of 1,000 per minute per dry gram at the 20 foot depth (Abrahams, 1963).
  6. In the east group of holes, the joints are more numerous with increasing depth. Waste water penetrated the fine line joints to depths of at least 22 feet and subsequently altered the tuff adjacent to the joint as much as one-quarter to one-half inch into the matrix away from the joint. Clays developed locally and impeded drainage so that the joints retained water to the extent that the moisture content of the tuff was locally as much as 35 percent (Abrahams, 1963).
  7. Water in the low moisture range apparently moved to depths greater than 90 feet. Water in unknown quantities apparently moves through open joints or joints which may have been enlarged by solvents in the wastes (Abrahams, 1963).
  8. Below a depth of about 15-20 ft the alpha activity was low, except for local areas of relatively high activity. Apparently, these local areas of high alpha activity are where water carried the activity along the joints. The occurrence of rapid movement of water through joints was substantiated during these infiltration studies (Abrahams, 1963).
  9. Total hardness and total solids are correlated with alpha activity (Appendix B) (Christenson and Thomas, 1962).
  10. Total solids and total hardness increase with depth, suggesting solution or re-solution of previously deposited material (Christenson and Thomas, 1962).
-

11. There is some indication of an inverse relationship between gross alpha content and pH. It is possible that at the lower pH values the plutonium is oxidized to +6 and although it is fairly unstable, it is more mobile than the  $\text{Pu}^{+4}$  and  $\text{Pu}^{+3}$  species (Christenson and Thomas, 1962).
12. The irregularity of the saturation curves (sudden decrease in percent moisture) obtained from field data suggests that percolating water may cause perched zones, or may travel rapidly along fissures. Fracture transport and perched water will exert a marked influence on the accumulation and sorption of radionuclides in the areas involved (Christenson and Thomas, 1962).
13. Under field conditions, plutonium species have been shown to penetrate to at least 28 feet. Moisture and flow rate data, and physical inspection indicate that the penetration apparently takes place along fissures (Christenson and Thomas, 1962).
14. It is apparent that one cannot extrapolate from laboratory studies on intact core samples to conditions which prevail in the field (Christenson and Thomas, 1962).

In 1974, a detailed series of laboratory studies were initiated with crushed and intact Bandelier tuff at Argonne National Laboratory. Results suggest that waste and aqueous solutions of plutonium and americium exhibit anomalous migration behavior (Fried and others, 1975, 1976, 1977, 1978). This research shows that plutonium may exist in two forms, one of which (probably a hydrolyzed form) migrates much more rapidly than the "ionic" form when moving by aqueous percolation. The experimental results suggest a penetration rate of the more mobile plutonium species of about 217 cm/y when transported by unsaturated water flow in the tuff (Fried and others, 1975).

The objective of a comprehensive field study performed by Nyhan and others, (1984) was to determine the distribution of plutonium, americium and water beneath two absorption beds at MDA T as a function of depth. Results of their study indicate that the vertical distributions of radionuclides and water are related to the occurrences of fractures and variations in geologic properties of tuff units in each profile.

---

## 2.0 SITE CONDITIONS

### 2.1 Hydrogeological Setting

The Los Alamos facilities are located on the western part of the Pajarito Plateau (Figure 2.1), which forms an apron of volcanic and sedimentary rock around the eastern flanks of the Jemez Mountains. The MDA T site is situated along the northern border of the Los Alamos facilities (Figure 1.1). The Pajarito plateau is aligned approximately north-south and is about 20 to 25 miles in length and five to ten miles wide. The Plateau is bounded to the east by White Rock Canyon, which contains the Rio Grande. The Puye Escarpment borders the Plateau on the north and northeast while the Sierra de los Valles are adjacent to the Plateau on the west. The Plateau dips gently eastward from an elevation of about 7,500 feet near the mountains toward the Rio Grande where it vanishes at an elevation of about 5,400 feet. The Rio Grande has cut steep slopes and cliffs into the Plateau. The Plateau is dissected into a number of narrow mesas by intermittent streams that trend southeastward.

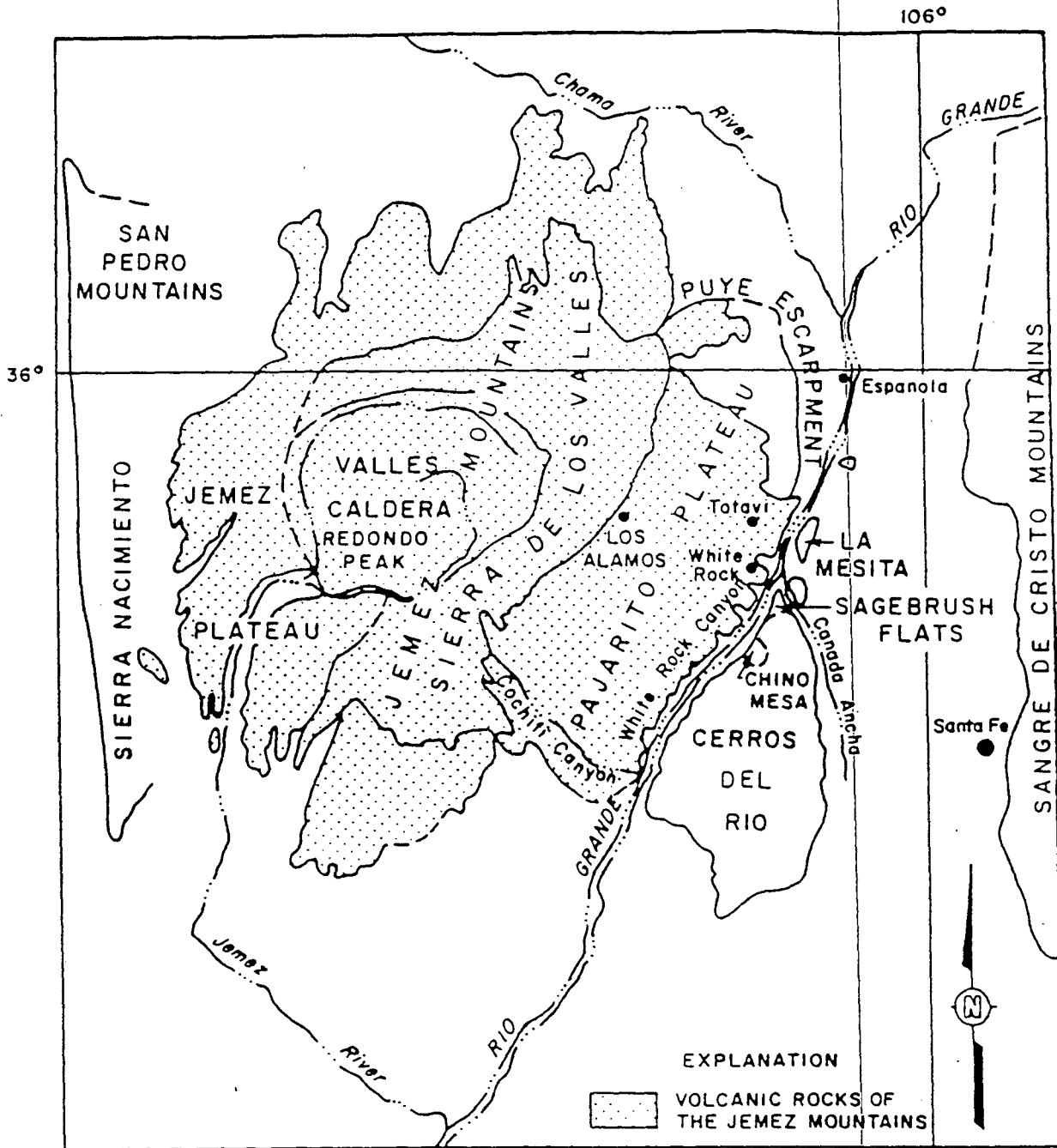
The volcanic and sedimentary rocks that are present in the Los Alamos area range in age from Miocene to Holocene (Abee and others, 1981). Rock types include sandstones and siltstones, crystalline rocks, and ash-flow tuffs (Figure 2.2). The oldest rock unit in the Los Alamos area is the Tesuque Formation of Miocene age which consists of fossiliferous siltstones and sandstones with lenses of clay that were deposited as basin fill in the Rio Grande structural trough (Abee and others, 1981). The main water supply for LANL and domestic use is groundwater from the Tesuque Formation (Abee and others, 1981).

The Puye Conglomerate overlies the Tesuque Formation in the central and eastern parts of the Pajarito Plateau. The Puye Conglomerate consists of well-rounded pebbles, cobbles, and small boulders of Precambrian quartzite and granite in a matrix of coarse arkosic sandstone grading into a poorly consolidated, silty, sandy conglomerate containing interlayered lapilli-tuff beds and volcanic mudflow deposits (Abee and others, 1981).

The Puye Conglomerate is overlain by the Tschicoma Formation which forms the major part of the interior mass of the central Jemez Mountains. Rock types are porphyritic dacite, rhyodacite, and quartz latite containing phenocrysts of pyroxene, hornblende, biotite, plagioclase and quartz. The maximum thickness of the Tschicoma Formation exceeds 900 m (Abee and others, 1981).

The volcanic rocks of Chino Mesa are 0-460 m thick and were deposited less than 2.8 million years ago over the Tschicoma Formation. These volcanic rocks are mostly basaltic andesite flows and tuffs containing xenocrysts of quartz (Abee and others, 1981).

The Bandelier tuff was formed during the Pleistocene by volcanic activity in the Jemez Mountains and consists of a series of rhyolite and quartz latite domes, ash flows, air-fall



Reference; R.L. Griggs, 1954

Figure 2.1. Physiographic features of the Jemez Mountains (Griggs, 1954).

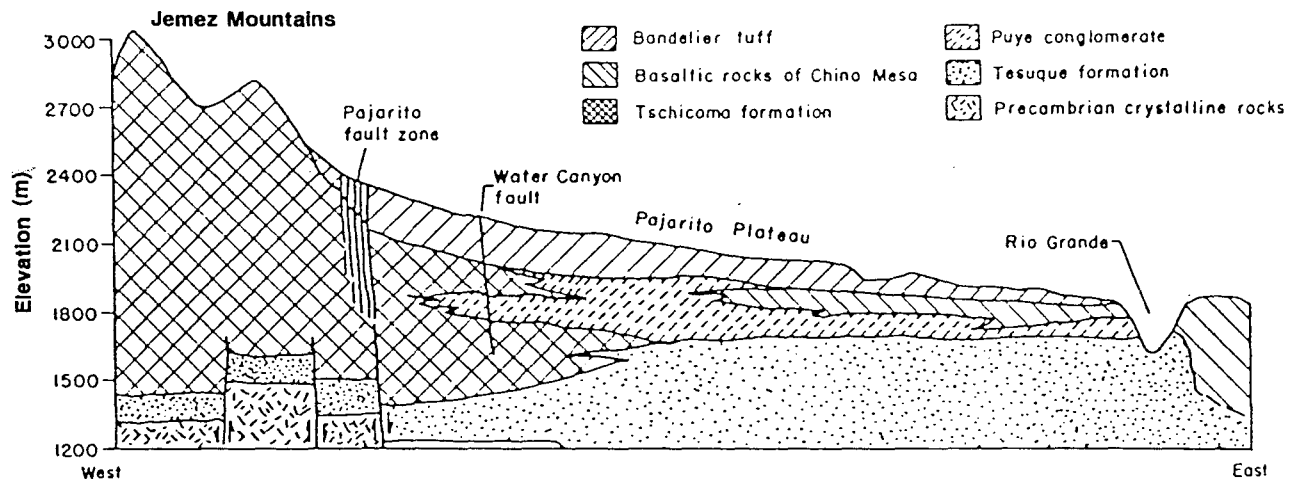


Figure 2.2. Geologic cross section from the Jemez Mountains on the west, through the Pajarito Plateau, to the Rio Grande River on the east (modified from Abee and others, 1981).

pumice, and obsidian. The Bandelier tuff forms the upper parts of the Jemez Plateau on the western flanks of the Jemez Mountains and the Pajarito Plateau on the eastern flanks of the Jemez Mountains. It is therefore the most extensive unit at Los Alamos. The formation is divided into two members, the lower Otowi and upper Tshirege. Each member is composed of a basal air-fall pumice overlain by a series of ash-flow units. The thickness of the tuff ranges from 10 to 320 m.

In the Los Alamos area, the 1.4-million-year-old Otowi Member consists of a 0- to 10-m-thick basal bedded air-fall pumice overlain by massive to poorly bedded nonwelded ash-flow deposits containing abundant lithic fragments. Ash flow units in the Otowi often easily erode to form characteristic pinnacle-shaped features. The thickness of this member in the Los Alamos area ranges from 0 to 80 m (Abee and others, 1981).

The Tshirege Member is 1.1 million years old and consists of a 0.3-m-thick basal bedded air-fall pumice overlain by nonwelded ash flows containing hornblende-rich quartz latite pumice and accidental lithic fragments. The base of the Tshirege rests on the irregular erosional surface of the Otowi.

Physical properties of the tuff that may affect fluid flow result primarily from induration (which includes vapor-phase crystallization, devitrification, and welding) and jointing (Abee and others, 1981).

Joints, formed by cooling of ash flows, commonly divide the tuff into irregular blocks. The predominant joint sets are vertical or nearly vertical and joint frequency generally increases with a greater degree of welding (Abee and others, 1981).

## 2.2 Primary Aquifer System

The main aquifer of the Los Alamos area rises westward from the Rio Grande through the Tesuque Formation into the lower part of the Puye Conglomerate, beneath the central and western parts of the plateau (Figure 2.3). The water in the aquifer moves from the major recharge area in the Valles Caldera eastward toward the Rio Grande. This is the only aquifer capable of yielding municipal and industrial supplies (Purtymun, 1984). The upper surface of the main aquifer rises westward from the Rio Grande, and partially discharges into the river through seeps and springs. The major recharge area for the aquifer is the intermountain basin formed by the Valles Caldera. The upper parts of the sediments in the basin are lacustrine deposits of clay, sand and gravels. These deposits are underlain by volcanic debris resulting from collapse of the caldera. The sediments and volcanics in the basin are highly permeable and saturated.

LOS ALAMOS, NM

MEAN ANNUAL PRECIP. - 15 inches.  
460 mm.

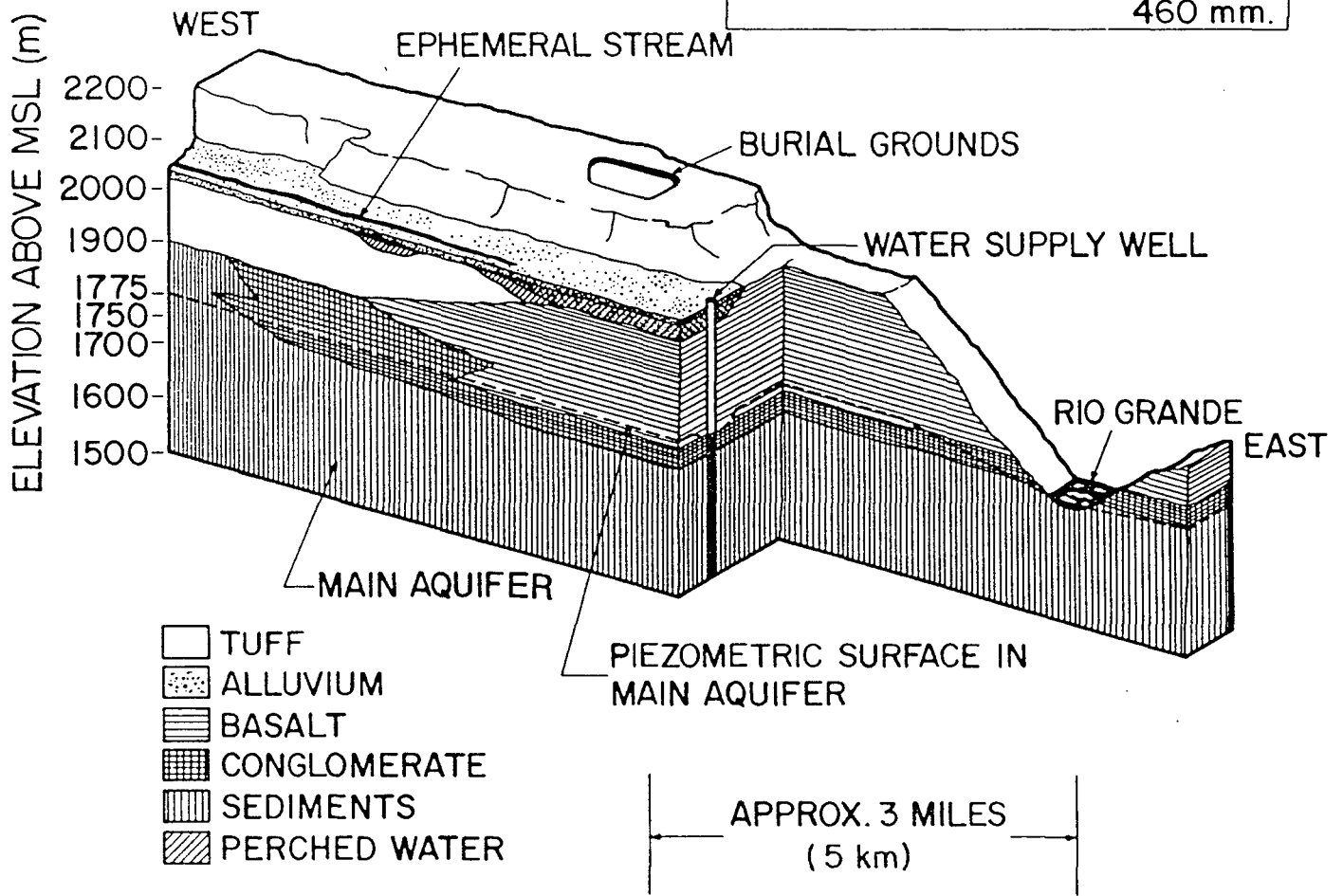


Figure 2.3. Illustration of geologic-hydrologic relationships in the Los Alamos area (LANL, 1987).

Characterization of the hydraulic and chemical properties of the main aquifer is based on information obtained from supply wells, stock wells, test wells and springs. Aquifer tests and pumping from production wells and test holes have enabled the determination of the physical characteristics of the main aquifer (Figure 2.4) (Purtymun, 1984). The physical characteristics of the aquifer will govern the quantity and the rate at which the water will move. The rate of water movement in the geologic formations of the main aquifer is presented as Figure 2.5.

## 2.3 Vadose Zone Conditions

### 2.3.1 General

The term moisture is defined in this report to include both liquid water and water vapor. Moisture flow and storage therefore include the combined flow and storage of liquid water and water vapor. Under partially saturated conditions, water vapor will be present within the pore gas. The pore gas may be regarded as a mixture of air and water vapor. Under most natural conditions, water vapor and liquid water will be in local thermodynamic phase equilibrium within the pore and fracture space. In partially saturated porous media, the equilibrium vapor pressure is a function of both temperature and matric potential and at constant temperature decreases with decreasing saturation. Liquid-water movement in a partially saturated porous media is described using Darcy's law (flux is dependent upon hydraulic gradient, cross-sectional area and a constant of proportionality), whereas water-vapor movement proceeds either as molecular diffusion under a water-vapor concentration gradient or by advection accompanying bulk pore-gas flow.

For this study, degree or percent saturation refers to liquid-water saturation and is defined to be the fractional pore volume or fracture space occupied by liquid water. Degree of saturation and other bulk hydrologic properties are meaningful only when defined as averages over volumes of rock sufficiently large to enclose many pores or fractures (over which the saturation and other bulk hydrologic properties may be taken to be averaged) but yet must be small compared with the overall size of the macroscopic hydrologic system.

Under partially saturated conditions, liquid water is bound to the solid within the pore and fracture openings either by surface-tension (capillary) forces or, at very low saturations, by physical or chemical adsorption. The strength of the bonding force is measured in terms of an equivalent negative pressure, or pressure head, designated as the matric potential.

In a fractured medium, the matric potential within the fractures need not be equal to that within the enclosing rock matrix, although pressure equilibration will tend to be

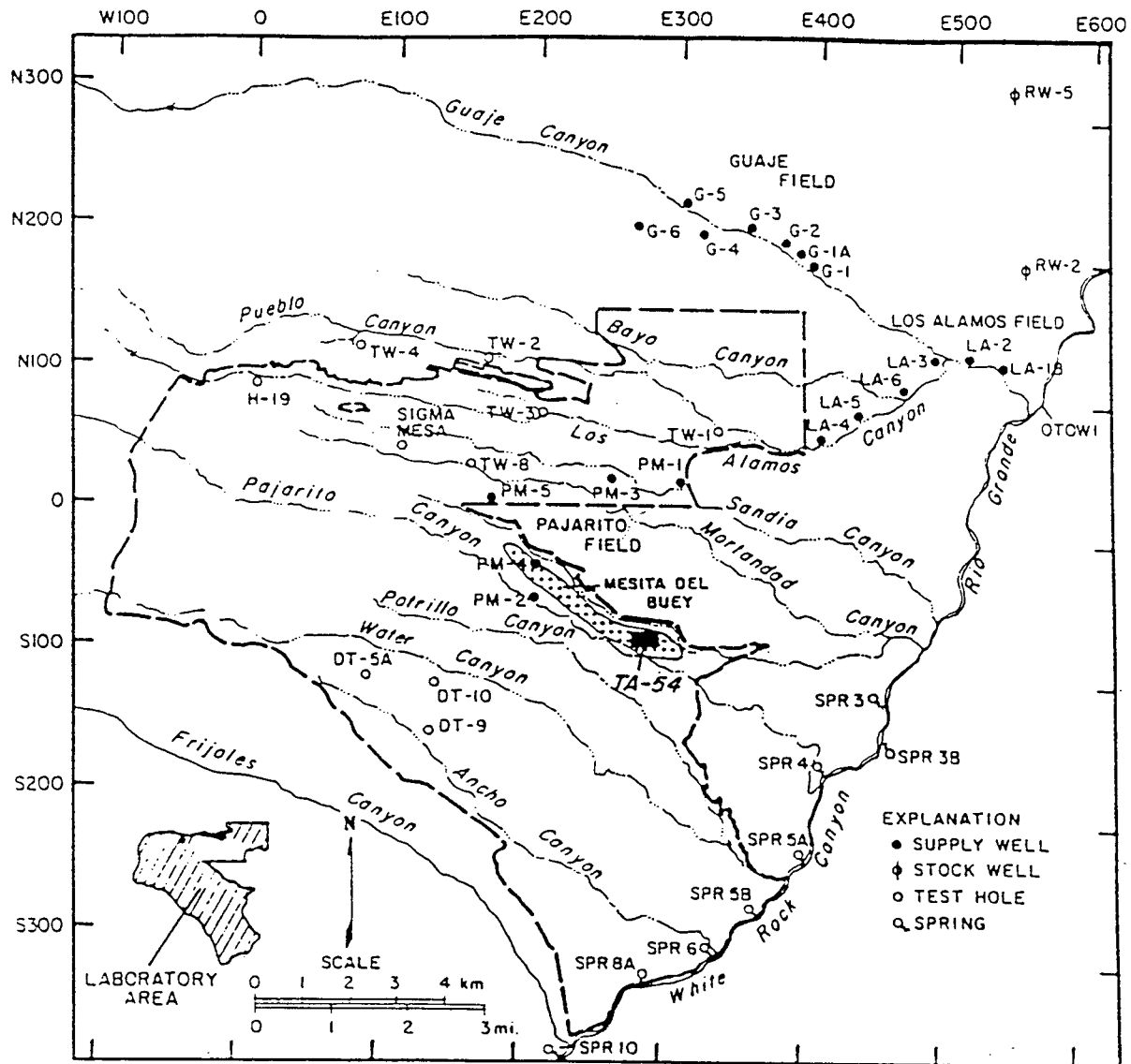


Figure 2.4. Location of supply wells, test wells, stock wells, springs in the Main Aquifer in the Los Alamos Area (Purtymun, 1984).

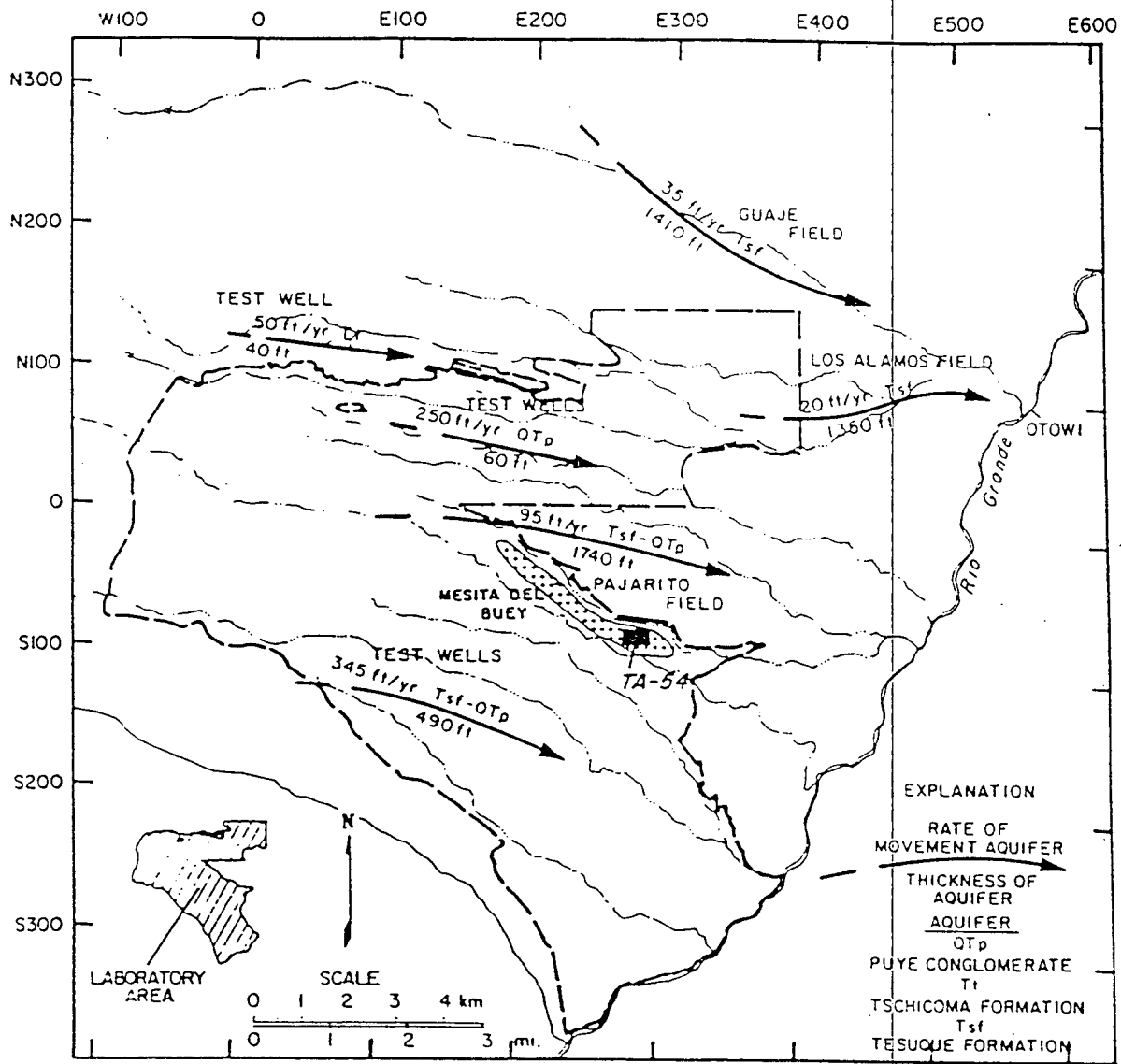


Figure 2.5. Rate of movement of water in the main aquifer in the Los Alamos Area (Purtymun, 1984).

---

established over time. Large differences in matric potential between rock matrix and fractures may occur under transient conditions, and thus may affect moisture movement under such conditions.

Matric potential is a function of liquid-water saturation. An analytic or graphical representation of the functional relationship defines the moisture-retention curve for the porous medium. Moisture-retention curves for most media are not unique; they display hysteresis in which the precise relation between matric potential and saturation depends on the wetting and drying history of the medium.

Standard techniques, using mercury intrusion, pressure-plate apparatus, thermocouple psychrometers, and centrifuges are developed to measure the moisture-retention curves for small soil or rock samples. However, there are few, if any, reliable means of measuring the moisture-retention capacity of discrete fractures.

Depending on the representative linear pore dimensions relative to the representative fracture spacings, a considerable difference may exist between the scale of (1) the bulk-rock volume appropriate for defining the rock-matrix hydrologic properties, which are averaged over the pore space, and (2) the volume containing many fractures that is required to define the bulk properties for the fractures. Under these conditions, the pores and fractures may define two overlapping continuum systems, each regarded as equivalent porous media. Such a double-porosity model may be appropriate, for example, to describe a highly fractured but otherwise homogeneous tuff in which the fractures bound distinct matrix blocks. At the opposite extreme, the fracture density may be so low that bulk fracture properties cannot be defined meaningfully, in which case the fractures that are present would have to be regarded as discrete entities. At this time, there is not enough information pertaining to which fracture-matrix relationships most accurately describe the system at MDA T. The Pathway Analysis followed a continuum approach with the properties of the matrix dominating the system.

The vector volumetric flux of liquid water moving under isothermal and iso-osmotic conditions through a partially saturated, natural hydrogeologic unit, regarded as an equivalent porous-medium continuum system, is determined by the spatial gradients of matric and gravitational potentials and by the hydrologic properties. This functional dependence is expressed mathematically by Darcy's law for unsaturated liquid-flow.

The moisture-retention curve together with the relationship between relative hydraulic conductivity and saturation or, equivalently, matric potential, constitute the set of moisture-characteristic relations for a particular porous medium under partially saturated conditions.

In addition to the storage and transport of moisture as liquid water within the unsaturated zone, moisture may be stored and transported as water vapor within the air-filled pore space. The bulk flow of air in pores and fractures is usually regarded to be Darcian in which the potential gradients are determined by the local pore-gas pressure.

---

---

### 2.3.2 Hydrologic and Transport Properties

A fair amount of information is available on the hydrologic properties of the rocks in the vicinity of Los Alamos (Abeelee, 1979, 1981, 1984, 1986). However, very little research has been performed investigating the transport properties of the rocks. Estimates of distribution coefficients and other rock transport properties are presented in the section on sensitivity analysis (Section 5.2).

### 2.3.3 Climatology

Maximum temperatures are generally below 32°C, with the extreme recorded at 35°C (Abeelee and others, 1981). A large diurnal variation keeps summer nocturnal temperatures in the 12° to 15°C range. Winter temperatures are typically in the range of -10°C to 5°C, with the extreme recorded at -28°C. The average relative humidity is 40%, ranging from 30% in May and June to above 50% in July, January, and February. The mean annual precipitation for Los Alamos is 457 mm (Abeelee and others, 1981).

## 2.4 Waste Characteristics

### 2.4.1 General

Records pertaining to the volume, type and quantity of wastes disposed at MDA T have deficiencies and in some cases are nonexistent. Nonetheless, the available data were reviewed and compiled to enable a historical reconstruction to be used as input into the pathway analysis. Currently, archive searches and interviews are being conducted to better define the composition and quantity of waste stream input into the four absorption beds.

### 2.4.2 Radionuclide Releases to Material Disposal Area T

Material Disposal Area T (MDA T) was one of the first disposal areas used at LANL (Rogers, 1977). Untreated wastes from the processing of plutonium were released to the pits from 1945 to 1952 (Rogers, 1977). In 1952 a waste disposal treatment plant (DP-West/Building 35) was installed to remove plutonium and other radionuclides because the tuff had become clogged with suspended solids. The completion and operation of the treatment plant resulted in a sharp drop in concentrations of radionuclides being released to the absorption beds (Table 2.1). Furthermore, when the quantity of wastes discharged to the absorption beds had reached the order of several thousand gallons per day, the beds had to be abandoned (Rogers, 1977).

---

Table 2.1. On-site estimates of radioactivity to absorption beds<sup>1</sup>  
(covered seepage pits, Area T and Area V).

---

Year	Plutonium Ci
1945	1.4035
1946	1.4035
1947	1.4035
1948	1.4035
1949	1.4035
1950	1.4035
1951	1.4035
1952	0.0035
1953	0.0035
1954	0.0035
1955	0.0035
1956	0.0035
1957	0.0035
1958	0.0035
1959	0.0035
1960	0.0035
1961	0.0035
TOTAL	9.8595

<sup>1</sup> Area T beds were operated through 1951, Area V beds through 1961. Most of the plutonium was <sup>239</sup>Pu, but analyses were not performed to determine specific isotopes. Data are estimated (Christenson, 1973).

---

At infrequent intervals, slugs consisting of a few hundred gallons each of treated wastes were released from DP-West to the absorption beds from 1952 until 1967 (Rogers, 1977). From 1965 through 1967, absorption beds 1 and 2 also received radioactive wastes from Disposal Treatment Plant-East (Table 2.2). A new treatment plant was built which eliminated liquid waste discharged to the absorption beds in 1968 (Rogers, 1977).

#### 2.4.2.1 Method of Disposal

The configuration of the four absorption beds is presented in Figure 2.6. Each bed is 36.6 m long, 6.1 m wide, and about 1.2 m deep. The east and west sides of the beds are sloped so that only the center 30.5 m of each bed has a depth of 1.2 m. The original surface of the site sloped to the north at 12 to 1 (Rogers, 1977). The distance between the centers of beds 1 and 3 and beds 2 and 4 is 24.4 m (Rogers, 1977).

The beds were filled with stone, gravel, sand and earth. To form a deck for the gravel the stone was graded from large at the bottom to small at the top. Sand was placed over the gravel. The top layer of fill was earth (Rogers, 1977).

Liquid wastes moved through a 15.2-cm iron pipe from DP West Buildings 2, 3, 4, and 5 to a concrete distribution box between beds 1 and 2. The distribution box was 1.2 m long, 0.9 m wide, and 1.2 m deep with 15.2-cm walls (Rogers, 1977).

Wastes were probably diverted into either bed 1 or bed 2 instead of allowing the waste to flow to both (Rogers, 1977). The floor drain from Filter Building 12, TA-21-12, emptied into a 15.2 cm iron pipe leading into bed 1. Overflow pipes of 15.2 cm iron connect beds 1 and 3 and beds 2 and 4. The overflow pipes are positioned in beds 1 and 2 at the top of the stone layer and in beds 3 and 4 at the bottom (Rogers, 1977).

"Reportedly more water [liquid wastes] moved into pits [Beds] 1 and 3 than moved into 2 and 4, and at times some of the pits became clogged and overflowed, the overflow moving northward toward a canyon" (Rogers, 1977).

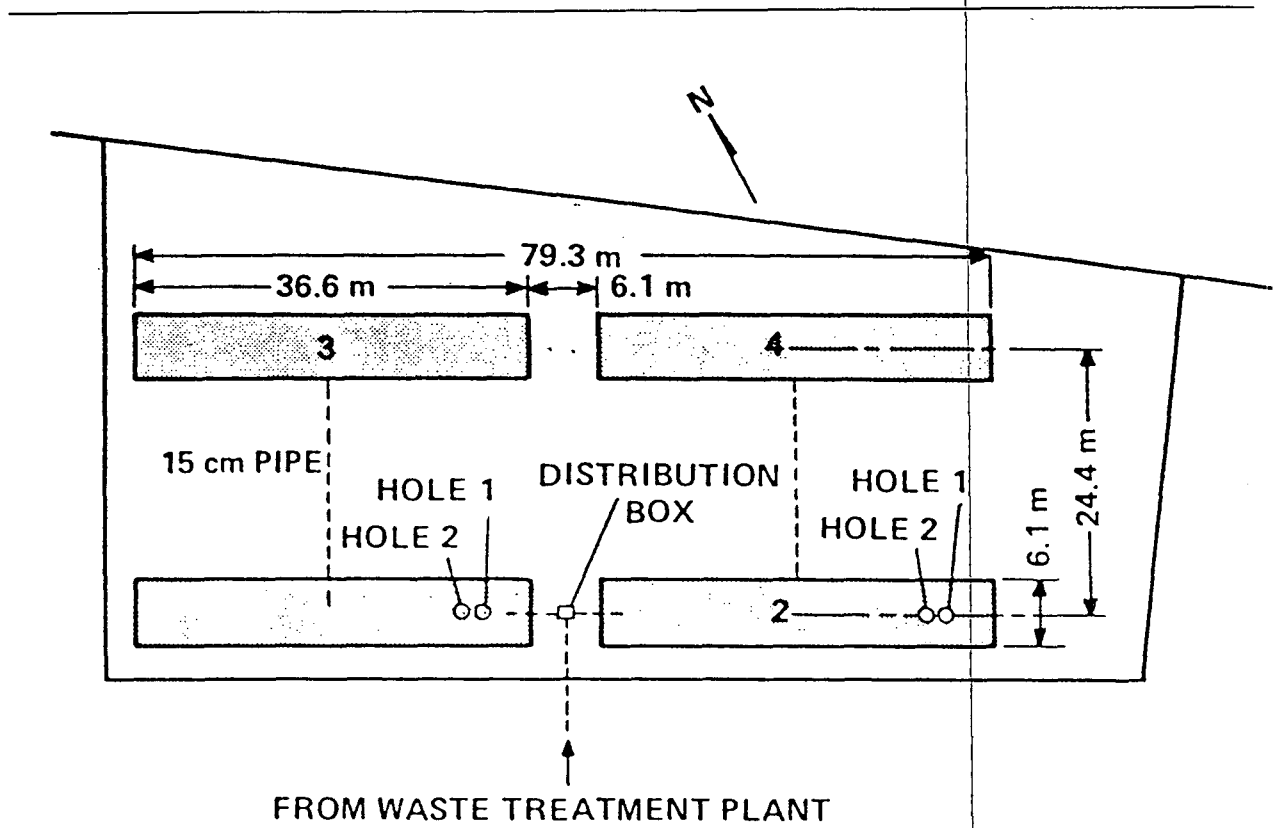
#### 2.4.2.2 Contamination Volumes

The amount of untreated waste released into the absorption beds during the period 1945 to 1952 was reported to be approximately 53,000 m<sup>3</sup> (Table 2.3) (Rogers, 1977). During this time it is estimated that the concentration of plutonium was 120 dis/min/ml with an average fluoride concentration of 160 ppm. In addition, 39.6 m<sup>3</sup> of effluent, with high concentrations of ammonium citrate, was released to the beds from June 1951 to July 1952. The plutonium concentration in this waste averaged about 14,000 dis/min/ml, while fluoride concentrations were about 200 ppm (Rogers, 1977).

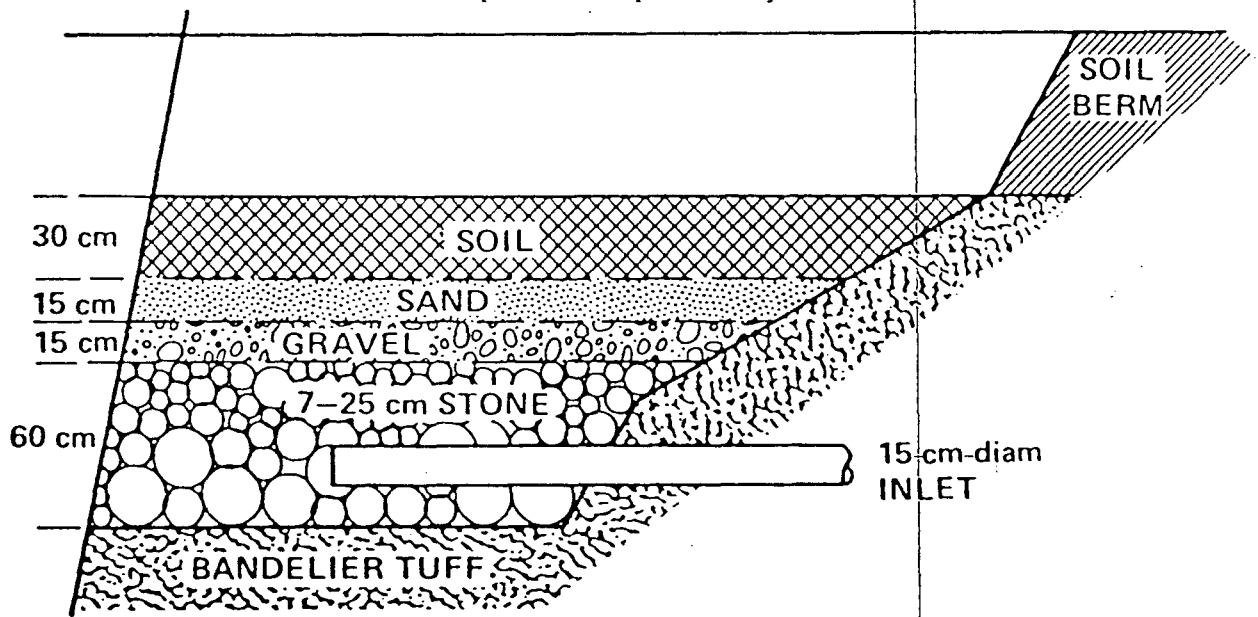
Table 2.2. Reported volumes of wastes discharged to Area T absorption beds (in cubic meters).

Year	From DPE	From DPW	Year	From DPE	From DPW
1945	0	3,000 (est)	1966	4,355	0
1946	0	4,000 (est)	1967	666	0
1947	0	5,000 (est)	1968	0	0
1948	0	6,000 (est)	1969	0	0
1949	0	5,971	1970	0	0
1950	0	10,030	1971	0	0
1951	0	13,600	1972	0	0
1952	0	5,400	1973	0	0
1953	0	822			
1954	0	206			
1955	0	1,389			
1956	0	1,970			
1957	0	1,587			
1958	0	657			
1959	0	731			
1960	0	750			
1961	0	117			
1962	0	51			
1963	0	230			
1964	0	98			
1965	2,492	137			

Compiled by L.A. Emelity, H-7, May 1974.



a. Site plan of absorption bed system.



b. Cross section of an absorption bed.

Figure 2.6. Design of absorption beds at Area T.

---

Table 2.3. Historical Pu-239 releases to MDA T (Rogers, 1977).

---

Time duration	Effluent Volume (m <sup>3</sup> )	Plutonium Concentration (dis/min/ml)
1945-1952	53,000	120
June 1951- July 1952	40	14,000
1953-1967	16,000	0.2

---

---

### 3.0 PATHWAY ANALYSIS MODELS

#### 3.1 Initial Conceptual Model

The hydrogeologic system in the vicinity of the site appears to be controlled by interrelated hydraulic properties and processes which, most likely, are complex and vary widely in space, has boundary conditions with irregular geometries, and has inputs and outputs that vary in space and time.

Mathematical models may be used effectively to quantify physical systems, provided the limitations and uncertainties of the models are reasonably well understood.

Before starting the pathway analysis it was important to select a computer code(s) that would satisfactorily handle the initial and boundary conditions. These conditions at MDA T are particularly difficult to simulate due to the numerical instabilities caused by the large volumes of liquid introduced into a very dry system. The selection of the computer codes was relatively easy because there are few codes that can accommodate the numerical difficulties posed by the addition of large pulses into a very dry system.

#### 3.2 Rationale for Code Selection

Two numerical codes, HYDRUS (Kool, 1987) and SOILSIM (Huyakorn, 1989), were chosen to simulate variably-saturated flow and transport under conditions at MDA T.

HYDRUS and SOILSIM are both finite element codes for simulating water flow and solute transport under transient variably saturated conditions. HYDRUS simulates vertical (one-dimensional) flow and transport and SOILSIM can perform two-dimensional cross-sectional, areal or axisymmetric problems. The two codes were selected for this investigation because of their demonstrated ability and numerical efficiency in simulating highly non-linear, transient variably saturated flow and contaminant transport problems. The use of both one and two dimensional codes permits evaluation of both the importance of multi-dimensional flow and transport as well as the use of an efficient one-dimensional code for sensitivity analysis.

SOILSIM is a finite element code that is based on the VAM2D code (descendant of SATURN). Differences between SOILSIM over VAM2D are discussed in Section 3.4.2. These differences do not affect the simulations performed for the pathway analysis.

### 3.2.1 HYDRUS (one dimensional)

#### General Features

HYDRUS (Kool, 1987) is a modification of the program WORM, developed by M. van Genuchten at the United States Department of Agriculture-Agricultural Research Service (USDA-ARS) Salinity Lab. Enhancements incorporated in HYDRUS include the ability to simulate the effects of hysteresis in the water retention characteristic on flow and transport, automatic mass balance computation, and expanded capabilities for handling varying transient boundary conditions. During flow simulations performed for the pathway analysis, it was discovered that due to the manner in which the storage coefficients were computed in HYDRUS, sometimes appreciable mass balance errors would occur. The code was modified using the procedure described by Milly (1985) to correct this problem. This correction has since also been implemented in the original WORM code (M.Th. van Genuchten, personal communication).

HYDRUS solves the one-dimensional Richard's equation for vertical water flow, and the advection-dispersion equation for solute transport.

#### 1-D Flow Equation (HYDRUS)

$$\frac{\partial}{\partial z} [K k_r \left( \frac{\partial \psi}{\partial z} - 1 \right)] = C \frac{\partial \psi}{\partial t} \quad (1)$$

where  $\psi$  is pressure head (L),  $K$  is the saturated hydraulic conductivity (L/T),  $k_r$  is the relative hydraulic conductivity (Dimensionless),  $C$  is the storage coefficient (1/L),  $z$  is vertical distance taken to be positive downward (L), and  $t$  is time (T). The coefficient  $C$  is defined as

$$C = S_w S_s + \phi \frac{dS_w}{d\psi} \quad (2)$$

where  $S_w$  is the water saturation (Dimensionless),  $S_s$  is the coefficient of specific storage (1/L), and  $\phi$  is the porosity (Dimensionless).

---

### 1-D Transport Equation (HYDRUS)

$$\frac{\partial}{\partial z} \left( D \frac{\partial c}{\partial z} \right) - V \frac{\partial c}{\partial z} = \theta \left( R \frac{\partial c}{\partial t} + \lambda c \right) \quad (3)$$

where  $c$  is the solute concentration ( $M/L^3$ ),  $D$  is the dispersion coefficient ( $L^2/T$ ),  $V$  is the Darcy velocity ( $L/T$ ),  $R$  is the retardation coefficient (Dimensionless),  $\theta = \phi S_w$  is the volumetric water content, and  $\lambda$  is the first-order decay coefficient ( $1/T$ ). The dispersion coefficient is defined as

$$D = \alpha_L V + \theta D_o \quad (4)$$

where  $\alpha_L$  is the dispersivity ( $L$ ) and  $D_o$  is the effective molecular diffusion coefficient ( $L^2/T$ ).

The retardation coefficient  $R$  is defined as

$$R = 1 + \frac{\rho k_d}{\theta} \quad (5)$$

where  $\rho$  and  $k_d$  are the bulk density and distribution coefficient, respectively.

The governing flow equation is solved using a fully implicit, mass-lumped Galerkin finite element formulation with optional upstream weighting of the relative conductivity. The evaluation of storage coefficients in HYDRUS has recently been revised to ensure a mass-conservative formulation. This new formulation results in mass-balance errors of typically less than 0.5 percent. The solute transport equation is solved using an implicit Galerkin solution to the classical advection-dispersion equation. The solution allows for linear equilibrium adsorption and first-order decay reactions. The solution incorporates an automatic correction of the dispersion coefficient for numerical dispersion.

---

### 3.2.1.1 Assumptions of HYDRUS

HYDRUS contains both flow and single species solute transport models. The code can perform variably saturated analysis using pressure head as the dependent variable. Major assumptions of the flow model are:

- Flow of the fluid phase is considered isothermal and governed by Darcy's law;
- Vapor-phase water flow is negligible;
- The fluid is considered slightly compressible and homogeneous;
- The fractured rock is treated as an equivalent porous medium;
- For variably saturated flow analysis, hysteresis effects in the constitutive relationships of relative permeability versus saturation, and saturation versus pressure head are allowed.

Major assumptions of the solute transport model are:

- Hydrodynamic dispersion and molecular diffusion in the porous medium system are governed by Fick's law. The hydrodynamic dispersion coefficient is defined as the sum of the coefficients of mechanical dispersion and molecular diffusion. The medium dispersivity is assumed to correspond to that of an isotropic porous medium and hence related to longitudinal dispersivity;
- Adsorption and decay of the solute are described by a linear equilibrium isotherm and a first order decay constant, respectively.

### 3.2.1.2 Limitations of HYDRUS

- In performing a variably saturated flow analysis, the code handles only one dimensional single-phase flow (liquid water) and ignores the flow of the second phase (water vapor and air) which, in some instances, can be significant;
- Flow and transport in fractures are not explicitly simulated;
- The code simulates only transport of a single species solute and does not simulate chain reactions;

- The code does not take into account kinetic sorption effects or other chemical reactions which, in some instances, can be important;
- The code accounts for only one dimension of flow and transport; if significant flow components occur in the second and third dimensions, significant simulation errors could result.

### 3.2.2 SOILSIM (two dimensional)

#### General Features

SOILSIM (Huyakorn, 1989) uses a Galerkin finite element solution to the two-dimensional Richard's equation for variably saturated flow. The code can use either fully implicit or Crank-Nicholson approximations of the time derivatives, and mass-lumping of the storage matrix.

#### Governing Flow Equation

$$\frac{\partial}{\partial x_i} [K_{ij} k_r \left( \frac{\partial \psi}{\partial x_j} + 1 \right)] = c \frac{\partial \psi}{\partial t} \quad (6)$$

where  $K_{ij}$  is the saturated hydraulic conductivity tensor and  $x_i$  ( $i = 1,2$ ) are spatial coordinates, where  $x_1$  is the horizontal direction and  $x_2$  is the vertical direction which is taken as positive upwards, and the remaining terms are as defined previously.

#### 2-D Transport Equation

$$\frac{\partial}{\partial x_i} \left( D_{ij} \frac{\partial c}{\partial x_j} \right) - v_i \frac{\partial c}{\partial x_i} = \phi S_w R \left( \frac{\partial c}{\partial t} + \lambda c \right) \quad (7)$$

where  $D_{ij}$  is the dispersion tensor, with elements defined by

$$D_{11} = \frac{\alpha_L (v_1)^2}{|v|} + \frac{\alpha_T (v_2)^2}{|v|} + D_o \quad (8a)$$

$$D_{22} = \frac{\alpha_L (V_2)^2}{|V|} + \frac{\alpha_T (V_1)^2}{|V|} + D_o \quad (8b)$$

$$D_{12} = D_{21} = (\alpha_L - \alpha_T) \frac{V_1 V_2}{|V|} \quad (8c)$$

where  $\alpha_L$  and  $\alpha_T$  are longitudinal and transverse dispersivities, respectively.

The solute transport equation is solved by the upstream weighted residual finite element method designed to circumvent oscillations and negative concentrations. Solute movement may include linear equilibrium adsorption and first order decay reactions.

### 3.2.2.1 Assumptions in SOILSIM

SOILSIM contains both flow and single species solute transport models. The code can perform two types of flow analysis: (1) variably saturated analysis using pressure head as the dependent variable, and (2) fully saturated confined or unconfined groundwater analysis using hydraulic head as the dependent variable. Major assumptions of the flow model are:

- Flow of the fluid phase is considered isothermal and governed by Darcy's law;
- Vapor-phase water flow is negligible;
- The fluid considered is slightly compressible and homogeneous;
- The fractured rock can be treated as an equivalent porous medium;
- For variably saturated flow analysis, hysteresis effects in the constitutive relationships of relative permeability versus saturation, and saturation versus pressure head are assumed to be negligible;
- For areal unconfined saturated flow below the water table, vertical flow components and seepage faces are assumed to be negligible.

---

Major assumptions of the solute transport model are:

- Hydrodynamic dispersion and molecular diffusion in the porous medium system are governed by Fick's law. The hydrodynamic dispersion coefficient is defined as the sum of the coefficients of mechanical dispersion and molecular diffusion. The medium dispersivity is assumed to correspond to that of an isotropic porous medium and hence related to two constants, the longitudinal and transverse dispersivities;
- Adsorption and decay of the solute is described by the linear equilibrium isotherm and a first order decay constant.

#### 3.2.2.2 Limitations of SOILSIM

- In performing a variably saturated flow analysis, the code handles only single-phase flow (liquid water) and ignores the flow of the second phase (water vapor and air) which, in some instances, can be significant;
- In performing an areal unconfined saturated flow analysis, the presence of seepage faces is neglected and the simplified Boussinesq equation is used;
- Flow and transport in fractures is not explicitly taken into account;
- The code simulates only transport of a single species solute and does not simulate daughter products;
- The code does not consider kinetic sorption effects or other chemical reactions which, in some instances, can be important;
- The code accounts for only two dimensional flow and transport, and if significant flow components occur in the third dimension, significant simulation errors could result.

### 3.3 Numerical Accuracy

The accuracy of numerical approximations of time-dependent partial differential equations depends on the size of the nodal or grid spacings and time increments employed as well as other numerical factors. The variably saturated flow equation, particularly for infiltration problems with very dry initial conditions, is highly non-linear. Even with robust and efficient codes, convergence difficulties may be encountered unless sufficiently fine spatial and temporal resolutions are used. These requirements make a significant contribution to the overall computational costs of performing variably

---

saturated flow simulations. The solute transport equation in contrast, is a linear equation, and is thus free of convergence problems. On the other hand spurious solutions exhibiting excessive oscillations and numerical dispersion may be obtained unless the grid spacings and time step sizes are selected carefully so they are consistent with the magnitude of the dispersivity coefficients and flow velocities. For the pathway analysis time intervals and grid spacings were carefully selected to avoid numerical instabilities in the flow and transport solutions.

Once the flow equation has been adequately solved for the specific conditions, it is generally a straightforward process to establish the appropriate time and spatial discretization to obtain accurate solute transport solutions.

The temporal and spatial discretization criteria for accurate transport simulation results are represented by the Courant and Peclet numbers (Huyakorn and Pinder, 1983). In general, numerical oscillations in the computed concentration distribution do not occur if the grid size is chosen such that the local Peclet number does not exceed 2 or 3. If an upstream weighted transport solution is employed (as in SOILSIM/VAM2D) oscillations are suppressed even when the local Peclet number is as high as 10.

The methods employed for discretization of the problem domain and the selection of the time stepping-scheme are discussed in Sections 4.2.6 and 4.2.7, respectively.

### 3.4 Regulatory Acceptance

#### 3.4.1 HYDRUS

As mentioned, HYDRUS (Kool, 1987) is a descendent of the code WORM, which has been developed by the US Department of Agriculture. Both WORM and HYDRUS are publicly available. WORM is currently used by the State of Texas in site evaluation studies for low level nuclear waste disposal. HYDRUS is currently used in a joint project between the New Mexico Institute of Mining and Technology and HydroGeoLogic involving characterization of tracer migration through Yucca Mountain tuffs. This project involves documentation and use of HYDRUS under NNWSI-USGS Quality Level I QA requirements.

#### 3.4.2 SOILSIM

SOILSIM (Huyakorn, 1989) is among the most robust and full featured codes available for simulation of multi-dimensional variably saturated flow and transport. An enhanced version of SOILSIM, called VAM2D, has been adopted by the US NRC for performance assessment studies of low level nuclear waste facilities. The VAM2D code is published by the NRC as NUREG/CR-5352. VAM2D is also currently being used by both the US NRC and Sandia National Laboratory for modeling studies under the international

---

INTRAVAL model validation program. SOILSIM has been purchased by the State of Texas to be used in the review of license applications for unsaturated zone waste disposal facilities. Differences between VAM2D and SOILSIM are that VAM2D has ability to simulate effects of hysteresis and saturation dependent anisotropy and can handle chain decay reactions for multispecies transport simulations. Apart from this, the codes are identical.

---

## 4.0 MODEL APPLICATION

### 4.1 General

Before performing the pathway analysis the information available for MDA T was converted to a form that could be used as model input. Model input was obtained from a general reconstruction of past events that may have had an effect on the hydrogeologic system.

The following expressions have been used in this study to describe the moisture characteristics of the Bandelier tuff

$$\begin{aligned} S_w &= S_{wr} + (1 - S_{wr}) [1 + |\alpha\psi|^\beta]^{-\gamma} & \psi < 0 \\ &= 1 & \psi \geq 0 \end{aligned} \tag{9}$$

$$k_r = \left( \frac{S_w - S_{wr}}{1 - S_{wr}} \right)^n \tag{10}$$

where  $\psi$  is the soil-water pressure head,  $S_w$  is the water saturation,  $S_{wr}$  is the residual saturation,  $k_r$  is the relative hydraulic conductivity and  $\alpha$ ,  $\beta$ ,  $\gamma$  and  $n$  are curve shape parameters. The parameter  $\gamma$  is related to  $\beta$  as  $\gamma = 1 - 1/\beta$ . The expression for water saturation as a function of pressure head given by Eq. (9) is known as the van Genuchten relationship (van Genuchten, 1978). The expression for relative conductivity (Eq. 10) was derived by Brooks and Corey (1964).

The values of residual saturation,  $S_{wr}$ , and the shape parameters  $\alpha$ ,  $\beta$ , and  $n$  in (9) and (10) for the Bandelier tuff were determined by least-squares fitting of observed water retention data. In this procedure the parameters  $S_{wr}$ ,  $\alpha$ , and  $\beta$  are determined by fitting Eq. (9) to experimental  $S_{wr}$ - $\psi$  data. The exponent  $n$  in Eq. (10) is determined similarly by least-squares fitting of the following relationships to the experimental  $S_w$ - $\psi$  data

$$\begin{aligned} S_w(\psi) &= S_{wr} + (1 - S_{wr}) \left[ \frac{\psi_a}{\psi} \right]^m & \psi < \psi_a \\ &= 1 & \psi \geq \psi_a \end{aligned} \tag{11}$$

where  $\psi_a$  is the air-entry pressure and  $m$  is a parameter related to  $n$  as  $n = 3 + 2/m$ .

---

---

The relationship for saturation as a function of pressure head given by (11) is not used in the simulations since it has been found (e.g., van Genuchten and Nielsen, 1985) that the van Genuchten relationship (9) gives a more accurate description of the water retention characteristic of most natural geologic materials. In contrast, the Brooks-Corey conductivity function (10) with parameter  $n$  as determined according to the procedure followed here has been found to predict actual unsaturated hydraulic conductivity reasonably well.

## 4.2 Data Preparation

The data necessary to perform the pathway analysis were largely acquired from published reports. In cases where site-specific data are unavailable, either approximations were made or values were obtained from other sites with similar hydrogeologic conditions (Table 4.1).

### 4.2.1 Input Parameters

For each simulation it was necessary to supply a variety of input parameters. The range of values that are used in the sensitivity and actual simulation runs are listed in Table 4.1.

#### 4.2.1.1 Rock Matrix Properties

Little direct information on matric potentials and moisture fluxes is available for the Bandelier tuff in the vicinity of MDA T. For this pathway analysis, an equivalent porous medium is assumed to represent the combined rock matrix and fracture system. The basis for the determination of the soil matrix properties for this study was largely obtained from Abeele and others (1981).

The saturated hydraulic conductivity of solid tuff has been measured often yielding measurements ranging from  $2 \times 10^{-7}$  m/s to  $4.7 \times 10^{-6}$  m/s when corrected for a temperature of 288°K (Abeele and other, 1981).

In the studies performed by Abeele and others (1981) a saturated hydraulic conductivity of  $2.35 \times 10^{-6}$  m/s was obtained. Unsaturated hydraulic conductivity was not measured. However, Abeele and others (1981) did predict the unsaturated hydraulic conductivity of crushed tuffs from the matric potential-water content relationship (moisture characteristic curve).

Table 4.1. Source and range of model input parameters.

Input Parameter	Range	Source
1. Saturated hydraulic conductivity	6.3-148 m/y	Abeele and others 1981
2. Residual water saturation	.0097	least-squares fit to exp. data (Appendix D)
3. Power index (n) of the relative permeability relationship <sup>1</sup>	3.0-3.69	least-squares versus fit to exp. data (Appendix D)
4. Leading coefficient ( $\alpha$ ) of saturation versus capillary head relationship	.423 m <sup>-1</sup>	least-squares fit to exp. data (Appendix D)
5. Power index ( $\beta$ ) of the saturation versus capillary head relationship	2.217	least-squares fit to exp. data (Appendix D)
6. Porosity	20-40 Percent	Abeele and others, 1981
7. Bulk Density	1280-1840 kg/m <sup>3</sup>	Abeele and others, 1981
8. Dispersivity	1-3.5 m	Probable range <sup>2</sup>
9. Retardation coefficient	5-3000	Estimation from literature review and field data
10. Flux rates	See Table 5.6	
11. Concentration values	See Figure 5.63	

1) To overcome numerical instabilities n was lowered for input into SOILSIM, the effect of this was evaluated during the sensitivity analysis (Section 5.2)

2) Dispersivity is often found to be scale dependent. Empirical evidence suggests that a dispersivity value on the order of 1% of the total travel distance is realistic for field conditions (Gelhar and others, 1985). The total distances in the simulations were 100 and 350 m.

---

The relationship for water saturation versus pressure head used for this problem is presented in Figure 4.1 (Abeele and others, 1981). The curves are based on measured water characteristics curves obtained from crushed Bandelier tuff samples.

#### 4.2.1.2 Physical and Chemical Properties

The majority of the plutonium disposed at MDA T is composed of Pu-239 with a half-life of 24,400 years. A very small amount of Pu-241 was also probably disposed at MDA T. Plutonium-241 has a half-life of 13.2 years and undergoes continuous beta decay to americium-241.

The common weapons-grade plutonium mix manufactured at Los Alamos, is similar to that which was disposed at MDA T and typically contains .4 percent 241-Pu by weight (Nyhan, 1984).

#### 4.2.2 Uncertainty of Input Data

The predictive capability of any numerical model depends on the model assumptions and limitations, the reliability of input data encompassing various physical parameters including relevant coefficients appearing in the governing partial differential equations (granted that the accuracy of the numerical approximation of these equations is adequate). For the problem considered, critical input parameters and their degree of uncertainty are summarized in Table 4.2.

#### 4.2.3 Boundary Conditions

Boundary conditions are a set of conditions in mathematical terms that serve to tie the modeled domain into the surrounding physical framework. The different types of boundary conditions are:

- prescribed transient or steady-state head (pressure) for surfaces bounding the flow region (Dirichlet conditions);
- prescribed transient or steady-state flow is known across surfaces bounding the region (Neumann conditions);
- transient or steady-state solute flux is known across surfaces bounding the region (Robbins conditions).

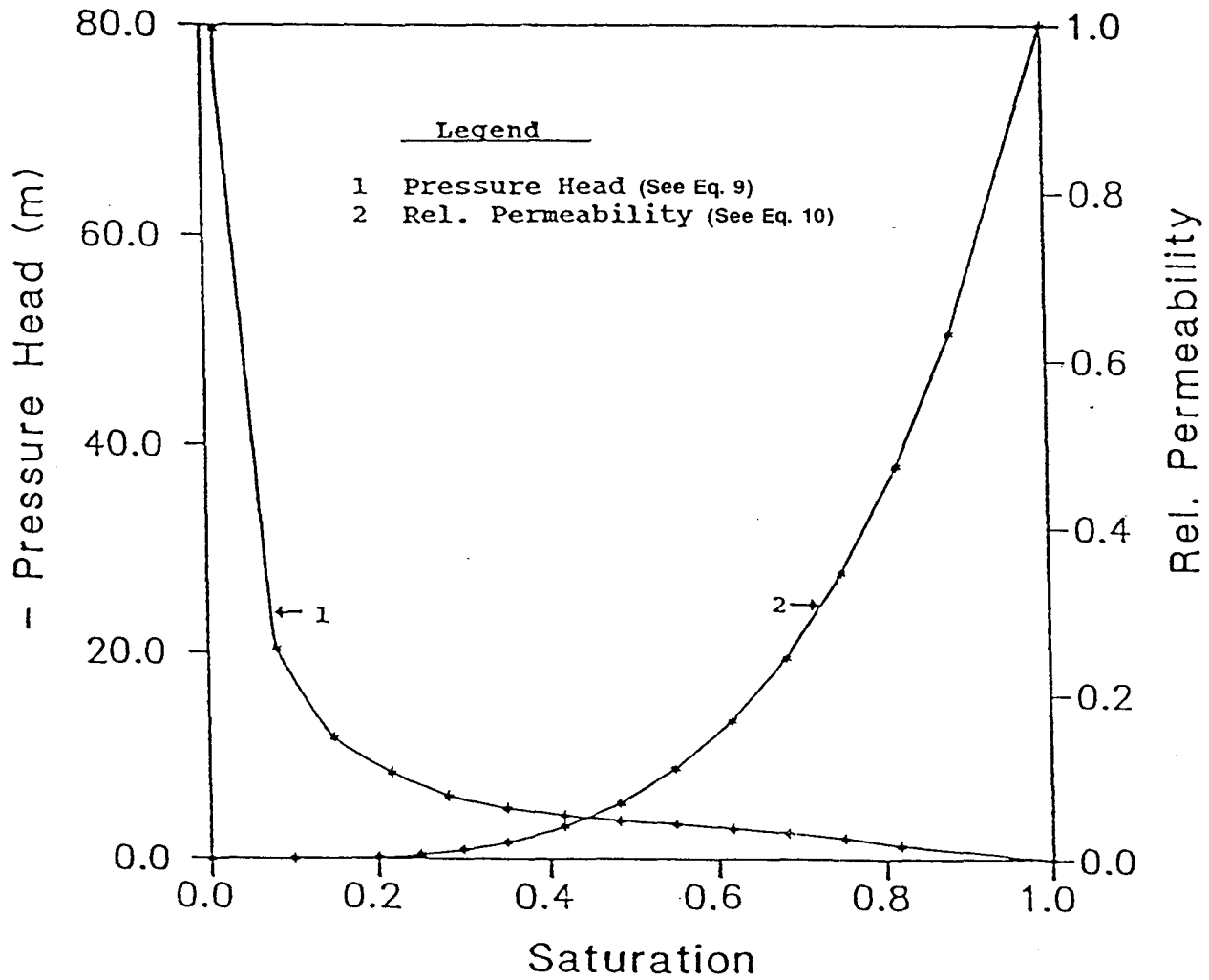


Figure 4.1. Relationships for water saturation versus pressure head, and relative permeability versus saturation.

Table 4.2. Input parameter relative uncertainties.

Input Parameter

1. Saturated hydraulic conductivity

Although saturated hydraulic conductivity (K) has been measured on tuffs in the vicinity of the site, no measurements are available at MDA T. Therefore, there is still a relatively high degree of uncertainty associated with this parameter.

2. Residual water saturation

Properties of the moisture characteristic curves have been estimated through the van Genuchten analysis which relates the physical properties of the rock to the water saturation characteristics. The degree of relative uncertainty associated with these estimates is not known, but is probably less than other major uncertainties.

3. Power index (n) of the relative permeability versus saturation relationship

Properties of the moisture characteristic curves have been estimated through the van Genuchten analysis. The degree of relative uncertainty associated with these estimates is not known, but is probably less than other major uncertainties.

4. Leading coefficient ( $\alpha$ ) of the saturation versus capillary head relationship

Properties of the moisture characteristic curves have been estimated through the van Genuchten analysis. The degree of relative uncertainty associated with these estimates is not known, but is probably less than other major uncertainties.

5. Leading coefficient ( $\beta$ ) of the saturation versus capillary head relationship

Properties of the moisture characteristic curves have been estimated through the van Genuchten analysis. The degree of relative uncertainty associated with these estimates is not known, but is probably less than other major uncertainties.

---

Table 4.2. Continued.

---

Input Parameter

---

6. Porosity and Bulk Density

Lab measurements of porosity and bulk density of tuffs collected from the general vicinity of the site are available. Measured ranges indicate that unless site specific data are collected there will remain a relatively high degree of uncertainty. However, the impact on flow and transport predictions is much less than that of uncertainties in K, material and boundary conditions.

7. Dispersivity

No field or laboratory information is available on dispersivity values. A range of values consistent with the hydrogeologic framework was selected (1.0 - 3.5 m). The effect of uncertainties associated with this parameter are relatively insignificant.

8. Retardation Coefficient

No field or laboratory information is available. A wide range of values considered to be characteristic of rocks/contaminants are investigated during the sensitivity analysis. Uncertainties associated with this parameter can have major impacts on simulated solvent transport results.

9. Waste Discharge Rates

Waste discharge rates are estimated from historical records that are considered to be relatively complete. Although total discharges are known on a year to year basis, the exact temporal variation, and the partitioning between individual disposal beds are not known.

10. Concentration Values

The concentrations of radionuclides entering the absorption beds are taken from measurements and estimates made at different times. These records are incomplete.

---

#### 4.2.3.1 HYDRUS

The upper boundary conditions are set as specified surface fluxes. The flux consists of ambient recharge plus the volume of water added to bed 1 from 1945 through 1967. Because HYDRUS is one dimensional the side boundaries must be no-flow (zero flux).

The lower boundary was varied depending on whether the simulations were performed with the coarse grid or fine grid (Section 4.2.6). In simulations performed with the coarse grid, the modeled domain extended to the water table and therefore the boundary condition was set as a zero pressure head. The modeled domain discretized by the fine grid covered only the upper 100 m of the system (which did not include the water table) and therefore the lower boundary was specified as a zero pressure head gradient. This type of boundary condition is consistent with a freely draining boundary and allows both the pressure head and flux to change in response to surface water applications.

#### 4.2.3.2 SOILSIM

The boundary conditions for SOILSIM are specified as follows:

- Disposal bed 1 - transient flux boundaries;
- Land surface - steady flux boundaries;
- Water table surface - steady Dirichlet boundaries;
- Pipe leak (when applicable) - steady Dirichlet boundaries;
- Lateral boundaries - zero flux boundaries.

#### 4.2.4 Initial Conditions

Vadose zone moisture flow at steady state may be simulated if the boundary conditions are known and do not change with time. For nonsteady-state conditions, boundary conditions in addition to a meaningful set of initial head (pressure) values must be supplied at the start of the simulation.

#### 4.2.4.1 HYDRUS

To provide initial conditions for HYDRUS, moisture release curves were used in conjunction with estimated recharge rates to match measured saturations at depth. Abeele (1981) reports that "moisture monitoring by means of a neutron moisture probe indicates that at depths exceeding 10 m the tuff rarely exceeds 10% of saturation."

---

Therefore, the initial saturation profile was estimated during Scenario II.1 (Section 5.5.2.1) to approximate 10 percent saturation.

#### 4.2.4.2 SOILSIM

The initial conditions for SOILSIM are identical to those specified for HYDRUS, except for the addition of the second dimension.

#### 4.2.5 Time Dependent Input Data

For the pathway analysis the only input parameters that were varied with time were radionuclide concentrations and volumes of fluid applied to absorption bed 1. Precipitation and evapotranspiration rates were accounted for by estimating effective recharge (precipitation less evapotranspiration) using ambient saturations and moisture release curves (Section 5.5.1).

##### 4.2.5.1 Waste Discharge

Estimates of total fluid discharged to MDA T absorption beds is presented in Column 2 (Table 4.3). It is assumed that 55 percent of the total volume of wastes discharged to MDA T was applied to bed 1. In addition to the estimated volume of wastes applied to bed 1 between 1945 and 1967 a known quantity of waste and water were applied in 1960 and 1961 (Table 4.3). The earth and sand cap over the absorption beds would have severely limited the evaporation of water from the beds (Figure 2.6). Therefore, evaporation was not considered an important factor in the flux approximation.

Rogers (1977) states that "Reportedly more water [liquid wastes] moved into beds 1 and 3 than moved into 2 and 4, and at times some of the pits became clogged and overflowed, the overflow moving northward toward a canyon. However, overflow from the beds never reached the canyon." The canyon is roughly 100 m from disposal beds 1 and 2 and approximately 75 m from disposal beds 3 and 4.

##### 4.2.5.1.1 HYDRUS

The one-dimensional analysis performed with HYDRUS used input fluxes directly from the far right column Table 4.3, after correcting for the area of application (dimensions of bed 1).

Table 4.3. Flux input to absorption bed 1.

Year	Estimated volumetric flux from DPE & DPW (m <sup>3</sup> /y)	55% of total flux (m <sup>3</sup> )	Linear flux <sup>1</sup> (m/y)	Ambient recharge (m/y)	Flux input to model (m/y)
1944	--	--	--	--	--
1945	3,000	1,650	7.39	.00254	7.39
1946	4,000	2,200	9.85	.00254	9.86
1947	5,000	2,750	12.30	.00254	12.30
1948	6,000	3,300	14.78	.00254	14.80
1949	5,971	3,284	14.70	.00254	14.70
1950	10,030	3,517	24.70	.00254	24.70
1951	13,600	7,480	33.50	.00254	33.50
1952	5,400	2,970	13.30	.00254	13.30
1953	822	452	2.02	.00254	2.03
1954	206	113	.506	.00254	.51
1955	1,389	764	3.40	.00254	3.40
1956	1,970	1,023	4.85	.00254	4.86
1957	1,587	873	3.91	.00254	3.91
1958	657	361	1.61	.00254	1.62
1959	731	402	1.80	.00254	1.80
1960	750	413	1.84	.00254	1.85 <sup>2</sup>
1961	117	64	.28	.00254	.29 <sup>2</sup>
1962	51	28	.125	.00254	.128
1963	230	127	.569	.00254	.569
1964	98	54	.24	.00254	.244
1965	2,629	1,446	6.47	.00254	6.48
1966	4,355	2,394	10.70	.00254	10.70
1967	666	366	1.63	.00254	1.64
1968	--	--	--	--	--

<sup>1</sup>Area of bed 1 is 223.26 m<sup>2</sup>

<sup>2</sup>Water added by Christenson (1961) has not been included

---

#### 4.2.5.1.2 SOILSIM

To overcome large numerical instabilities that were encountered during initial simulation runs with SOILSIM, a linearly time-varying approximation was adopted for the surface flux boundary condition (Figures 4.2 and 4.3). Whereas the relationship between loading rate and time used in the HYDRUS simulations can be represented by a histogram, a linearly varying flux was used in the SOILSIM simulations. The piecewise linear approximation was chosen such that on a year to year basis, the same total amount of water was applied in the SOILSIM and HYDRUS runs.

At any particular point in time during the simulation, the loading rates used by HYDRUS and SOILSIM may not be identical. However, over time scales of 2-3 years or more, the two approximations give consistent results. Moreover, both ways of specifying the input fluxes are only approximations to the actual historic conditions and it is difficult to argue which of the two is the more accurate. While actual disposal rates probably did not vary as regularly as assumed in the SOILSIM runs, the abrupt year-to-year changes as modeled by HYDRUS will not be completely realistic either.

#### 4.2.5.2 Radionuclide Loading

The radionuclide concentrations and loading rates are some of the most critical data necessary for the analysis. Unfortunately, the records pertaining to concentration and loading rates are incomplete.

A brief tabulation of historical concentrations of Pu-239 contained in the waste water disposed at MDA T is presented in Table 4.4. The sharp decrease in plutonium concentrations in 1953 is due to the completion and operation of a new treatment facility.

Application rates and concentrations of Am-241 are not available. Only partial records for loading concentrations of ammonium citrate are available.

To overcome the difficulty of obtaining reliable concentrations for americium and ammonium citrate the concentrations of these constituents were normalized to a concentration of 1.0 for the pathway analysis. The normalization of their concentrations will enable future comparisons to be made if more information becomes available.

#### 4.2.5.2.1 HYDRUS

The concentration of Pu-239 input into the one-dimensional model HYDRUS are presented in Table 4.4. The high concentration of Pu-239 reported in 1951

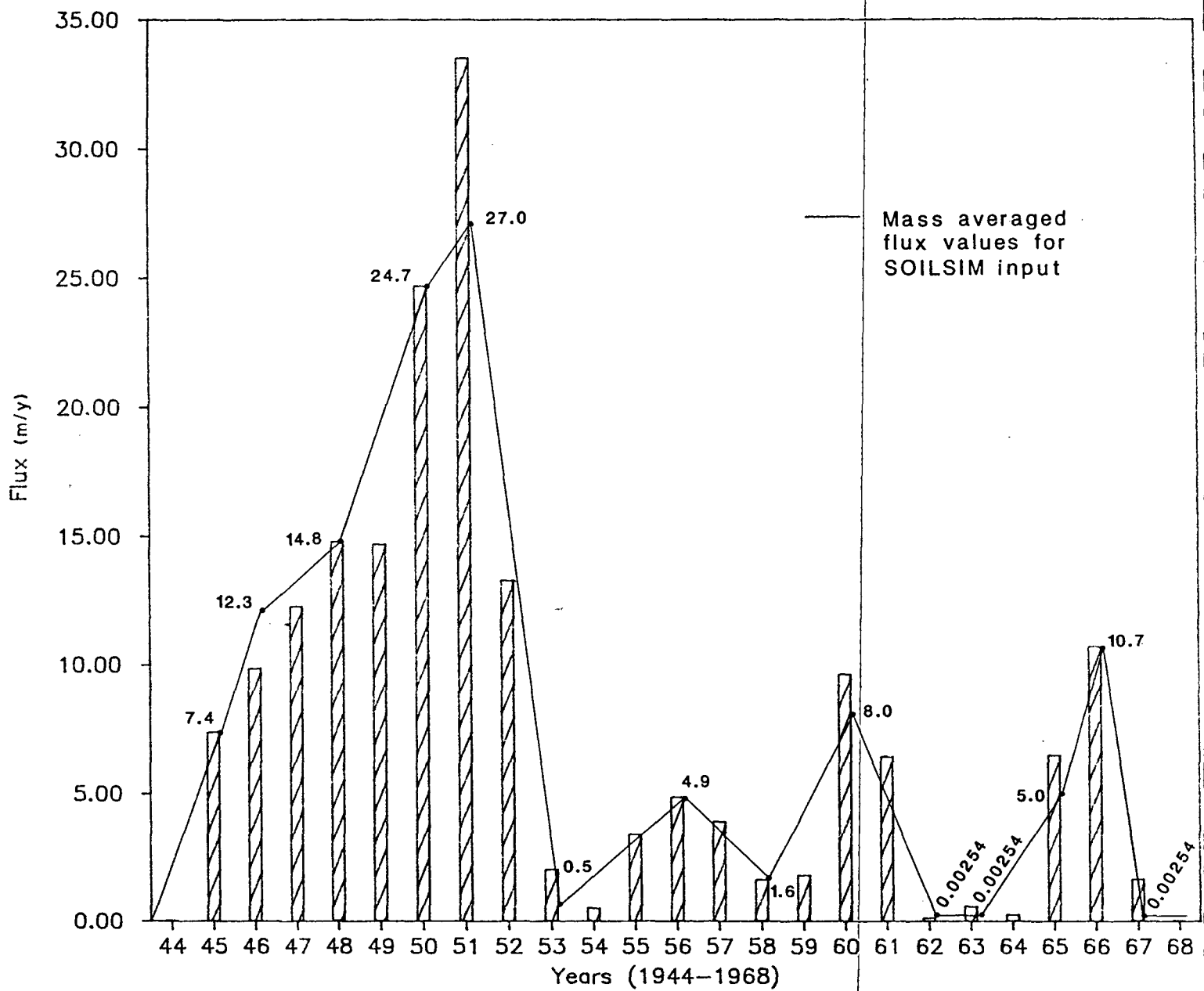


Figure 4.2. Yearly mass averaged flux rates for 2-D SOILSIM simulations (including pulse in 1960-61).

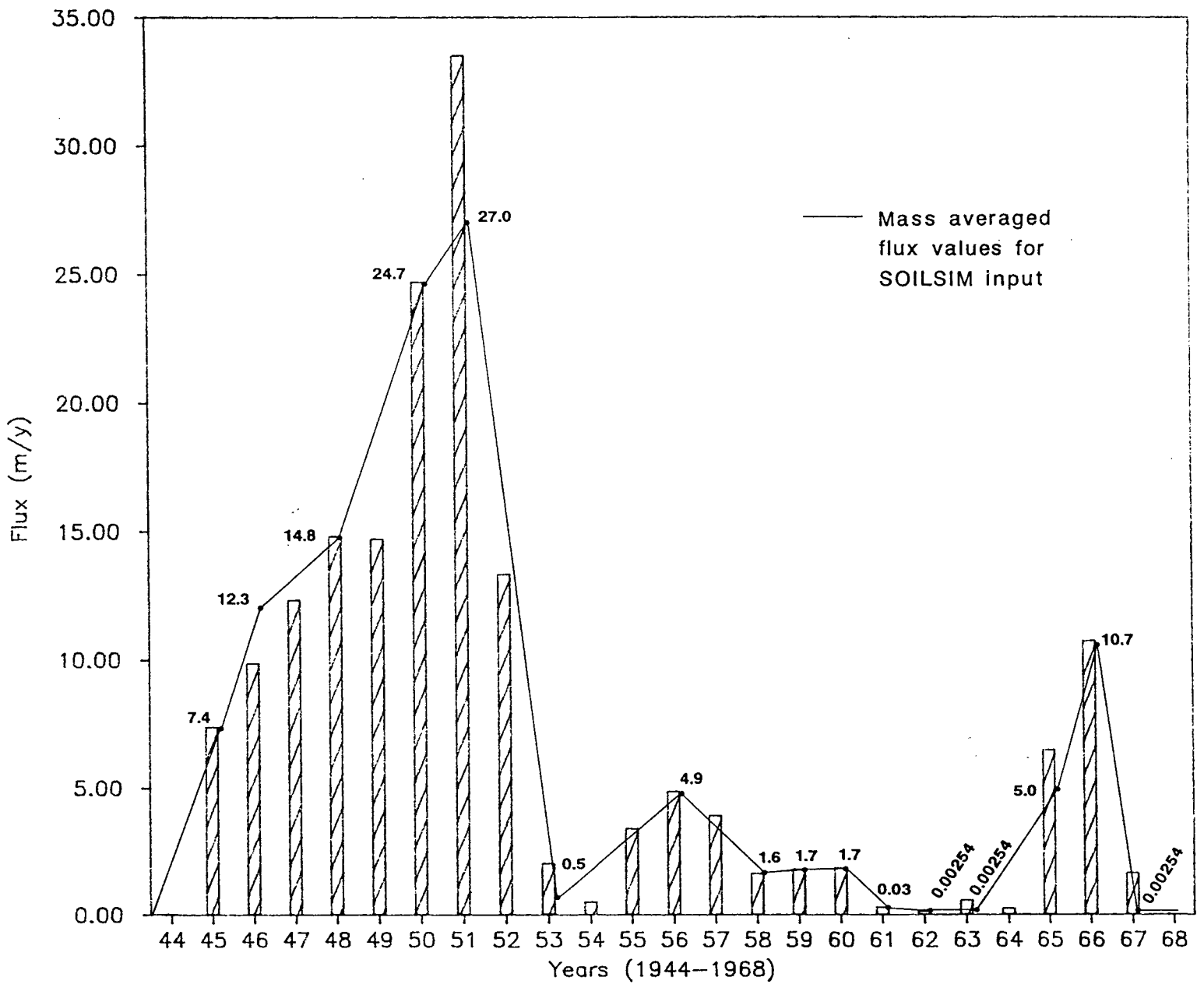


Figure 4.3. Yearly mass averaged flux rates for 2-D SOILSIM simulations (excluding pulse in 1960-61).

Table 4.4. Reported Pu-239 concentrations released to absorption beds at MDA T.

Year	Pu-239 concentration (dpm/ml)
1945	120
1946	120
1947	120
1948	120
1949	120
1950	120
<sup>1</sup> 1951	160
1952	120
<sup>2</sup> 1953	.2
1954	.2
1955	.2
1956	.2
1957	.2
1958	.2
1959	.2
<sup>3</sup> 1960	.114
<sup>3</sup> 1961	.106
1962	.2
1963	.2
1964	.2
1965	.2
1966	.2
1967	.2

<sup>1</sup> 40 m<sup>3</sup> of 14,000 dis/m/ml

<sup>2</sup> Treatment facility completed

<sup>3</sup> Addition of tap water to absorption bed 1 lowered concentration (Christenson and others, 1961)

---

(160 dis/min/ml) was due to the release of 40 m<sup>3</sup> concentrated wastes to the beds from June 1951 through July 1952. In 1960 and 1961 the radionuclide concentrations in wastewater added to bed 1 were lowered because of the addition of tap water to bed 1 during this time (Christenson and others, 1961).

#### 4.2.5.2.2 SOILSIM

Concentration data input (Figure 4.4) to SOILSIM followed that used in HYDRUS. Note that because the fluid discharges were mass averaged in SOILSIM, the actual radionuclide mass loading in SOILSIM was also mass averaged.

#### 4.2.6 Mesh Design

Mesh selection to accomplish the one and two dimensional analyses required several different grids and discretization methods. The original discretization of the problem domain was relatively coarse. Vertical grid spacings for both the one and two dimensional simulations ranged between 3.5 and 7.5 meters. This permitted first approximations to be made of the vertical distances that the solutes would migrate. Horizontal grid spacing in the two dimensional case (SOILSIM) ranged from 1.5 to 7.0 meters and was the same throughout all of the simulations. After the initial simulations were completed the grids of the simulated area were refined by methods discussed in the following sections.

##### 4.2.6.1 HYDRUS (1-D Mesh)

Initial flow and transport simulations performed in one dimension used a coarse grid to roughly determine the approximate rate and extent of radionuclide movement. Vertical grid lines were evenly spaced at 3.5 m to a depth of 350 m (Figure 4.5). To facilitate the computation of nodal flux the distance between the two nodes in the horizontal direction was 2 m (effective nodal distance equal to 1 m). This configuration yields a mesh consisting of 100 elements and 202 nodes.

Results from these preliminary simulations indicated that plutonium and americium have not moved deeper than 40 m. To obtain better resolution and greater numerical accuracy the simulated vertical domain was reduced from 350 m to 100 m. The length between the two nodes in the horizontal direction remained at 2 m, while the vertical spacing was reduced to 1 m (Figure 4.5). This configuration also yields a mesh of 100 elements and 202 nodes.

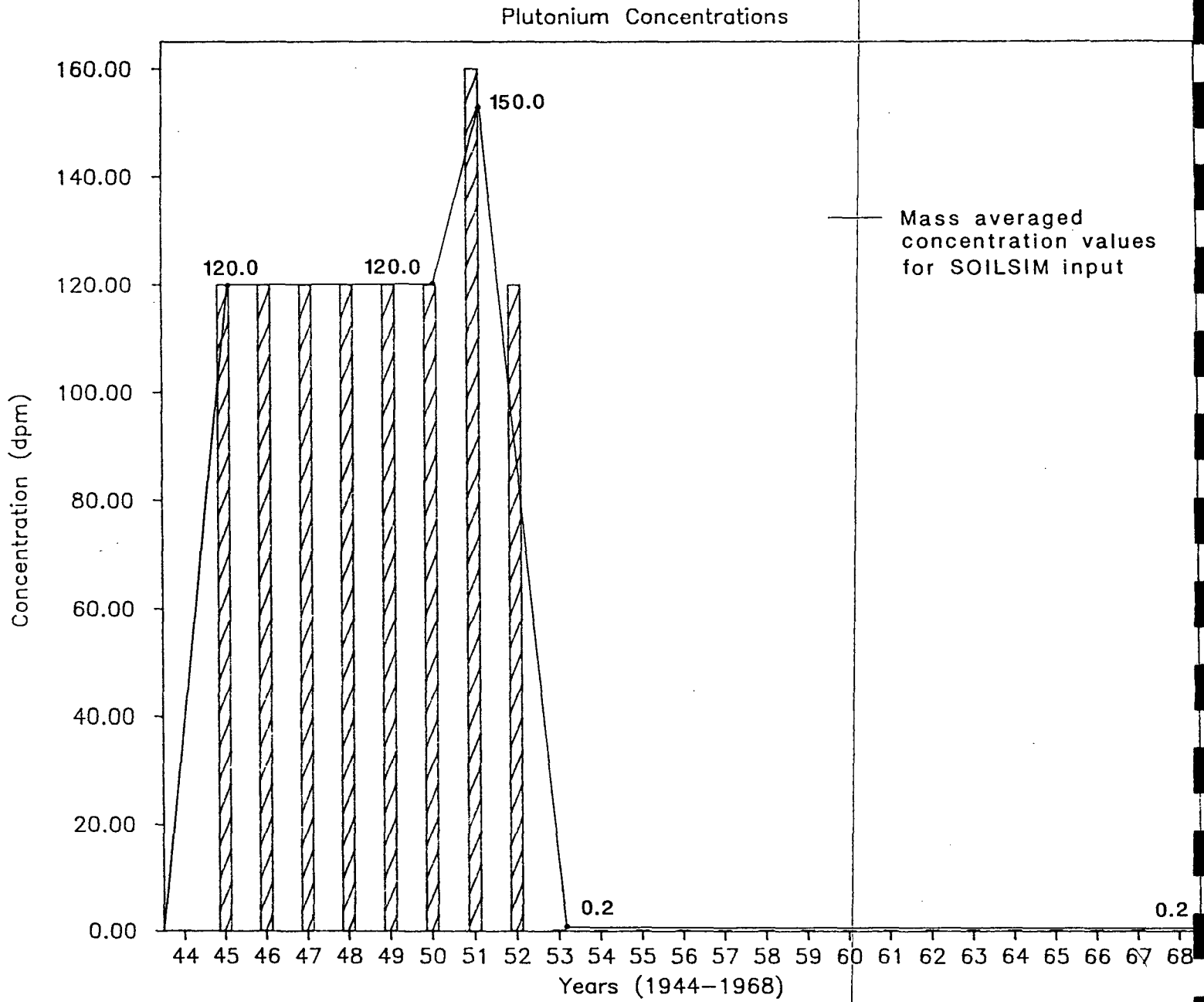


Figure 4.4. Pu-239 input concentrations for 2-D SOILSIM simulations.

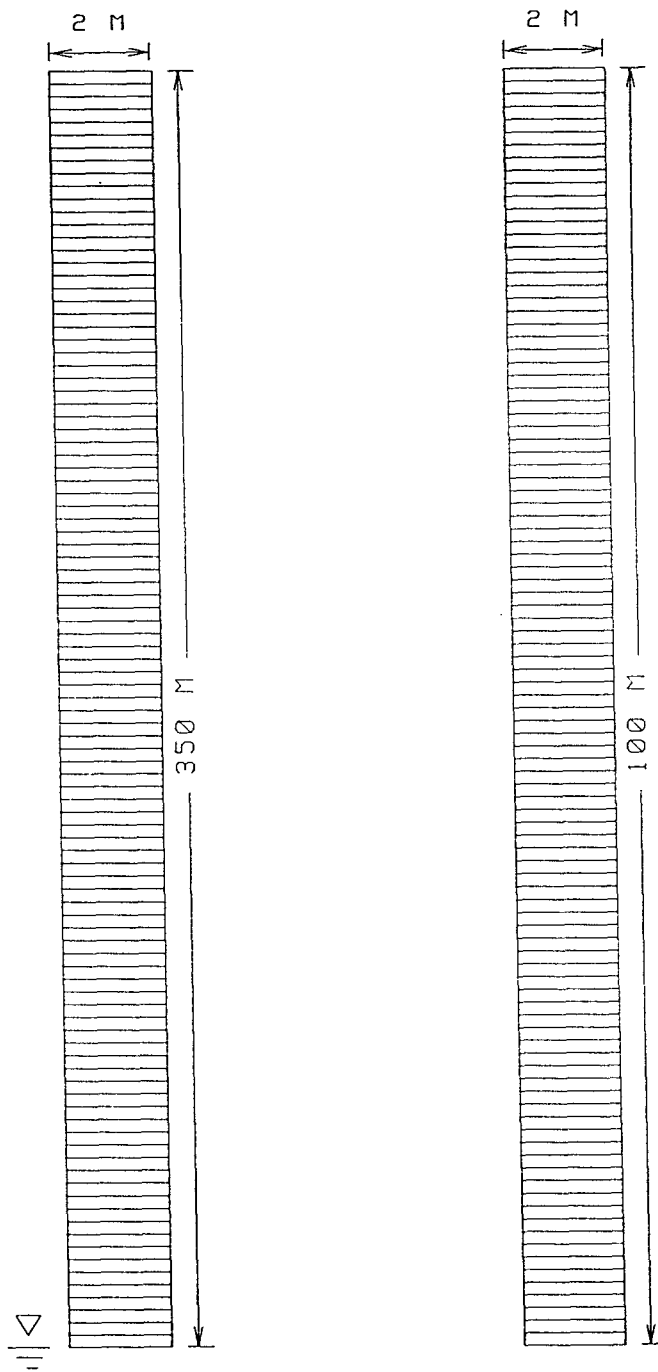


Figure 4.5. Fine and coarse mesh utilized for 1-D HYDRUS simulations.

---

The longitudinal dispersivity is estimated to be approximately 3.5 m for the tuff material. This translates to a mesh Peclet number of 1.0 for the coarser grid and .286 for the finer mesh.

#### 4.2.6.2 SOILSIM (2-D Mesh)

The preliminary two-dimensional grid employed by SOILSIM covered a cross-sectional area of 14,700 m<sup>2</sup> (Figure 4.6). Vertical grid lines are spaced at intervals ranging from 1.5 m to 7.0 m to a depth of 350 m. Horizontal grid lines are spaced at intervals ranging from 1.5 m to 7.0 m over a distance of 42 m. The mesh consists of 1080 nodes and 994 elements.

Rectangular elements are used in preference to irregular quadrilateral elements to increase the efficiency and the ease of output processing, checking and interpretation of computed results. Nodes and elements are numbered sequentially from the bottom to the top along each vertical line. This is done to obtain a reasonable matrix bandwidth and to simplify the procedure for plotting of contours and profiles of saturations and concentrations.

Preliminary results suggested that radionuclides would not migrate greater than 40 m. Therefore, to obtain better resolution and greater numerical accuracy, during the transport runs, the simulated vertical domain was refined and narrowed to the upper 48 m and 29 m laterally (Figure 4.7).

The longitudinal dispersivity was estimated to be approximately 3.5 m for the tuff material, which translates to a mesh Peclet range of .43 - 2.0 for the coarser grid and a range of .666 - .428 for the finer mesh. Peclet numbers less than 10 are acceptable for the upstream-weighted-residual finite-element scheme used in the model (Huyakorn and Pinder, 1983).

#### 4.2.7 Convergence Criteria and Time Discretization

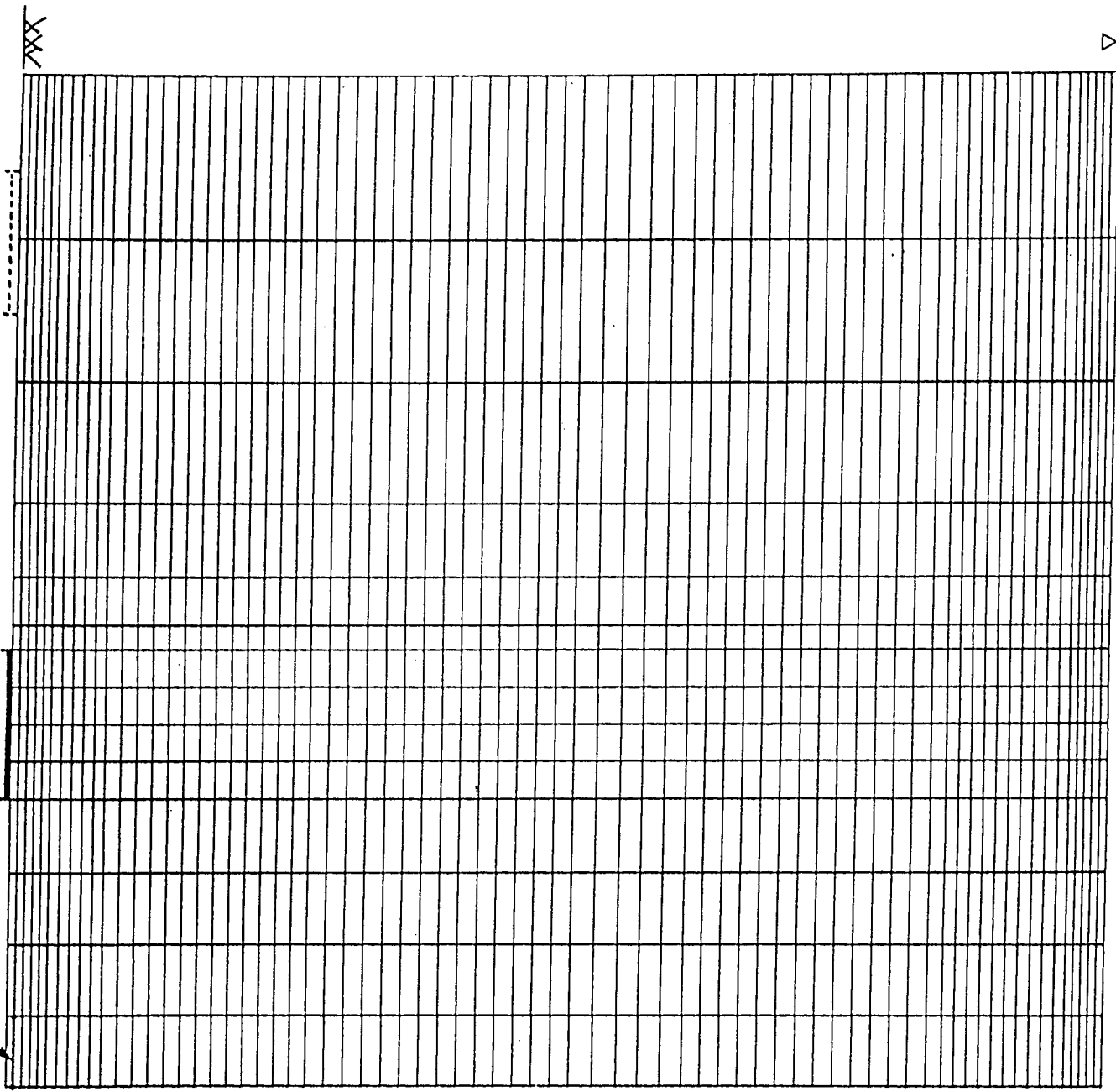
Due to nonlinearity of the unsaturated flow equation, the flow solution at every time step is obtained using an iterative procedure, where iteration is used until the pressure head error at every node is less than a given convergence criterion. The convergence criteria for both HYDRUS and SOILSIM were set to 0.1 meter. This value was selected to ensure an accurate solution without unduly increasing computational requirements.

Simulation time is divided into stress periods that represent time intervals during which all external stresses are constant. Stress periods are further divided into time steps.

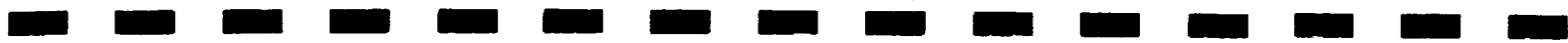
LOCATION OF DISPOSAL BED 3

DISPOSAL BED 1

LEAKY PIPE



350 m



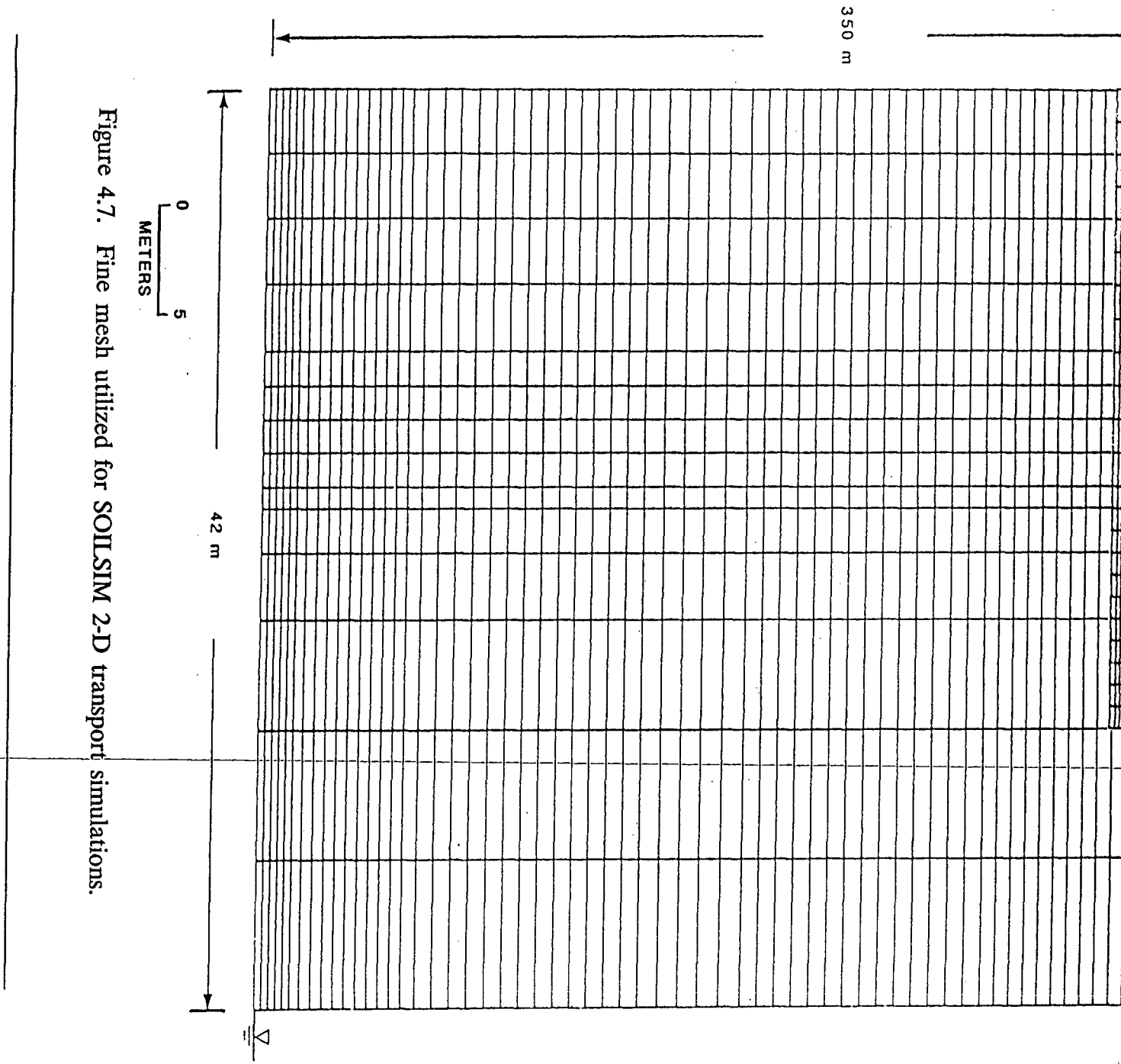


Figure 4.7. Fine mesh utilized for SOILSIM 2-D transport simulations.

---

For model input the length of the simulation period is specified in addition to the number of time steps into which it is to be divided. To permit flexibility, a time step multiplier allows the length of each time step to vary. Both HYDRUS and SOILSIM have features for automatic adjustment of time steps when convergence difficulties occur. Small time steps are used during periods of high water input, with larger time steps as redistribution time increases. This procedure minimizes any sensitivity of model output to the time step values.

#### 4.2.7.1 HYDRUS

In general, HYDRUS converges better when shorter time-step intervals are assigned. If convergence difficulties arise in HYDRUS, the code will automatically reduce the time interval to improve the convergence. The following are the specified values for the time-related input:

- maximum number of time steps permitted            2000
- initial time step    .01
- maximum allowable time step                            2
- duration of the simulation                                50

#### 4.2.7.2 SOILSIM

As in HYDRUS, if SOILSIM simulations do not converge, the code will automatically reduce the time-step interval. To increase the efficiency of the two-dimensional simulations and to minimize convergence problems initial time step intervals were set to relatively small values in years corresponding to the addition of high flux rates. The following are specified values for the time-related input:

Time Steps	Corresponding Years	Time Step Interval
0.0- 2.0	1944-1946	0.1
2.0- 7.0	1946-1953	0.05
7.0- 9.0	1953-1955	0.025
9.0-10.0	1955-1956	0.1
10.0-24.0	1956-1980	0.25
24.0-26.0	1980-1982	0.5
26.0-50.0	1982-2004	1.0

---

## 5.0 PATHWAY ANALYSIS

### 5.1 General

The pathway analysis is designed, through the application of numerical models, to develop, test and refine a site conceptual model from which remedial investigation data requirements may be identified. To achieve this goal, the following steps were taken and are illustrated in Figure 5.1:

- Formulation of initial conceptual model;
- Development of numerical models which quantify the conceptual model;
- Sensitivity analysis;
- Historical reconstruction and comparison of actual field measurements to simulated model output;
- Simulation of site specific cases;
- Revision of site conceptual model;
- Identification of RI data requirements.

Formulation of initial conceptual model - available geologic, hydrologic, and waste disposal data were used to develop a qualitative conceptual model of the variably saturated subsurface flow, transport, and waste disposal system, as described in previous sections of this report.

Development of numerical models - available parametric and geometric data were used to quantify geometric and temporal boundary conditions and unsaturated flow and transport characteristics into two numerical models which incorporate all the key features of the conceptual model. The numerical modeling approach is discussed in the preceding section of this report.

Sensitivity analysis - the sensitivity of the system to various parameters was evaluated to identify which processes and parameters should receive priority emphasis during the remedial investigation program.

Historical reconstruction - to develop, test and refine the conceptual model, pathway analysis results were compared and calibrated to observed radionuclide profiles.

Simulation of site-specific cases - a series of case scenarios, as described below, were performed that resemble the history of the waste disposal practices as closely as possible.

---

### Case I - Ambient Flow Simulations

The first case involves one scenario designed to simulate the ambient conditions of the natural system without any effects of waste disposal.

### Case II - Waste Discharge Flow Simulations

The second case involves three waste discharge flow scenarios (Section 5.5.2). During this case, the documented or estimated man-induced liquid discharges since 1945 are superimposed on the natural hydrologic system obtained from Case I. The three scenarios are:

- Addition of known volumes of wastes from 1945 through 1967 to absorption bed 1;
- In addition to the known volumes of waste applied from 1945 through 1967, Christenson (1961) applied a large volume of tap water to absorption bed 1 during a field investigation;
- Simulation of a pipe located south of the absorption beds that has been leaking 1-2 gpm for many years (due to numerical instabilities that occurred because of the high volume of water leaking from the pipe, the pipe leak was simulated at .03 gpm).

### Case III - Contaminant Transport Simulations

The transport simulations performed in the Case III scenarios are analogous to the Case II flow simulations except that they simulate contaminant transport.

Modification and refinements of site conceptual model - the site conceptual model is revised, based on pathway analysis results, as described in Section 7.0 and provides the hydrogeologic framework from which the remedial investigation data requirements are identified.

Identification of remedial investigation data requirements - after the completion of the pathway analysis and the development of a site refined conceptual model the Remedial Investigation (RI) data requirements are identified in Section 8.0.

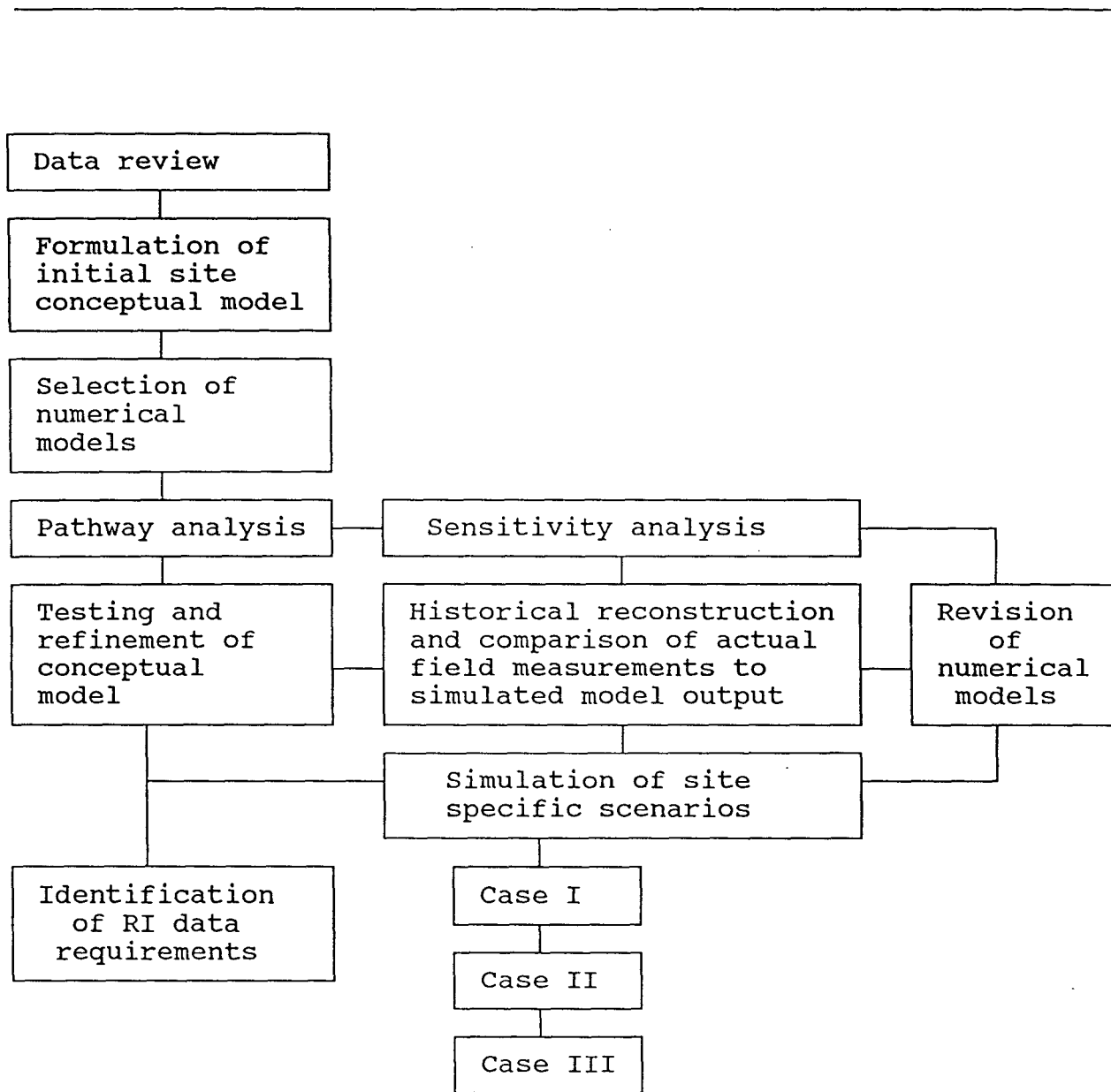


Figure 5.1. Strategy to identify RI data requirements.

---

## 5.2 Sensitivity Analysis

The wide variance and uncertainty of the input data necessitated that a series of sensitivity runs be performed. Because these runs are designed to estimate parameters in gross terms, there was little justification to perform sensitivity simulations in two dimensions. Furthermore, the present lack of appropriate field information precludes a detailed sensitivity analysis in two dimensions.

The one-dimensional sensitivity analysis was performed by using measured rock properties and estimated recharge rates to determine the ambient conditions. After ambient conditions were established (Section 5.5.1), the actual waste disposal loading rates (Section 5.5.2 and 5.5.3) were superimposed on the ambient conditions and the sensitivity analysis was performed.

The actual mechanics of the sensitivity analysis involves a systematic sequence of simulation runs in which each key parameter of interest is varied through its estimated range of uncertainty, while holding all the other variable parameters constant. Thus, any dissimilarities between otherwise identical simulations are attributed to a single parameter.

The parameters of most interest in the sensitivity analysis are the distribution coefficients, mesh spacing, shape and position of the soil moisture curve, saturated hydraulic conductivity, dispersivity, and the volumetric water loading rates for bed 1.

### 5.2.1 Distribution Coefficients

Estimates for the distribution coefficients ( $K_d$ ) of americium and plutonium were obtained from studies performed on the tuff underlying Yucca Mountain Nevada (Table 5.1). These estimates for distribution coefficients of americium and plutonium were input into the model as first approximations.

Figures 5.2 through 5.4 indicate that if actual  $K_d$ 's are in the range of those given in Table 5.1, americium would have only migrated approximately 3.5 meters vertically. In 1978, detectable concentrations of plutonium and americium were found to depths of 30 meters at MDA T. This inconsistency between the model results and field measurements suggest that either the actual  $K_d$  for americium at MDA T is far lower than  $K_d$ 's measured at Yucca Mountain or there are other factors affecting the migration of americium at MDA T.

Table 5.1. Typical distribution coefficients and approximate retardation factors for welded and nonwelded Yucca Mountain hydrogeologic units (Heiken, 1982).

Element	Distribution coefficient, $K_d$ (ml/g)		Retardation factor, $^aR_m$	
	Welded	Nonwelded	Welded	Nonwelded
Americium	1,200	4,600	28,000	24,000
Carbon	0 <sup>b</sup>	0 <sup>b</sup>	1	1
Curium	1,200	4,600	28,000	24,000
Cesium	290	7,800	6,700	41,000
Iodine	0 <sup>b</sup>	0 <sup>b</sup>	1	1
Neptunium	7	11	160	58
Protactinium	64	140	1,500	740
Lead	5	5	120	27
Plutonium	64	140	1,500	740
Radium	25,000 <sup>c</sup>	25,000 <sup>c</sup>	580,000	130,000
Tin	100	100	2,300	530
Strontium	53	3,900	1,200	21,000
Technetium	0.3	0 <sup>b</sup>	8	1
Thorium	500	500	12,000	2,600
Uranium	1.8	5.3	27	45
Zirconium	500	500	12,000	2,600

<sup>a</sup> Calculated using values of moisture content of 10 and 28 percent and bulk densities of 2.33 and 1.48 g/cm<sup>3</sup> for welded and nonwelded tuff.

<sup>b</sup> No data available; assumed to be zero.

<sup>c</sup> Barium used as a chemical analog.

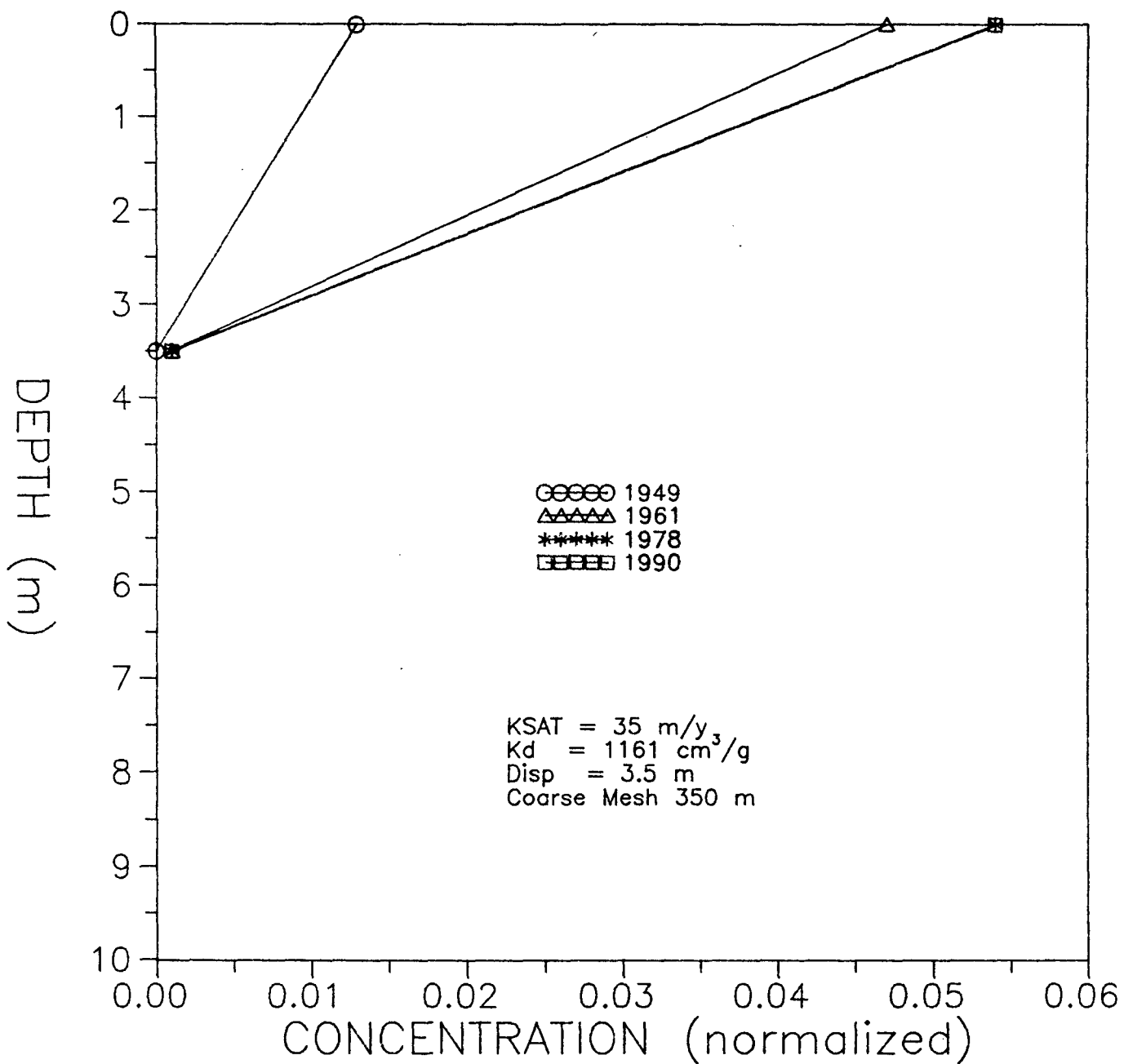


Figure 5.2. Simulated americium concentrations versus depth assuming  $K_d$  values in the lower range of Yucca Mountain tuffs.

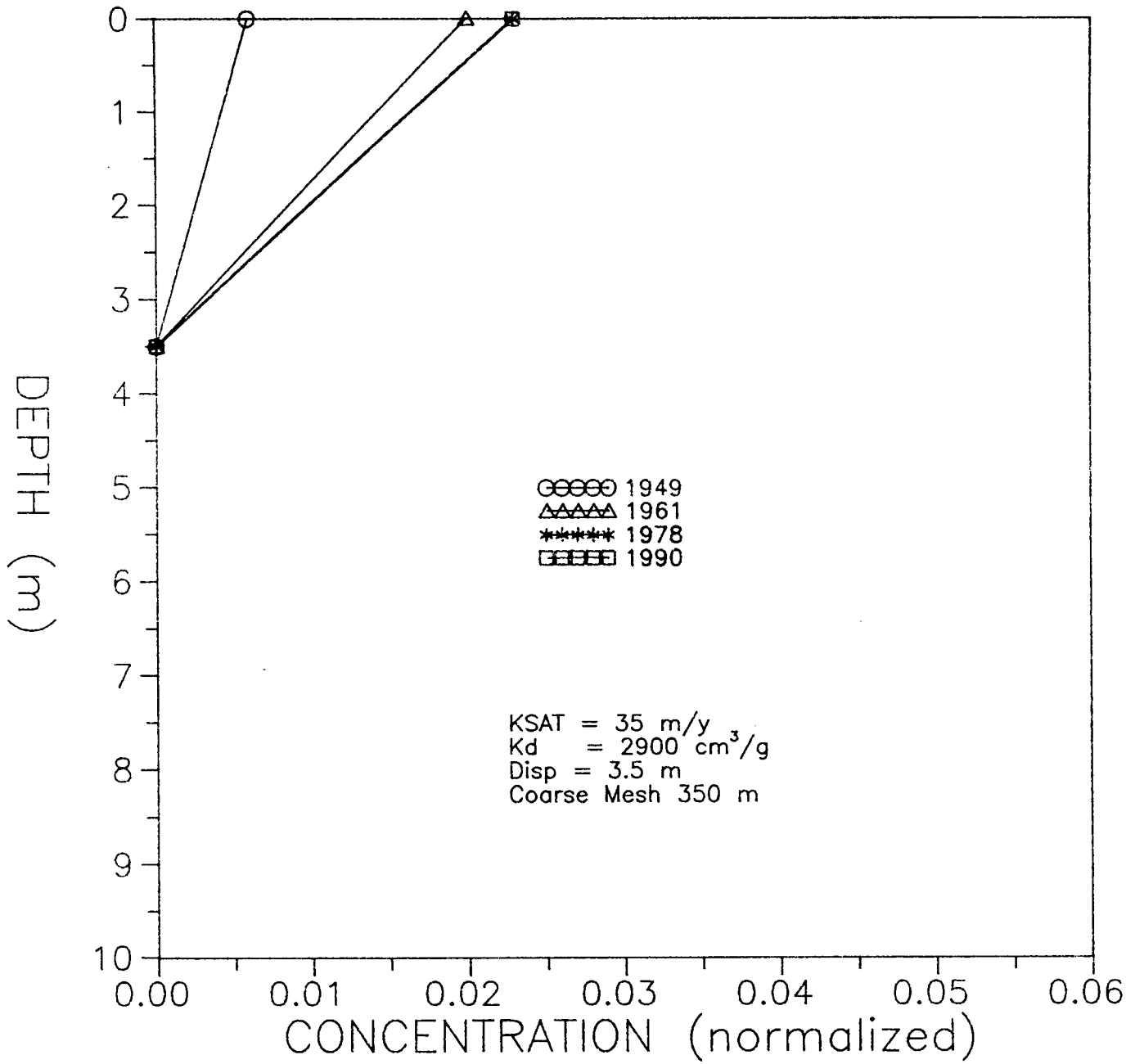


Figure 5.3. Simulated americium concentrations versus depth assuming  $K_d$  values in the moderate range of Yucca Mountain tuffs.

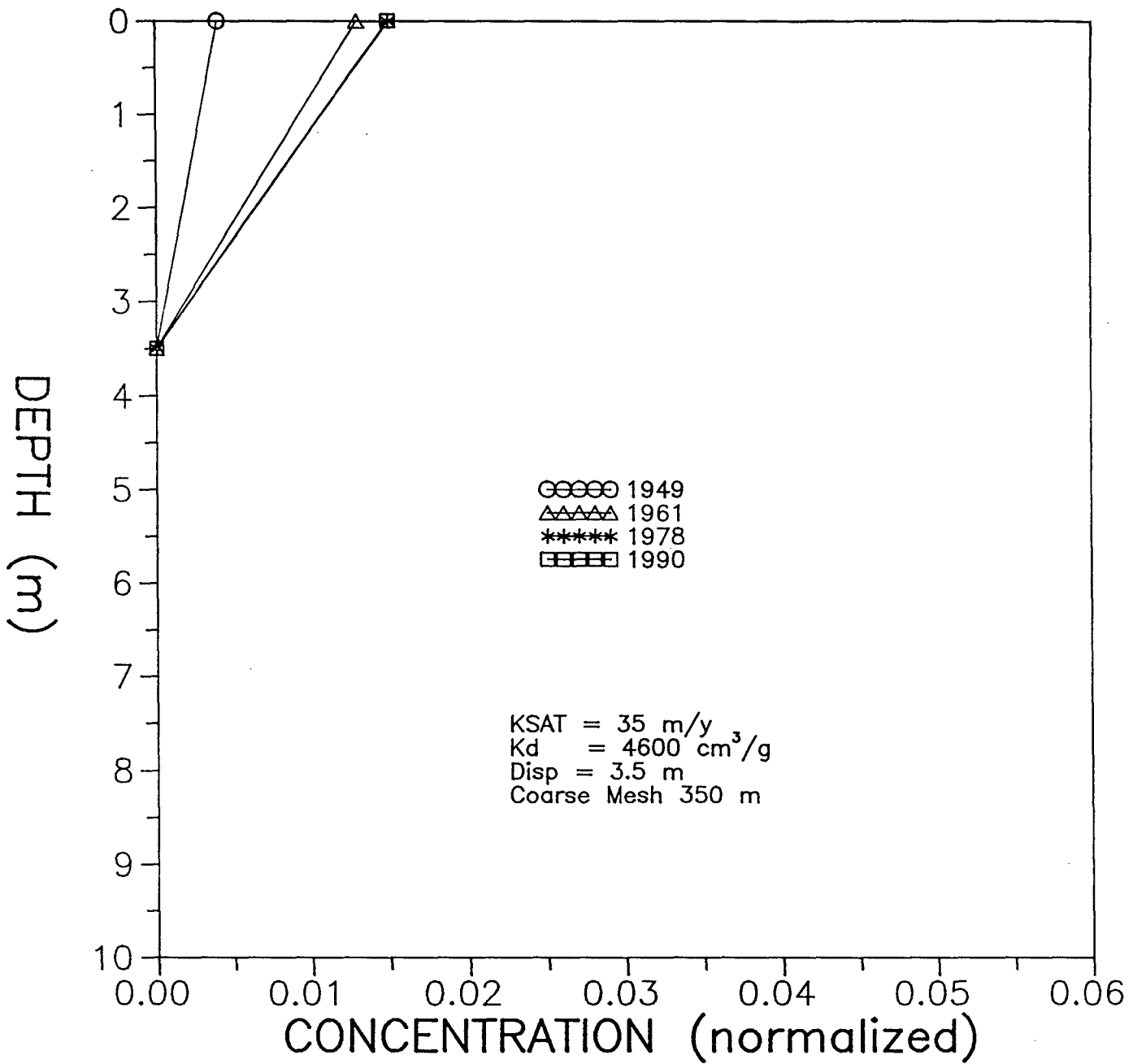


Figure 5.4. Simulated americium concentrations versus depth assuming  $K_d$  values in the high range of Yucca Mountain tuffs.

---

HYDRUS results indicate that the range of  $K_d$ 's for plutonium at the site are also considerably lower than those reported for the tuff at Yucca Mountain (Figures 5.5 through 5.8). Figures 5.9 and 5.10 illustrate the sensitivity of the system to ranges of plutonium  $K_d$  values that are more in accordance with the observed concentrations at MDA T.

## 5.2.2 Mesh Spacing

The initial simulation runs performed with HYDRUS utilized a uniform finite element mesh with 3.5 m vertical nodal spacing from land surface to the water table at 350 m depth. To evaluate the sensitivity of predicted concentration distributions, the model spacing was reduced to a 1 m spacing to a depth of 100 m. Results presented in Figures 5.11 through 5.14 indicate that the simulated concentration profiles are indeed relatively sensitive to the selected nodal spacing. Simulations performed with a 3.5 m node spacing show a deeper penetration of radionuclides compared to the 1 m node spacing. This result is related to the tendency of the numerical solution to produce a more smeared concentration profile when a coarser grid is used. In the present case, the grid spacing of 3.5 m is large relative to the actual depth of penetration of the solute front (5-15 m). The smearing tendency thus results in over prediction of the radionuclide penetration depth. The finer, 1 m, mesh results in a more accurate simulation. Therefore, the one-dimensional flow and transport scenarios presented in Section 5.5 are all performed with the fine (1 m) mesh in addition to the 3.5 m mesh.

The two-dimensional transport simulations utilized a finite element grid of variable nodal spacing, varying between 1.5 m near the source, to 7.5 m near the water table (Figure 4.7). The latter value is again relatively large, but since the radionuclides never reached this distance, this is inconsequential.

## 5.2.3 Shape of Moisture Release Curves

### 5.2.3.1 Power Index (n) of the Relative Permeability Versus Saturation Relationship

The addition of large pulses of liquid wastes into the very dry system at MDA T causes steep saturation fronts, which are difficult to simulate numerically. These difficulties are reflected in slow convergence of the numerical solution and the need to use very small time steps. The complications become much more pronounced as the dimensionality of the modeling is increased. Whereas the nonlinearity of the flow problem did not cause undue difficulties with the one-dimensional HYDRUS simulations, initial model runs did indicate severe convergence difficulties with the two-dimensional SOILSIM runs. To overcome these numerical problems, the difficulty of the flow simulation was reduced by releasing the exponent (n) in the assumed Brooks-Corey relationship between relative conductivity and saturation from 3.69 to 3.0. This in turn necessitates evaluation of the

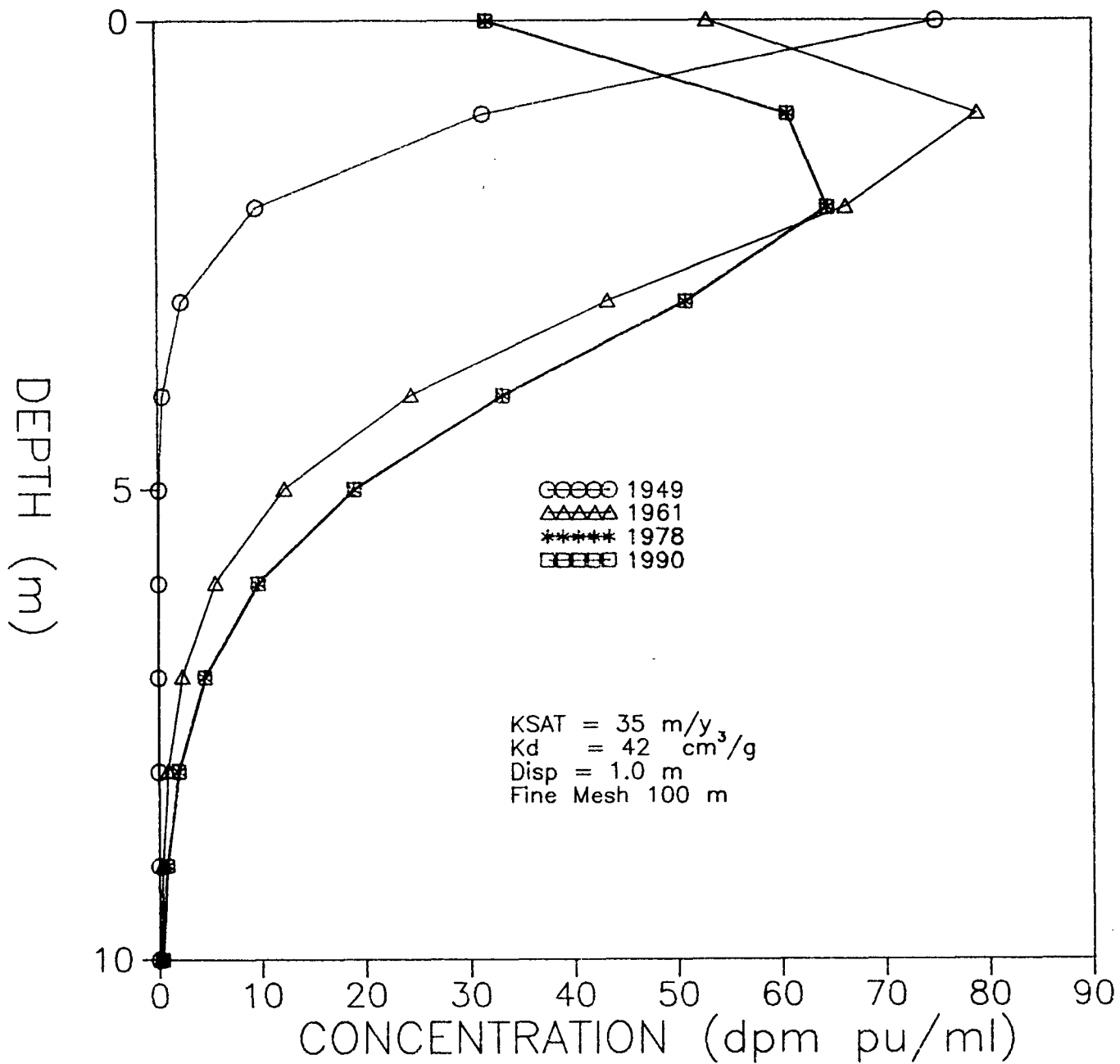


Figure 5.5. Sensitivity simulation of Pu transport to  $K_d$ , run 1.

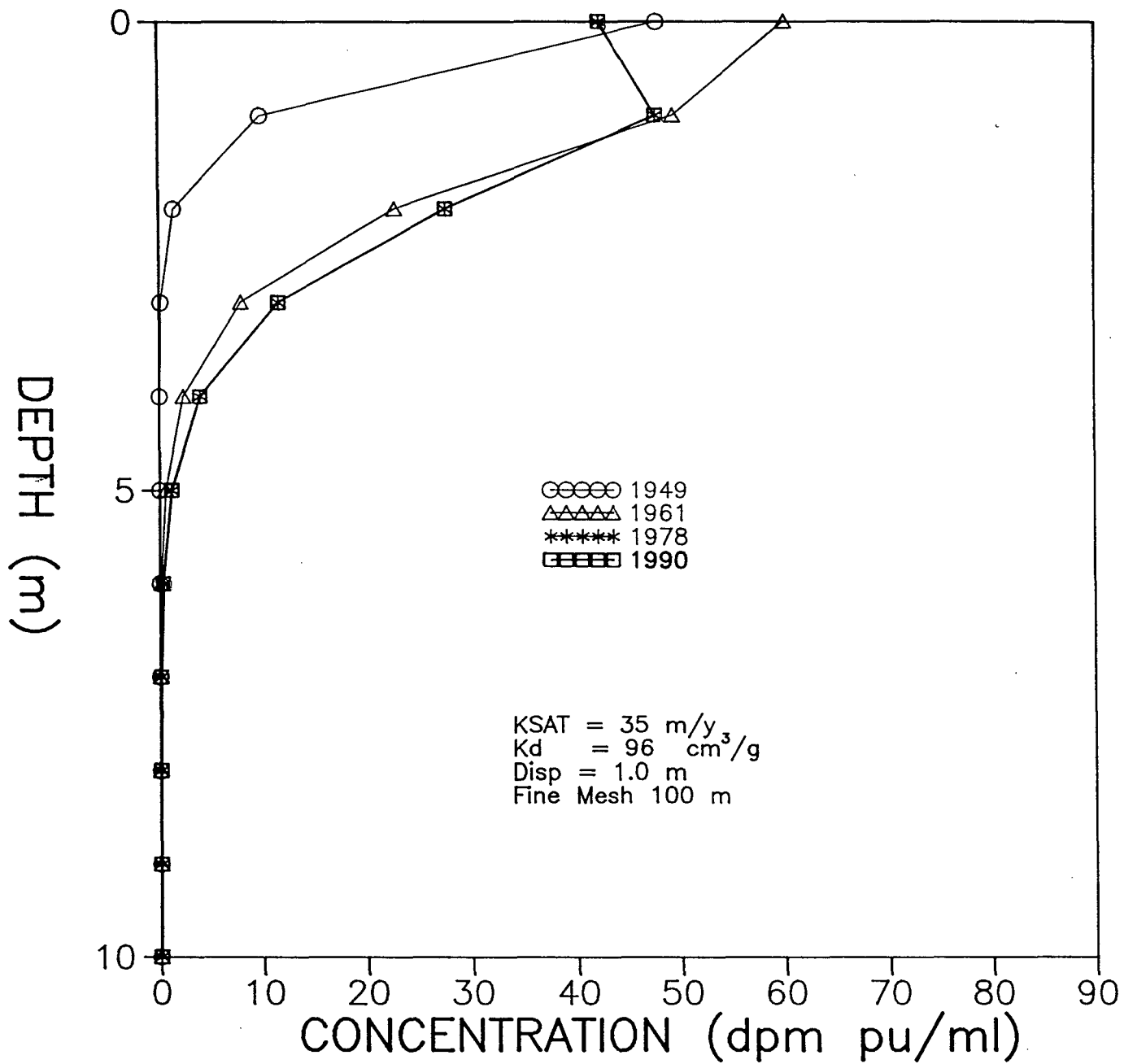


Figure 5.6. Sensitivity simulation of Pu transport to  $K_d$ , run 2.

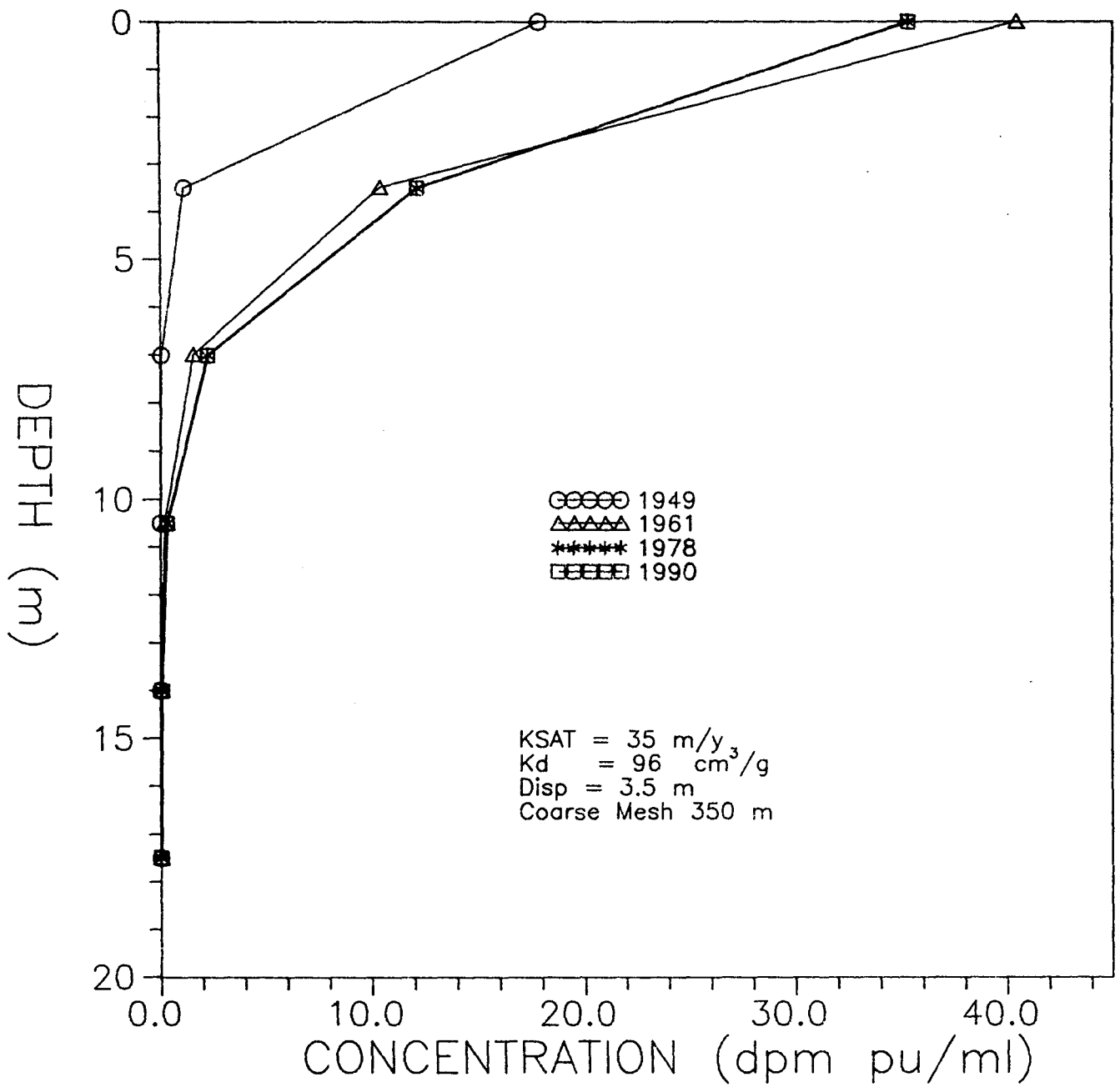


Figure 5.7. Sensitivity simulation of Pu transport to  $K_d$ , run 3.

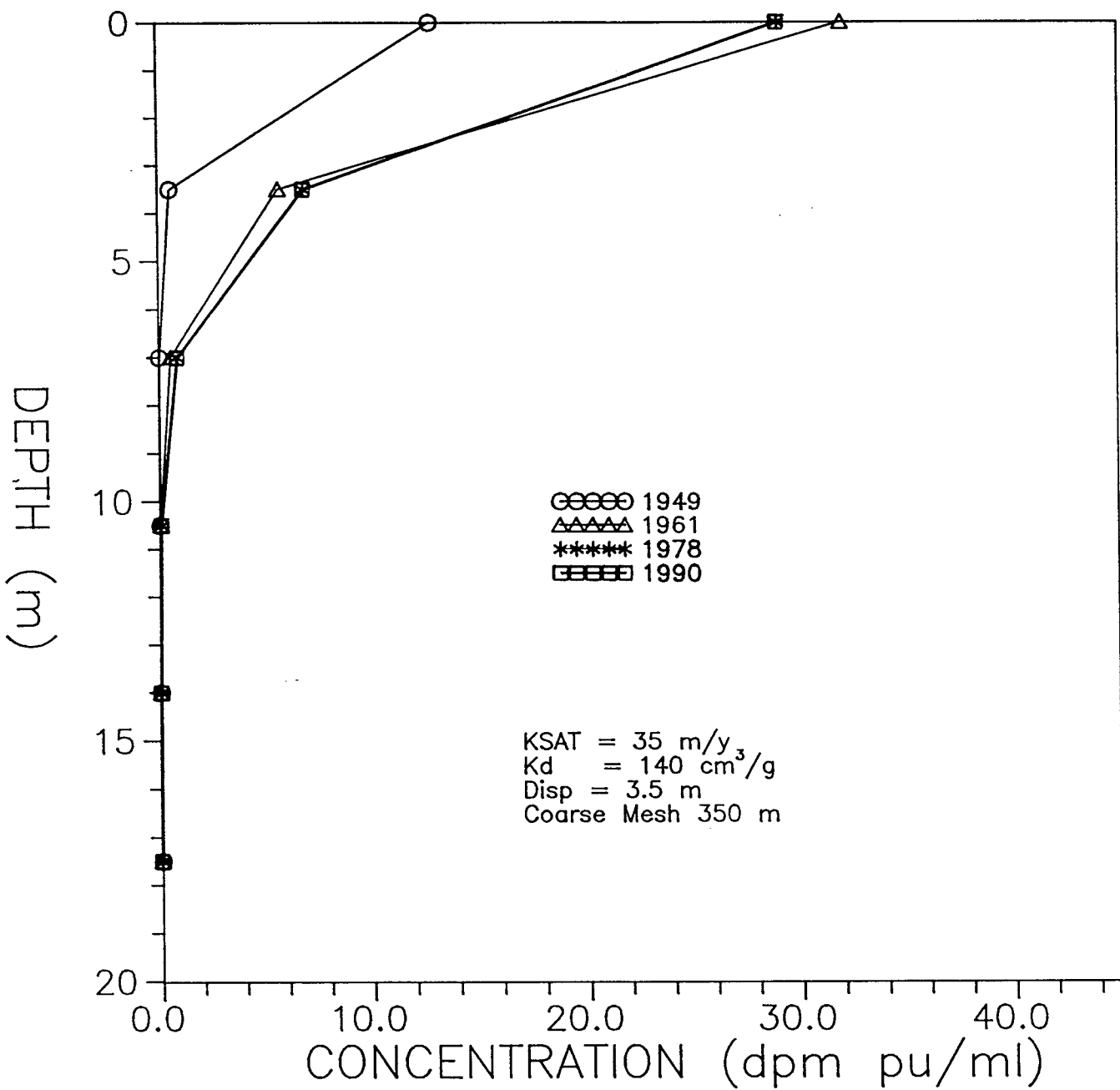


Figure 5.8. Sensitivity simulation of Pu transport to  $K_d$ , run 4.

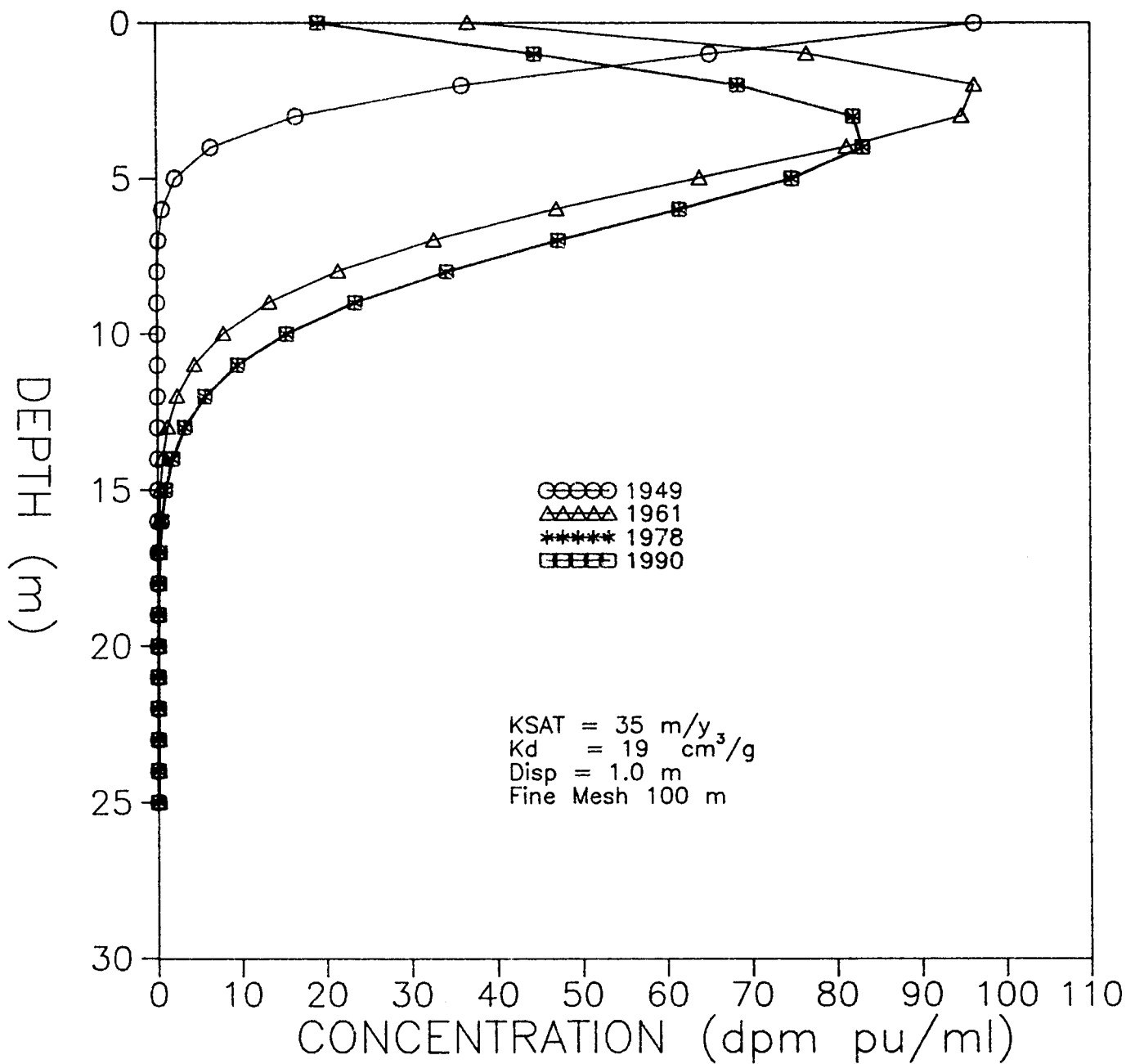


Figure 5.9. Sensitivity of Pu transport to  $K_d$ , run 5.

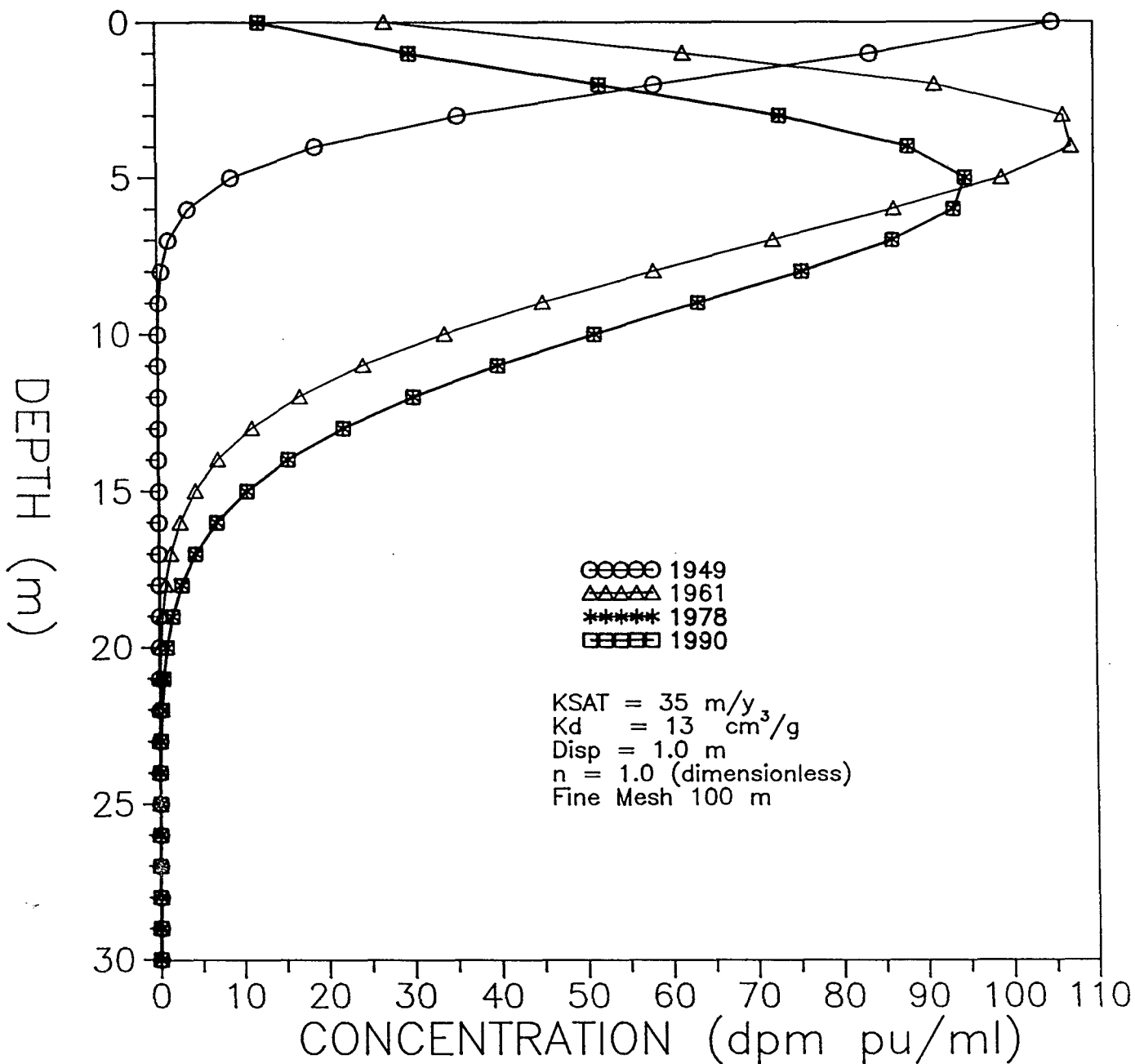


Figure 5.10. Sensitivity of Pu transport to  $K_d$ , run 6.

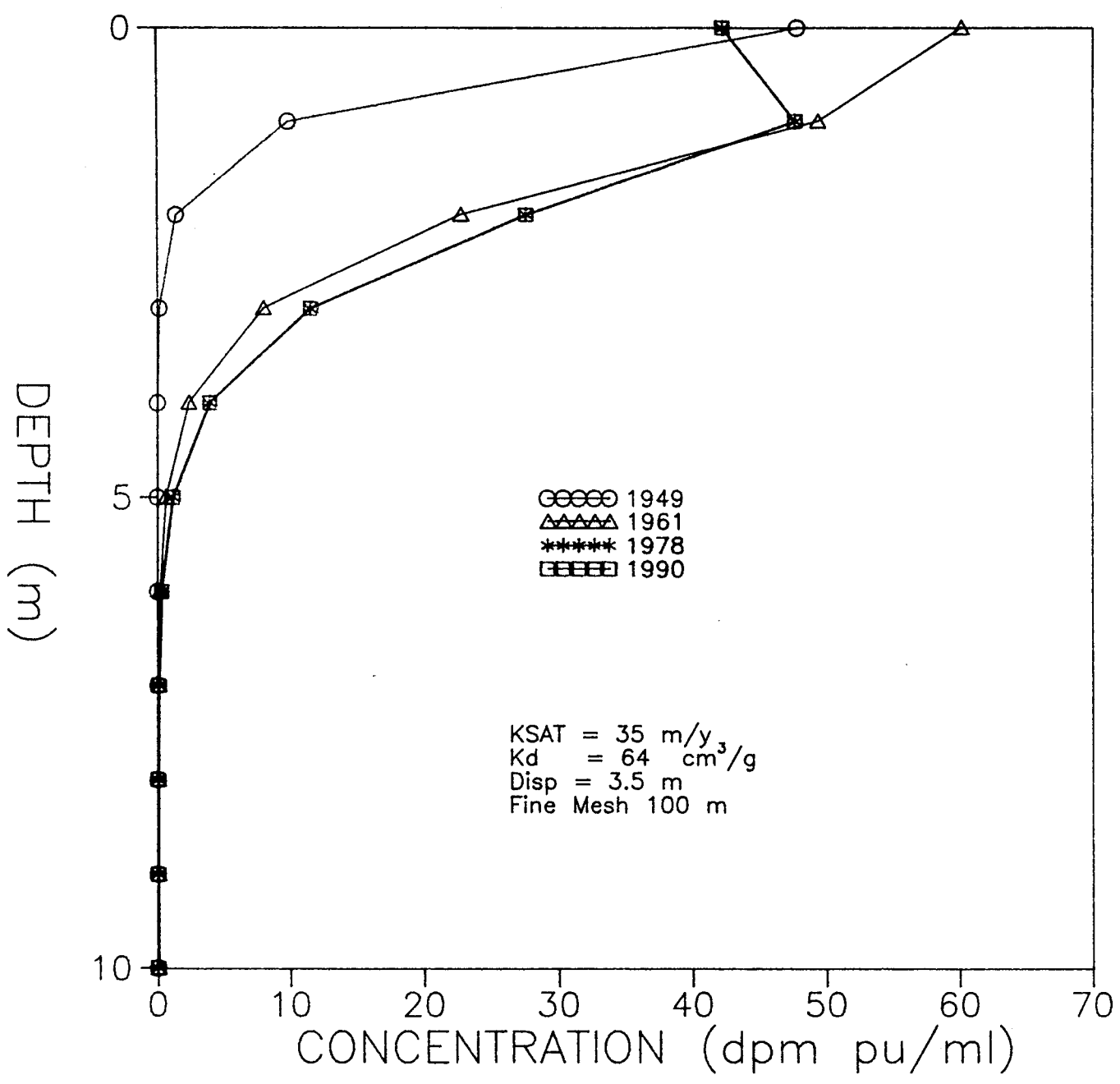


Figure 5.11. Sensitivity of Pu transport to mesh spacing (fine mesh).

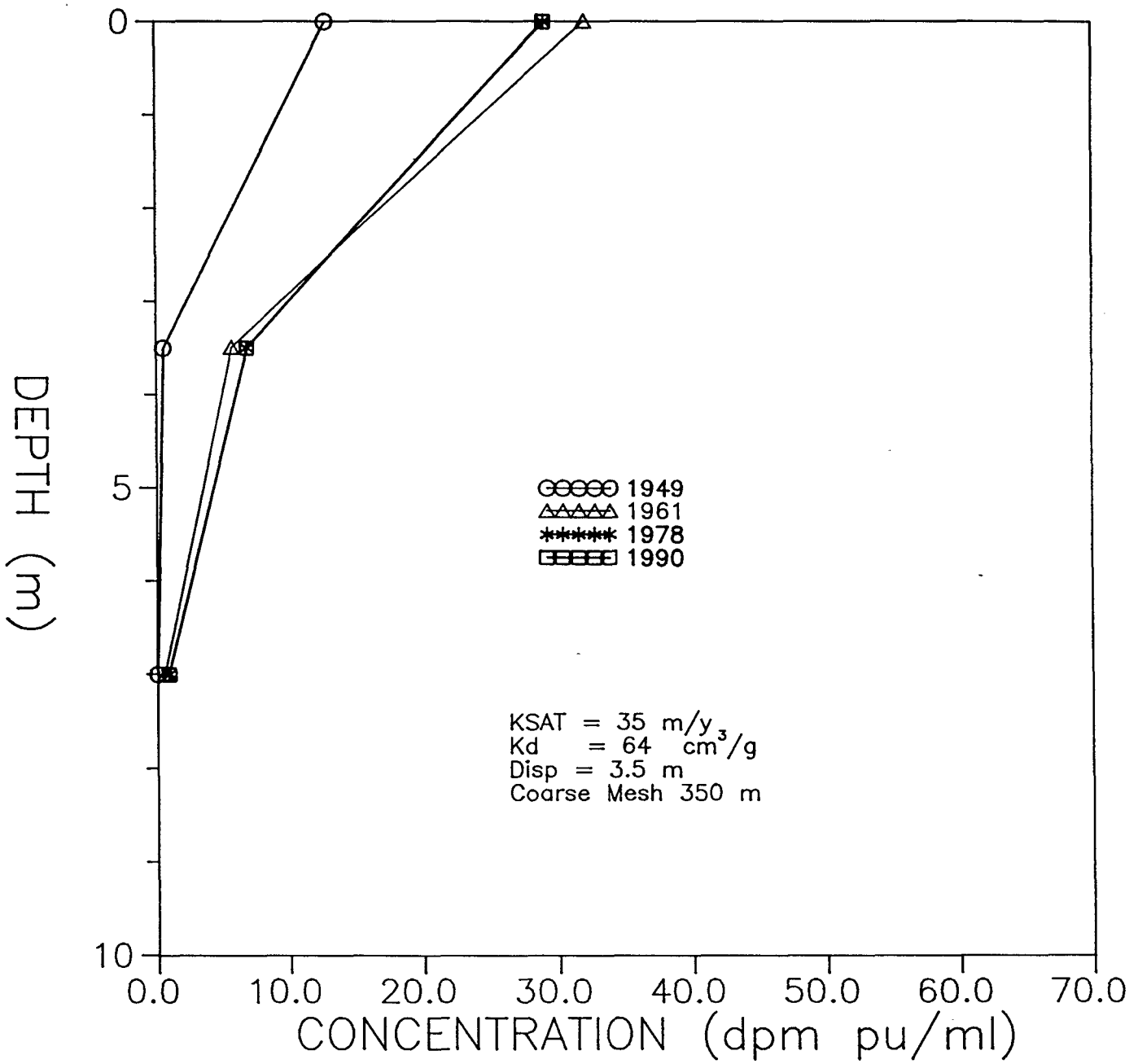


Figure 5.12. Sensitivity of Pu transport to mesh design (coarse mesh).

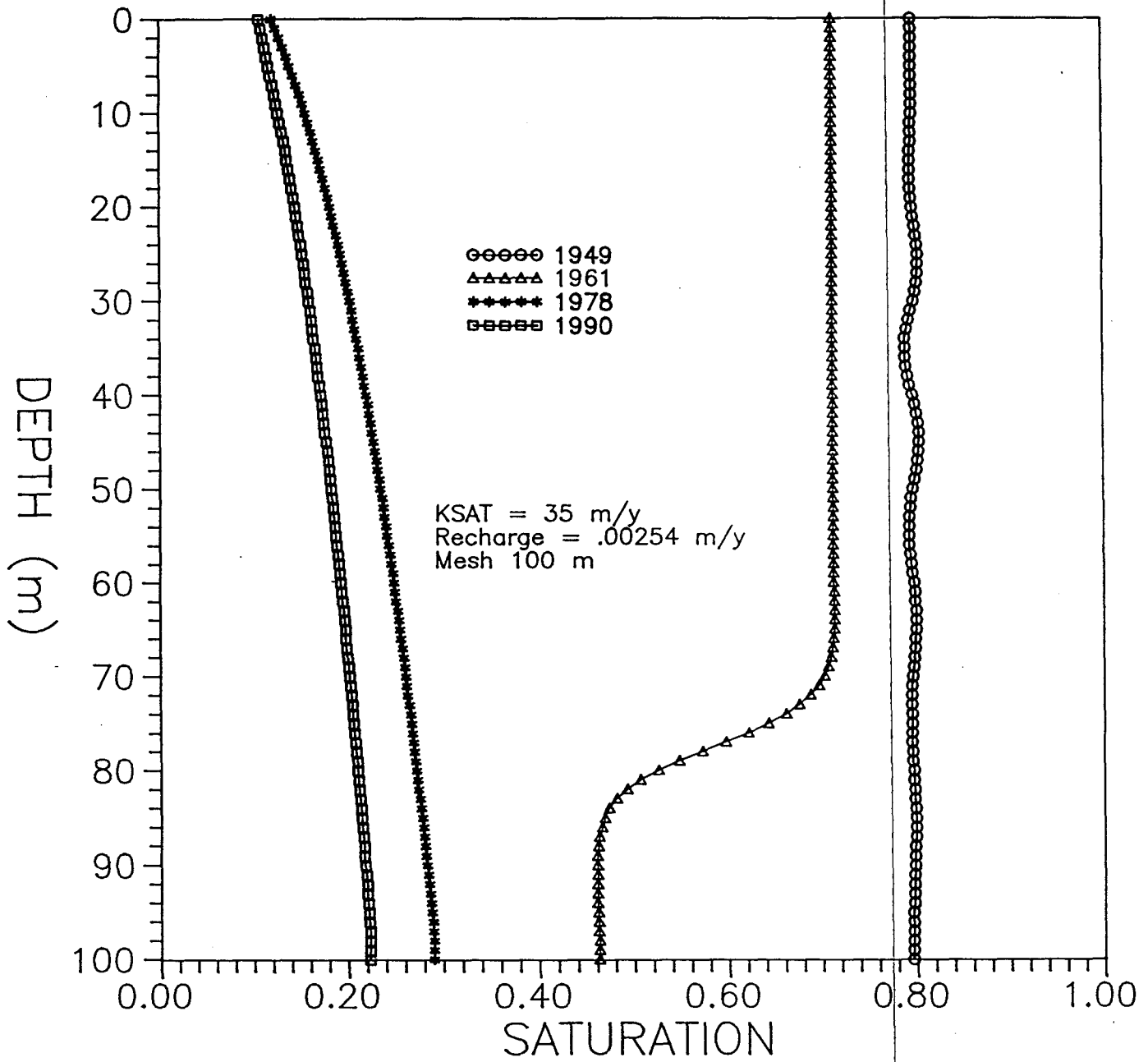


Figure 5.13. Sensitivity of saturation distributions to mesh design (fine mesh).

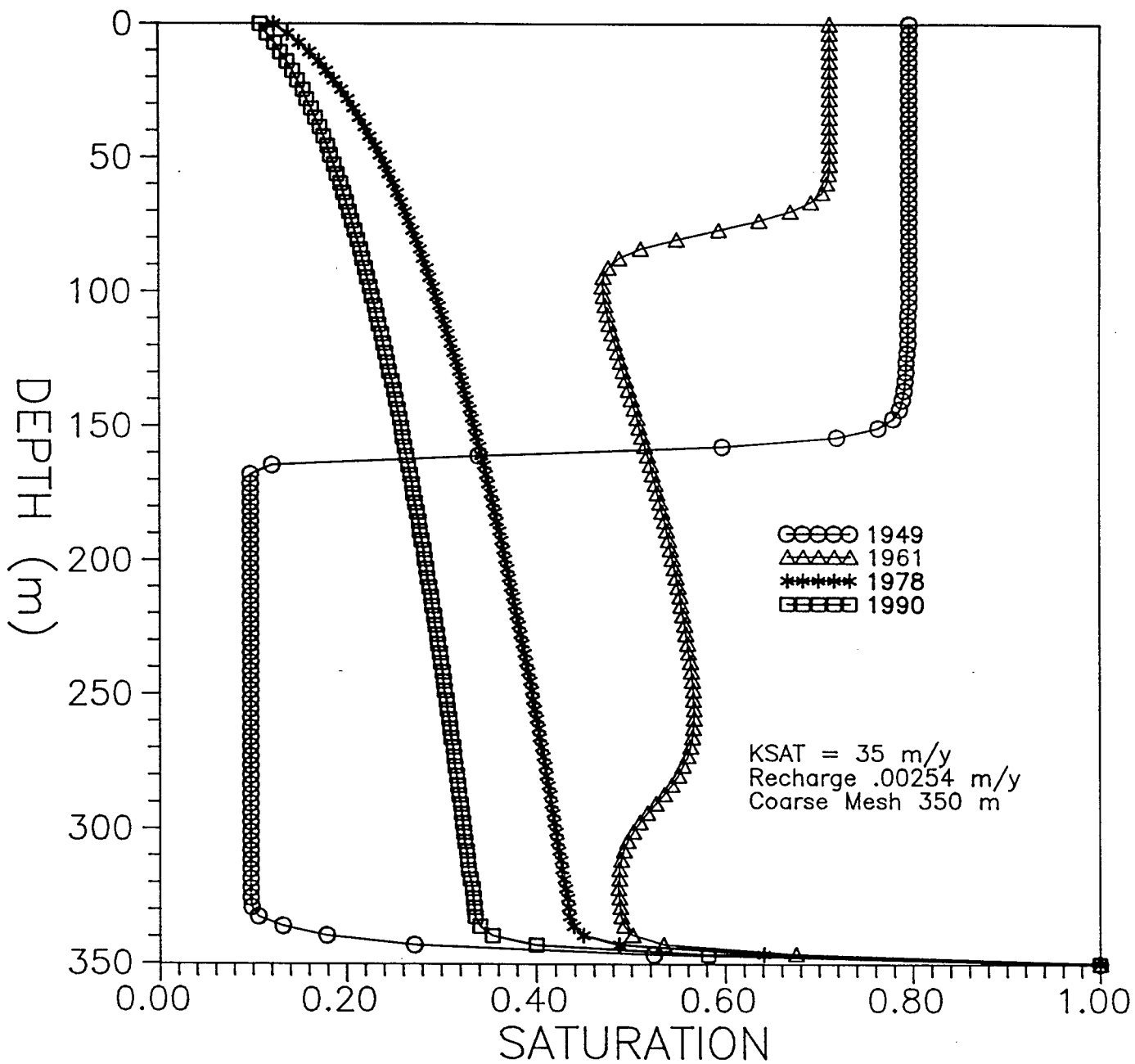


Figure 5.14. Sensitivity of saturation distributions to mesh design (coarse mesh).

---

sensitivity of predicted radionuclide transport to this variation in the hydraulic parameters for the Bandelier tuff. Results of varying  $n$  between 1.0 and 4.5 on plutonium transport are shown in Figure 5.15 through 5.18. It can be seen that the lower value of  $n$  results in a more dispersed concentration profile and faster travel times. Although the location of the peak concentration at a given time value is little affected by changes in  $n$ , a lower value of  $n$  results in a greater predicted depth of radionuclide penetration.

#### 5.2.3.2 Leading Coefficient $\alpha$ of the Relative Permeability versus Saturation Relationship

The  $\alpha$  value obtained from the least squares fit discussed in Section 4.2 is  $0.423 \text{ m}^{-1}$ . The sensitivity of the radionuclide transport to this  $\alpha$  value was evaluated by performing two sensitivity simulations. In the first simulation  $\alpha$  was assigned a value of 0.1 (Figure 5.19), while in the second simulation  $\alpha$  was assigned a value of 0.8 (Figure 5.20). The results from these simulations indicate that at a  $K_d$  of 13, which was used for all of the Case scenarios discussed in Section 5.5, the transport of radionuclides is very insensitive to  $\alpha$ .

#### 5.2.3.3 Leading Coefficient $\beta$ of the Relative Permeability versus Saturation Relationship

The  $\beta$  that was obtained from the least squares fit discussed in Section 4.2 has a value of 2.217. The sensitivity of the radionuclide transport to this value of  $\beta$  was evaluated by performing two sensitivity simulations. In the first simulation  $\beta$  was assigned a value of 1.5 (Figure 5.21), while in the second simulation  $\beta$  was assigned a value of 4.0 (Figure 5.22). The results from these simulations indicate that at a  $K_d$  of 13, which was used for all of the Case scenarios discussed in Section 5.5, the transport of radionuclides is very insensitive to  $\beta$ .

#### 5.2.4 Saturated Hydraulic Conductivity

Restricting the sensitivity analysis to one-dimension precludes evaluation of the effects of variations in the ratio of horizontal to vertical hydraulic conductivity. The effect of hydraulic conductivity was investigated in the sensitivity analysis by varying the saturated hydraulic conductivity while maintaining the same relationship between relative conductivity and saturation. Since the actual hydraulic conductivity at any saturation value is the product of saturated and relative conductivity, varying saturated hydraulic conductivity also changes conductivity over the entire range of saturations.

The saturated hydraulic conductivity is estimated for the Bandelier tuff to range from 6.3 - 148 m/y (Abee and others, 1981). To estimate the sensitivity of the system to the saturated hydraulic conductivity several runs were made at different saturated hydraulic conductivities. The results indicate that the lower bound of saturated hydraulic conductivity is approximately 35 m/y; at values lower than 35 m/y, HYDRUS predicted

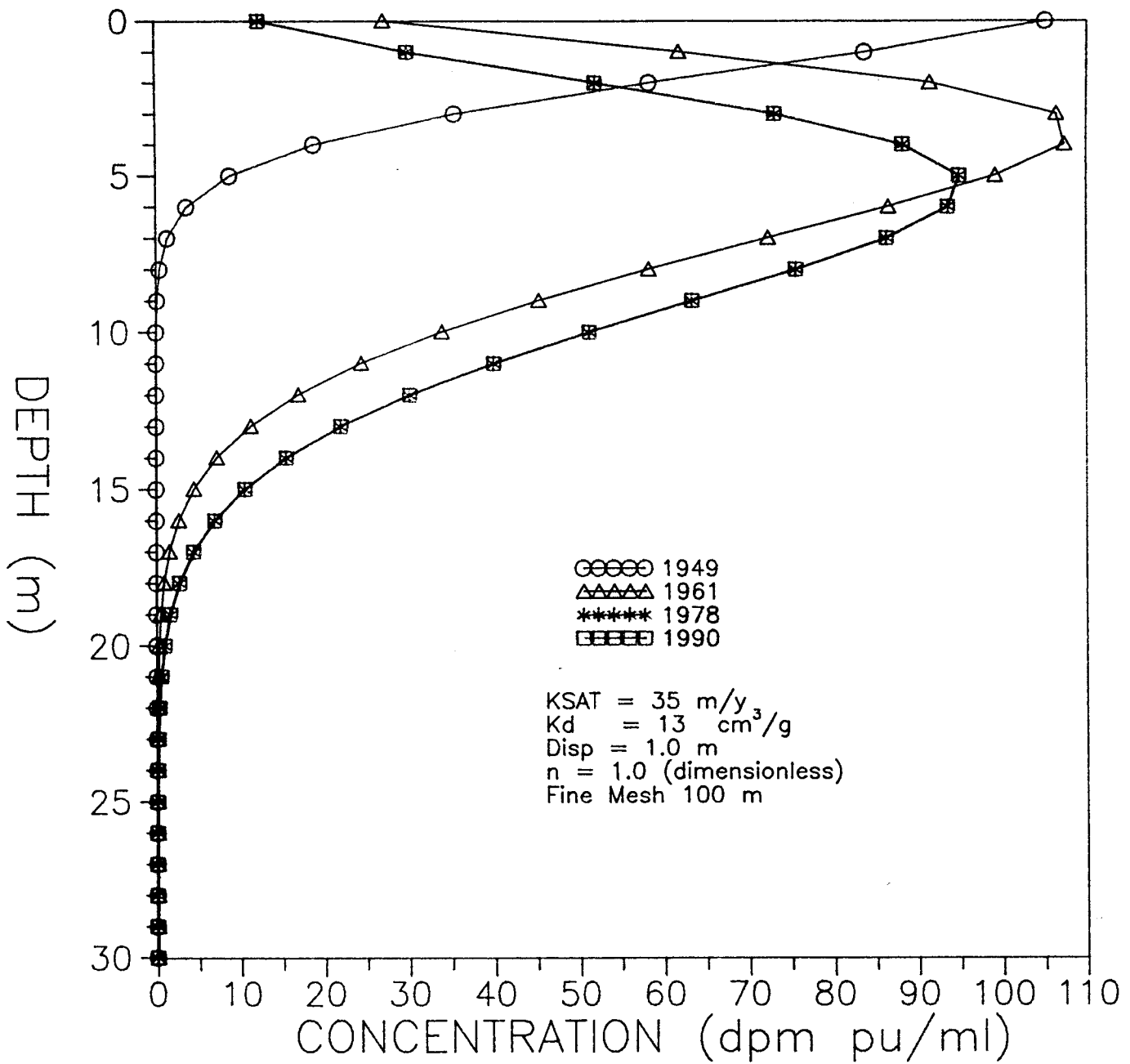


Figure 5.15. Sensitivity of transport to power index (n) of the relative permeability versus saturation relationship.

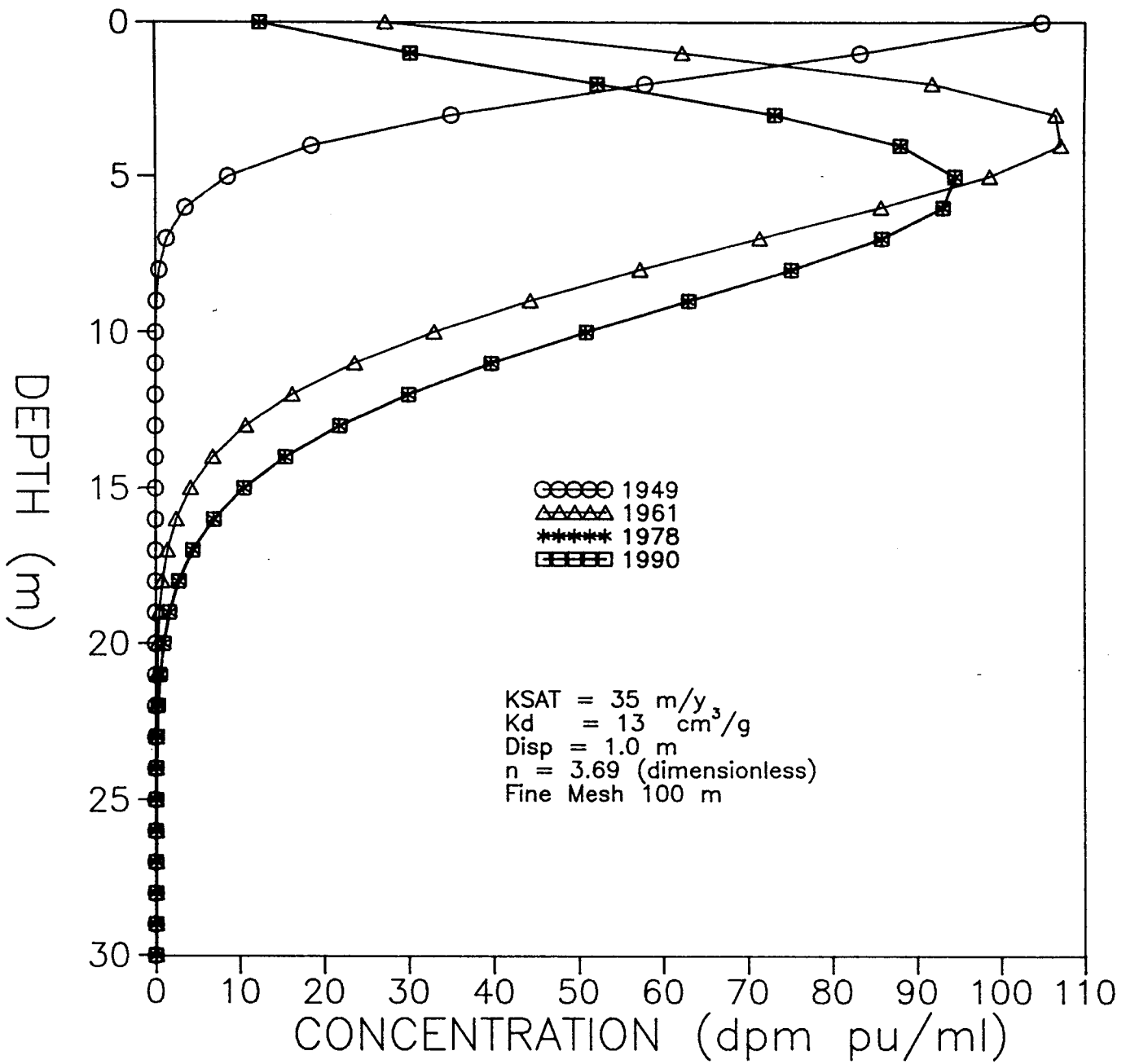


Figure 5.17. Sensitivity of transport to power index (n) of the relative permeability versus saturation relationship.

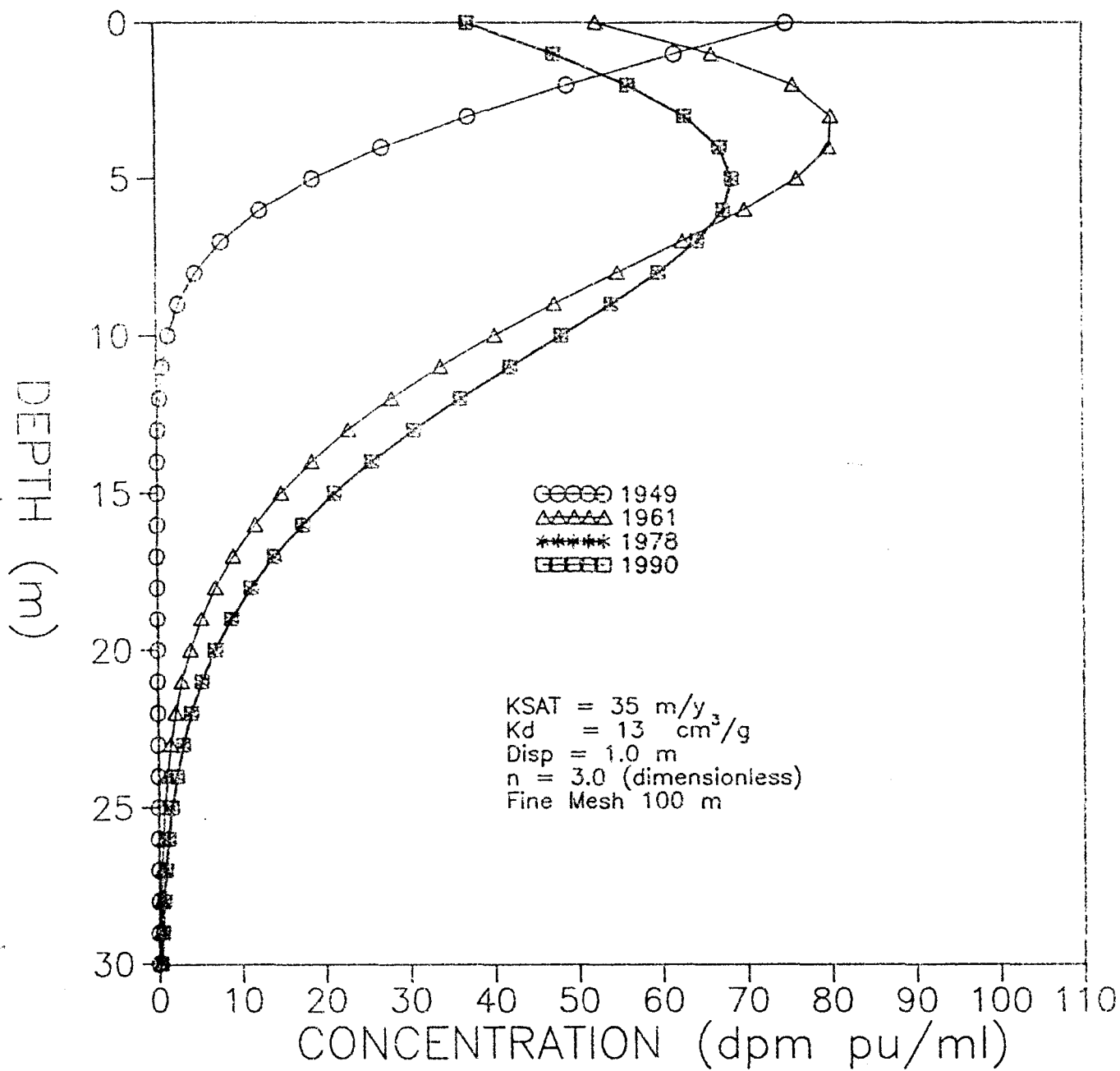


Figure 5.16. Sensitivity of transport to power index (n) of the relative permeability versus saturation relationship.

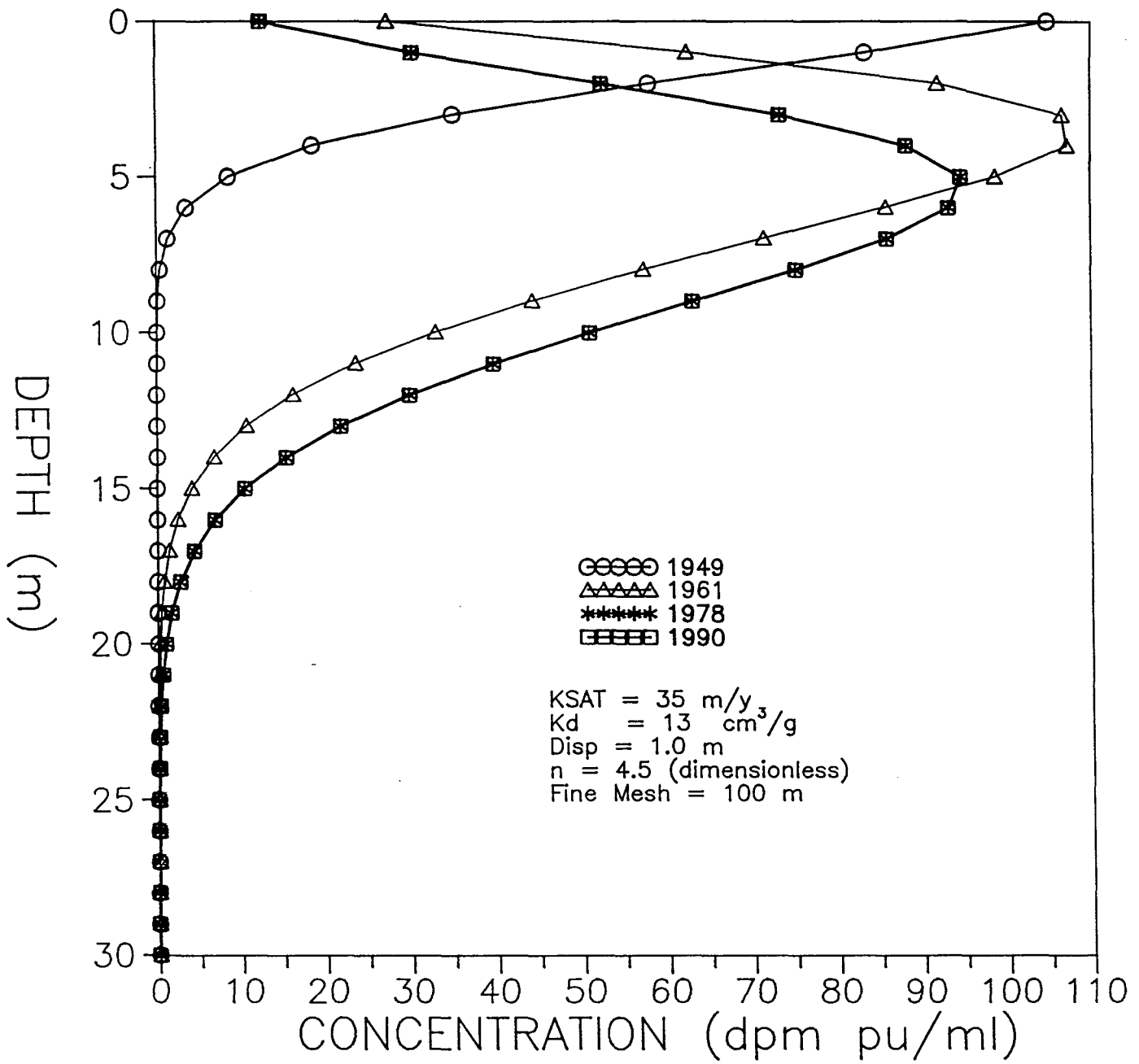


Figure 5.18. Sensitivity of transport to power index (n) of the relative permeability versus saturation relationship.

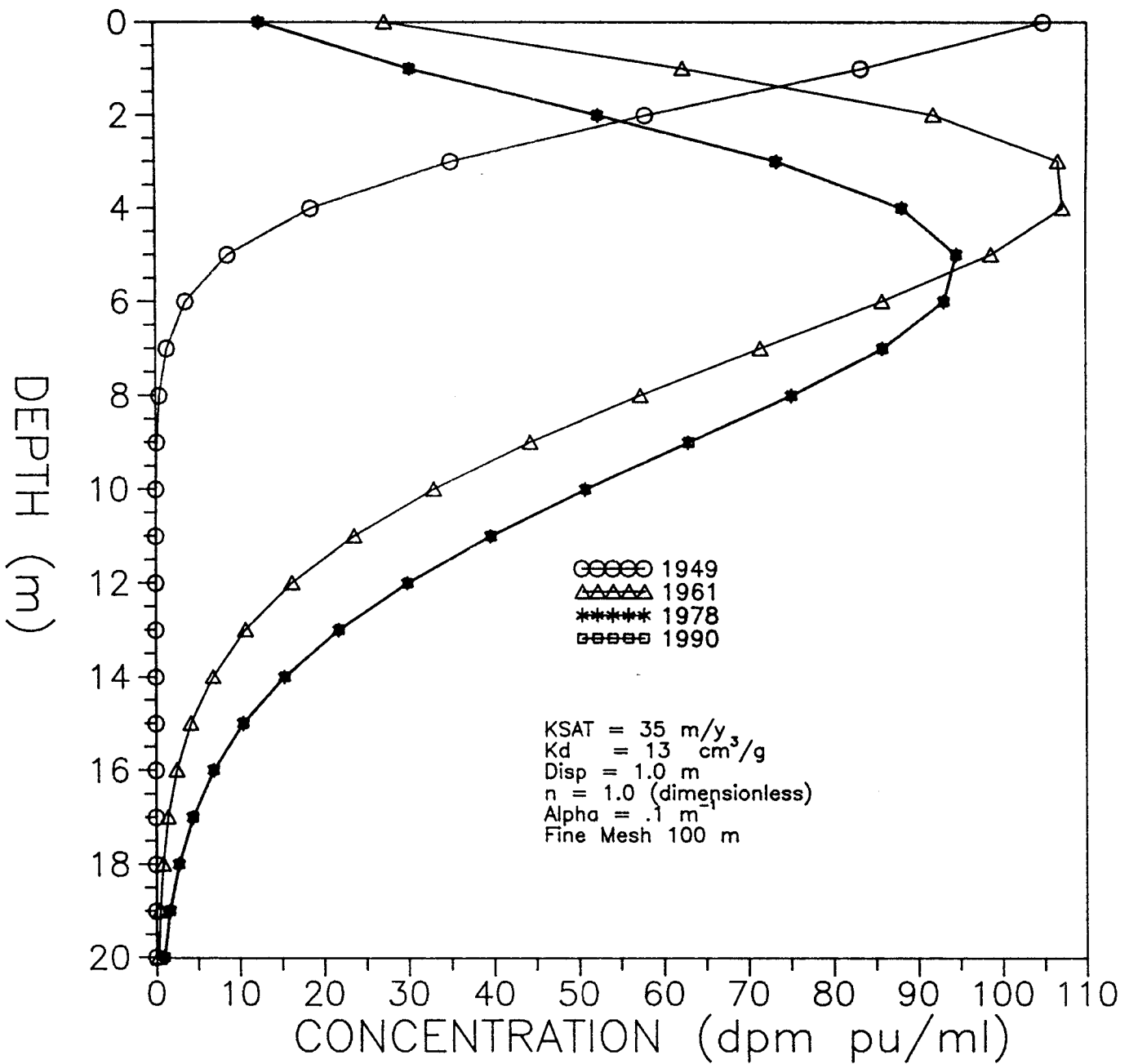


Figure 5.19. Sensitivity of transport to the leading coefficient ( $\alpha$ ) of the saturation versus capillary head relationship.

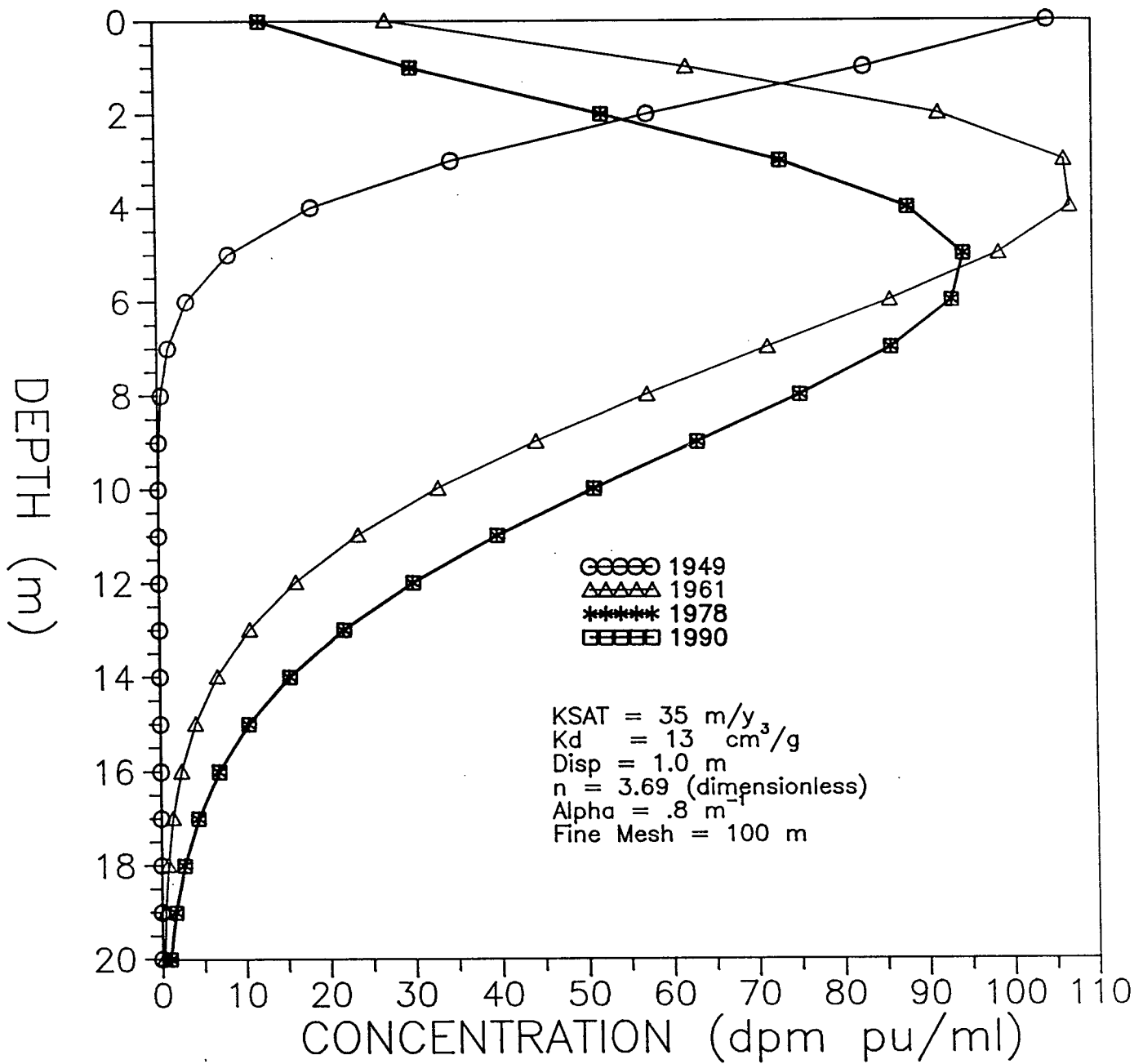


Figure 5.20. Sensitivity of transport to the leading coefficient ( $\alpha$ ) of the saturation versus capillary head relationship.

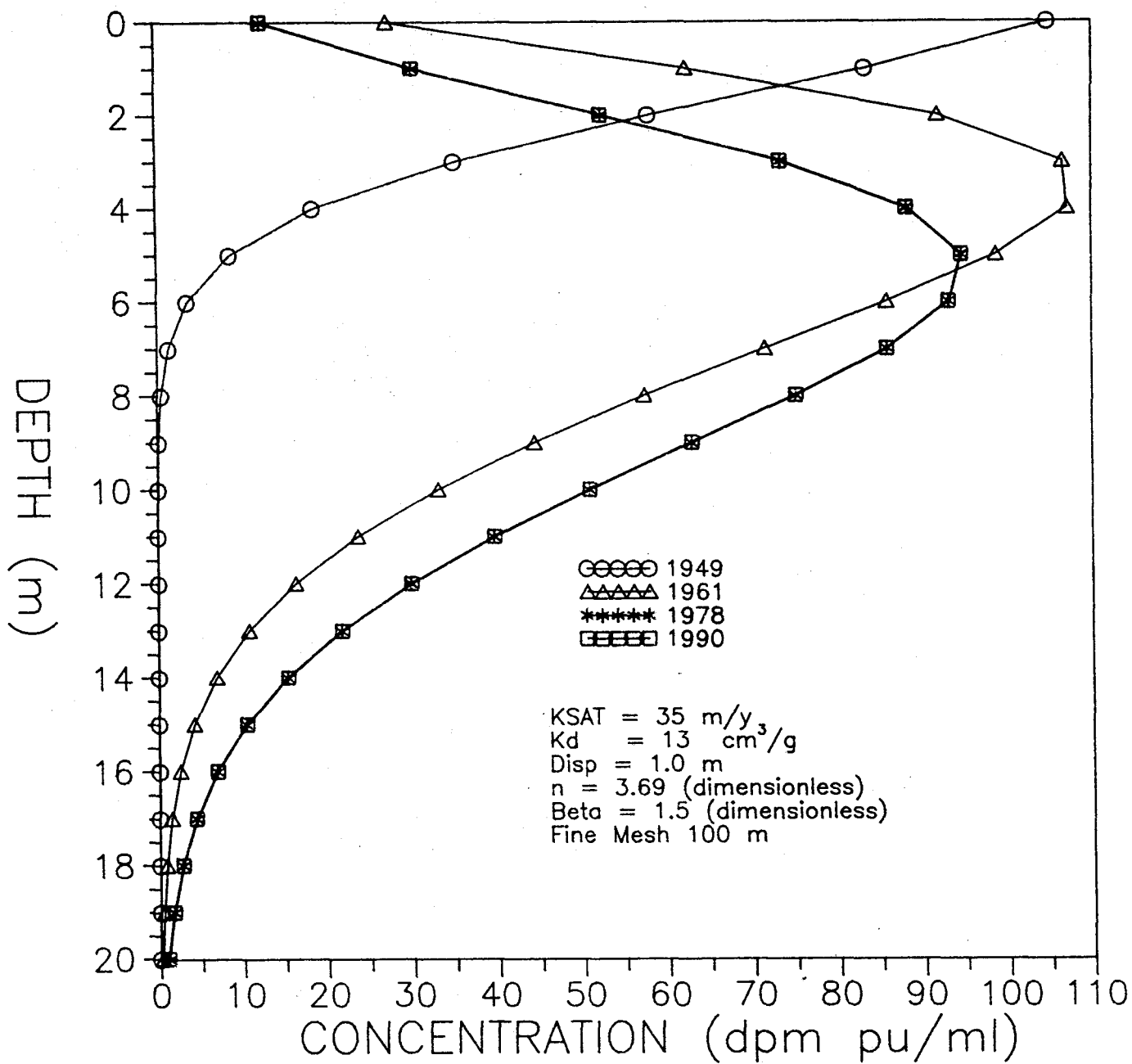


Figure 5.21. Sensitivity of transport to the power index ( $\beta$ ) of the saturation versus capillary head relationship.

NO. 10000 CLEARPRINT

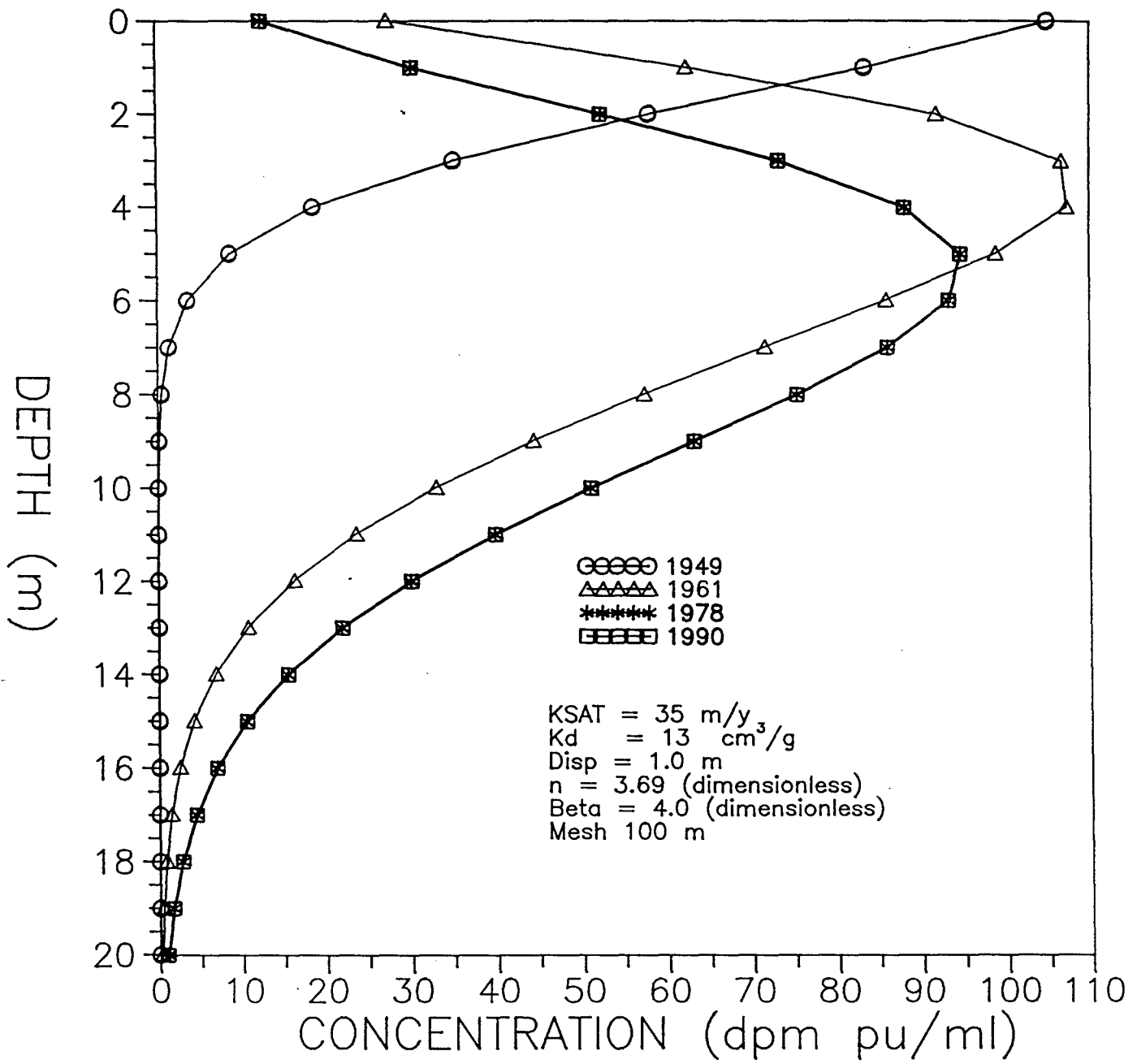


Figure 5.22. Sensitivity of transport to the power index ( $\beta$ ) of the saturation versus capillary head relationship.

---

the occurrence of fully saturated conditions underneath the bed during the periods of highest waste water discharges. The flow simulations performed in Section 5.5 all used a saturated hydraulic conductivity of 35 m/y.

Changes in the saturated hydraulic conductivity will alter the simulated vertical distribution of moisture content (Figures 5.23 and 5.24) and radionuclides (Figures 5.25 and 5.26).

The analysis suggests that saturated hydraulic conductivity must be raised by an order of magnitude before there are significant differences in transport times.

### 5.2.5 Dispersivity

Site specific data are lacking on the magnitude of dispersivity. The value of 3.5 m used in the transport simulations was determined as 1 percent of the total distance between disposal bed and the water table and are in accordance with accepted estimates (Gelhar and others, 1985). This range of values is not unrealistic for the site. Dispersivity values on the order of several meters are consistent with the fractured nature of the tuff underneath the disposal bed.

The sensitivity of the transport simulations to dispersivity is evaluated through a simplified approach. The value of vertical longitudinal dispersivity for the rocks at Los Alamos is unknown, but is estimated to lie within the range of 1 to 3.5 meters. This is based on the general indication that dispersivity is dependent on the scale of the problem and commonly falls within the range of 1 to 30 percent of the pathway length. The majority of the initial sensitivity runs are performed with dispersivity set to 1 meter. For comparison, additional simulations are performed with dispersivity set to 3.5 meters. The results illustrated in Figures 5.26 and 5.27 indicate that dispersivities of 3.5 m allow radionuclides to migrate faster than dispersivities of 1.0 m, although mean velocities are not significantly different. Therefore, to be conservative a value of 3.5 m is used for dispersivities in the transport scenarios discussed in Section 5.5.3.

### 5.2.6 Volume of Water Added to Bed 1

The volume of water added to bed 1 is one of the most important factors controlling the rate and distance of radionuclide migration. The scenarios performed in Section 5.5 all assumed that 55 percent of the total flux added to the absorption beds was actually received by absorption bed 1. Historical records and field evidence suggest that 55 percent of the total flux is probably an upper bound to the actual volume of water that infiltrated below bed 1. However, this conservative approach was adopted to ensure that the fastest anticipated travel times are obtained for the design of the remedial investigation.

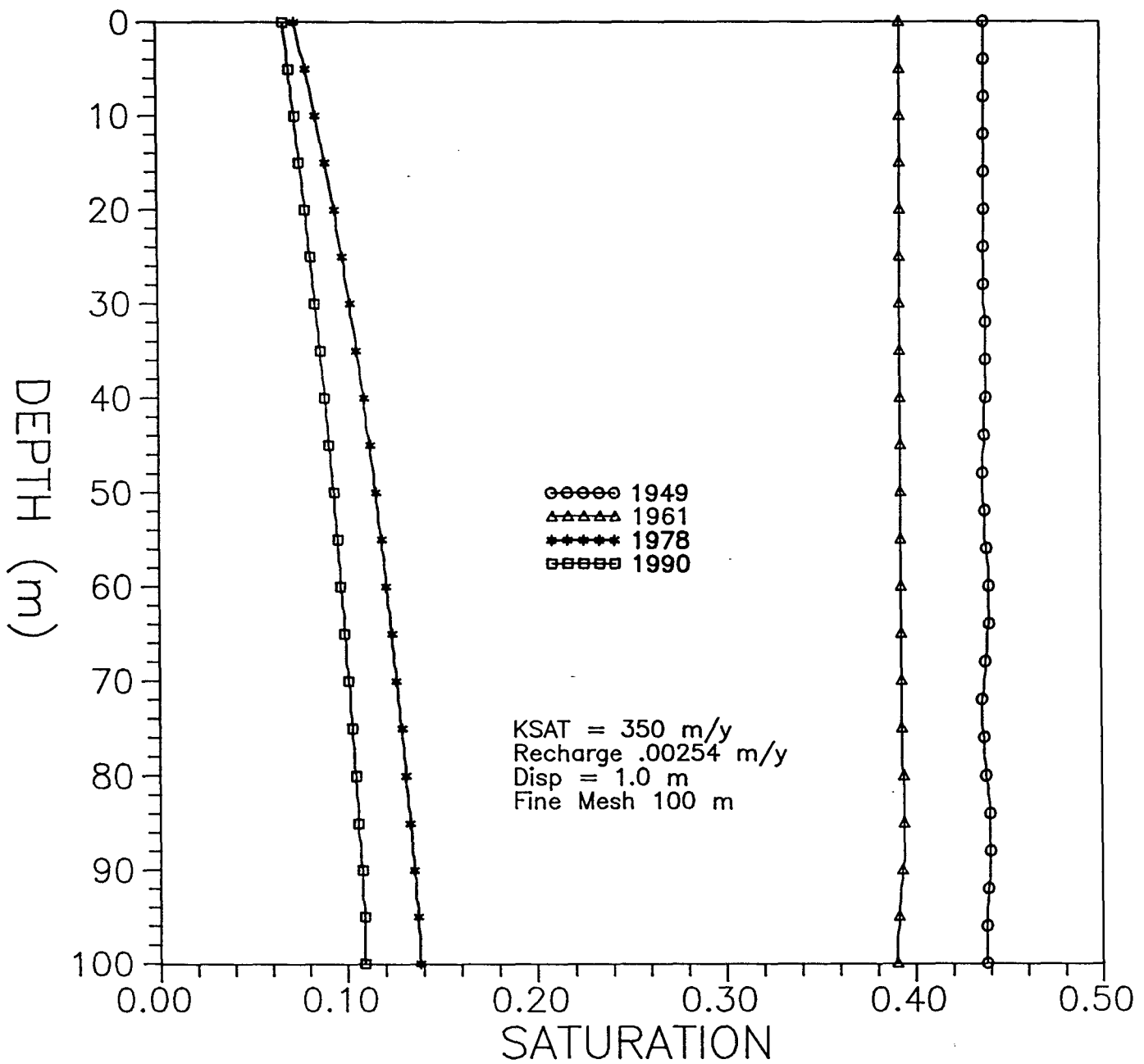


Figure 5.23. Sensitivity of saturation distributions to saturated hydraulic conductivity.

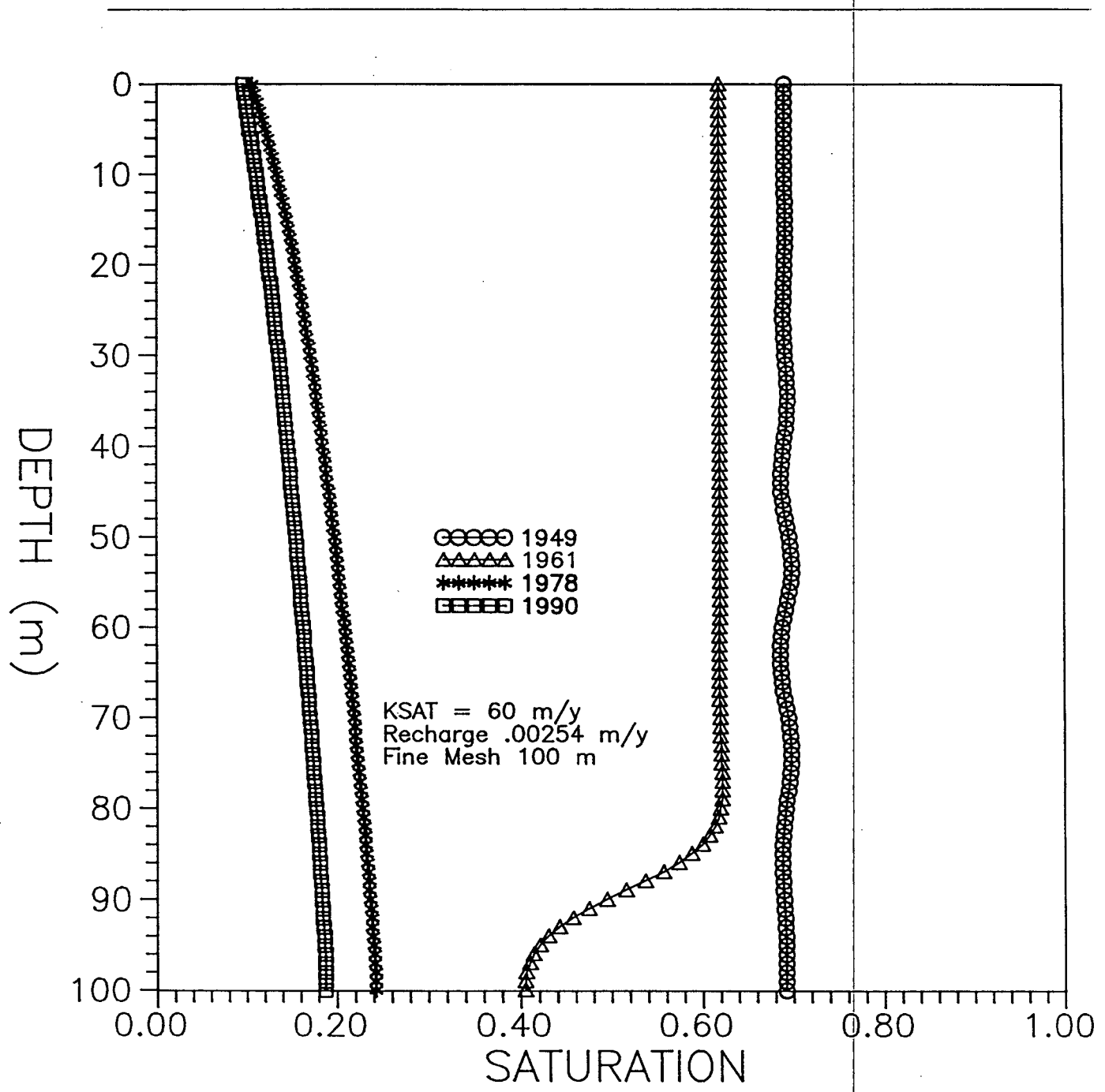


Figure 5.24. Sensitivity of saturation distributions to saturated hydraulic conductivity.

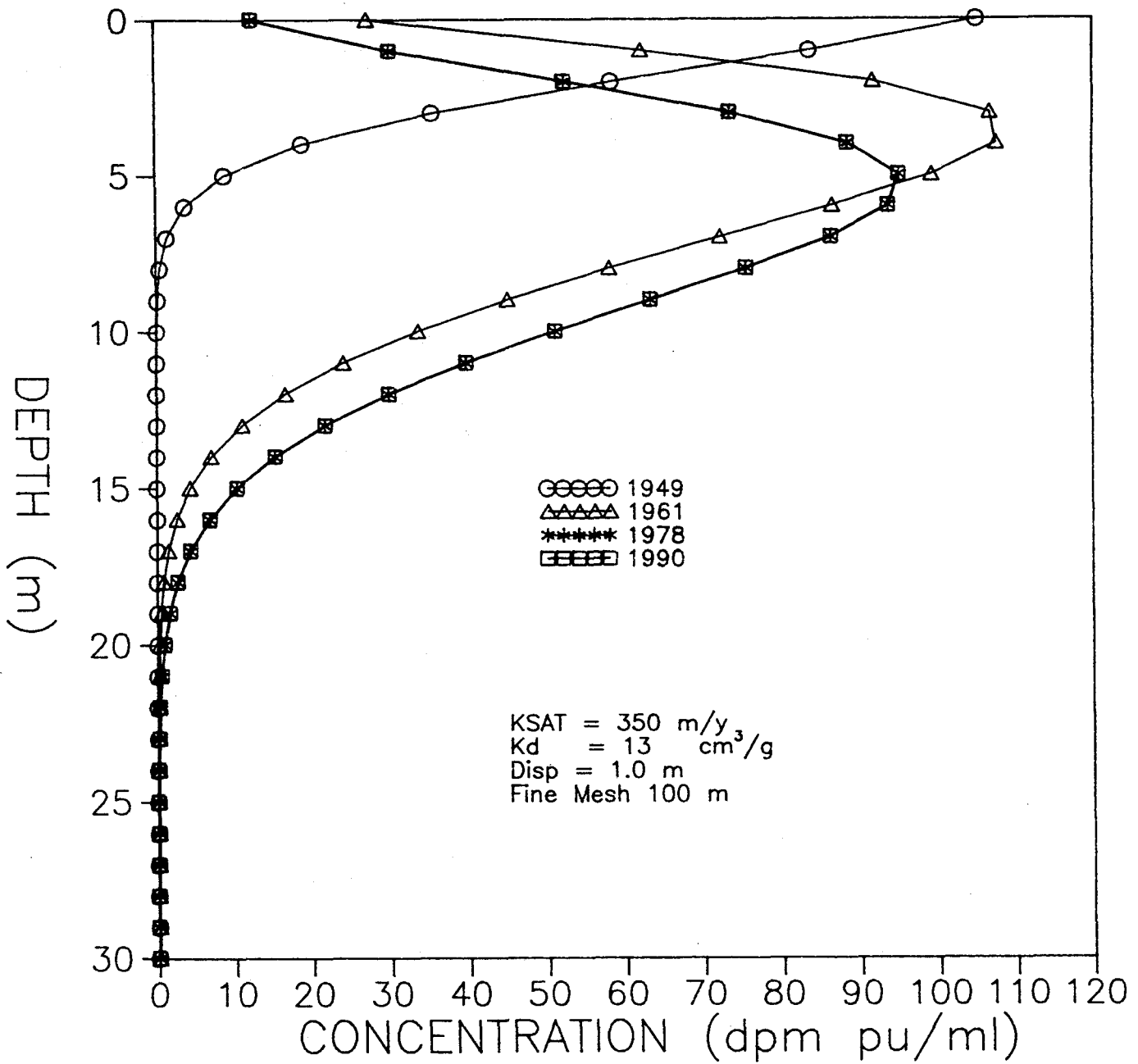


Figure 5.25. Sensitivity of Pu transport to saturated hydraulic conductivity.

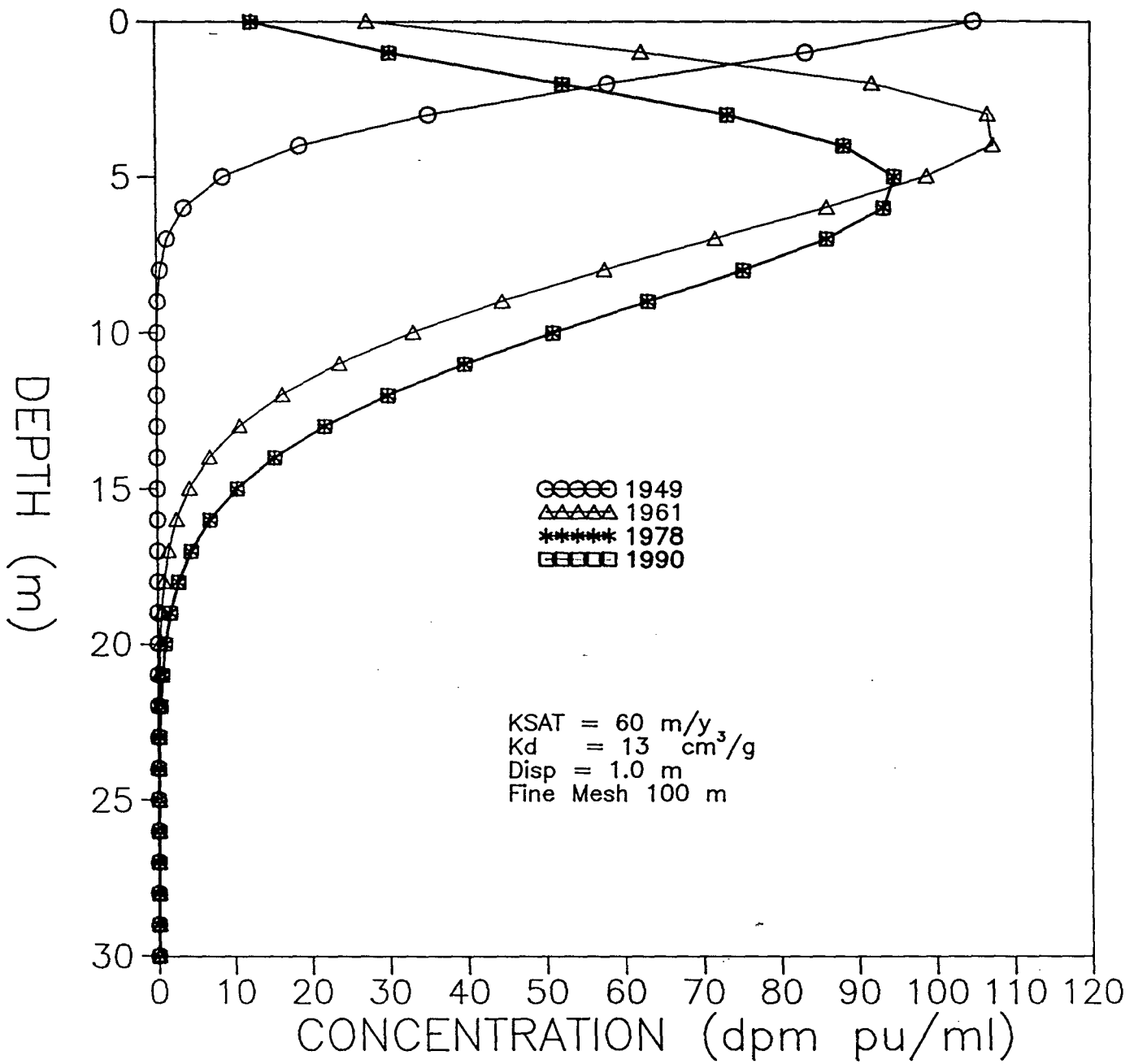


Figure 5.26. Sensitivity of Pu transport to saturated hydraulic conductivity and dispersivity.

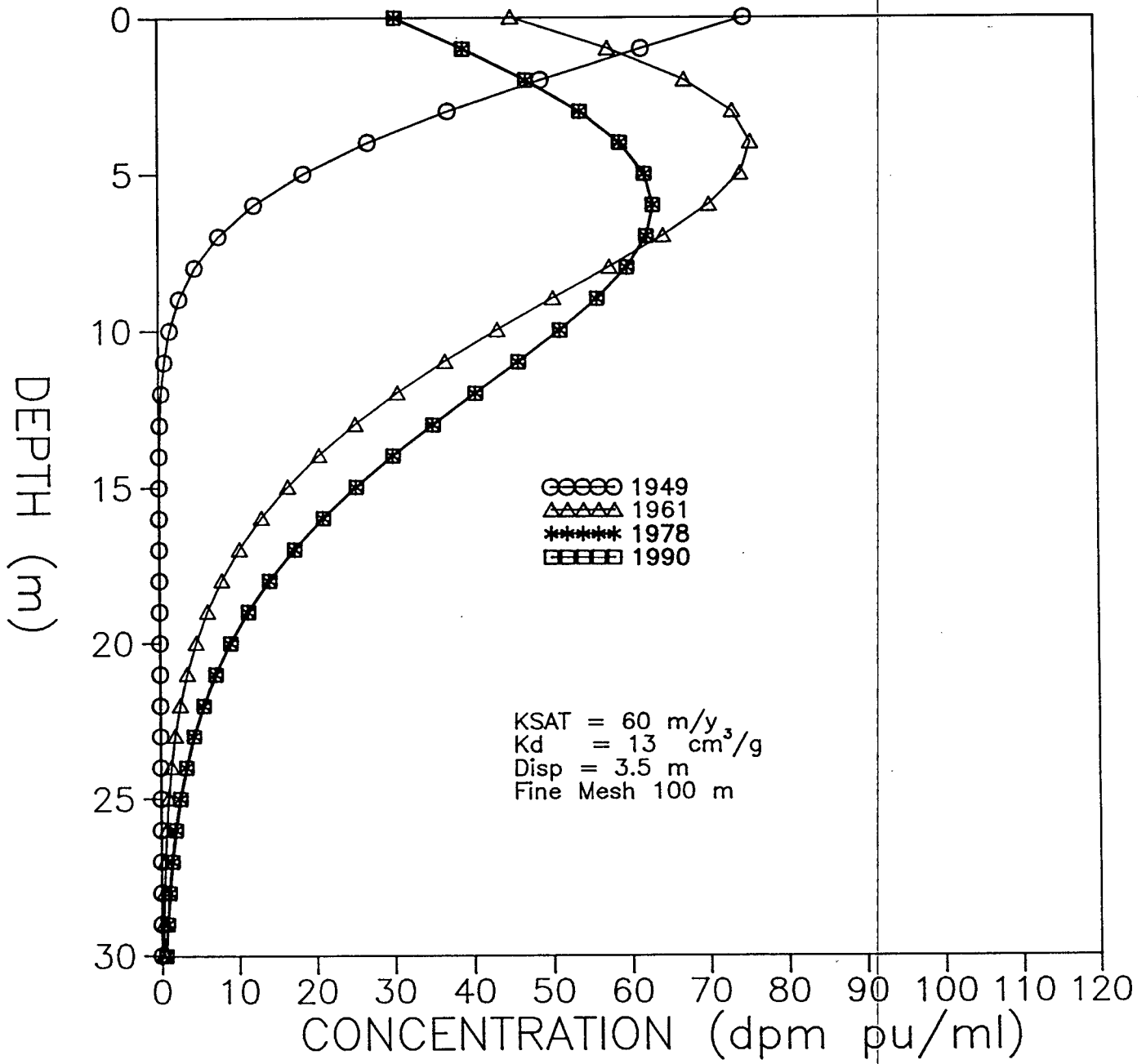


Figure 5.27. Sensitivity of Pu transport to dispersivity.

---

The uncertainty associated with the estimated volume of water added to bed 1 required that several simulations be performed in which the volume of water is sharply reduced. The first simulation used identical input as Scenario II.2 (Section 5.5.2.2), except that only 25 percent of the total flux was added to the absorption bed (Figure 5.28). The second simulation not only input 25 percent of the total flux but also reduced the saturated hydraulic conductivity from 35 m/y to 20 m/y (Figure 5.29).

The results of the simulations illustrate that even at reduced fluxes and saturated hydraulic conductivities, water would have infiltrated well beyond the upper 30 meters in the very early history of MDA T.

### 5.3 Historical Data Comparisons

Field data pertaining to moisture and radionuclide values are available for the years 1961 and 1978. Due to the undefined heterogeneity in the subsurface rocks and uncertainties in waste discharge rates and chemistry, a strict matching between the simulation results and the measured saturation and radionuclide values cannot be made. However, if general trends between the simulated output and the field data are compared and explained, a better understanding is gained of the processes that govern the water movement and migration of radionuclides in the unsaturated zone.

The sensitivity analysis (Section 5.2) suggests that the factors exhibiting the most control over the movement of water and transport of radionuclides are the saturated hydraulic conductivity and the distribution coefficients. To investigate the respective roles of these properties a series of simulations were performed in which all other input remained constant (Table 5.2). The objective of these simulations is to further characterize the probable rates, distributions, and controlling mechanisms of radionuclides and moisture movement through the rocks.

Field sampling results for subsurface distribution of moisture content and plutonium concentration in 1978 are shown in Figures 5.30 and 5.31. The sharp spikes on the measured moisture and radionuclide curves recorded in the field during 1978 have several interpretations. One interpretation is that these spikes are representative of high moisture and radionuclide pulses moving slowly downward through the rock strata. An alternative interpretation is that the spikes are related directly to the rock properties of the strata in which they are exhibited. That is, rocks that are very fine grained and have a high clay content will tend to adsorb greater amounts of radionuclides and will also maintain a greater water saturation through stronger forces of capillary attraction. Therefore, the spikes may not be discharge pulses but rather a measure of the ability of the different strata to adsorb radionuclides and to retain water.

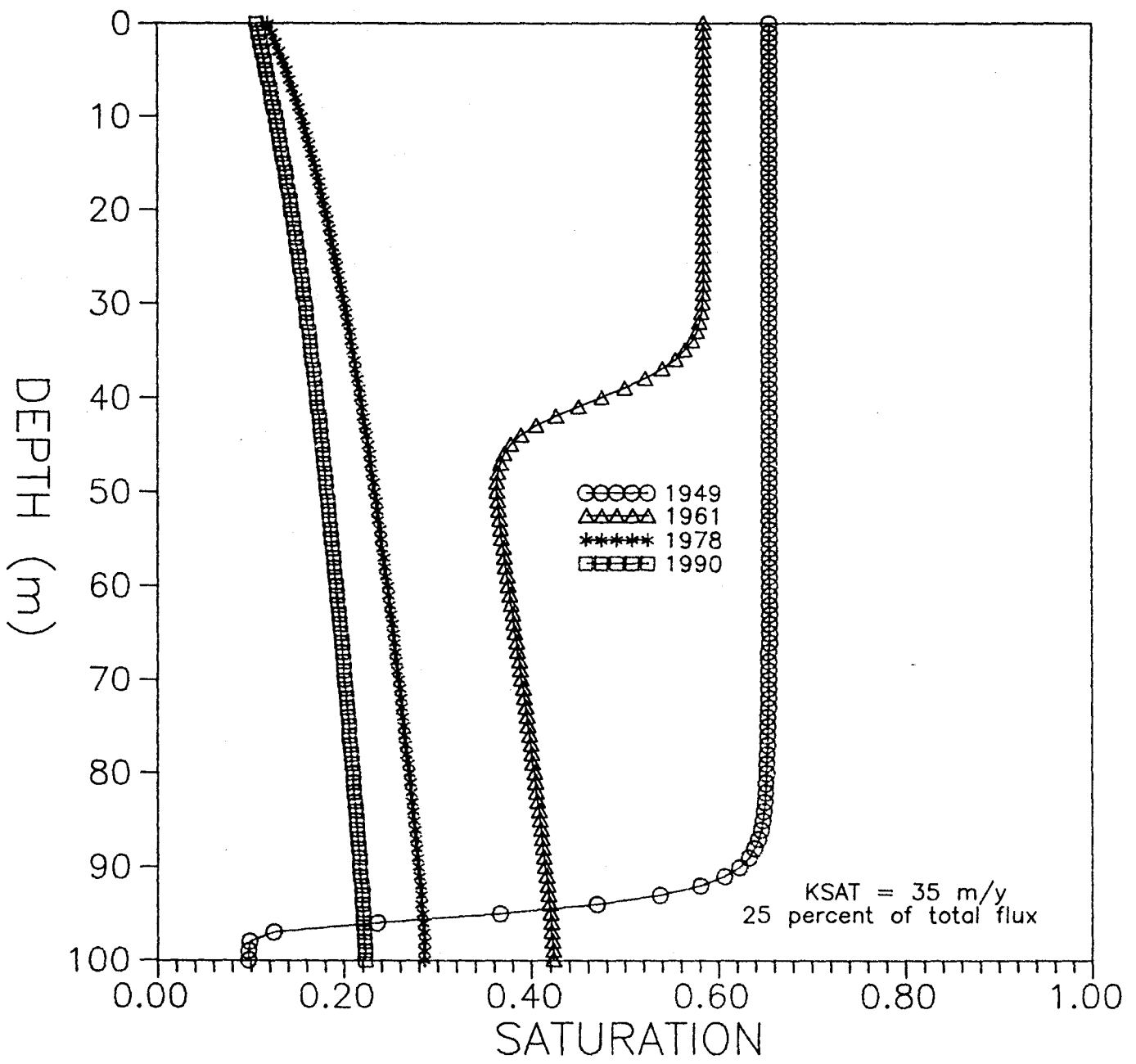


Figure 5.28. Sensitivity of saturation distribution to volume of water added to absorption bed.

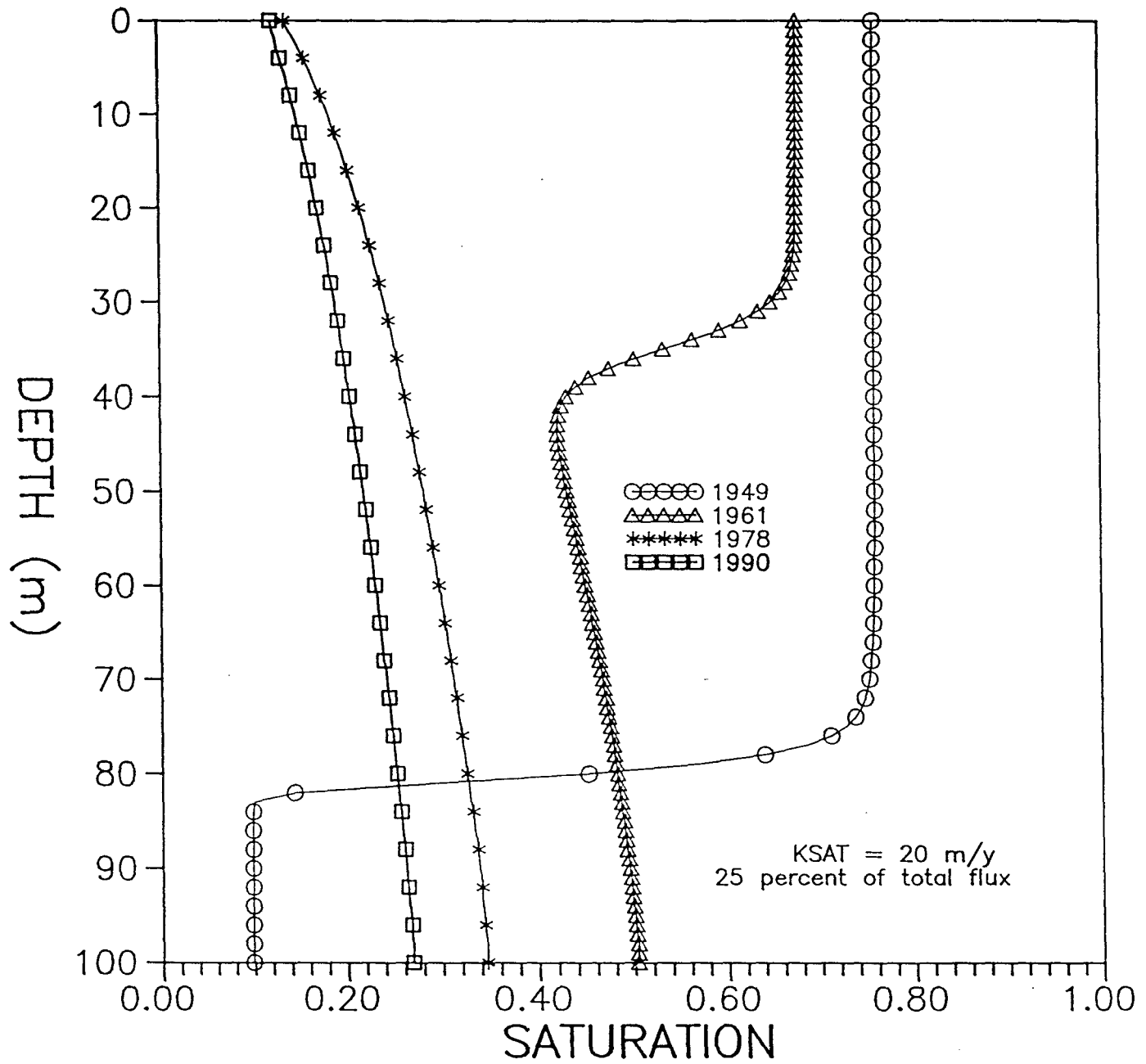


Figure 5.29. Sensitivity of saturation to volume of water added to absorption bed in conjunction with a lower hydraulic conductivity.

Table 5.2. Parameter input for historical comparisons.

Input Parameter	Value
1. Saturated hydraulic conductivity (m/y)	Variable
2. Residual water saturation	.0097
3. Power index (n) of the relative permeability versus saturation relationship (dimensionless)	3.69
4. Leading coefficient (alpha) of the saturation versus capillary head relationship ( $m^{-1}$ )	.423
5. Power index (beta) of the saturation versus capillary head relationship (dimensionless)	2.217
6. Porosity (dimensionless)	.4
7. Bulk Density ( $g/cm^3$ )	1.55
8. Longitudinal Dispersivity (m)	3.5
9. Distribution coefficient	Variable
10. Flux rates	(see Table 5.8)
11. Concentration values	(see Figure 5.63)

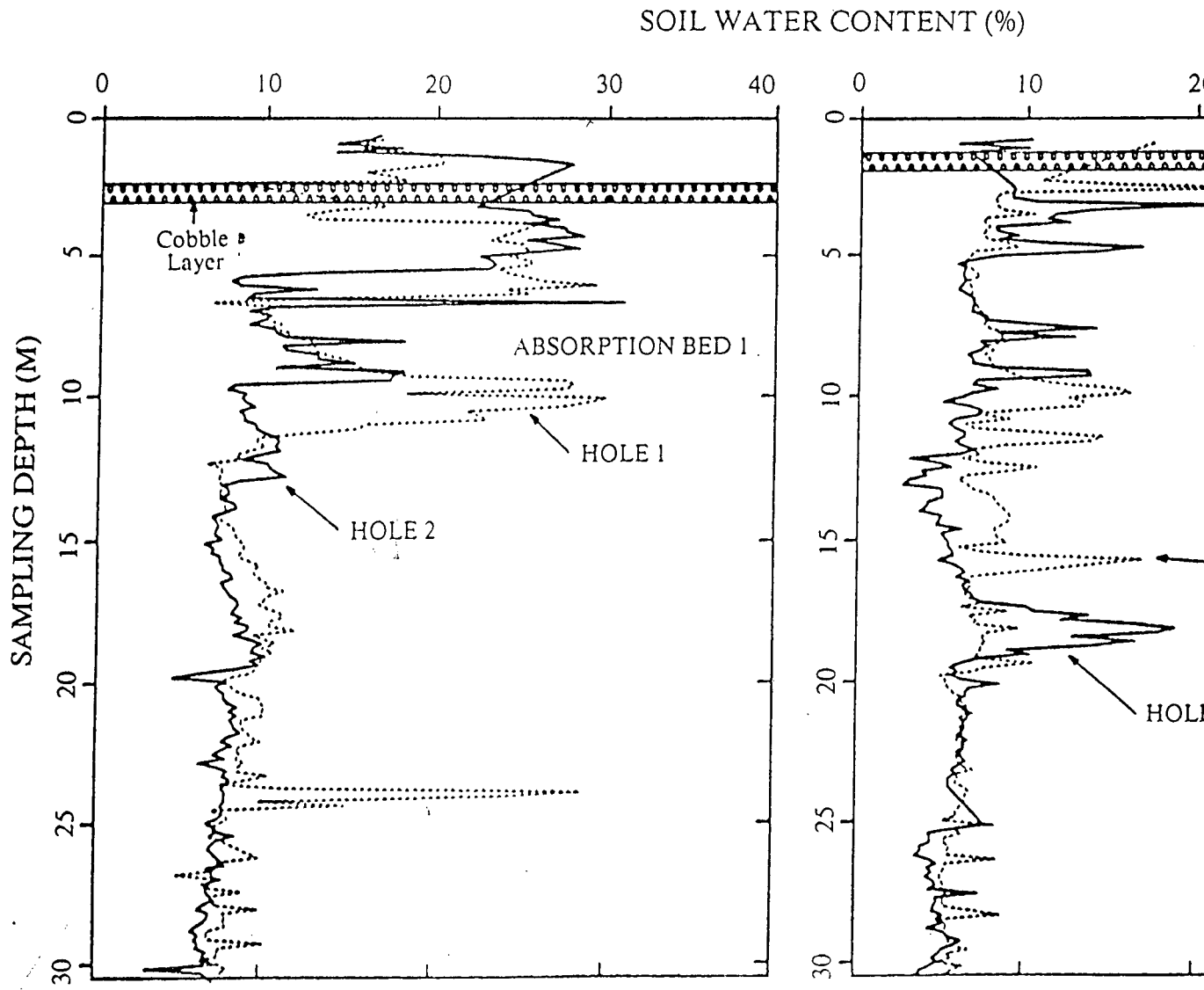


Figure 5.30. Gravimetric soil water content as a function of sampling depth for absorption beds 1 and 2 in 1978.

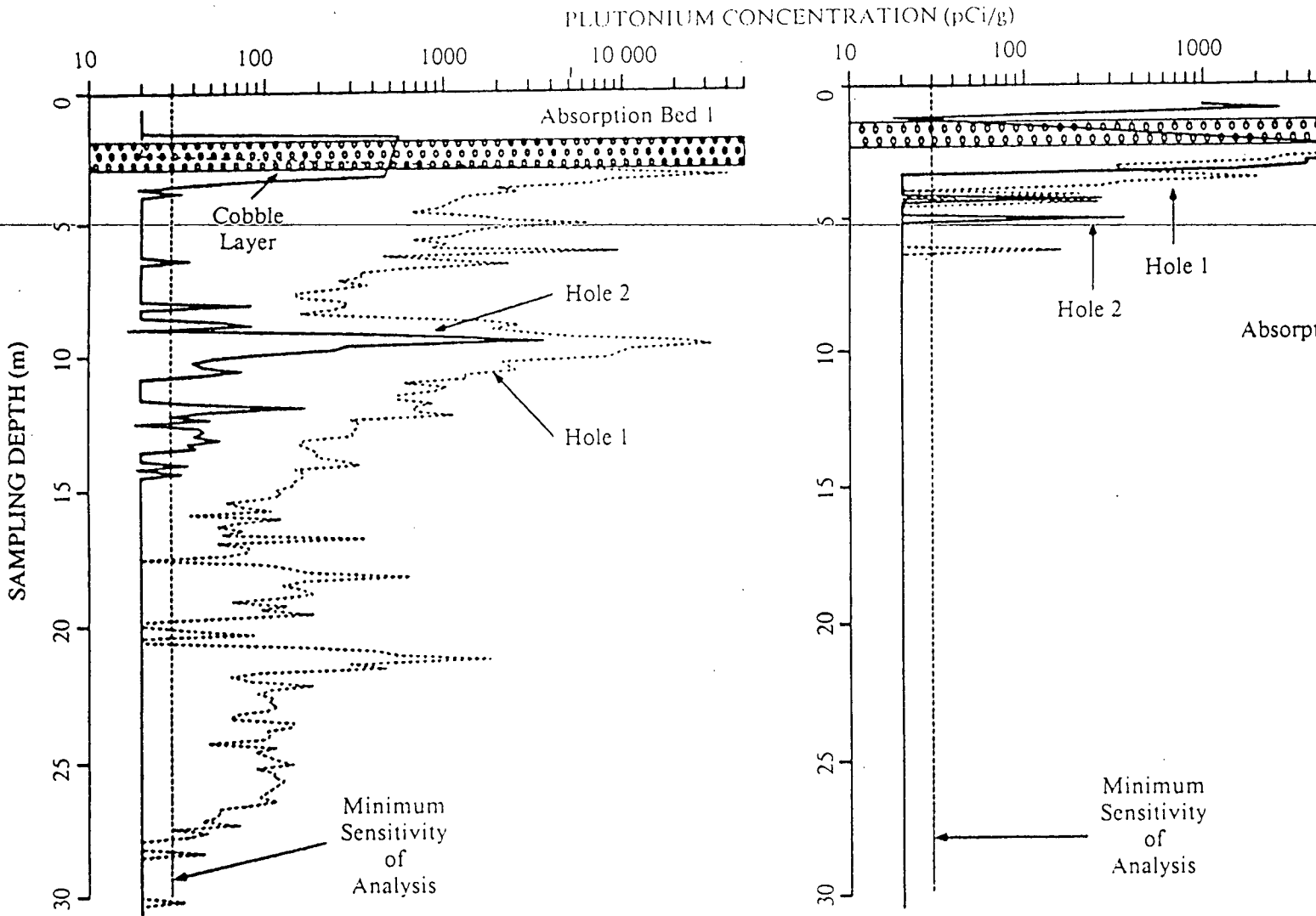


Figure 5.31. Concentration of plutonium as a function of sampling depth for absorption beds 1 and 2 in 1978.

---

It is important to determine which interpretation is more accurate as this will have major implications in the design of the remedial investigation program. If it is assumed that zones of elevated moisture content and radionuclide concentrations merely reflect the downward migration of past waste discharge pulses, then one could compute water flux and travel times by measuring the rate of vertical movement of these peaks with time. On the other hand, if the moisture and radionuclide peaks are controlled more by lithology, the moisture peaks would tend not to move vertically but simply decrease in magnitude as the fine grained rocks dry out. The movement and concentrations of radionuclides would be dependent on the distribution coefficients and hydraulic conductivities.

To investigate the role of distribution coefficients, and saturated hydraulic conductivities, the upper 100 m of the geologic system was divided into five separate layers. Each of the layers were assigned either different values of saturated hydraulic conductivities or different values of distribution coefficients in an attempt to reproduce the measured radionuclide and saturation curves.

In the following simulations, actual historical liquid waste flux and radionuclide loading rates are duplicated as closely as possible, corresponding to the input of Scenario II.2 (Section 5.5.2.2).

### 5.3.1 Distribution Coefficients

For each of these simulations the distribution coefficients are varied from one layer to the next while the saturated hydraulic conductivity is kept constant at 35 m/y. In general, the effect of changing the distribution coefficients in each of the layers independently, caused the predicted radionuclide concentrations in the rocks to exhibit sharp spikes that were similar to those observed in the field (Figures 5.32 through 5.36). Corresponding concentrations of radionuclides in the water phase tend to be relatively graded over the separate layers (Figures 5.37 through 5.41).

These observations support the premise that the sharp spikes are caused by different adsorption capacities of the individual layers and not by downward moving variable discharge pulses. Furthermore, the fact that the spikes represent concentrations of radionuclides measured in the rocks rather than in the water suggest that the spikes may be essentially independent of the waste-water pulses applied to the absorption beds.

### 5.3.2 Saturated Hydraulic Conductivity

To further investigate the relationship between the measured moisture distributions and hydraulic conductivity a series of simulations are performed in which the distribution coefficients are held constant for all five layers ( $K_d = 13 \text{ cm}^3/\text{g}$ ) and the saturated hydraulic conductivity is varied for individual layers. The saturated hydraulic conductivity

---

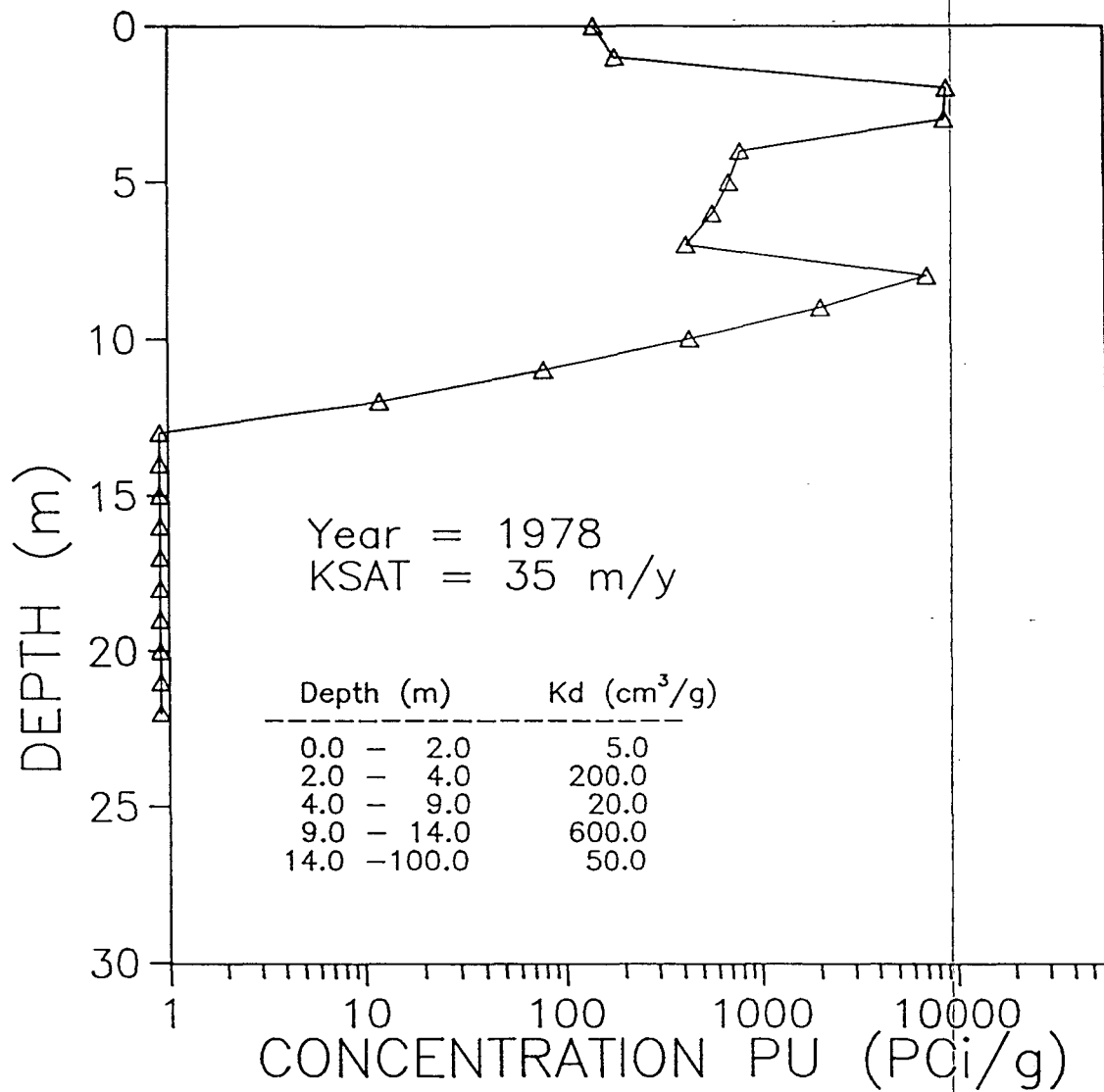


Figure 5.32. Simulated rock concentration of Pu in five layer system Run 1).

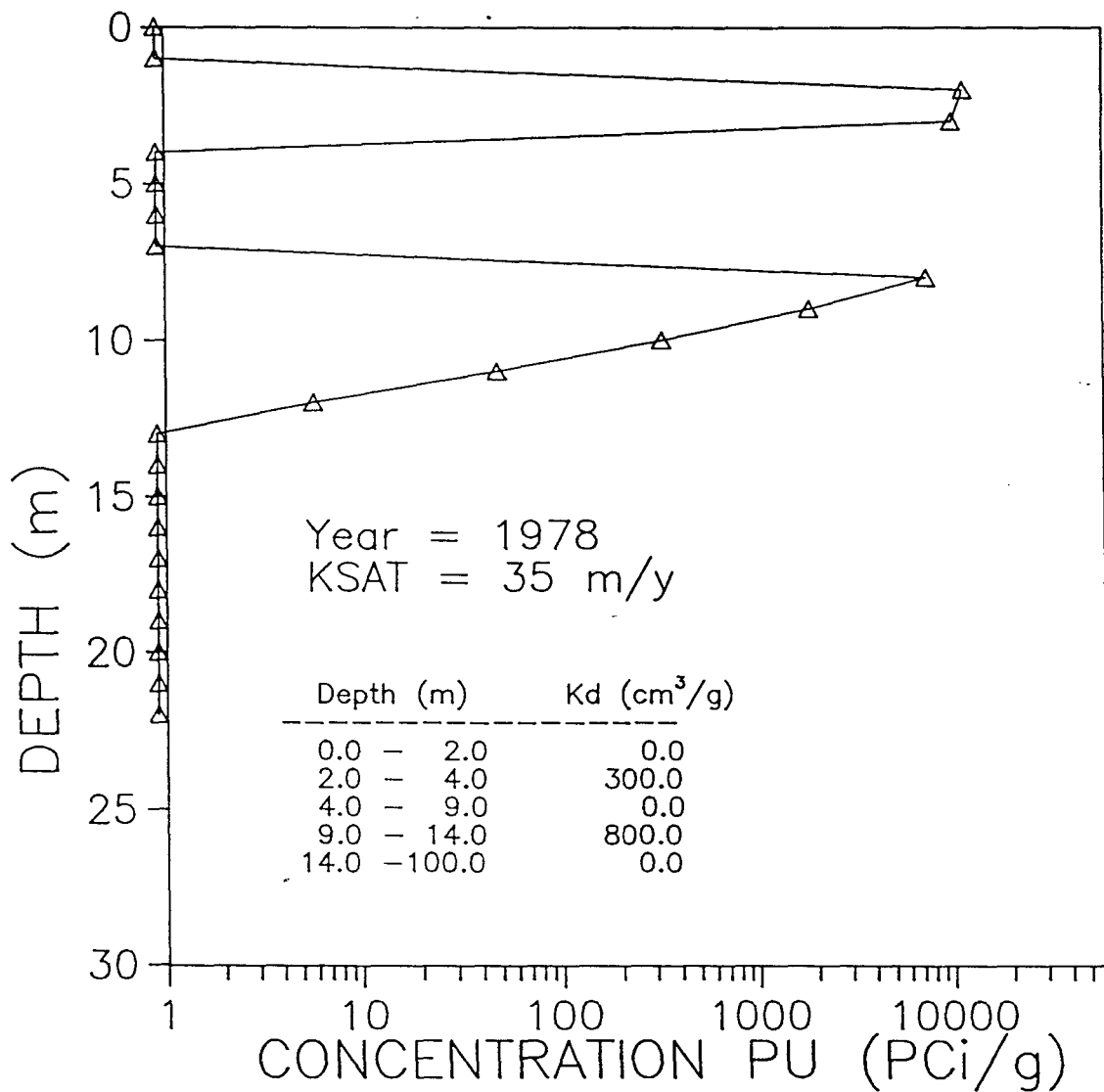


Figure 5.33. Simulated rock concentration of Pu in five layer system (Run 2).

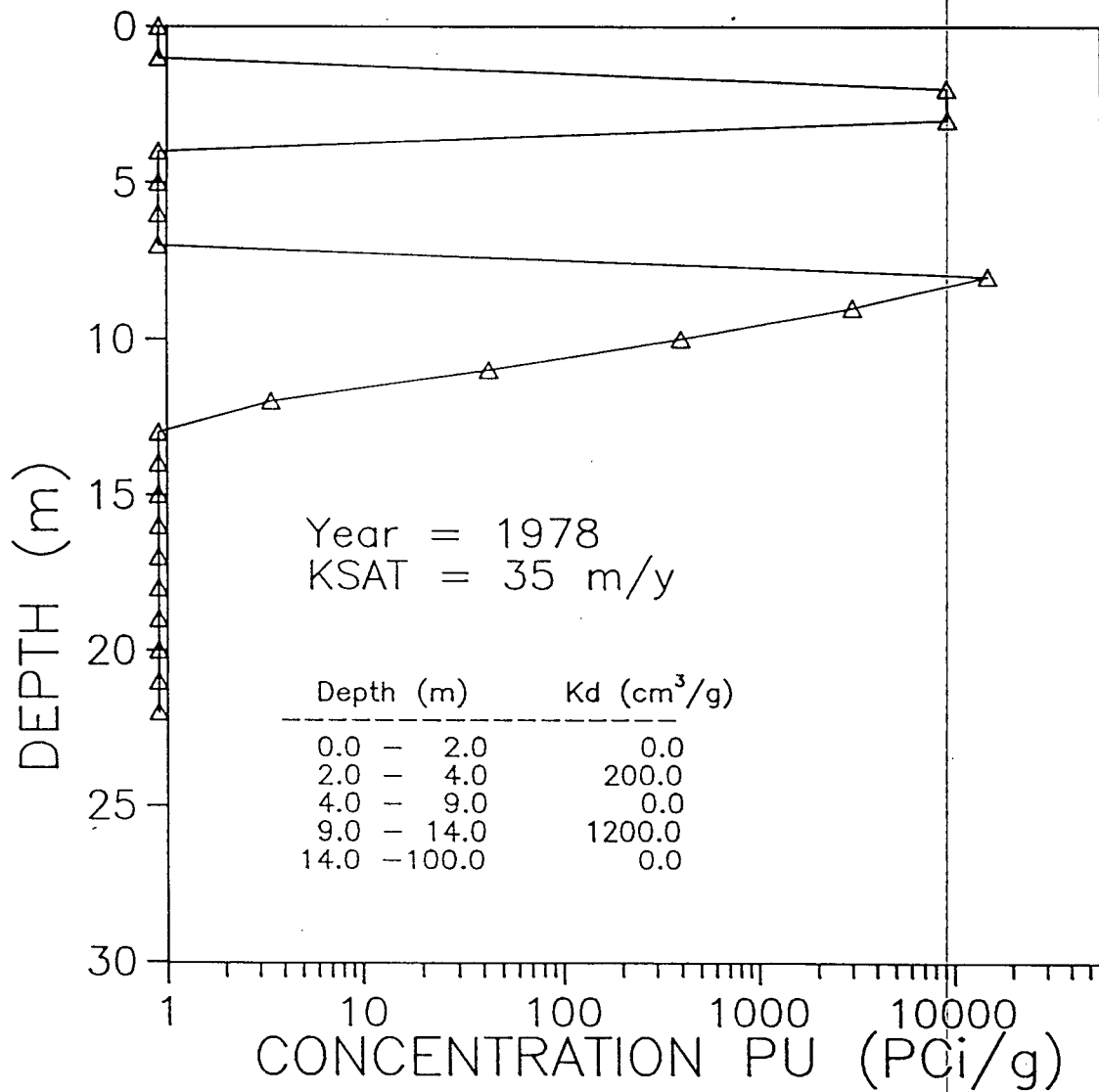


Figure 5.34. Simulated rock concentration of Pu in five layer system (Run 3).

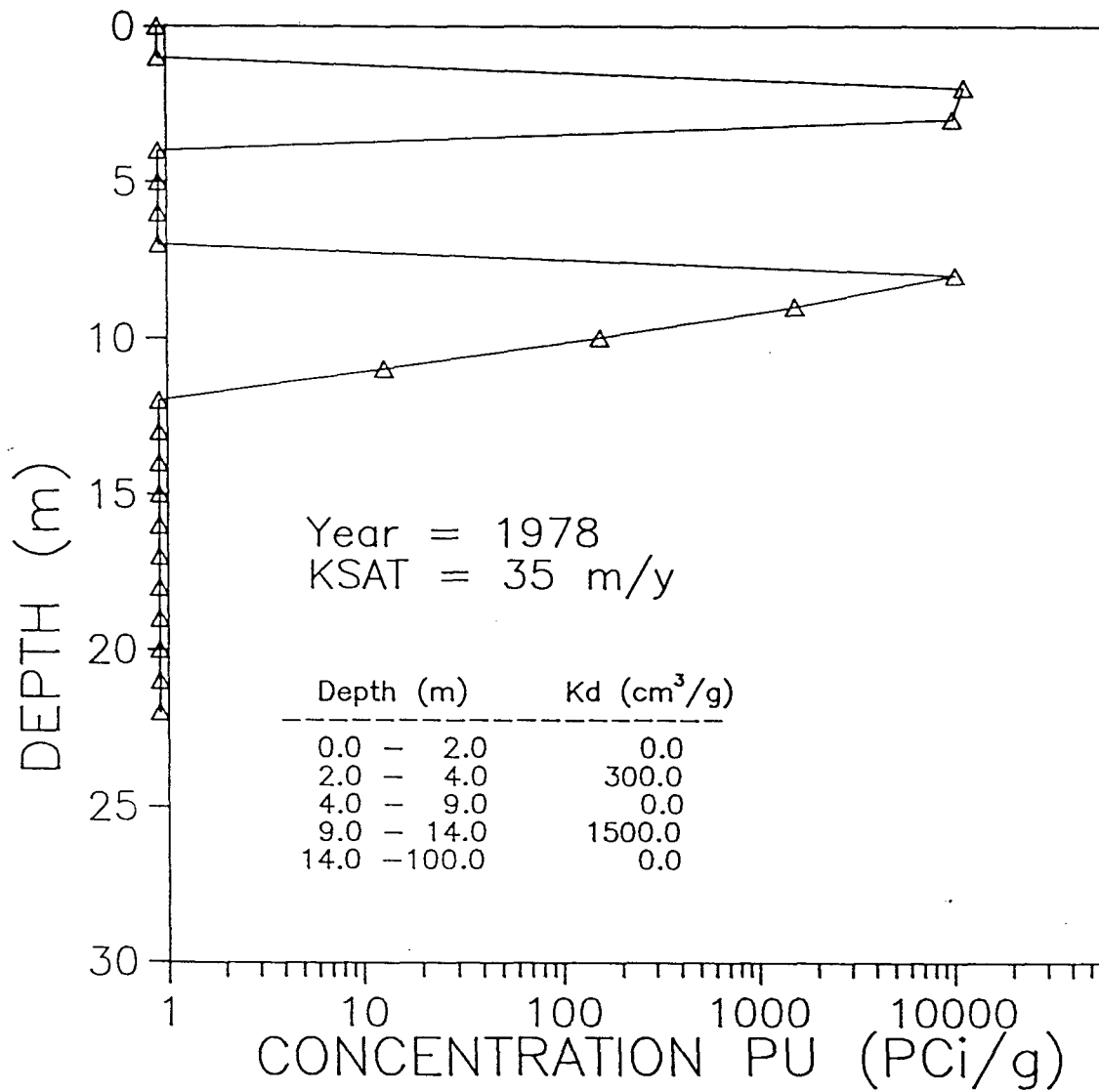


Figure 5.35. Simulated rock concentration of Pu in five layer system (Run 4).

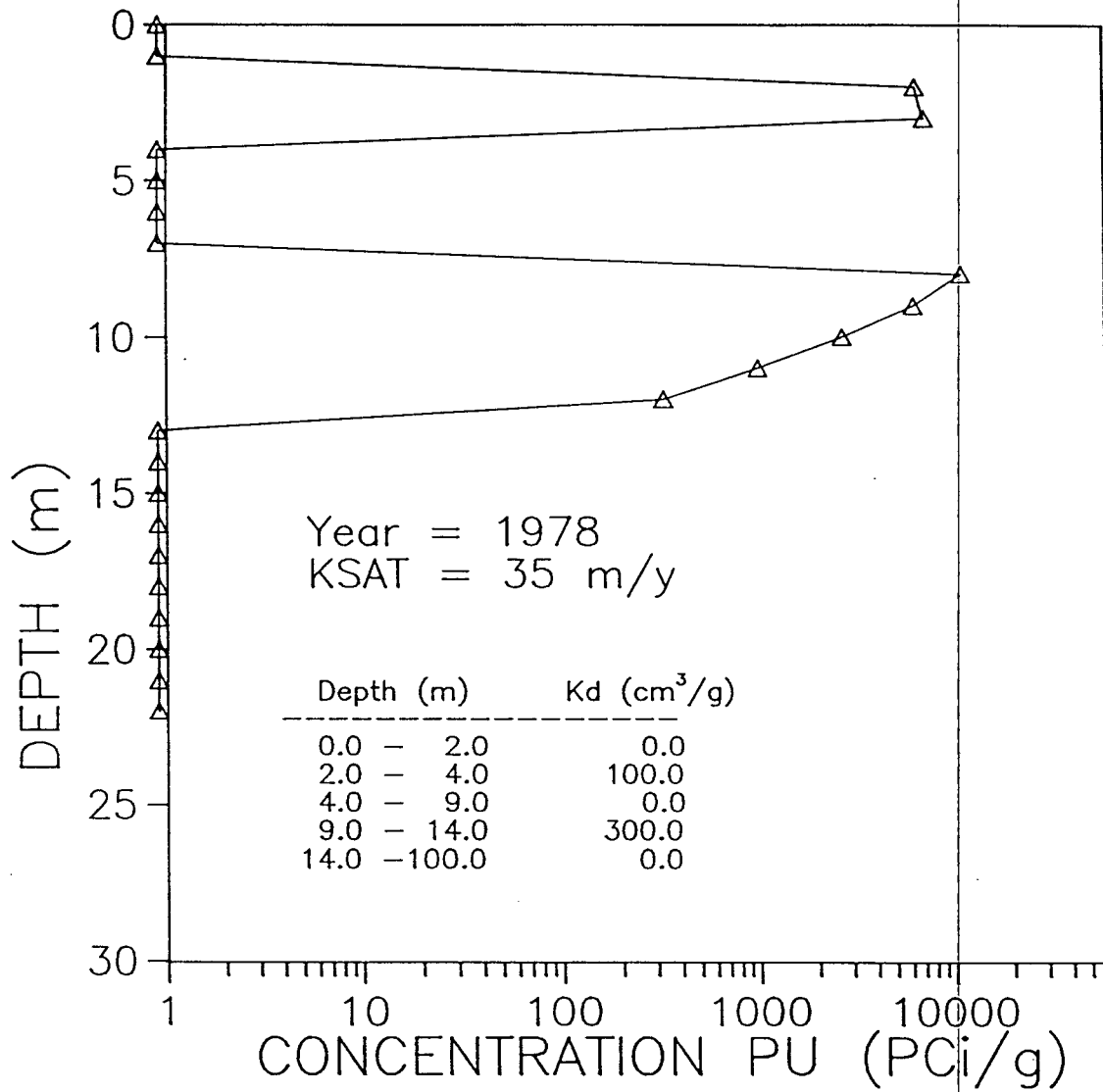


Figure 5.36. Simulated rock concentration of Pu in five layer system (Run 5).

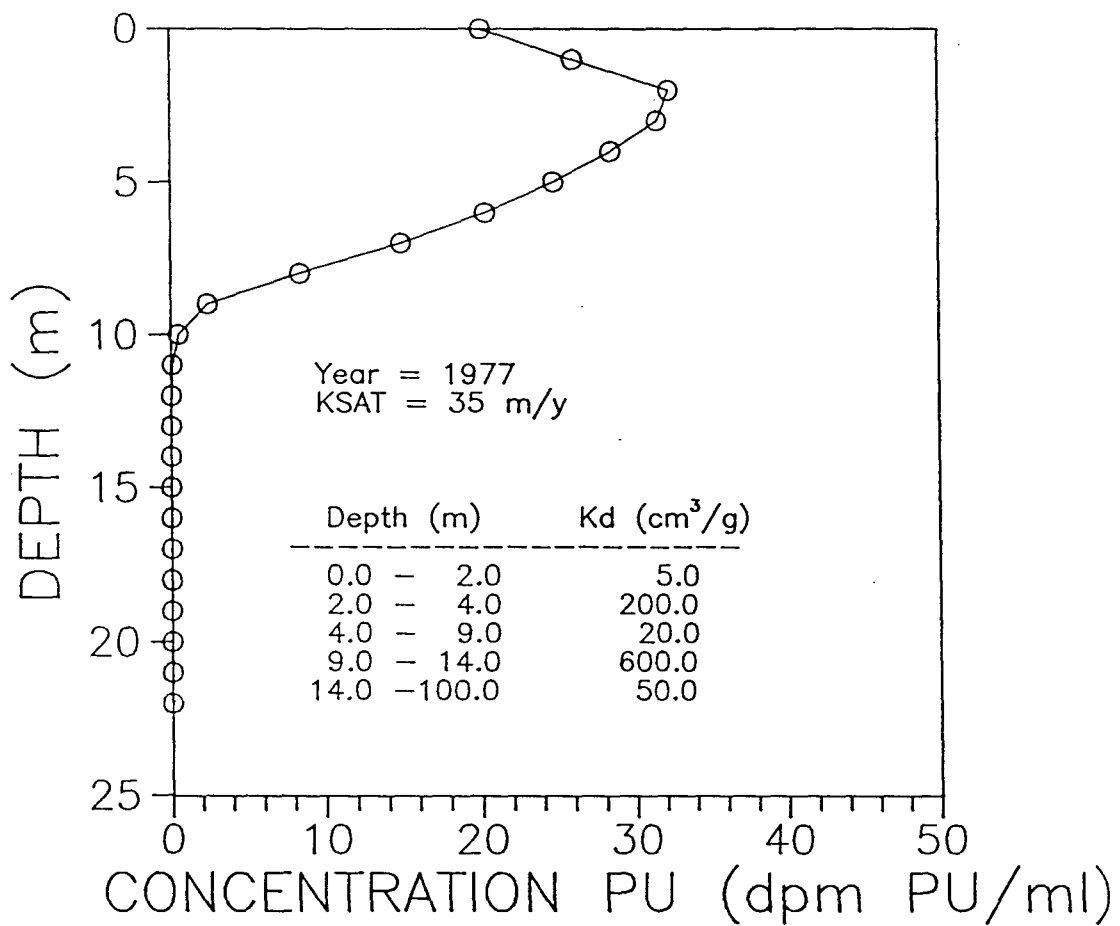


Figure 5.37. Simulated water concentration of Pu in five layer system (Run 1).

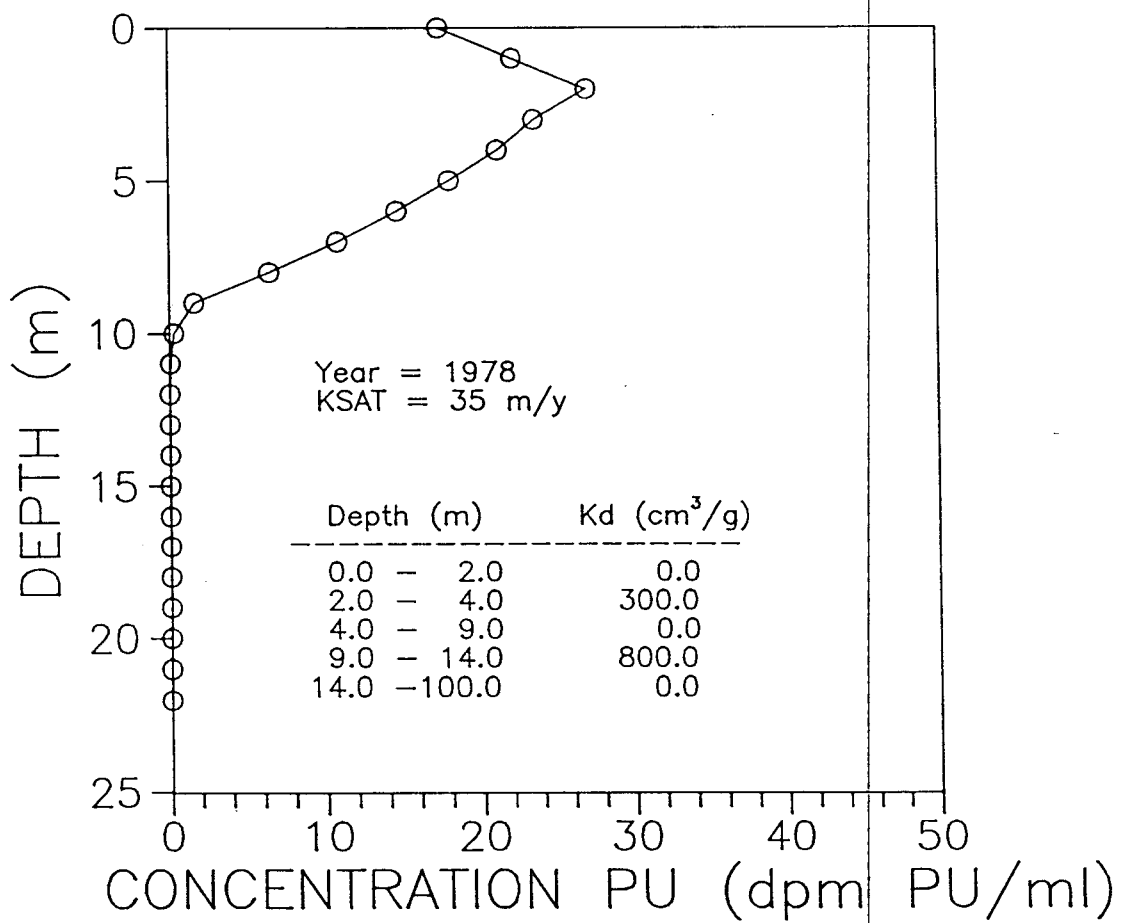


Figure 5.38. Simulated water concentration of Pu in five layer system (Run 2).

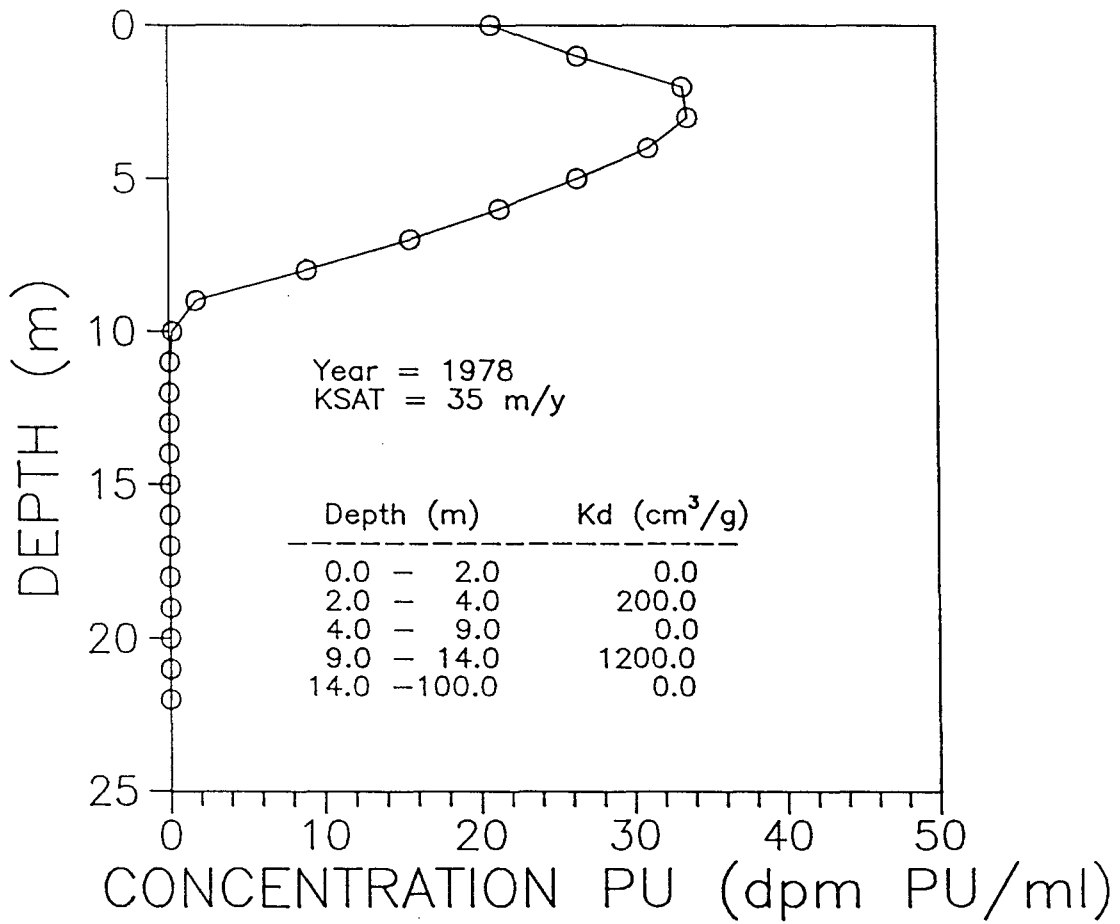


Figure 5.39. Simulated water concentration of Pu in five layer system (Run 3).

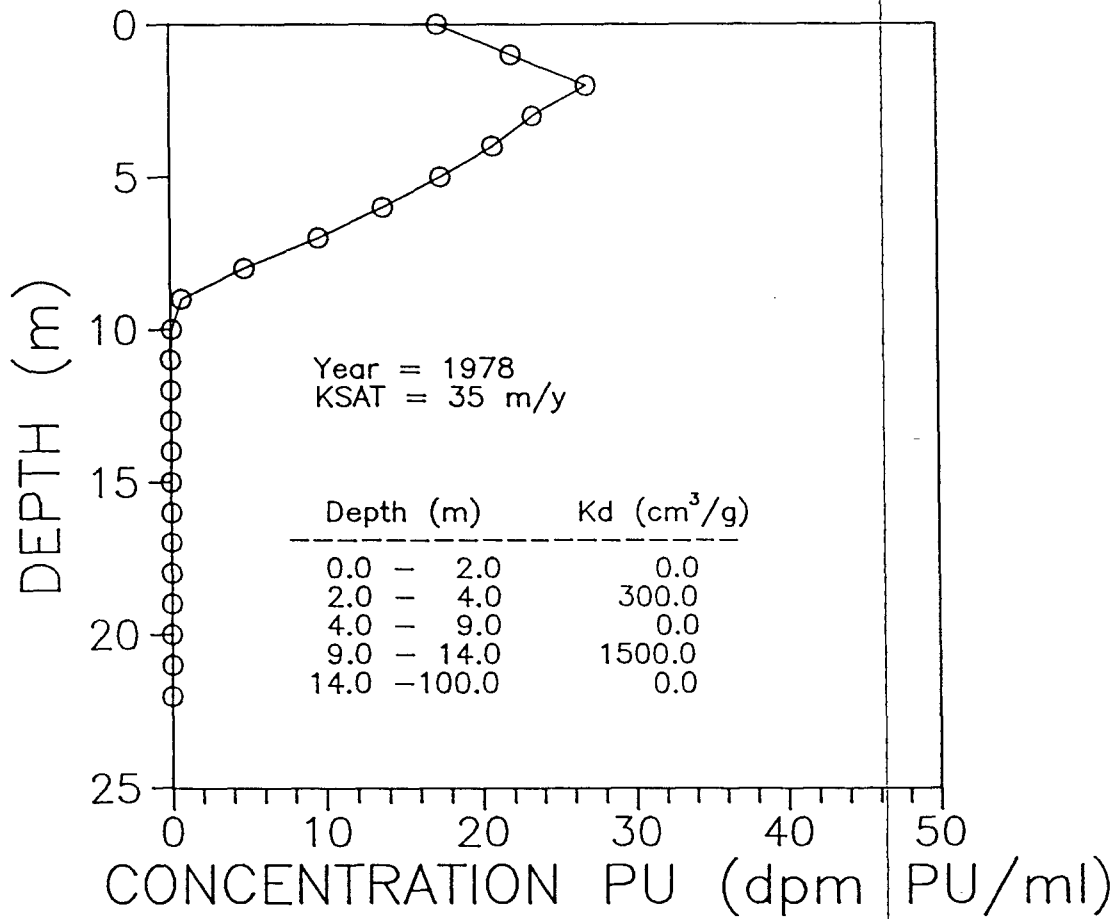


Figure 5.40. Simulated water concentration of Pu in five layer system (Run 4).

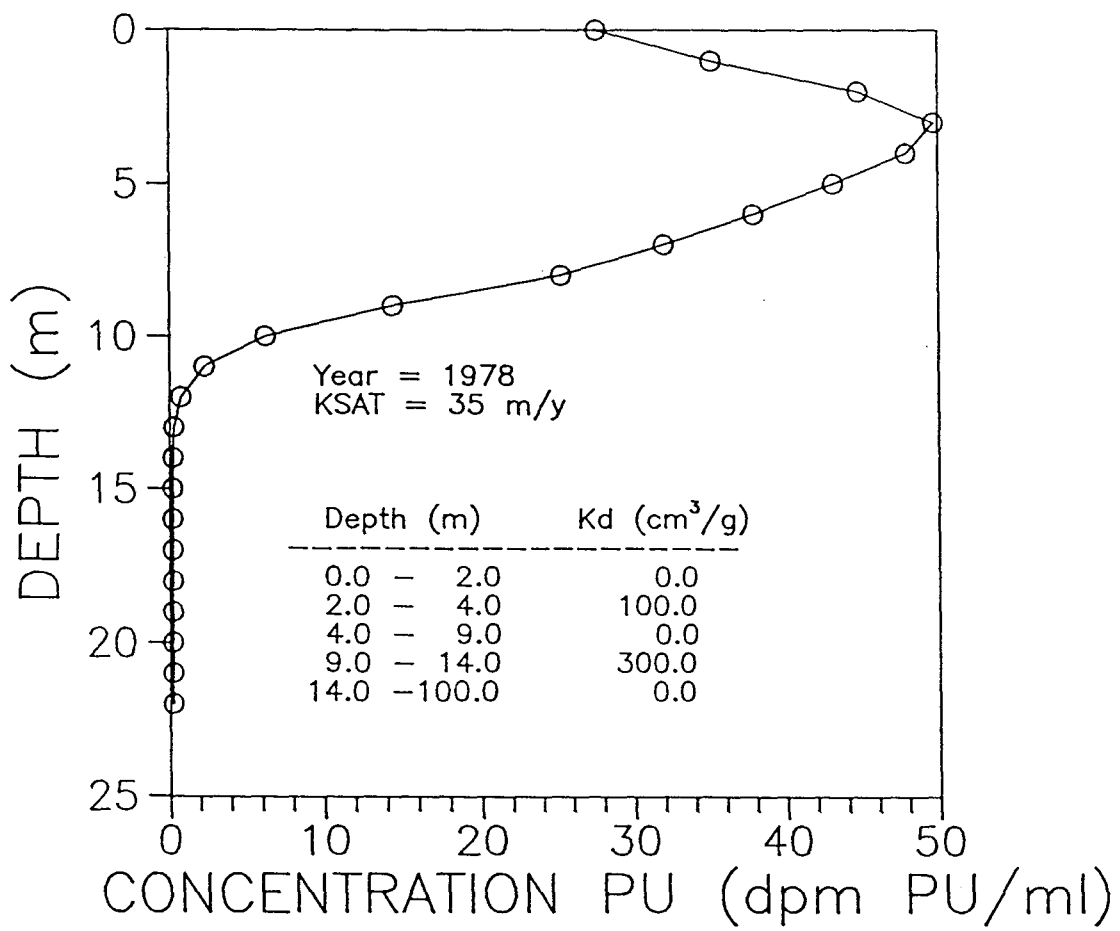


Figure 5.41. Simulated water concentration of Pu in five layer system (Run 5).

---

values assigned to the individual layers are all within a realistic range. In each of the simulations that follow, graphs of the rock saturation, concentration of plutonium in the rocks and concentration of plutonium in the water phase are presented and discussed.

Saturation distributions for years 1978 and 1951 are selected as illustrations because in 1951 the system is receiving the most flux and the highest saturations are reached. The simulated 1978 saturation and radionuclide profiles are also presented for comparison.

The following phenomena are observed in the simulated water saturation distributions and are illustrated in Figures 5.42 through 5.45:

- layers assigned lower saturated hydraulic conductivity values exhibit higher saturations and at times reached 100 percent saturation which could potentially create perched water;
- the high moisture spikes present in 1951 have all but dissipated by 1978;
- the high moisture spikes remain in the same vertical position and do not propagate downward;
- the different water pulses added to the system (Table 4.3) do not create discernable peaks as those observed in the field data, however contrasting values of hydraulic conductivity do create zones of high moisture content similar to those measured in the field.

The following phenomena are observed in the concentration distributions of plutonium in the rocks and are illustrated in Figures 5.46 through 5.49:

- concentrations are graded through the layers and do not exhibit separate zones of high concentration;
- higher saturated hydraulic conductivities tend to increase the concentrations with depth.

The following phenomena are observed in the concentrations of plutonium in the water phase and are illustrated in Figures 5.50 through 5.53:

- concentrations of plutonium in the water phase are considerably less than concentrations in the rocks contained in the same strata as would be expected from the  $K_d$ 's used;

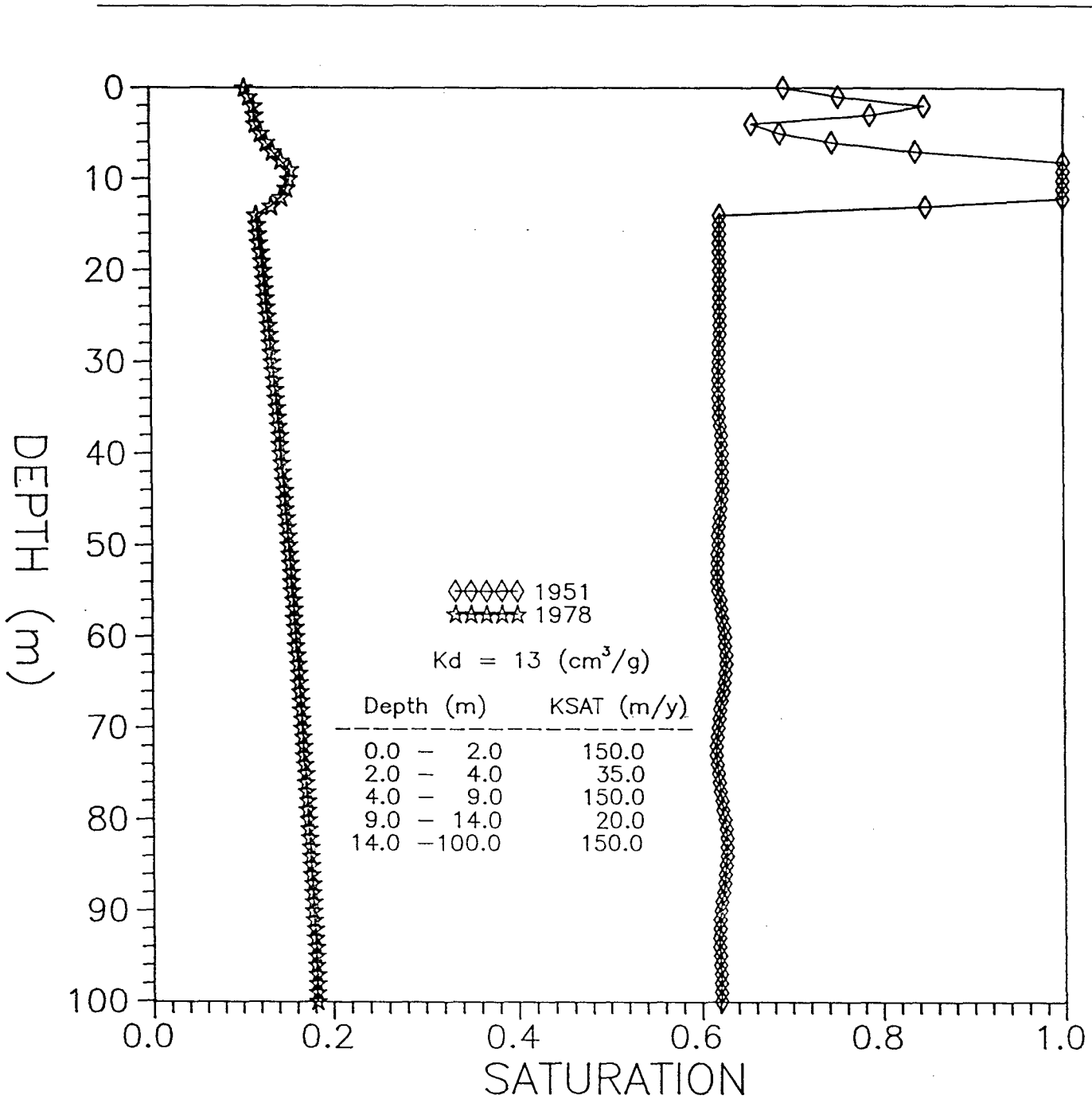


Figure 5.42. Simulated saturation distributions of five-layer system (Run 6).

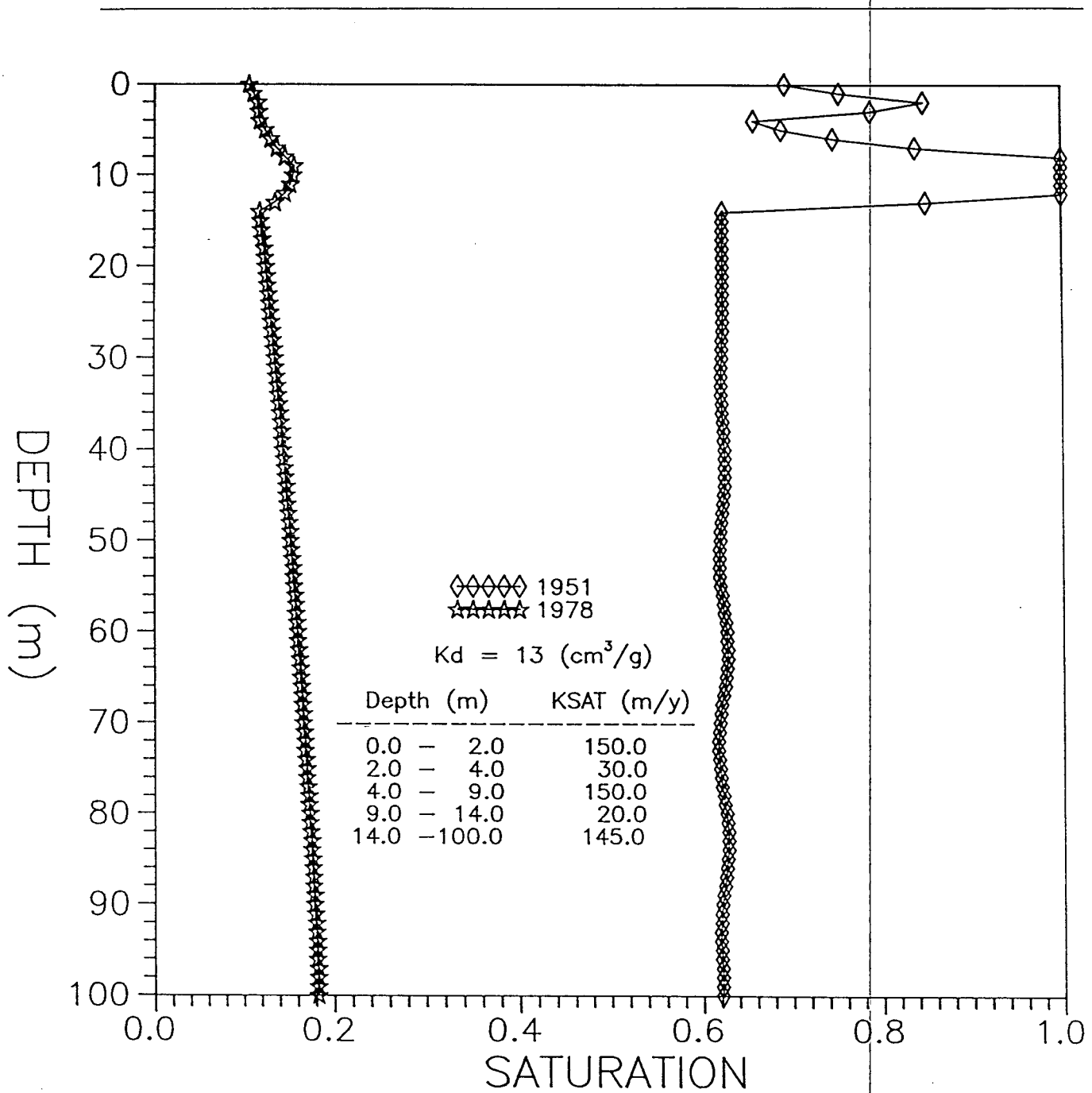


Figure 5.43. Simulated saturation distributions of five-layer system (Run 7).

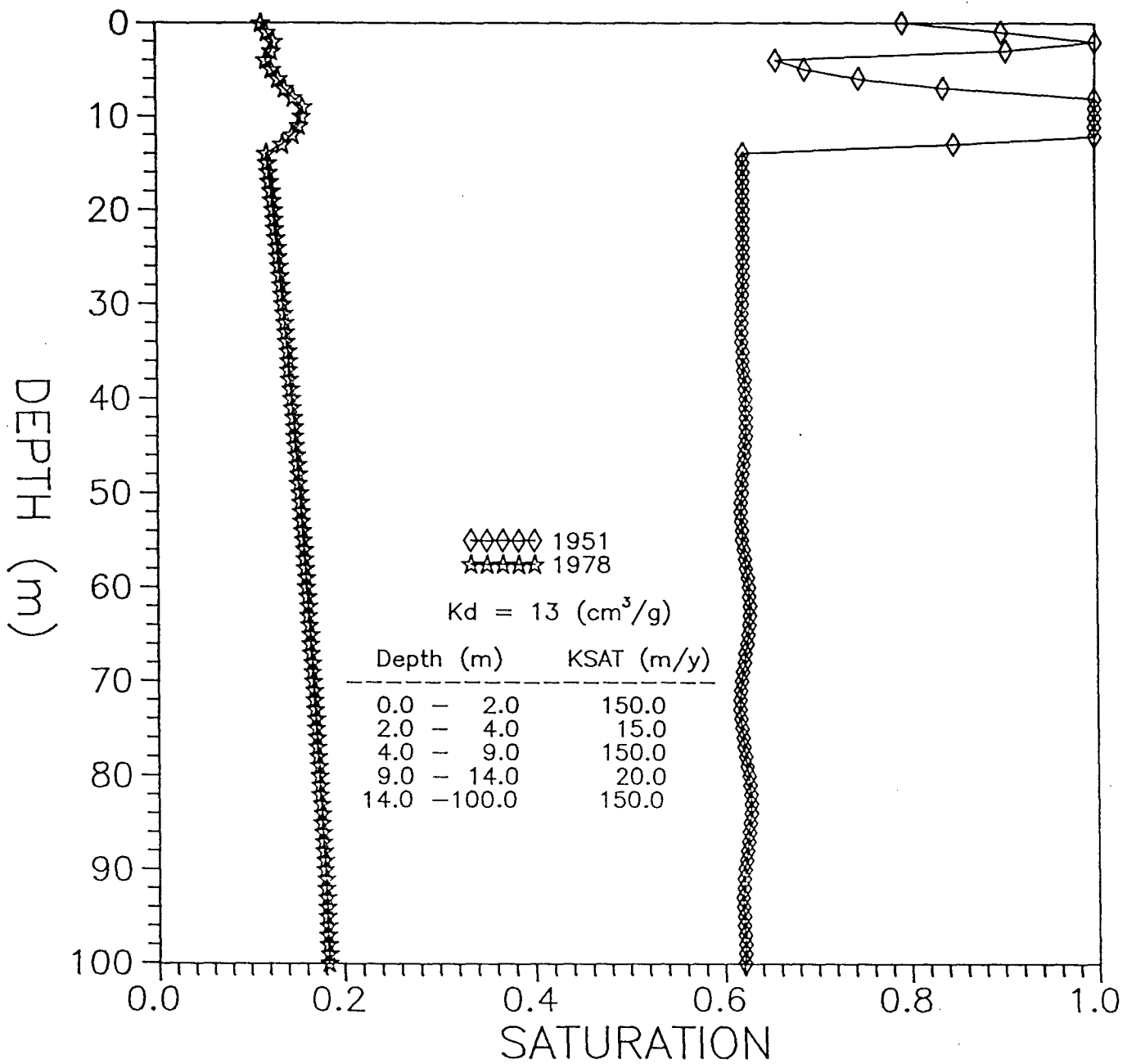


Figure 5.44. Simulated saturation distributions of five-layer system (Run 8).

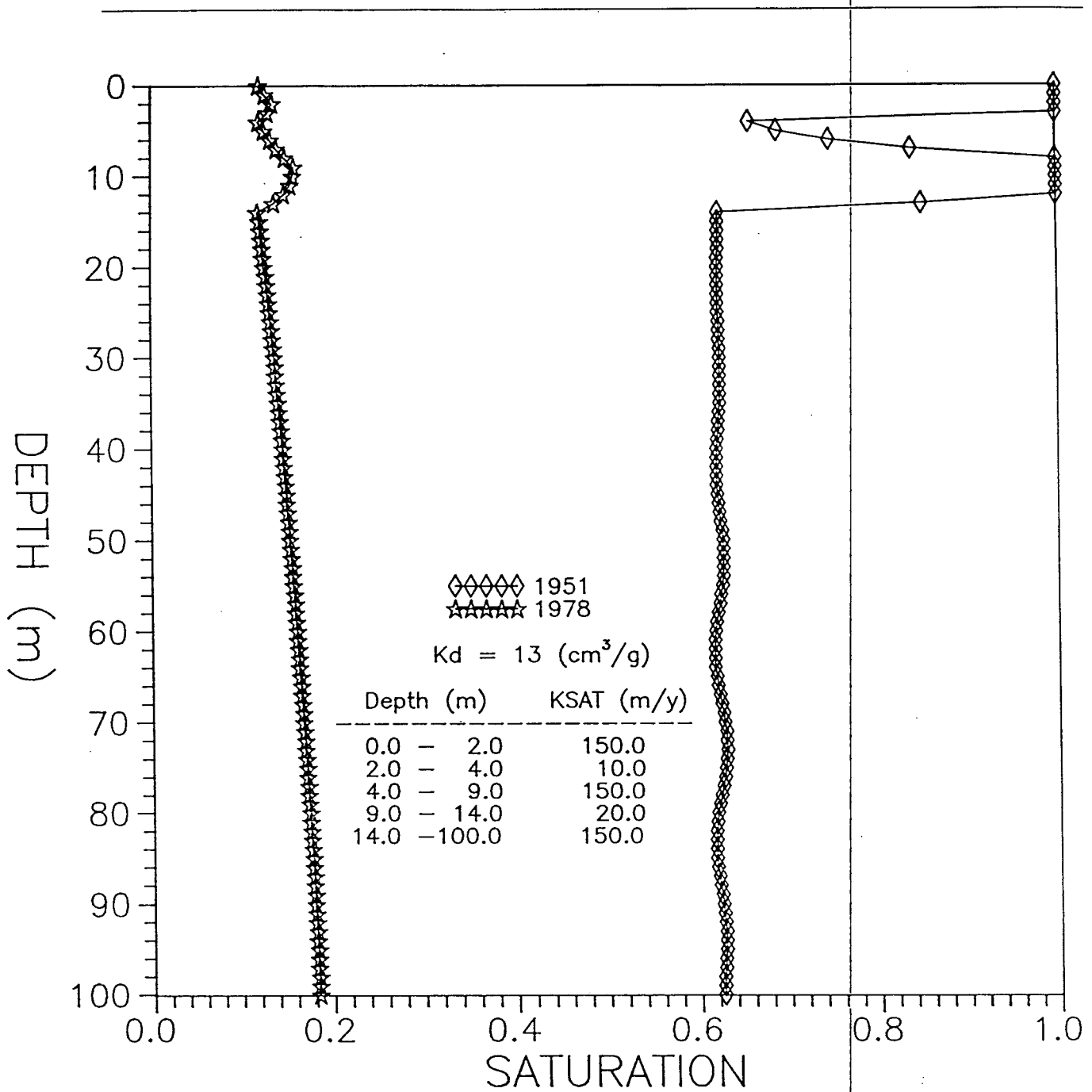


Figure 5.45. Simulated saturation distributions of five-layer system (Run 9).

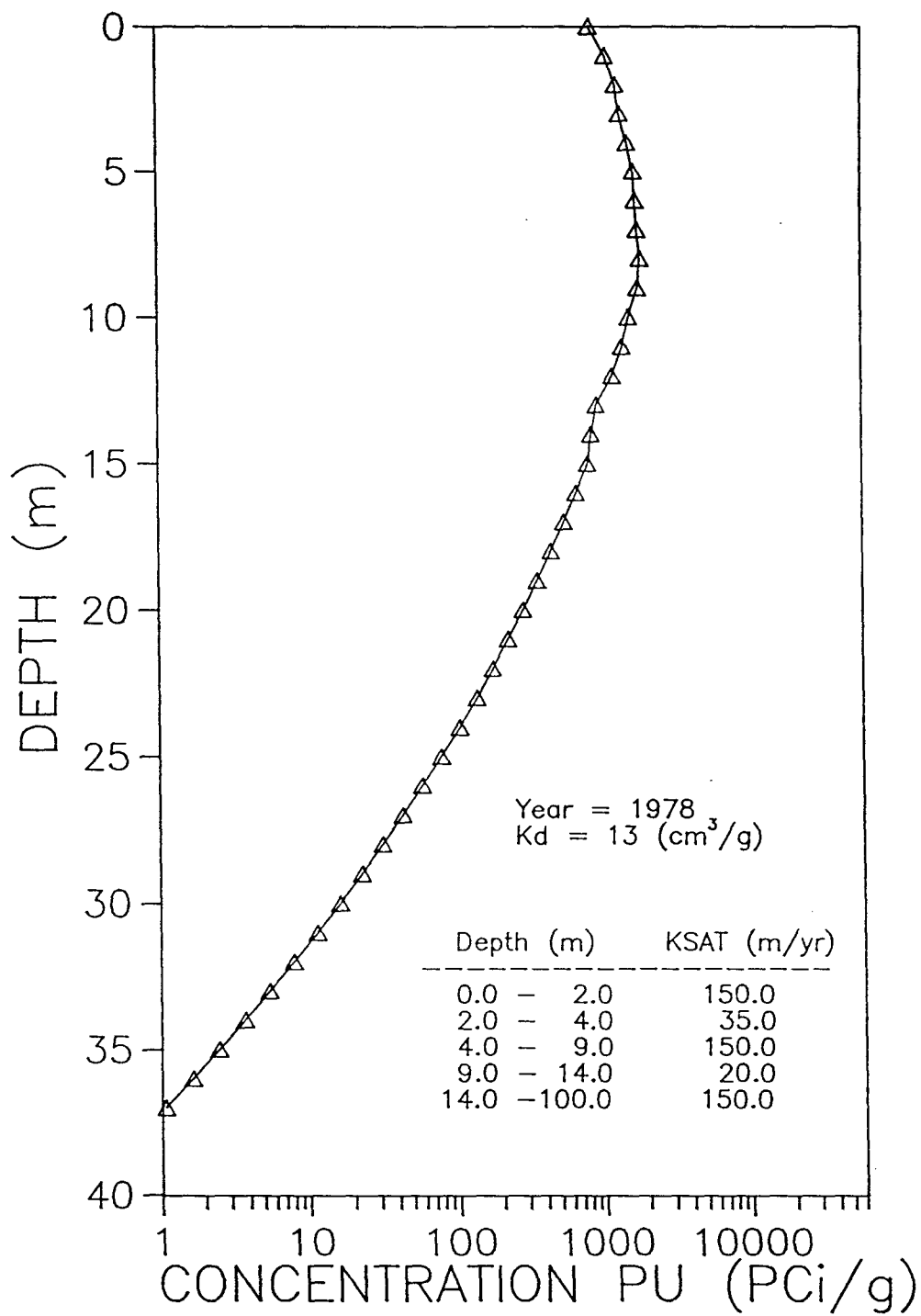


Figure 5.46. Simulated rock concentrations of Pu in five-layer system (Run 6).

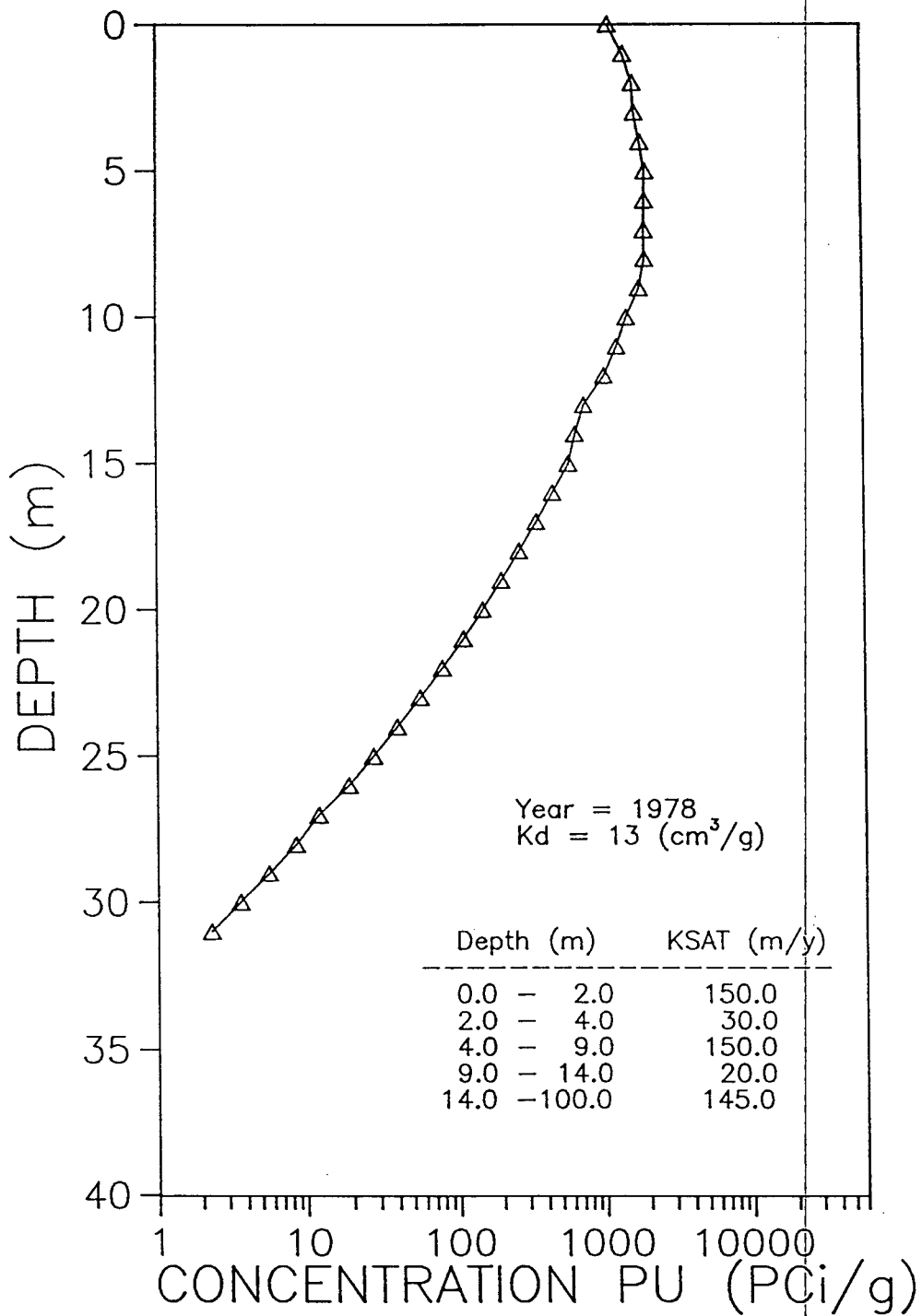


Figure 5.47. Simulated rock concentrations of Pu in five-layer system (Run 7).

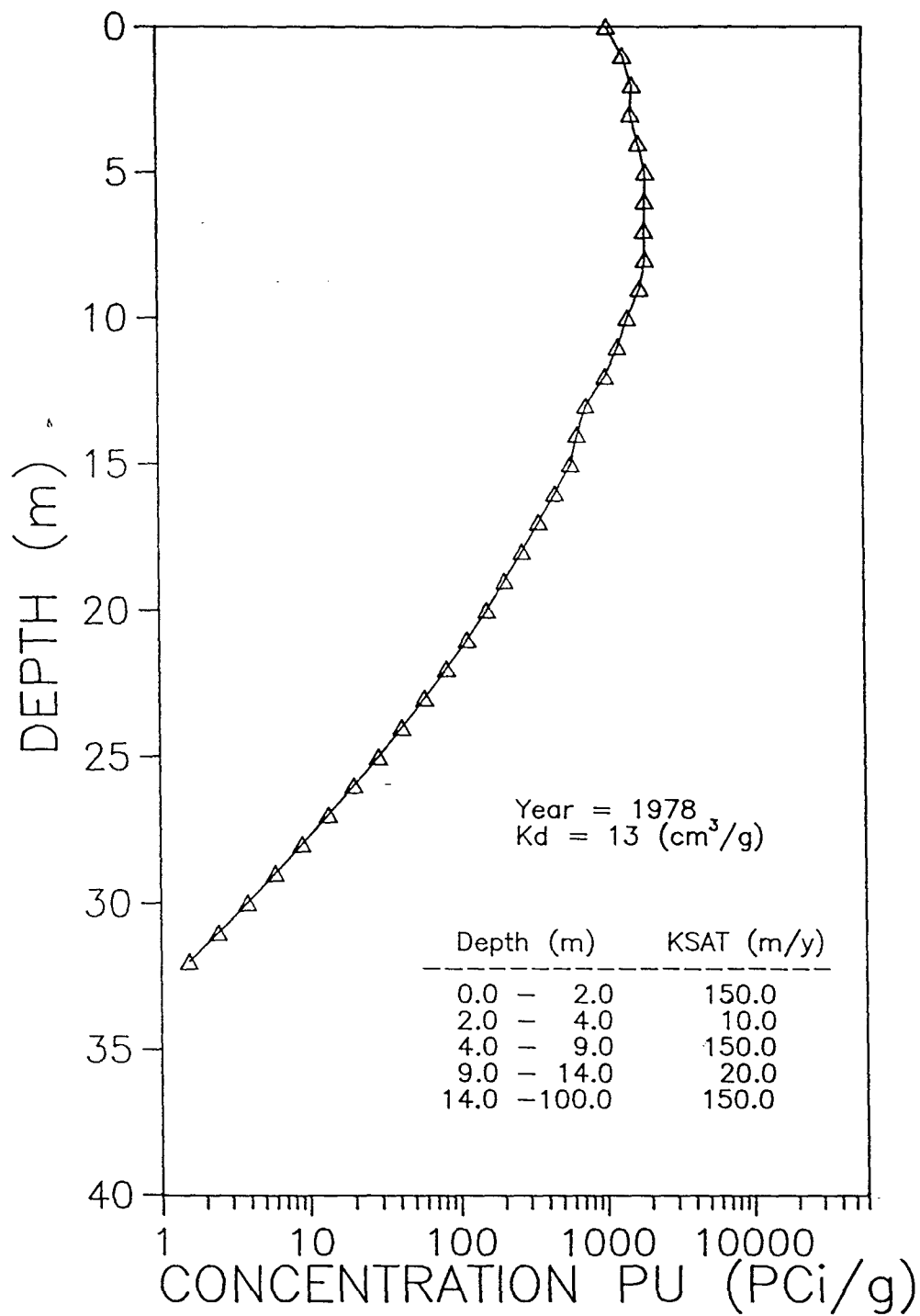


Figure 5.48. Simulated rock concentrations of Pu in five-layer system (Run 8).

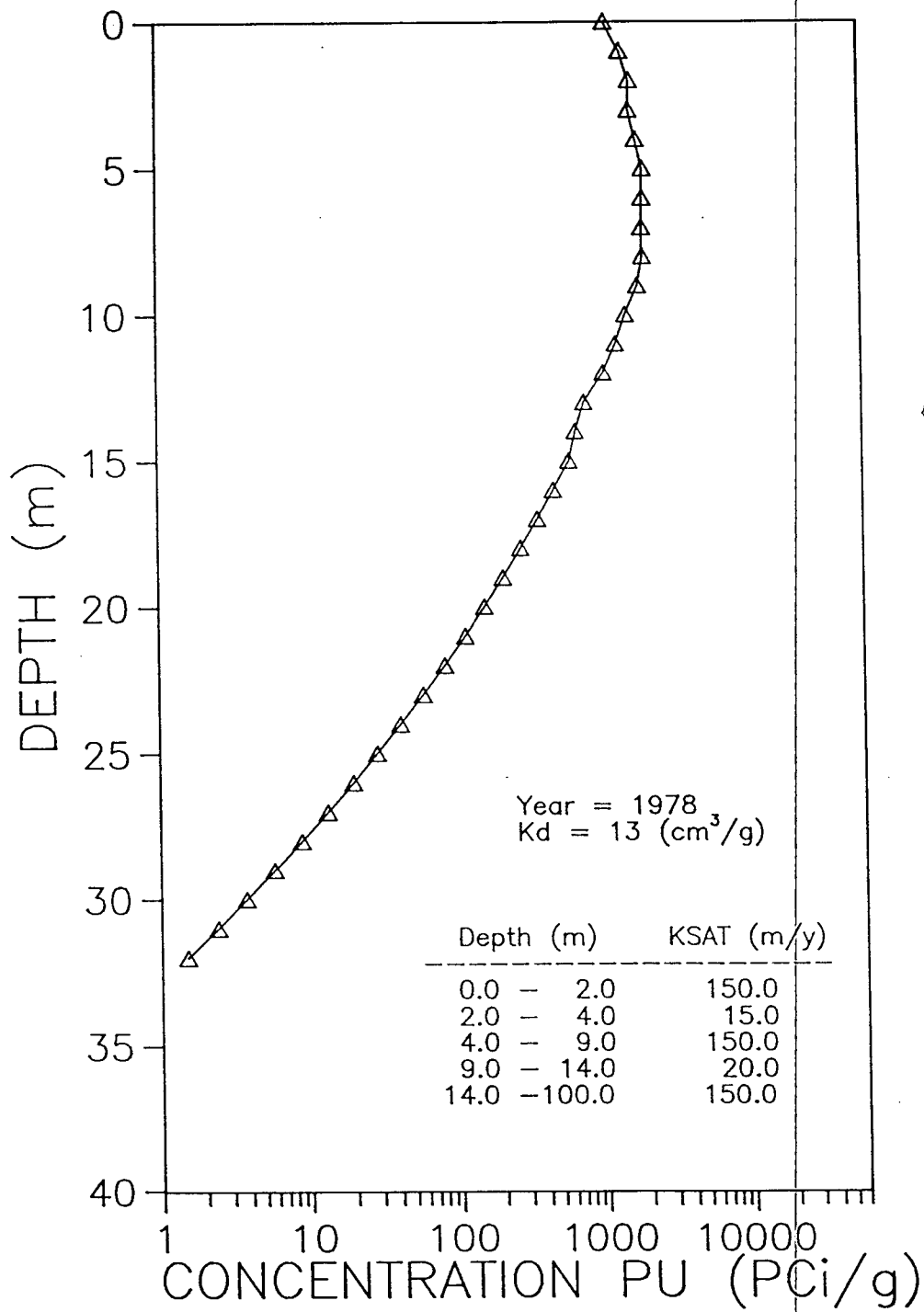


Figure 5.49. Simulated rock concentrations of Pu in five-layer system (Run 9).

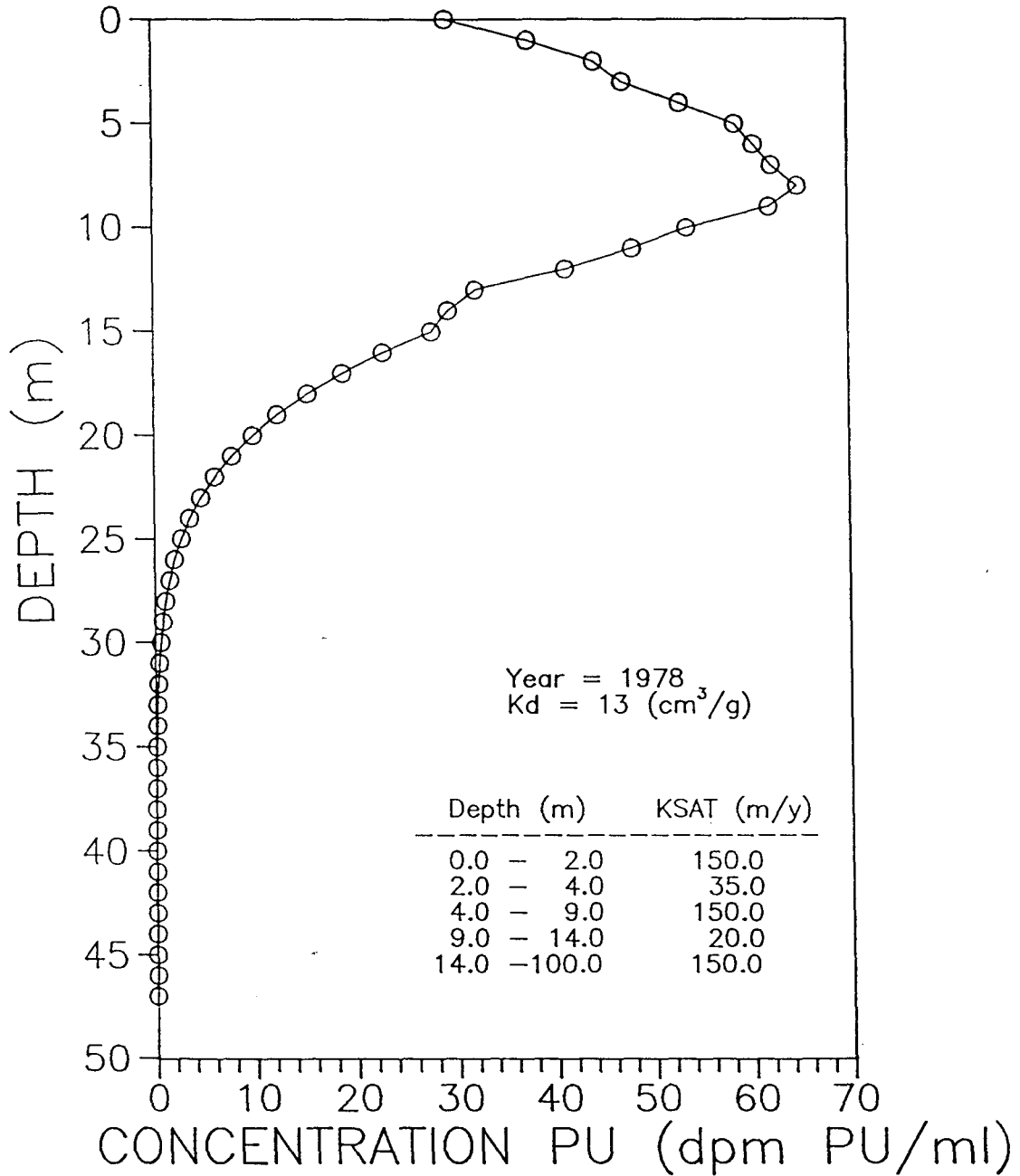


Figure 5.50. Simulated water concentrations of Pu in five-layer system (Run 6).

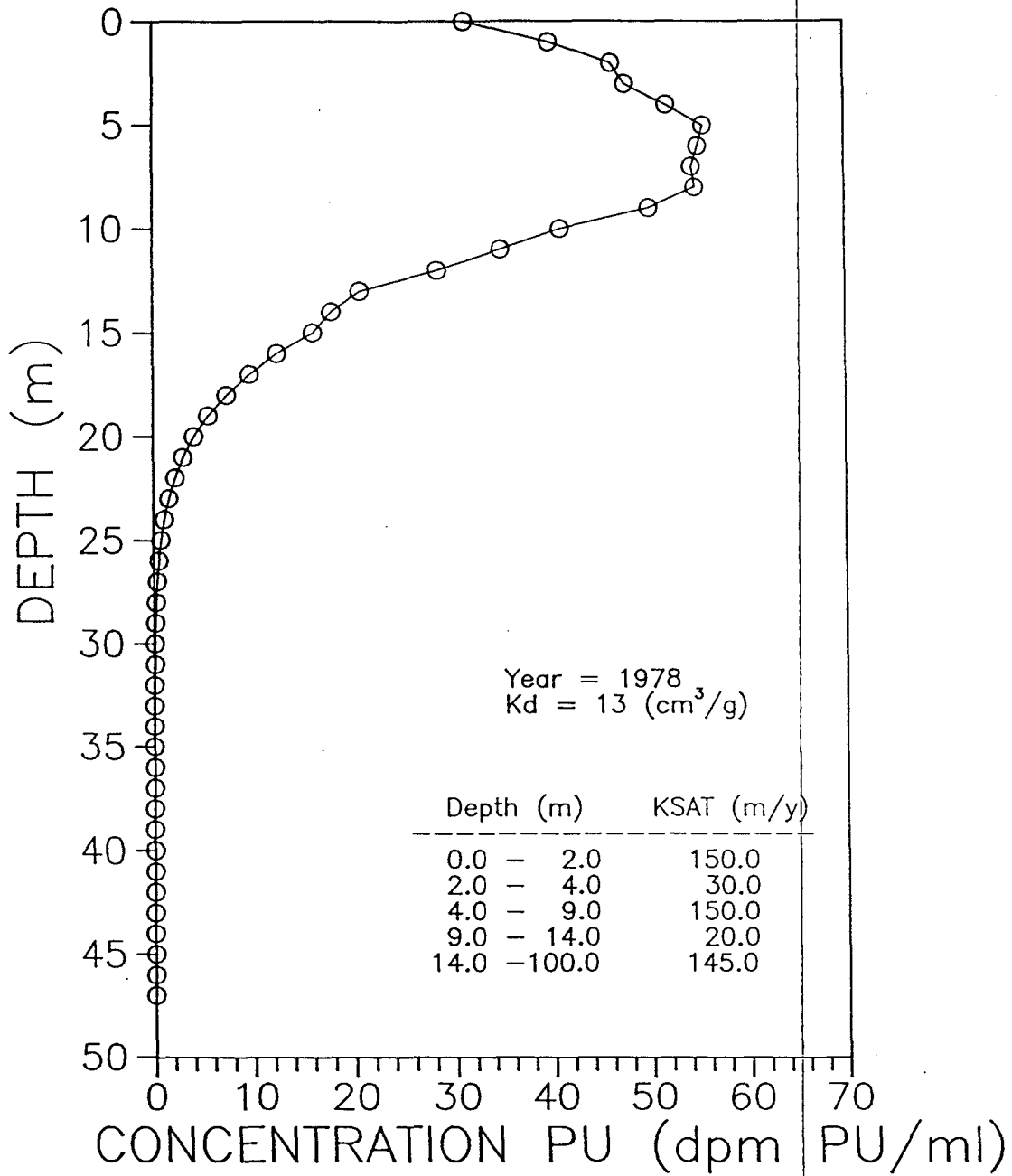


Figure 5.51. Simulated water concentrations of Pu in five-layer system (Run 7).

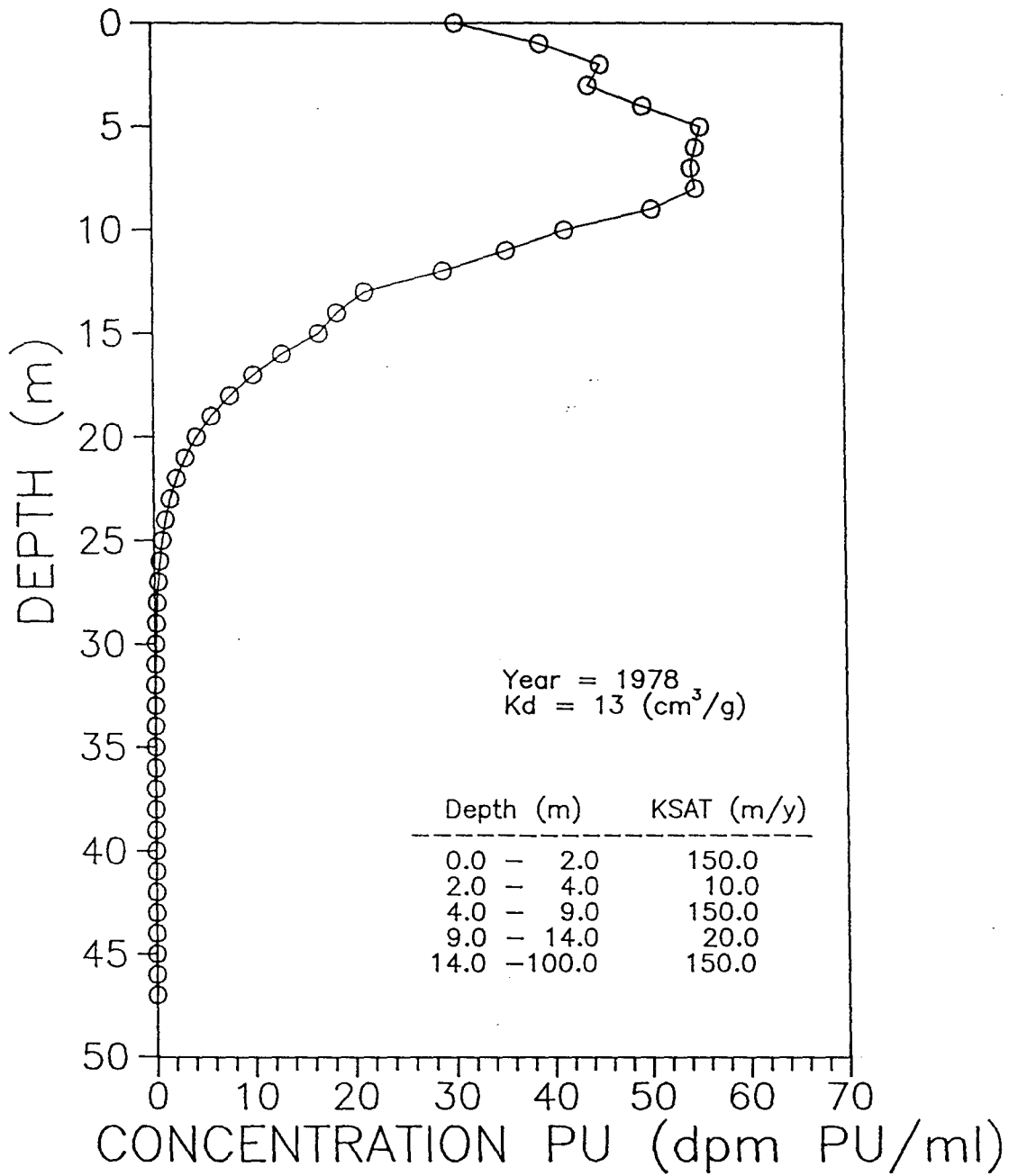


Figure 5.52. Simulated water concentrations of Pu in five-layer system (Run 8).

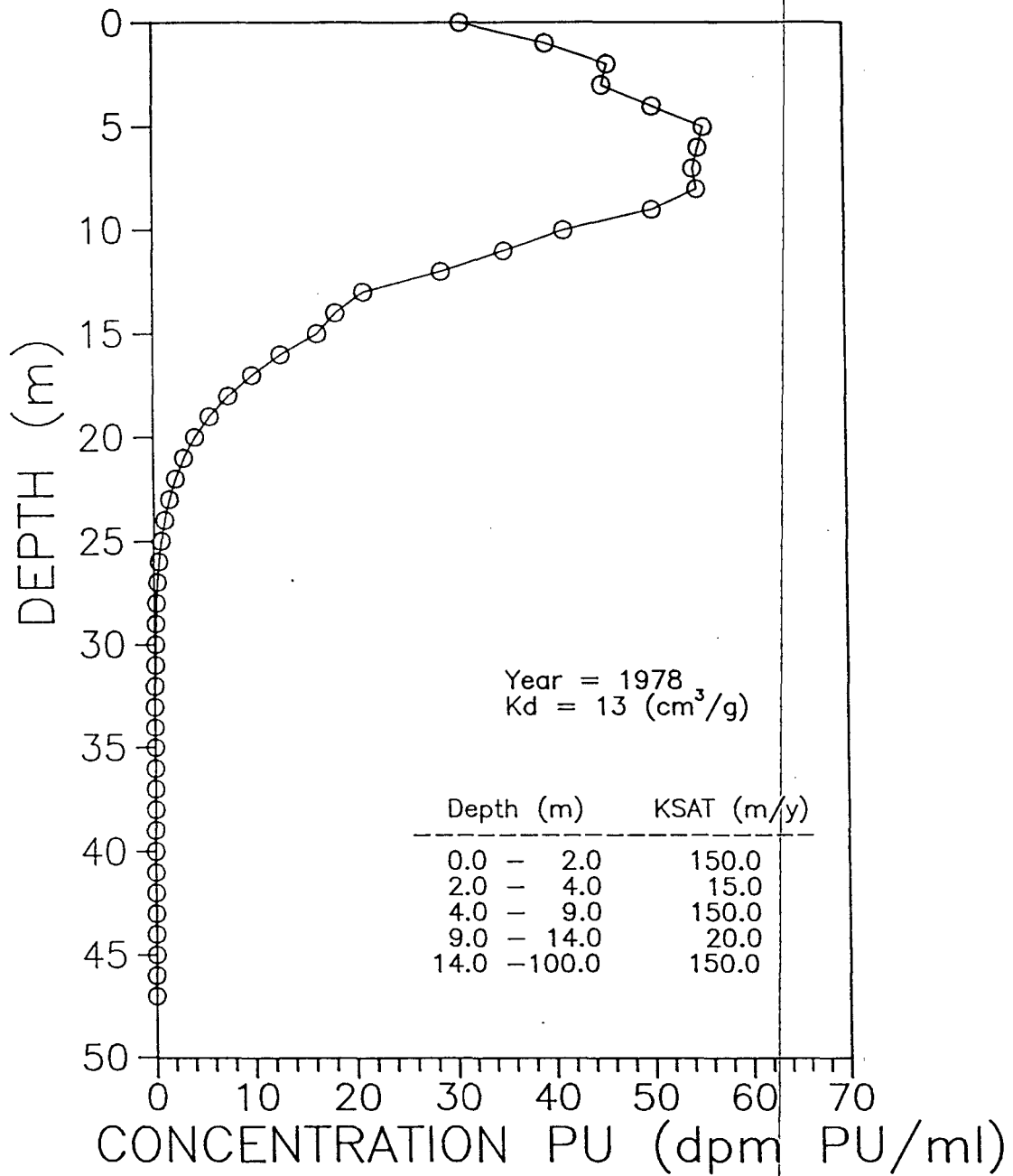


Figure 5.53. Simulated water concentrations of Pu in five-layer system (Run 9).

- 
- concentrations of plutonium in the water phase increase sharply in the zones of lower saturated hydraulic conductivities;
  - distinct peaks in the radionuclide distribution with depth are not evident despite the fact that radionuclides were added to the system in pulses of highly variable concentrations.

#### 5.4 Mass Comparison

Mass balance analyses are important in field assessments and in numerical flow and transport simulations to verify conservation of mass and to compare simulated mass distributions to observed mass distribution in the field. If the quantities of radionuclides introduced into the absorption beds cannot be completely accounted for, it may be an indication that radionuclides have migrated deeper than the upper 30 meters for which data are available.

To perform an approximate mass balance, Figures 5.32 through 5.36 were all plotted to the same scale as the measured radionuclide field data (Figure 5.31). A comparison was then made of the radionuclide mass under the simulated curves and that of the measured field curves.

The radionuclide field data and model output are plotted as semi-logarithmic graphs. Therefore, to determine the area under the respective curves the log axis of the graphs needed to be linearized. A short Fortran program was used to convert the log axis to a linear scale and to determine the area under the curves by numerical integration (Appendix E).

The results of this analysis, presented in Table 5.3, indicate that the radionuclide mass obtained from the modeling falls between the radionuclide mass measured in hole 1 of absorption bed 1 and the radionuclide mass measured in hole 2 of absorption bed 1.

Although the holes 1 and 2 are located within several meters of each other, the measured radionuclide concentration distributions are very different. Therefore, either the radionuclides were not uniformly loaded into absorption bed 1, or local heterogeneities have had a very strong control over radionuclide migration. The model assumes uniform conditions laterally and would necessarily average the radionuclide mass under the entire bed. Therefore, due to the relatively high uncertainty associated with this mass balance estimate, it is not possible to draw conclusions that radionuclides have or have not migrated deeper than 30 meters. However, when more data become available it may be possible and beneficial to perform multi-dimensional mass balances.

Table 5.3. Mass comparison between field measurements and simulations.

	Total Mass (Pci/m <sup>2</sup> )
Absorption Bed 1	
Hole 1	4.6 x 10 <sup>12</sup>
Hole 2	1.4 x 10 <sup>9</sup>
Area under simulated curves	3.0 x 10 <sup>11</sup>

---

## 5.5 Case Simulations

The pathway analysis simulations are divided into three general cases:

- Case I simulates the ambient conditions of the site prior to the introduction of wastes;
- Case II is comprised of three flow scenarios that simulate the effects of liquid waste discharges on the hydrogeologic system at MDA T;
- Case III is composed of three solute transport scenarios that are analogous to the flow scenarios of Case II.

### 5.5.1 Case I - Ambient Flow Simulations

The primary objective of the ambient flow simulations was to approximate the natural hydrogeologic system at MDA T before it was disturbed by the addition of liquid wastes. The hydraulic characteristics, initial conditions and boundary conditions of the natural system were established during these simulations and used as a basis for subsequent runs.

#### 5.5.1.1 Scenario I.1 - Natural Recharge

Data pertaining to ambient moisture conditions in the immediate site vicinity are scarce. Therefore, the ambient flow simulations incorporated several simplifying assumptions. In particular, flow was assumed to be vertical and the distribution of net infiltration was assumed to be spatially uniform and at steady state. Although these assumptions may be modified as more data become available, they should not significantly affect the validity of the model.

##### 5.5.1.1.1 Procedures and Input Parameters

Field evidence suggests that under ambient conditions the Bandelier tuff has a saturation of less than 10 percent of available pore space (Abee, 1981). Therefore, to simulate the natural conditions, hydraulic conductivity and recharge were adjusted in such a manner to establish ambient saturation distributions of less than 10 percent.

Measured saturated hydraulic conductivity measurements for the Bandelier tuff range from 6.3 - 148.0 m/y (Abee, 1981). Values of recharge were estimated from evapotranspiration data presented in Abee (1981). Sensitivity analysis indicated that, given the assumed rates of waste water discharge to absorption bed 1, the saturated hydraulic conductivity should be at least 35 m/y.

To achieve calibration, recharge and saturated hydraulic conductivity estimates were adjusted to stay within their respective probable ranges and to maintain a saturation profile of less than 10 percent. Model calibration resulted in a saturated hydraulic conductivity of 35 m/y and a recharge rate of 0.00254 m/y (.1 in/y). Although this combination is not necessarily a unique solution to the problem, no other combination would be found which met the criteria as well, while remaining within the estimated probable range.

Other data necessary for the simulation are the soil moisture characteristics (i.e., residual water content, alpha, beta and n). As was discussed in Section 4.0, these parameters were obtained from observed moisture retention data for the Bandelier tuff (Table 5.4).

#### 5.5.1.1.2 Saturation Distributions

The moisture distribution that is most consistent with the ambient hydrogeologic system at MDA T is presented in Figure 5.54.

#### 5.5.1.1.3 Discussion

Under steady state recharge, saturation values are less than 10 percent. The saturation distribution is essentially uniform, except in the immediate vicinity of the water table. The hydrologic input for this simulation is used as initial conditions for the Case II flow scenarios.

### 5.5.2 Case II - Flow Simulations

The second case involves three flow scenarios. Each of these uses the output from the flow analysis obtained during Case I to provide the initial conditions. During these scenarios, documented or estimated man-induced hydraulic stresses are superimposed on the natural hydrologic system. The velocity fields obtained as output from the Case II scenarios are used as input for the transport simulations performed in Case III.

Saturation profiles were obtained roughly bi-annually for a simulated time of 50 years. However, saturation profiles for only four years are plotted for each of the Case II scenarios. These years are 1949, 1961, 1978, and 1990, the reasons for plotting these specific years are:

- 1949 - Relatively early moisture distributions are provided to compare with later years;
- 1961 - Saturation distributions measured by Christenson (1961) are available for comparison with the simulation results (Appendix B);

---

Table 5.4. Parameter input for scenario I.1 (1-D).

---

Input Parameter	Value
1. Saturated hydraulic conductivity	35 (m/y)
2. Residual water saturation	.0097 (dimensionless)
3. Power index (n) of the relative permeability versus saturation relationship	3.69 (dimensionless)
4. Leading coefficient (alpha) of the saturation versus capillary head relationship	.423 (m <sup>-1</sup> )
5. Power index (beta) of the saturation versus capillary head relationship	2.217 (dimensionless)
6. Porosity	.4 (dimensionless)
7. Bulk Density	1.55 (g/cm <sup>3</sup> )
8. Ambient Recharge	.00254 (m/y)

---

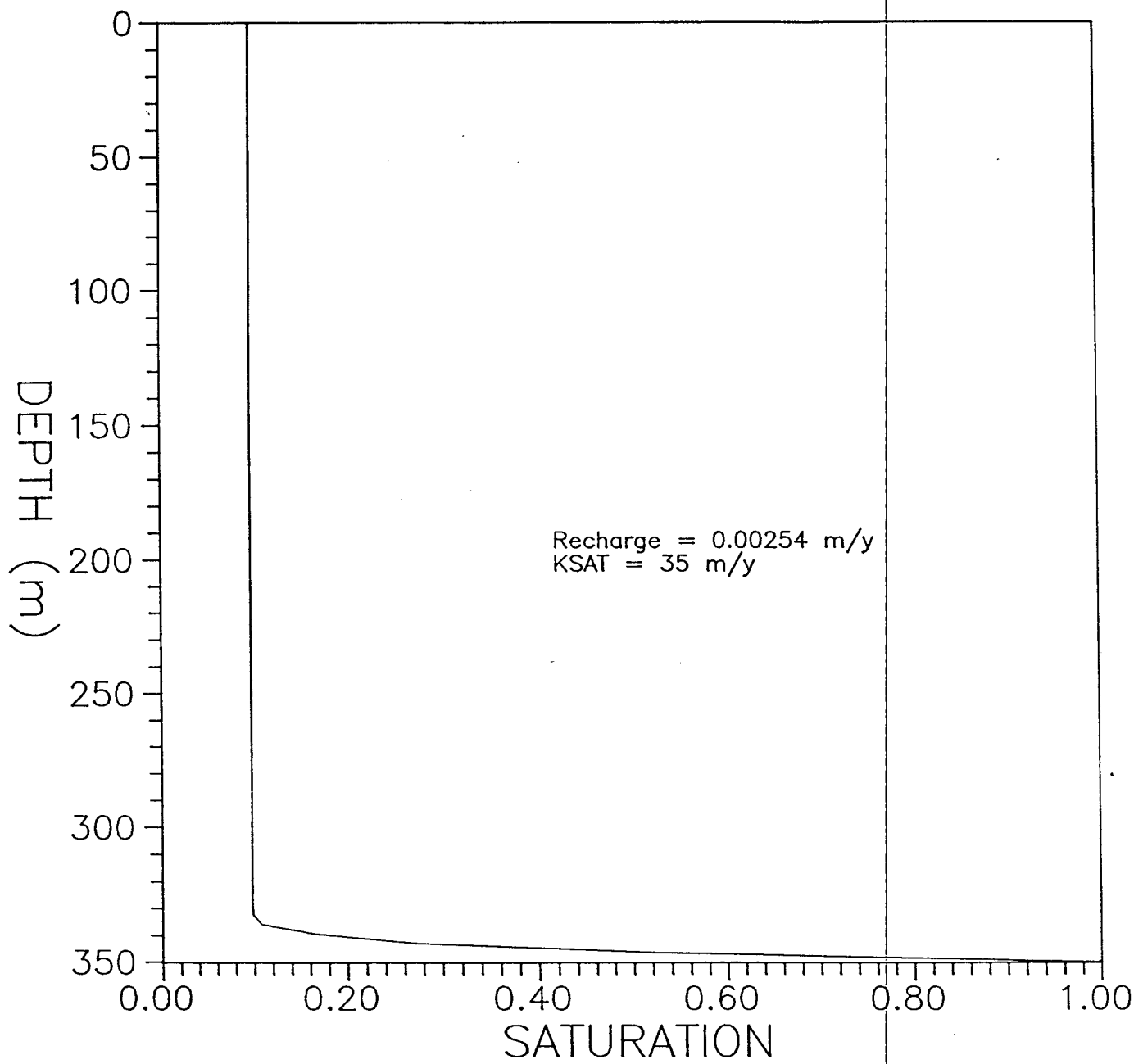


Figure 5.54. Steady state moisture distribution.

- 
- 1978 - Saturation and concentration distributions measured by Nyhan (1984) are available for comparison with the simulation results (Appendix F);
  - 1990 - Estimates of current site conditions are provided.

### 5.5.2.1 Scenario II.1 - Liquid Radionuclide Waste Addition

Scenario II.1 is a one-dimensional analysis that was performed to evaluate the effects on the hydrologic system caused by the intermittent disposal of liquid wastes.

#### 5.5.2.1.1 Procedures and Input Parameters

The input for this scenario is identical to Scenario I.1 with the exception that liquid waste discharges are introduced to the system (Table 5.5). The earliest data available on the volumes of waste added to the disposal beds are from 1945. As described in Section 4.0, it was assumed that 55 percent of the total flux released to beds 1 and 2 entered bed 1 (45 percent entered bed 2, see Table 5.6).

#### 5.5.2.1.2 Saturation Distributions

The simulated saturation profiles are presented in Figures 5.55 and 5.56 for the 350- and 100-meter meshes, respectively.

#### 5.5.2.1.3 Discussion

Modeling results indicate that by 1949, water has infiltrated to a depth of approximately 150 m and the system has approached 80 percent saturation. After 1967, the only flux entering the system is natural recharge (.00254 m/y). By 1990 the saturation has decreased substantially as the system approaches equilibrium.

The one-dimensional simulation does not allow for lateral movement of the infiltrating water which could slow the vertical movement significantly. However, predominantly vertical flow is consistent with the presence of vertical fractures in the tuff.

Despite the addition of a number of discrete waste liquid pulses there is no evidence of these pulses in the saturation profiles (i.e., sharp variations in moisture content are not present); rather, initial sharp contrasts in saturation have been smoothed out over the entire rock interval, due to the natural tendency for associated strong moisture tension gradients to dissipate quickly with time.

Table 5.5. Parameter input for scenario I.1 (1-D).

Input Parameter	Value
1. Saturated hydraulic conductivity	35 m/y
2. Residual water saturation	.0097 (dimensionless)
3. Power index (n) of the relative permeability versus saturation relationship	3.69 (dimensionless)
4. Leading coefficient (alpha) of the saturation versus capillary head relationship	.423 m <sup>-1</sup>
5. Power index (beta) of the saturation versus capillary head relationship	2.217 (dimensionless)
6. Porosity	.4 (dimensionless)
7. Bulk Density	1.55 g/cm <sup>3</sup>
8. Flux Rates	See Table 5.6

Table 5.6. Flux input to absorption beds at MDA T without 1960-1961 pulse.

Year	Estimated total flux from DPE & DPW (m <sup>3</sup> )	55% of total flux (Bed 1)	Areal correction of total flux <sup>1</sup>	Ambient recharge (m/y)	Flux input to model (m/y)
1944	--	--	--	--	--
1945	3,000	1,650	7.39	.00254	7.39
1946	4,000	2,200	9.85	.00254	9.86
1947	5,000	2,750	12.30	.00254	12.30
1948	6,000	3,300	14.78	.00254	14.80
1949	5,971	3,284	14.70	.00254	14.70
1950	10,030	3,517	24.70	.00254	24.70
1951	13,600	7,480	33.50	.00254	33.50
1952	5,400	2,970	13.30	.00254	13.30
1953	822	452	2.02	.00254	2.03
1954	206	113	.506	.00254	.51
1955	1,389	764	3.40	.00254	3.40
1956	1,970	1,023	4.85	.00254	4.86
1957	1,587	873	3.91	.00254	3.91
1958	657	361	1.61	.00254	1.62
1959	731	402	1.80	.00254	1.80
1960	750	413	1.84	.00254	1.85 <sup>2</sup>
1961	117	64	.28	.00254	.29 <sup>2</sup>
1962	51	28	.125	.00254	.128
1963	230	127	.569	.00254	.569
1964	98	54	.24	.00254	.244
1965	2,629	1,446	6.47	.00254	6.48
1966	4,355	2,394	10.70	.00254	10.70
1967	666	366	1.63	.00254	1.64
1968	--	--	--	--	--

<sup>1</sup>Area of bed 1 is 223.26 m<sup>2</sup>

<sup>2</sup>Note additional flux added by Christenson (1961) has not been included

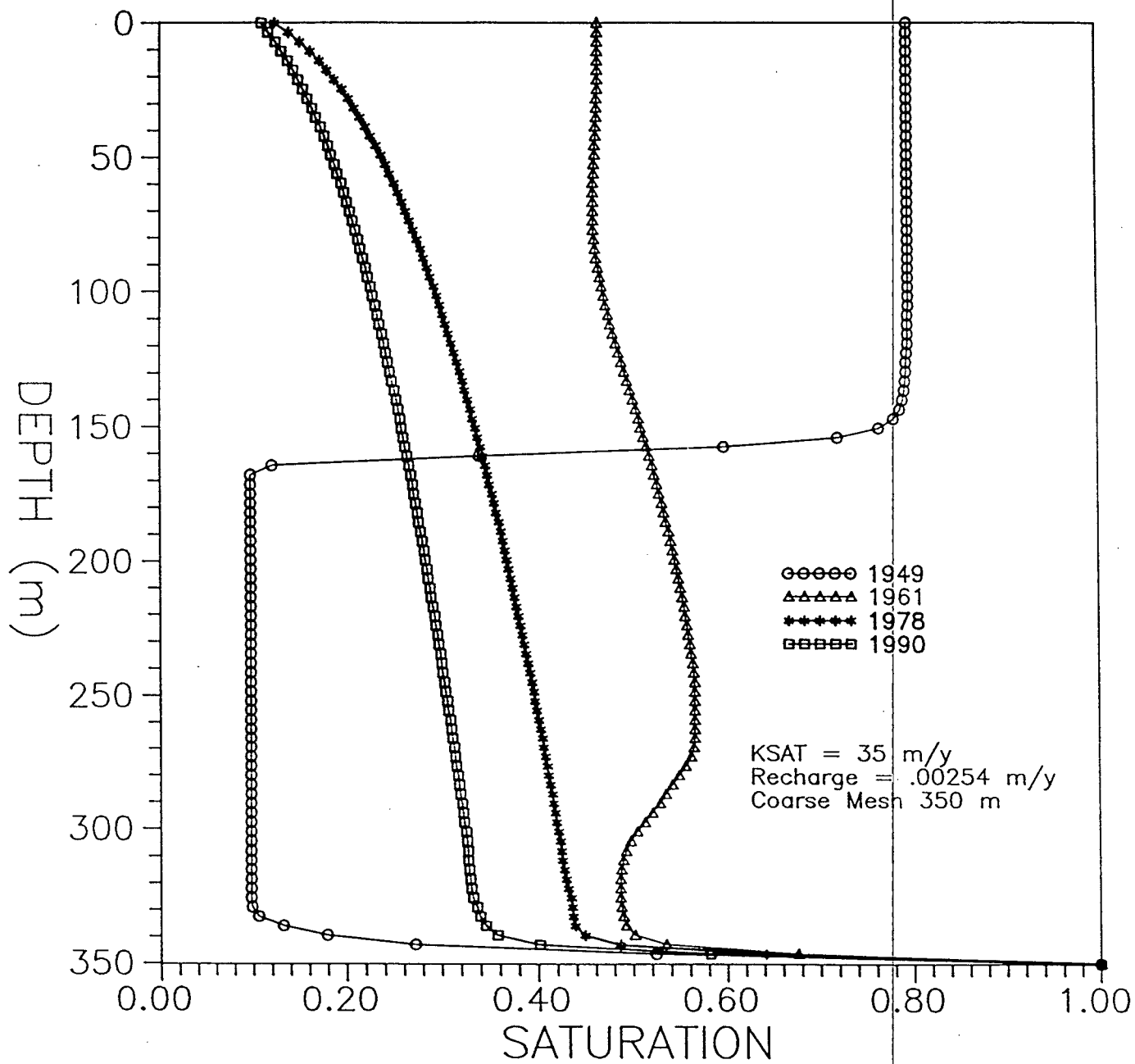


Figure 5.55. Saturation profile of Scenario II.1 (coarse mesh).

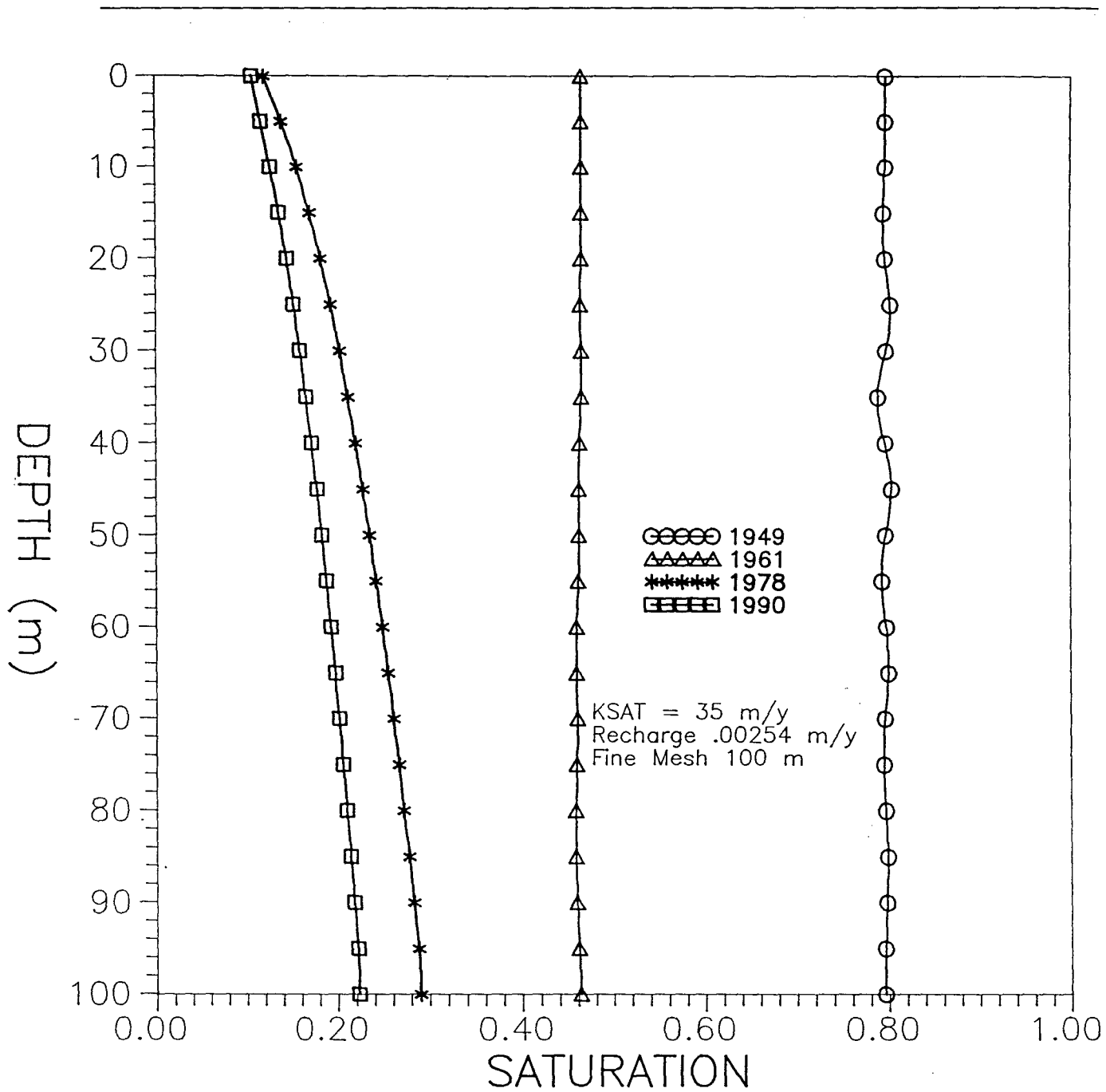


Figure 5.56. Saturation profile of Scenario II.1 (fine mesh).

---

### 5.5.2.2 Scenario II.2 - Moisture Pulse in 1960 and 1961

In 1960 and 1961, during two infiltration studies, several large pulses of water were discharged into bed 1 at MDA T (Christenson, 1961). The objective of this scenario is to evaluate the effect that these pulses of water, in addition to the waste discharges, have had on the hydrogeologic system.

#### 5.5.2.2.1 Procedures and Input Parameters

This scenario was simulated both in one-dimension (HYDRUS) and two-dimensions (SOILSIM). Except for the addition of two large moisture slugs in 1960 and 1961, the one dimensional simulation used identical input as Scenario II.1 (Tables 5.7 and 5.8).

To eliminate numerical instabilities in the two dimensional simulations, the addition of the water in 1960 and 1961 and liquid wastes, were mass averaged over specified years (Figure 5.57), rather than introduced as short term slugs.

In the SOILSIM analyses the power index of the relative permeability versus saturation relationship ( $n$ ) was relaxed from 3.69 to 3.0. Otherwise the parameter input was identical to HYDRUS (Table 5.7).

#### 5.5.2.2.2 Saturation Distributions

One dimensional saturation profiles and distributions are presented in Figures 5.58 and 5.59 for the coarse 350 meter mesh and the 100 meter mesh, respectively. In addition, Figure 5.60 illustrates the saturation distribution in two dimensions.

#### 5.5.2.2.3 Discussion

The most notable difference between the one dimensional simulation results of this scenario and the results from Scenario II.1, is that the slugs of water added in 1960 and 1961 have caused increased saturation (68 percent) to a depth of 70 m in 1961. In 1978, the only evidence of the pulses added in 1960 and 1961 are slightly higher residual saturations.

In both simulations the rocks approach nearly the same saturations by 1990. This suggests that above some threshold saturation and corresponding saturated hydraulic conductivity, the rocks will drain fairly rapidly.

Results from the two dimensional simulation suggest that if vertical and horizontal saturated hydraulic conductivities are the same, saturations would be increased over horizontal distances on the order of at least 42 meters (Figure 5.60). Data from

Table 5.7. Parameter input for Scenario II.2.

Input Parameter	Value	
	1-D	2-D
1. Saturated hydraulic conductivity	35 (m/y)	35 (m/y)
2. Residual water saturation	.0097	.0097
3. Power index (n) of the relative permeability versus saturation relationship	3.69	3.0
4. Leading coefficient (alpha) of the saturation versus capillary head relationship	.423 (m <sup>-1</sup> )	.423 (m <sup>-1</sup> )
5. Power index (beta) of the saturation versus capillary head relationship	2.217	2.217
6. Porosity	.4	.4
7. Bulk Density	1.55 (g/cm <sup>3</sup> )	1.55 (g/cm <sup>3</sup> )
8. Flux rates	See Table 5.8	See Figure 5.57

Table 5.8. Flux input to absorption beds at MDA T including 1960-1961 pulse.

Year	Estimated total flux from DPE & DPW (m <sup>3</sup> )	55% of total flux (Bed 1)	Areal correction of total flux <sup>1</sup>	Ambient recharge (m/y)	Flux input to model (m/y)
1944	--	--	--	--	--
1945	3,000	1,650	7.39	.00254	7.39
1946	4,000	2,200	9.85	.00254	9.86
1947	5,000	2,750	12.30	.00254	12.30
1948	6,000	3,300	14.78	.00254	14.80
1949	5,971	3,284	14.70	.00254	14.70
1950	10,030	3,517	24.70	.00254	24.70
1951	13,600	7,480	33.50	.00254	33.50
1952	5,400	2,970	13.30	.00254	13.30
1953	822	452	2.02	.00254	2.03
1954	206	113	.506	.00254	.51
1955	1,389	764	3.40	.00254	3.40
1956	1,970	1,023	4.85	.00254	4.86
1957	1,587	873	3.91	.00254	3.91
1958	657	361	1.61	.00254	1.62
1959	731	402	1.80	.00254	1.80
1960	750	413	1.84	.00254	9.63 <sup>2</sup>
1961	117	64	.28	.00254	6.43 <sup>2</sup>
1962	51	28	.125	.00254	.128
1963	230	127	.569	.00254	.569
1964	98	54	.24	.00254	.244
1965	2,629	1,446	6.47	.00254	6.48
1966	4,355	2,394	10.70	.00254	10.70
1967	666	366	1.63	.00254	1.64
1968	--	--	--	--	--

<sup>1</sup>Area of bed 1 is 223.26 m<sup>2</sup>

<sup>2</sup>Flux includes water added by Christenson in 1960 and 1961

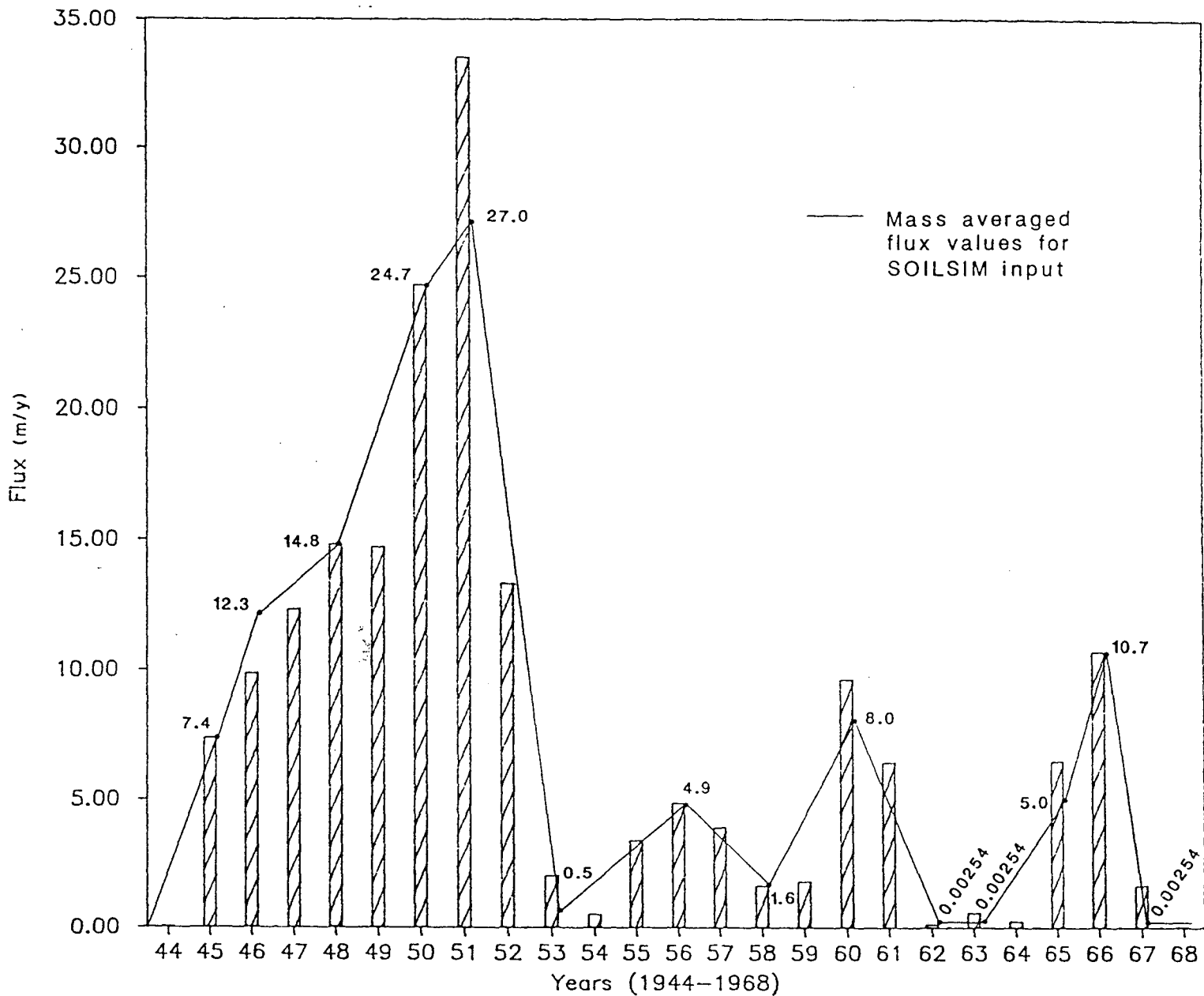


Figure 5.57. Hydrograph for flux input into SOILSIM and HYDRUS.

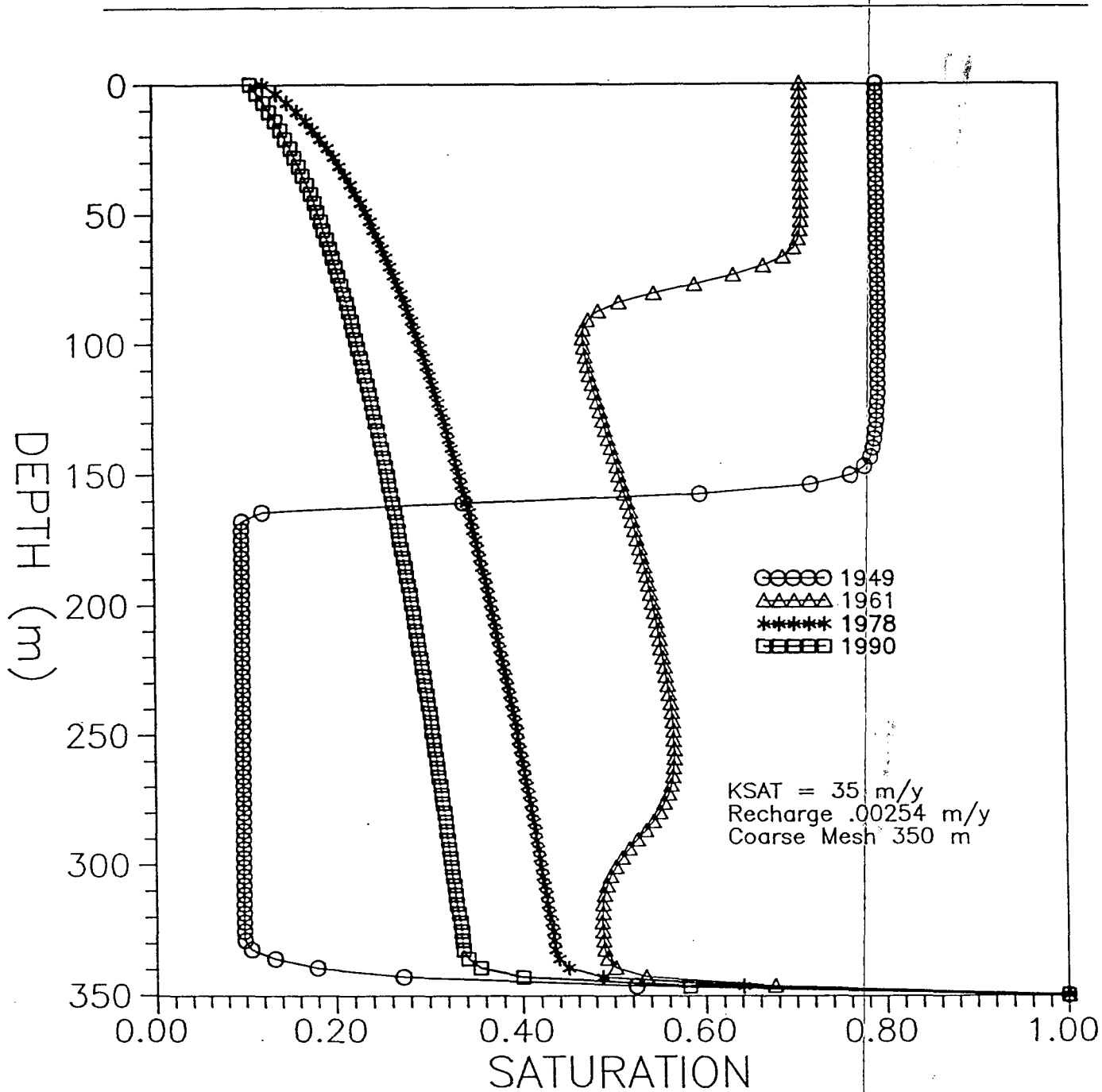


Figure 5.58. Saturation distribution for Scenario II.2 (with pulse in 1960-61) (coarse mesh).

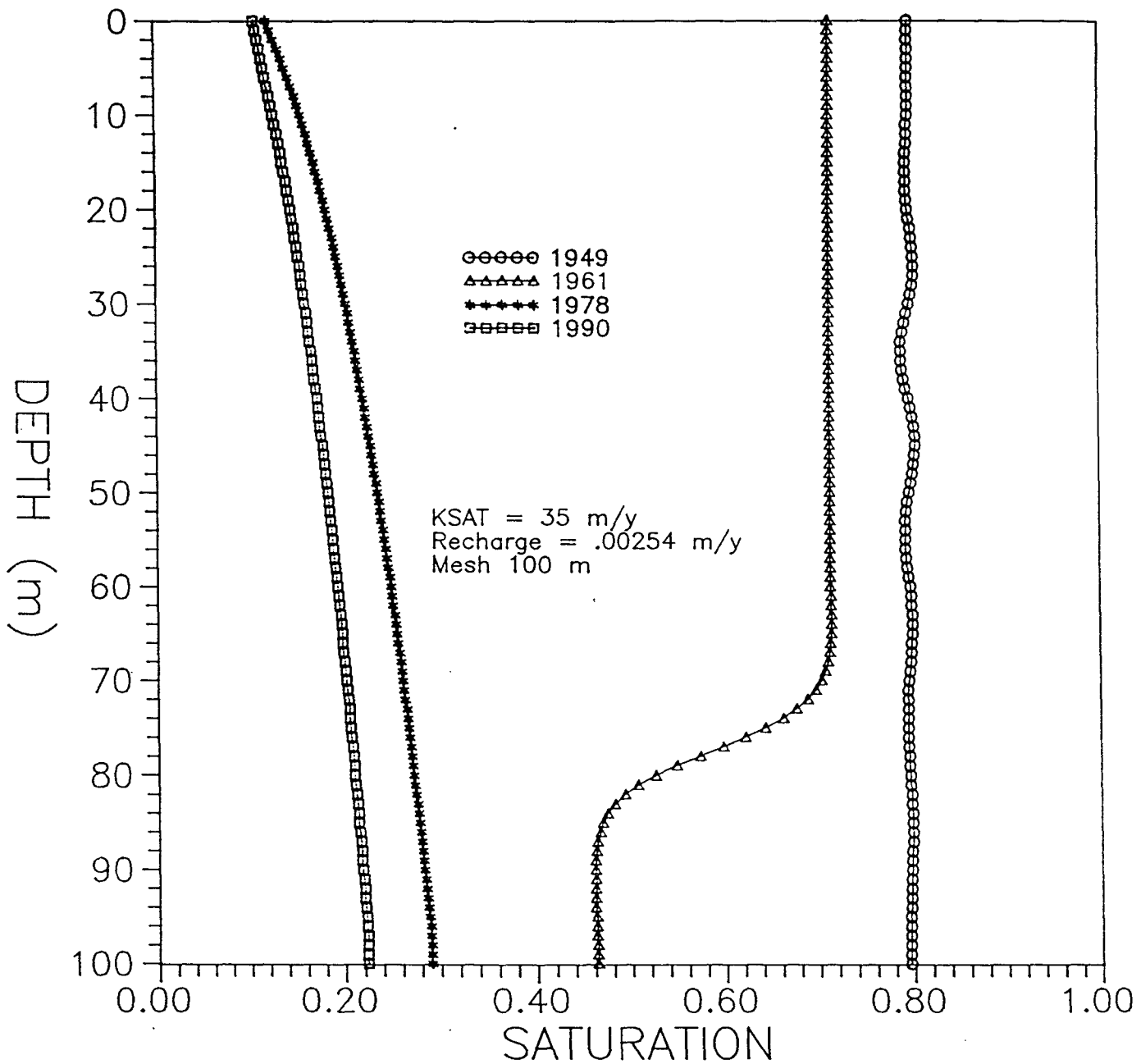


Figure 5.59. Saturation distribution for Scenario II.2 (with pulse in 1960-61) (fine mesh).

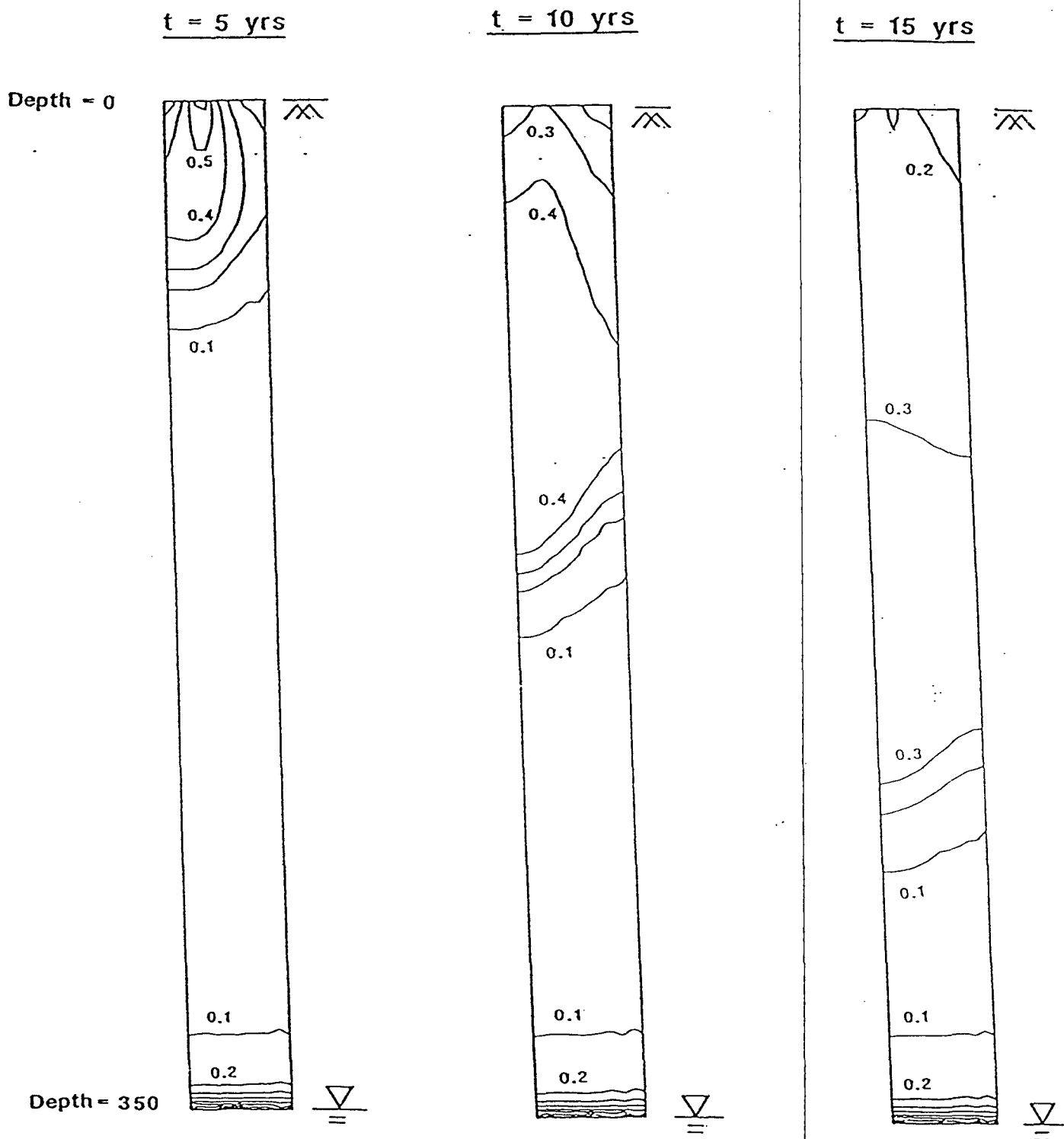


Figure 5.60. 2-D Scenario II.2 saturation distribution obtained from SOILSIM (pulse in 1960-61 applied/no pipe).

---

Abrahams (1963) indicates that the saturated hydraulic conductivity is approximately of the magnitude for horizontal and vertical directions in Bandelier tuff. The horizontal value is slightly higher (less than 10:1 horizontal to vertical) than the vertical.

Boundary effects must be taken into consideration when interpreting the results from the two dimensional simulations, as indicated by the saturation contours extending to the edges of the lateral domain. These boundary effects cause the water to flow faster vertically through the partially saturated zone. Normally, this might create problems with the interpretation of the modeling results. However, there is very little field information to compare the two dimensional modeling against; the modeling has been performed only to provide general approximations of system behavior. Furthermore, lateral moisture movement was probably overestimated in the two dimensional simulations that were performed by assuming horizontal and vertical hydraulic conductivities were equal. In reality, the presence of predominantly vertical fractures in the tuff probably results in a significantly greater vertical than horizontal hydraulic conductivity. In the absence of additional field data to define these conductivities there is little justification for additional two dimensional modeling.

#### 5.5.2.3 Scenario II.3 - Pipe Leak

In 1986, leaking pipes from a storm drain were discovered south of the absorption beds (Figure 5.61). It is unknown how long the pipes have been leaking but it is suspected that they may have been leaking at a rate of 1 to 2 gallons per minute (gpm) for a number of years.

##### 5.5.2.3.1 Procedures and Input Parameters

The original scope of work requested that two pipe leak simulations be performed, one at 2 gpm and one at 10 gpm. However, a flow rate of 2 gpm is equivalent to 3978 m<sup>3</sup>/y which is such a large volume of water entering the system, in addition to the direct discharges to the absorption beds, that this would likely have resulted in flooding of the site. This is even more true for a leakage rate of 10 gpm. Physically, the rate of leakage from a presorbed, non-pressurized pipe is related to the transmission capacity, i.e., hydraulic conductivity of the medium in which the pipe is buried. Therefore, the pipe leak was simulated by applying the water, from the leaking pipe, at approximately one half the saturated hydraulic conductivity of the surrounding rocks. This volume of water translates to a rate of approximately 0.03 gpm.

The location of the leaking pipe is adjacent to, but not directly underneath the absorption bed, and the presence of the leaking pipe cannot be accurately accommodated in a one-dimensional simulation. Therefore, the pipe leak scenario was only performed in two dimensions and incorporated identical stresses and input to those simulated in Scenario II.2, with the exception of the added flux of the pipe leak (Table 5.9).

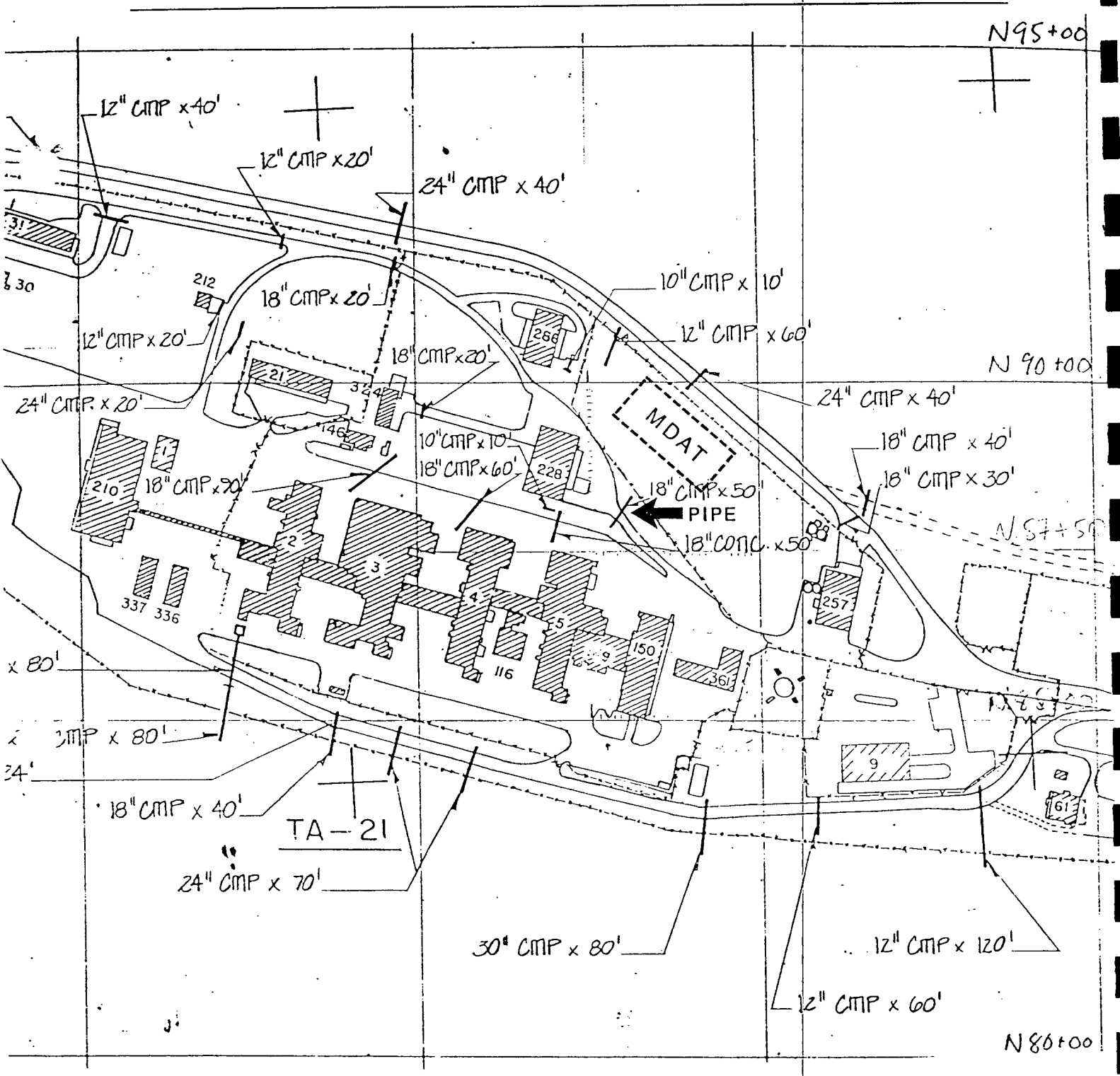


Figure 5.61. Location of buried pipe.

Table 5.9. Parameter input for scenario II.3 2-D.

Input Parameter	Value
1. Saturated hydraulic conductivity	35 m/y
2. Residual water saturation	.0097 (dimensionless)
3. Power index (n) of the relative permeability versus saturation relationship	3.0 (dimensionless)
4. Leading coefficient (alpha) of the saturation versus capillary head relationship	.423 m <sup>-1</sup>
5. Power index (beta) of the saturation versus capillary head relationship	2.217 (dimensionless)
6. Porosity	.4 (dimensionless)
7. Bulk Density	1.55 g/cm <sup>3</sup>
8. Flux rates	See Figure 5.57
9. Pipe leak	.03 gpm

---

#### 5.5.2.3.2 Velocity Field

The velocity field of this flow scenario is more illustrative than the saturation distribution and is presented in Figure 5.62.

#### 5.5.2.3.3 Discussion

The velocity field clearly depicts the effect of the leaking pipe in the upper left hand corner of the figure. The velocity arrows also indicate that there is a much greater vertical flow component underlying the leaking pipe than underlying bed 1.

The analysis also indicates that, if actual leakage rates were on the order of 2-10 gpm, the saturated hydraulic conductivity of the tuff must be much greater than previously estimated.

#### 5.5.3 Case III - Transport Simulations

The transport simulations performed in Case III of this analysis are analogous to the Case II flow simulations, that is, each transport scenario in Case III has the same flow scenario that was performed during the Case II simulations.

Unknown factors that may have influenced the distribution of americium include the initial concentrations of americium introduced to the waste pit, the weight fraction of  $^{241}\text{Pu}$  to  $^{239}\text{Pu}$  present in the original liquid wastes, and the respective migration rates of  $^{241}\text{Pu}$  and  $^{239}\text{Pu}$ . Nyhan and others (1984) performed a rough mass balance that indicated that not all of the americium in the rock stratum could be accounted for by the radioactive decay of  $^{241}\text{Pu}$  ( $^{241}\text{Pu}$  decays to  $^{241}\text{Am}$  with a half-life of 13.2 years). Therefore, a certain amount of americium must have been introduced by the liquid wastes. However, at this time, it is not possible to determine the relative importance of these two americium sources.

The lack of background information pertaining to americium precluded a detailed transport analysis. Therefore, Case III simulations only predicted concentration distributions for plutonium and a generic conservative species. The generic conservative species is presumed to display the general properties of fluoride and citrate.

Distribution coefficients are set to 13 for all of the transport runs in both one and two dimensions. This value was arrived at during the sensitivity analysis when it was found that a distribution coefficient of 13 allowed the plutonium in the water to migrate approximately 100 feet in depth, which is the approximate depth that plutonium has been encountered at the site.

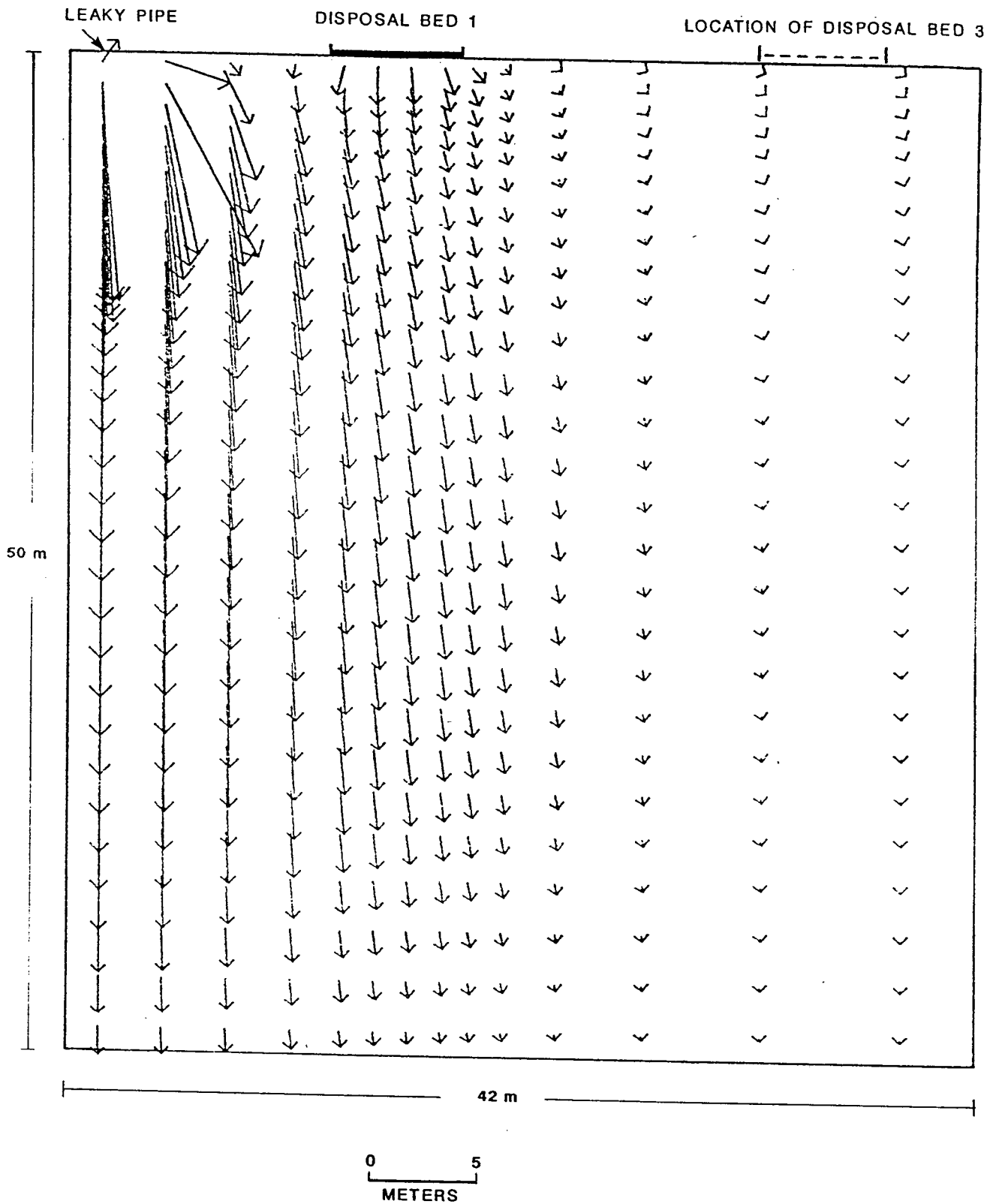


Figure 5.62. Velocity field of Scenario II.3 (pipe leak and pulse in 1960-61).

---

### 5.5.3.1 Scenario III.1

This scenario was performed in only one dimension to determine the rates of movement, and concentration distribution of plutonium. The only external stress placed on the system for this scenario is the intermittent introduction of liquid wastes.

#### 5.5.3.1.1 Procedures and Input Parameters

The velocity fields for the transport simulations performed during this scenario were obtained from the one dimensional flow output obtained during Scenario II.1. The specific input for this transport run is presented in Table 5.10. The concentration input is presented as a bar graph in Figure 5.63.

#### 5.5.3.1.2 Concentration Distributions

The simulated concentration distributions are presented in Figure 5.64.

#### 5.5.3.1.3 Discussion

The plutonium distribution profiles indicate that in 1978 the center of mass has reached a depth of approximately 6 meters. The leading edge of the plume on the other hand has already reached a depth of 15 meters in 1949 and 30 meters in 1961. It is also evident that under conditions of ambient recharge, migration rates are very slow, resulting in no noticeable differences in plutonium distribution between 1978 and 1990.

### 5.5.3.2 Scenario III.2

This scenario was performed in both one and two dimensions to determine the rates, directions and extent of plutonium radionuclide movement. The external stresses placed on the system are the intermittent introduction of liquid wastes and the water pulses applied in 1960 and 1961.

#### 5.5.3.2.1 Procedures and Input Parameters

The velocity fields for the transport simulations performed during this scenario were obtained from the outputs of the one- and two-dimensional flow runs performed during Scenario II.2.

---

Table 5.10. Parameter input for Scenario III.1.

---

Input Parameter	Value
1. Porosity	.4 (dimensionless)
2. Bulk Density	1.55 g/cm <sup>3</sup>
3. Dispersivity	3.5 m
4. Distribution Coefficient	13 cm <sup>3</sup> /g
5. Concentration Input	See Figure 5.63

---

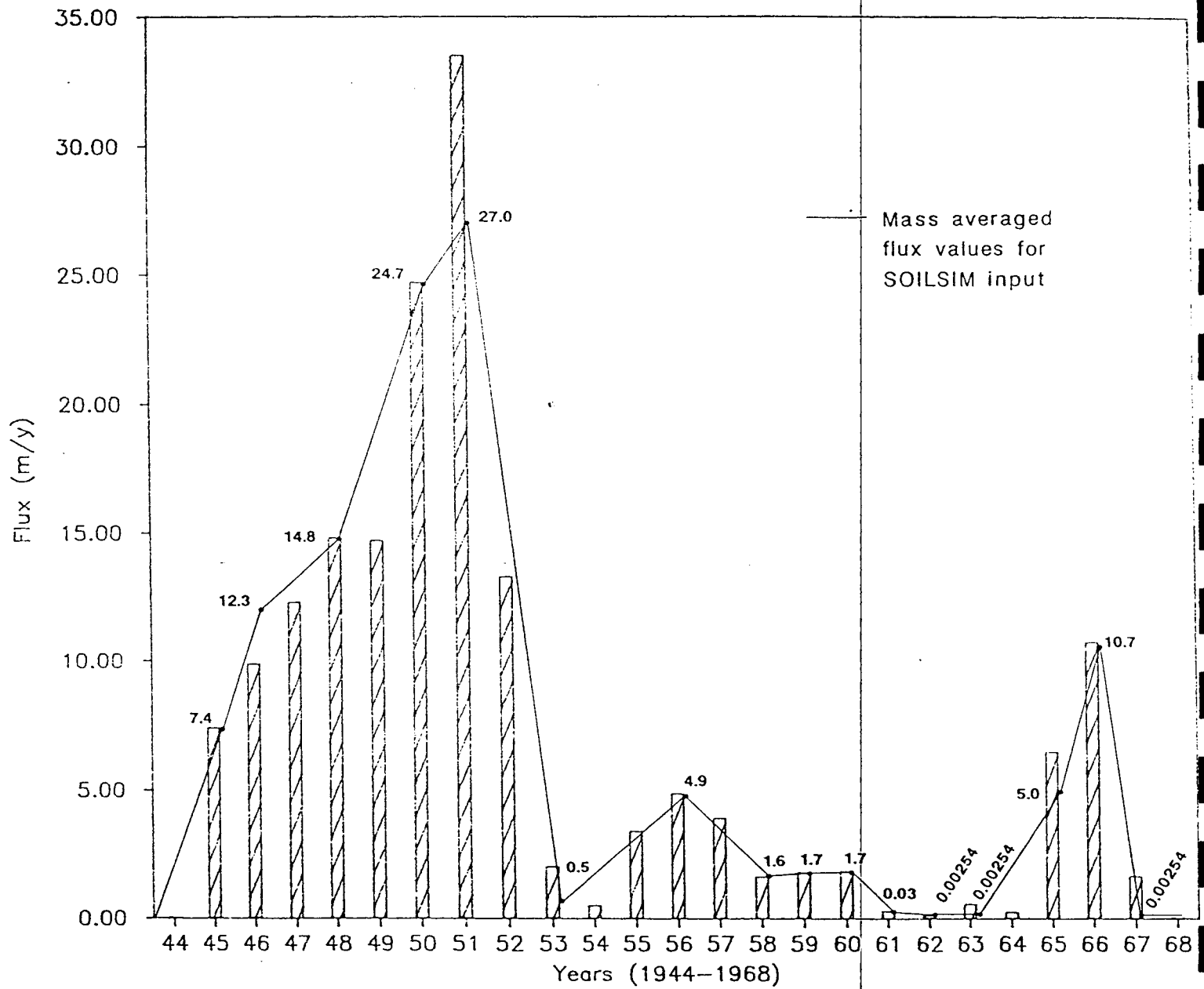


Figure 5.63. Concentration input for 1- and 2-D Scenarios.

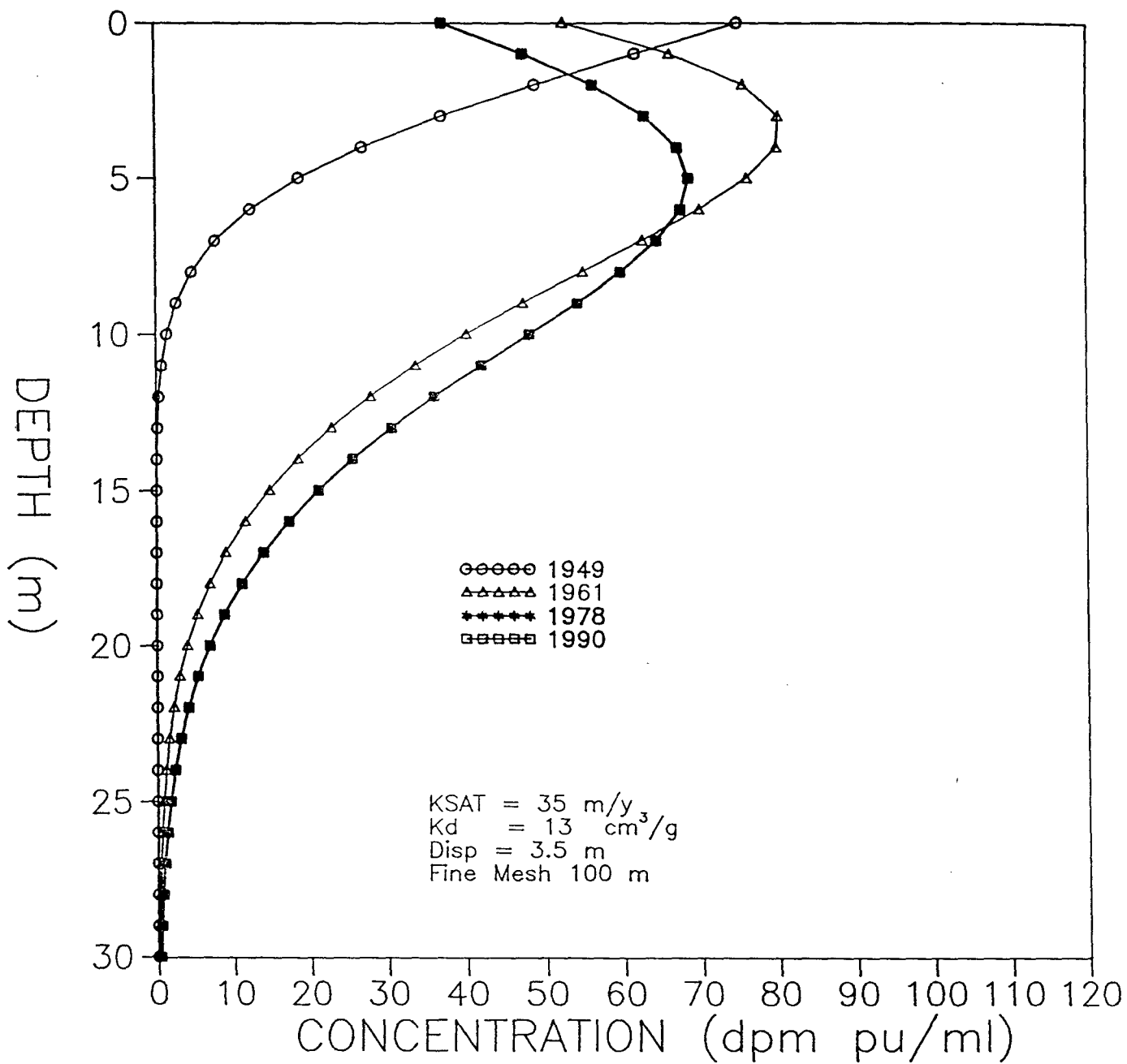


Figure 5.64. Simulated plutonium concentration profiles of Scenario III.1.

---

The parameter values and concentration input for the one dimensional simulations are presented in Table 5.11. The method by which water flux was mass-averaged for the two dimensional flow simulations dictated that the plutonium concentration input also be mass averaged (Figure 5.63).

#### 5.5.3.2.2 Concentration Distributions

Concentration profiles for the one dimensional simulation are presented in Figure 5.65.

Concentration profiles for a two-dimensional simulation involving a conservative species ( $K_d = 0.0$ ) are presented in Figure 5.66.

Concentration profiles for two dimensional simulations of plutonium are presented in Figures 5.68 and 5.69.

#### 5.5.3.2.3 Discussion

Comparison of the one dimensional simulations suggest that the additional water pulses added in 1960 and 1961 have had very little effect on the transport rates of the plutonium. The majority of the water added in 1960 and 1961 did not contain radionuclides and therefore probably decreased the water phase radionuclide concentrations in the water underlying MDA T.

In the two dimensional simulation of a conservative species (concentrations are normalized) it appears that the solute could have moved as deep as two hundred meters by 1969. However, there has most probably been some retardation even for fluoride and citrate.

The two dimensional simulation of plutonium indicates that under the conditions specified in the model, plutonium would have only migrated 12 meters in depth. Field evidence indicates that plutonium has migrated to a depth of at least 30 meters. The discrepancy between the field measurements and the simulation results demonstrate that either the assumed distribution coefficients are too high or the ratio of vertical to horizontal saturated hydraulic conductivity used in the model is too low.

#### 5.5.3.3 Scenario III.3

This scenario was performed in two dimensions to determine the rates, directions and extent of radionuclide and conservative species movement. The external stresses placed on the system are the intermittent introduction of liquid wastes, water pulses applied in 1960 and 1961, and a .03 gpm pipe leak.

---

Table 5.11. Parameter input for Scenario III.2.

---

Input Parameter	Value
1. Porosity	.4 (dimensionless)
2. Bulk Density	1.55 g/cm <sup>3</sup>
3. Dispersivity (longitudinal and transverse)	3.5 m
4. Distribution Coefficient	13 cm <sup>3</sup> /g
5. Concentration Input	See Figure 5.63

---

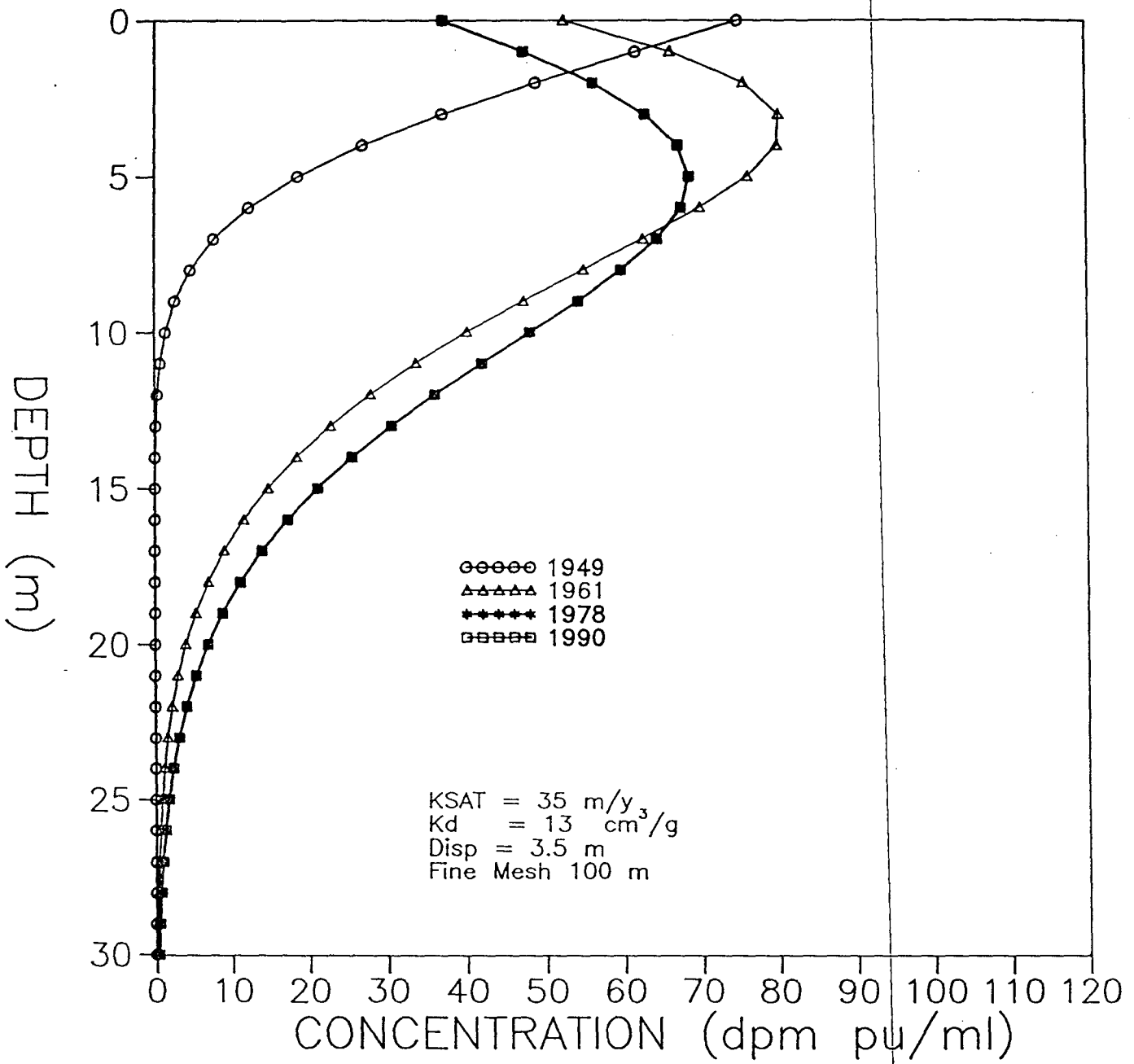


Figure 5.65. Simulated plutonium concentration profiles of Scenario III.2.

S6-S

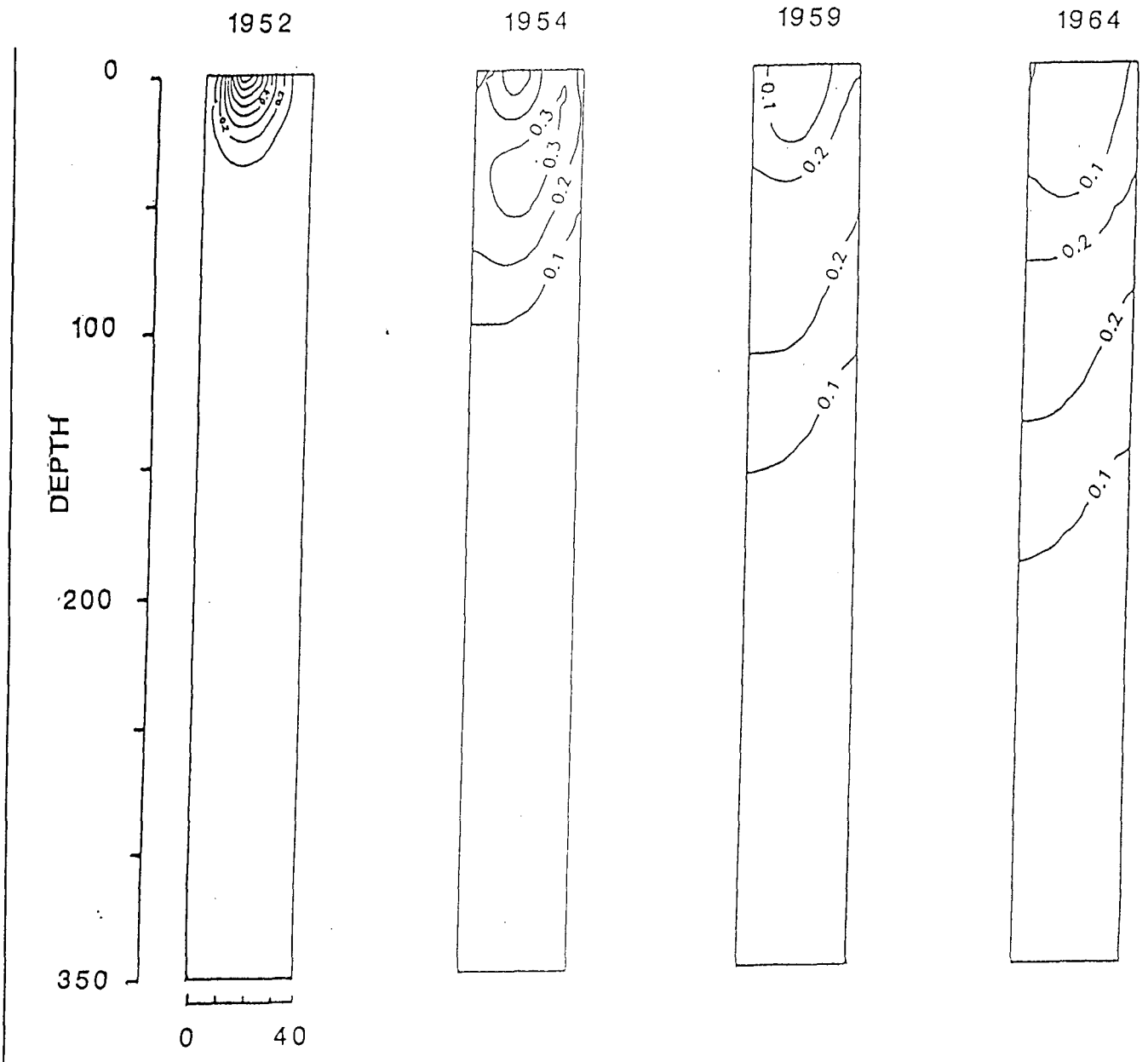


Figure 5.66. Simulated normalized concentration profiles for two-dimensional simulation involving a conservative species including 1960-61 pulses but without the pipe leak.

---

#### 5.5.3.3.1 Procedures and Input Parameters

The velocity fields for the transport simulations performed during this scenario were obtained from the outputs of the one and two dimensional flow runs performed during Scenario II.2.

Model input is identical to that of Scenario III.2 with the exception of a simulated pipe leak of .03 gpm (Table 5.12).

#### 5.5.3.3.2 Concentration Distributions

Concentration profiles for a two-dimensional simulation involving a conservative species ( $K_d=0$ ) is presented in Figure 5.67.

Concentration profiles for two dimensional simulations of plutonium are presented in Figures 5.68 and 5.69.

#### 5.5.3.3.3 Discussion

The lateral movement of water from the leaking pipe partially intercepts the radionuclide plume and increases the saturation of the rocks. The higher saturation increases the hydraulic conductivity and allows the radionuclides to move more rapidly.

---

Table 5.12. Parameter input for Scenario III.3.

---

Input Parameter	Value
1. Porosity	.4 (dimensionless)
2. Bulk Density	1.55 g/cm <sup>3</sup>
3. Dispersivity (longitudinal and transverse)	3.5 m
4. Distribution Coefficient	13 cm <sup>3</sup> /g
5. Concentration Input	See Figure 5.63
6. Pipe Leak	.03 gpm

---

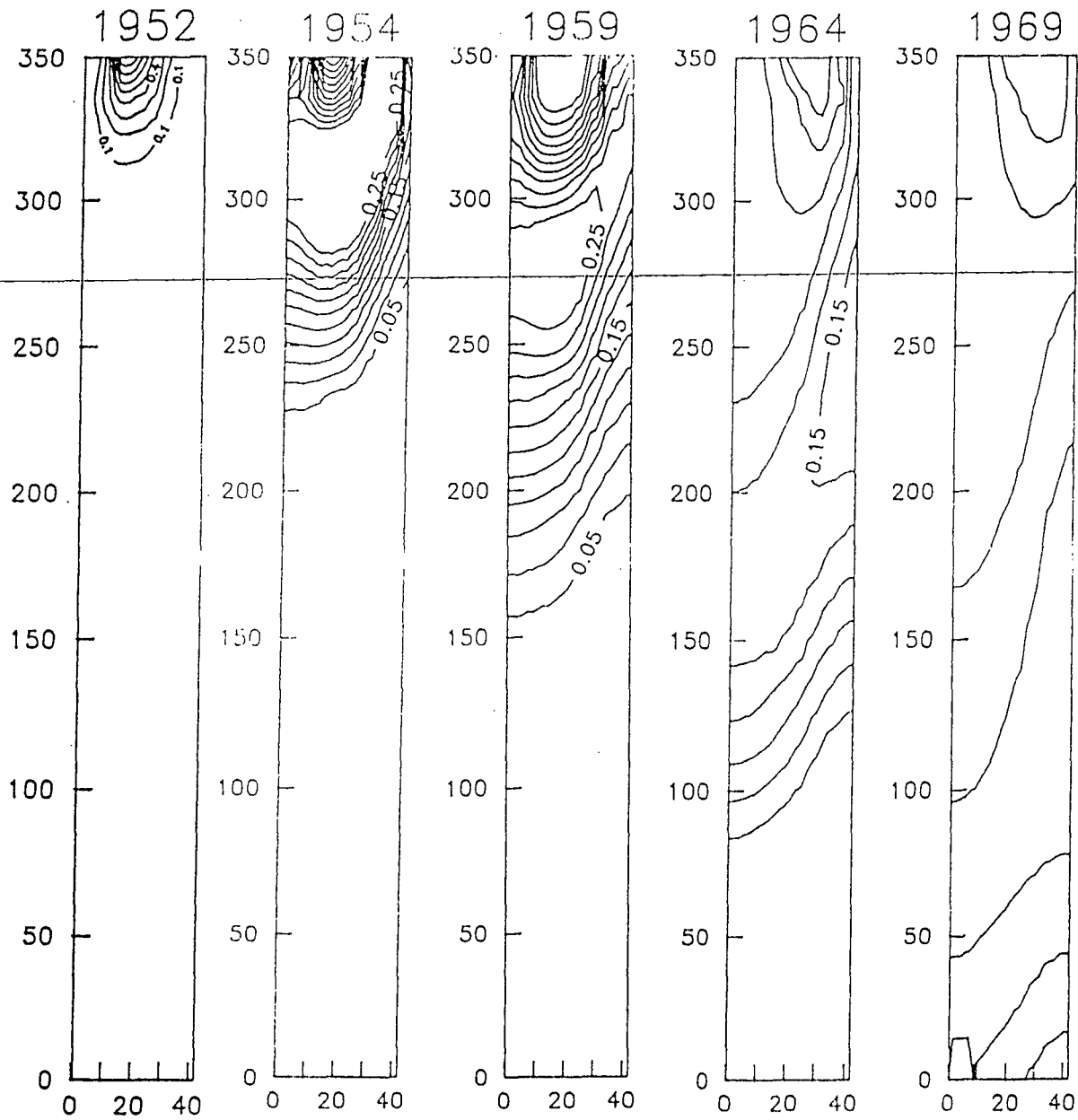


Figure 5.67. Simulated normalized concentration profiles for two-dimensional simulations involving a conservative species with pipe leak and 1961 pulses.

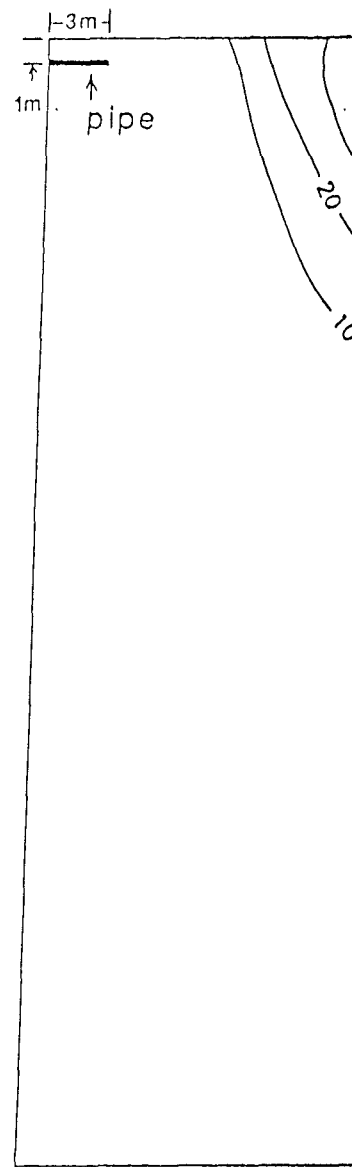
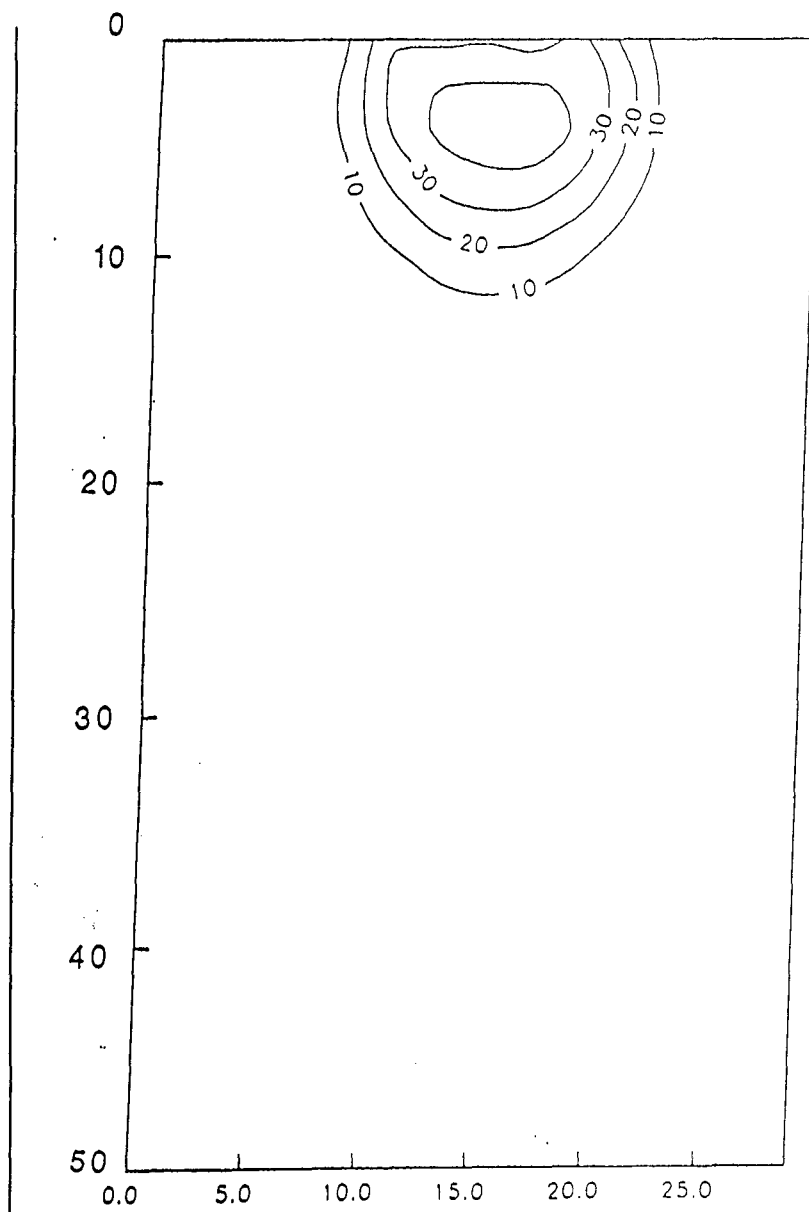
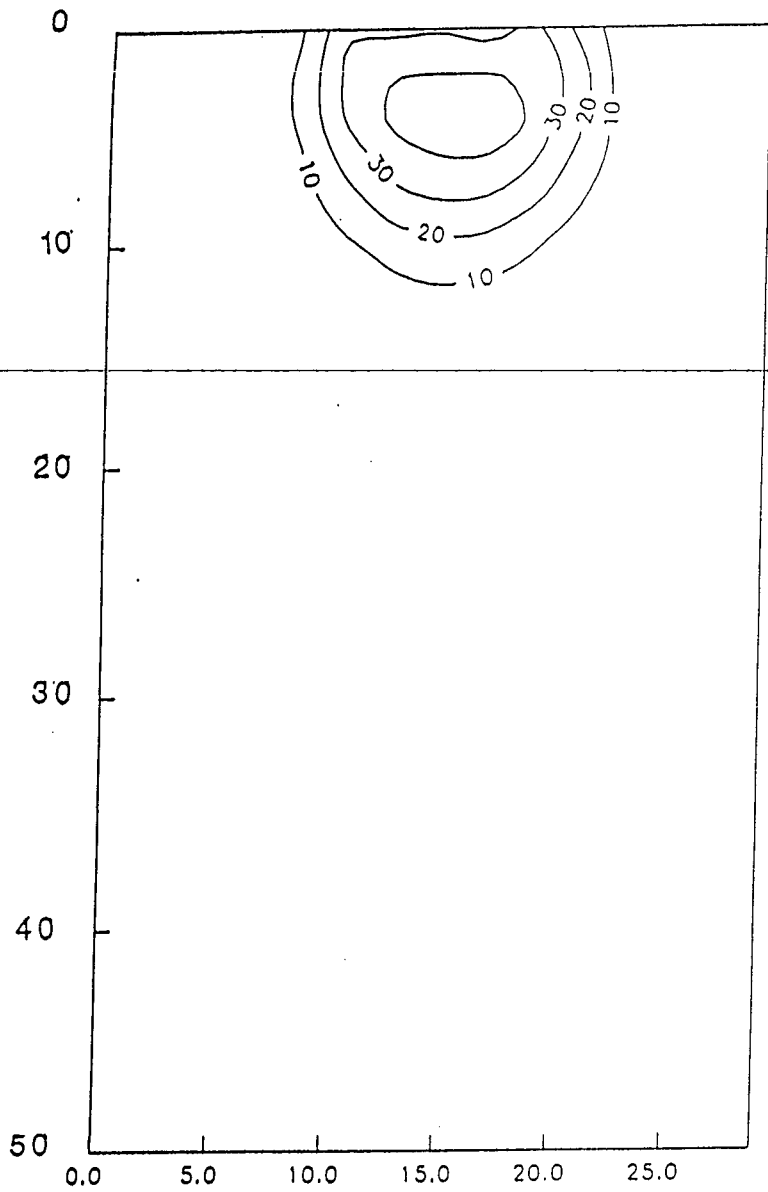
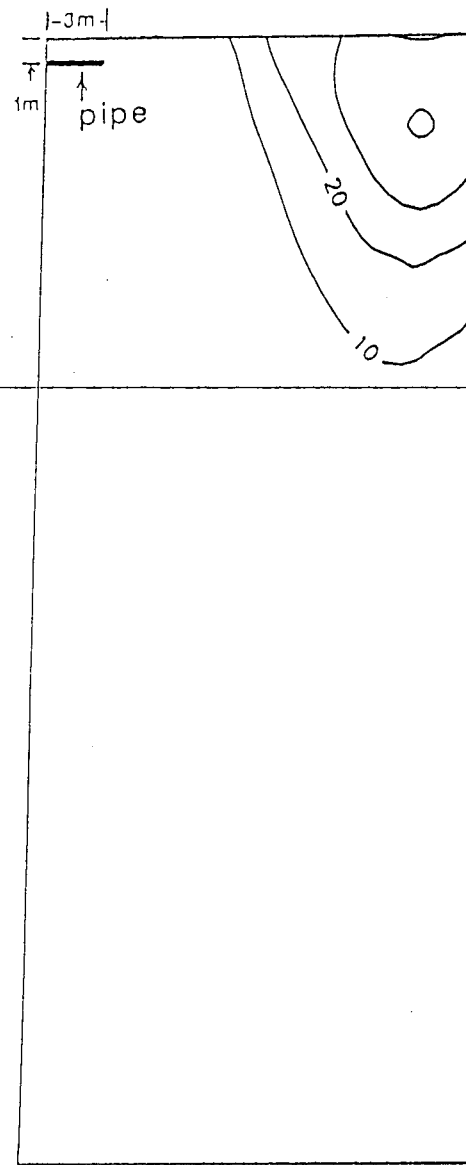


Figure 5.68. Simulated concentration profiles for two-dimensional simulations of Plutonium in 1978 with and without the pipe.



(a)



(b)

Figure 5.69. Simulated concentration (dpm) profiles for two-dimensional simulations of Plutonium in 1990 with and without the pipe.

---

## 6.0 PATHWAY ANALYSIS RESULTS AND CONCLUSIONS

Pathway analysis results are useful primarily for the development of a site conceptual model, from which the remedial investigation may be designed, implemented and evaluated.

It is important to recognize the transient nature of certain parameters (e.g., degree of saturation) which control flow and transport now and in the future. They may be very different from the conditions that governed flow and transport during the liquid-waste applications. Therefore, if future radionuclide movement is to be reliably predicted, some additional information must be obtained pertaining to the mechanisms that controlled the movement of water and radionuclides in the past.

Even the most conscientious remedial investigation program would provide only a relatively short observation period from which to recommend potential remedial measures. Evaluations based on such a limited history would have a significant degree of uncertainty. Furthermore, it is possible that the remedial investigation activities may conclude that major remedial options, such as the removal of the source to acceptable concentrations, are infeasible or ineffective when compared to other remedial options. In such a case, the pathway analysis may also be used as the quantitative framework from which to develop contingency plans for remedial measures and to provide a quantitative analysis in the defense of alternative remedial approaches to State and Federal regulatory agencies. Specific findings and conclusions from the pathway analysis are summarized below.

### 6.1 Fluid Movement

Pathway analysis results indicate that if the previous estimate (Abeele and others, 1981) of 27 m/y for the matrix saturated hydraulic conductivity of the Bandelier tuff was correct, the system could not have transmitted all of the liquid waste introduced into the beds without the occurrence of substantial surface ponding, runoff, and subsurface lateral spreading of perched water. There is evidence that surface ponding and overflow from the pits did occur as stated by Rogers (1977).

"Report[edly] more water [liquid wastes] moved into [Beds] 1 and 3 than moved into 2 and 4, and at times some of the pits became clogged and overflowed, the overflow moving north towards a canyon. Overflow from the beds never reached the canyon."

However, it may be assumed from this statement that the clogging of the beds was responsible for the overflow and not that the saturated hydraulic conductivity of the Bandelier tuff was exceeded. Reportedly, the beds were ultimately taken out of operation because they became so clogged.

---

The sensitivity analyses demonstrate that, at saturated hydraulic conductivities of 27 m/y, the volumes of discharge water reported by Christenson and others (1961) could not have been accommodated by matrix flow alone (Section 5.2). Therefore, either the matrix saturated hydraulic conductivity is substantially greater than previously estimated, or fractures are responsible for secondary permeability and played a significant role in the transmission of fluids and the transport of the accompanying solutes at the time of liquid wastes application. The minimum bulk vertical hydraulic conductivity (matrix and fractures combined) required to transmit liquids downward without considerable ponding is about 35 m/y.

The model layers with relatively low saturated hydraulic conductivities reached complete saturation by 1951 during the historical comparison simulation (Section 5.3). However, the water in the low permeability rocks had largely dissipated (moved vertically downward) by 1977. Furthermore, the yearly slugs of waste water added to the absorption beds are not discernable in the subsurface as discrete peaks but have dissipated over the entire stratigraphically layered profile.

In the event that recharge predominantly occurs as infrequent, high intensity events, such as snowmelts, the shallow distribution of moisture may differ from model predictions. However, at fairly shallow depths (less than 100 ft.) ambient moisture content is fairly constant at approximately 10 percent saturation (Abeele and others, 1979). These uniform moisture profiles suggest that moisture pulses associated with any high intensity recharge events are dampened at fairly shallow depths and are not observed as discrete pulses in the subsurface.

The pathway analysis results show that waste water discharged to the beds can move to the water table in a relatively short period of time (generally a few weeks to a few months). There is no evidence to indicate that radionuclides move with the water to these depths. The behavior of any other constituents is unknown. Currently, archive searches and interviews are being conducted to better define the composition and quantity of waste stream input into the four adsorption beds. Even if it is assumed that the distribution coefficients are far less than those measured on Yucca Mountain tuffs, the radionuclides at the MDA T site would have been retained in the upper 50 m.

#### 6.1.1 Lateral Fluid Movement

The moisture content distributions that were obtained from the two-dimensional simulations suggest that waste water disposal may have caused increases in saturation at substantial lateral distances from the absorption beds. This potential for lateral fluid movement presents the possibility for surface releases along the canyon wall to the north of the site. However, current field evidence suggests that even if water has moved laterally towards the canyon, the extent of any lateral radionuclide migration has been relatively limited. Recommendations for investigating the extent of lateral movement during the remedial investigation program are discussed in Section 8.0.

---

Results from the historical comparison simulations (Section 5.3), suggest that if the system contains rock layers of lower saturated hydraulic conductivity, the waste water applied to the absorption beds could saturate these layers and create perched water. Perched water would increase lateral water movement and thus tend to enhance lateral radionuclide transport.

## 6.2 Radionuclide Movement

The transport simulations performed during the pathway analysis used a range of distribution coefficients (Kd's) that were based on measured values for tuffs from Yucca Mountain, Nevada. Pathway analysis results indicate that the transport is very sensitive to distribution coefficients and that to approximate the observed concentrations, distribution coefficients (Kd's), particularly for americium, need to be considerably lower (allowing faster transport) than the values reported for Yucca Mountain tuffs. Two conclusions may be drawn from these results; either the sorption characteristics of the Bandelier tuff are considerably different from those reported for Yucca Mountain tuffs, or other factors involving the physical-chemical interaction of the waste solution and Bandelier tuff allow more rapid radionuclide transport. Abrahams (1963) suggests wastewater movement through the tuff may have changed some of the physical properties of the tuff, such as pore and particle sizes.

Discrepancies between the apparent retardation factors obtained from measured radionuclide travel distances, and retardation corresponding to the Kd's estimated from studies of other tuffs may be caused by the following processes: colloidal transport, Pu/Am oxidation and ionic state, complexing chemistry, decay of 241-Pu to 241-Am (half life 13.2 years), hydrolysis of plutonium, and preferential flow and transport down fractures during periods of high waste discharge, followed by diffusion of radionuclides into the rock matrix. Plans for investigating the role of these phenomena on the transport process during the remedial investigation are presented in Section 8.0.

Liquid waste addition to the absorption beds was stopped after 1967 and only ambient recharge (.1 in/y), continues to provide the dominant driving force for radionuclide transport. The transport simulation results for years 1978 and 1990 (Section 5.0), suggest that virtually no vertical movement of americium or plutonium occurred during this time interval. These results indicate that the transport rates prior to 1967 were considerably greater than those that can be expected today.

The sensitivity analysis shows that variations of the hydraulic parameters have relatively little effect on the predicted depths of concentration peaks at different times, and hence on average rates of contaminant migration. The shapes of the predicted radionuclide profiles are however more sensitive to variations in hydraulic parameters. This result is not unexpected since the average rate of contaminant migration is directly related to average flow rate, which is dictated by the magnitude and frequency of waste water discharges to MDA T. Variations of the hydraulic parameters do affect the saturation

---

levels and shape of the saturation profile, and through this, the shape of the radionuclide concentration profile.

### 6.3 Role of Fractures

The presence of fractures often complicates the interpretation of contaminant concentration data because, during relatively high flux periods, solutes may be rapidly transmitted through fractures to lower depths without leaving detectible concentrations in the matrix above. Evidence that this may be occurring is present in the profiles measured by Nyhan and others (1984) (Appendix F). The americium and plutonium profiles were constructed with data from approximately 800 samples which were collected to a depth of 100 ft (Appendix F). Occasionally, concentrations in these radionuclide profiles fall below detection limits only to reappear with values above detection limits at greater depths. This phenomenon could also be related to the presence of stratigraphic layers of contrasting distribution coefficients.

Abeele and others (1981) concluded that "the fractures in the tuff generally act as barriers to unsaturated flow of migrating waste solutions; however, fractures may play a role in conveying waste solutions through the tuff near the bottoms of the absorptions beds where saturated flow conditions were more commonly found." Abrahams (1963) found that below a depth of about 15-20 feet the alpha activity was low, except for local areas or relatively high activity. Abrahams concluded that these local areas of high alpha activity are where water carried the activity along the joints. The occurrence of rapid movement of water through joints was substantiated during these infiltration studies (Abrahams, 1963).

Pathway analysis results suggest that during the application periods of large volumes of liquid wastes, the fractures were probably saturated to considerable depths below the bottoms of the beds. The high saturations would have allowed flow through fractures and it may have been possible for the accompanying radionuclides to have moved further than the 100 feet currently reported to be the probable maximum vertical extent of the radionuclides (Nyhan and others, 1984).

The matrix saturations predicted for 1990 are relatively low and are probably not high enough to allow fracture flow. These simulation results suggest that fractures have probably been an important transport mechanism in the past during periods of large waste discharges, but are not expected to be a significant transport mechanism for fluid in the future under ambient conditions.

---

#### 6.4 Interpretation of Moisture and Radionuclide Profiles

Observations by Nyhan and others (1984) regarding their studies in which water saturations, americium and plutonium concentrations were measured with depth are stated as follows:

"The first high concentrations of radionuclides and water encountered in the tuff beneath the gravel cobble layer in Absorption Bed 1 were found at sampling depths of 4 to 5.5 m, where a highly weathered, light orange-gray tuff layer with a high clay content was found. This layer, previously described as Bed B (Rogers, 1977) would be less permeable than the rest of the surrounding tuff..." Furthermore, "the next major increase in tuff water content and radionuclide concentrations occurred at a sampling depth of about 8 to 9 m below Absorption Bed 1. At this depth we encountered a change in tuff units from the upper-lying, light brownish-gray, moderately welded tuff, to the lower lying...this contact zone was identified on the basis of color changes and the change in the total amount of force required to drive the split spoon sampler into the tuff... contact zones such as this exhibit increased welding, decreased porosity (Abeele and others, 1981), and, thus decreased conductivity relative to the adjacent tuff units."

Nyhan and others (1984) drew the conclusion that the correlation between fine grained rocks, high water content and high concentrations of plutonium and americium are related to the lower hydraulic conductivity of the fine-grained rocks and therefore the solutes and ground-water have slower travel times through these sections relative to the coarser grained units. If this was the case, the peaks (increases) in solute concentrations and moisture content could, and have previously been interpreted as moisture/solute pulses slowly moving downward (Nyhan and others, 1984).

In contrast to this interpretation the pathway analysis results offer an alternative explanation for the vertical changes observed in the measured water content and solute concentrations that is fundamental to our current conceptual model (Section 7.0).

The pathway analysis results provide strong evidence that at the time Nyhan and others (1984) were performing their study, the bulk of the waste water discharge had long since passed the depths being investigated. Instead of moisture and radionuclide pulses moving slowly downward, the profiles may represent variations in the moisture retention and radionuclide adsorption properties of the finer-grained units compared to coarser-grained units; that is, lithologic variations are responsible for the moisture and concentration fluctuations but not because they present a hindrance to flow. Under equilibrium or steady state soil moisture tension conditions, finer grained materials tend to retain more water (and drain more slowly) than do coarse grained materials. Furthermore, finer grained materials, especially clays, usually have a higher adsorption capacity for radionuclides, which could account for the higher concentrations of americium and plutonium in the finer grained units. Therefore, the saturation profiles may reflect

---

variations in moisture retention capacity while the radionuclide profiles may be correlated to the adsorption capacity of the rocks. Evidence to support this hypothesis was obtained from the results of the historical matching analysis (Section 5.3). It was observed that varying the saturated hydraulic conductivity in specified layers does not cause the development of the sharp variations in plutonium concentrations contained in the rocks; and that the yearly addition of varying amounts of liquid wastes will not generate multiple subsurface zones of high moisture saturation. However, if layers are assigned different distribution coefficients, zones of sharply varying radionuclide concentrations result.

The importance of distinguishing whether the flow and transport processes are controlled primarily by the permeabilities of the rocks or by other physical and chemical properties is crucial to the design of the remedial investigation program. If it is assumed that measured subsurface peaks in moisture content and radionuclide profiles merely reflect the downward pulse migration of past waste discharges, then one could compute water flux and radionuclide travel times on that basis. However, if the peaks reflect instead remnants of waste water and solutes (which have long since migrated deeper) retained by higher retention and adsorption capacity, then entirely different interpretations result.

#### 6.5 Implications on the Remedial Investigation

The selection of the proper instrumentation and methodologies to characterize the in-situ water flow and saturation relationships for the tuff will be one of the most difficult tasks of the remedial investigation. It is important to define moisture relationships with a meaningful degree of accuracy, while ensuring that, if the system is relatively insensitive to a particular parameter, time and resources are not needlessly spent collecting data.

Results from the pathway analysis have provided initial information on parameter sensitivity. These results suggest that the system probably approached ambient conditions relatively soon after the application of liquid wastes had ceased. This rebounding nature of the rocks towards ambient conditions indicates that long term flow and transport will be controlled by the hydraulic properties of the matrix at relatively low saturations. While fractures have likely been important during periods of high waste water discharge, they probably do not contribute to liquid flow and solute transport under ambient recharge conditions. At low ambient saturations moisture will be held in the matrix and the fractures will behave as barriers to liquid flow.

To characterize the in situ hydraulic properties of the tuff, boreholes need to be drilled and instrumented. Among the possible instruments are: pressure transducers, heat dissipation probes, thermocouple psychrometers, tensiometers, and neutron probes. Each of these instruments have specific advantages and limitations. A more complete discussion of the instrumentation is provided in Section 8.3.4.

---

## 7.0 CONCEPTUAL MODEL

A conceptual model of a hydrogeologic system uses available information to develop a general description and explanation of the hydrogeologic processes and controls which primarily govern the physical and geochemical dynamics of the real-world system.

A conceptual model is usually abstracted from an incomplete set of data, and generally consists of a collection of hypotheses that must be tested not only against existing data but also continually against new data as they become available. Specific knowledge of the hydrologic boundary conditions, initial conditions (hydrologic state), spatial distribution of matric potential, and system geometry and properties are supplied by field observations and/or developed from the fundamental concepts describing liquid and miscible component transport in permeable media. Consequently, one principal utility of a conceptual model is to guide data collection and to permit adequate testing and evaluation of hypotheses. The hypotheses, thus, may be accepted, rejected, refined, or replaced by alternatives in the light of new data and an improved understanding of the system.

The unsaturated zone beneath MDA T consists of stratified slightly eastwardly dipping hydrogeologic units composed of welded and nonwelded tuffs of contrasting hydraulic properties. Some of these units appear to be highly fractured, and the fractures may either enhance or retard the flow of moisture depending on the mechanisms of moisture flow and storage at any location and time within the system. The upper hydrologic boundary consists of the land surface, across which water enters the unsaturated zone as infiltration directly from precipitation or from runoff and is released through evapotranspiration. The lower hydrologic boundary is the water table, whose configuration is presumed to be steeply dipping towards the east (Figure 7.1).

The principal qualitative aspects of moisture flow and transport within the unsaturated zone beneath MDA T, are summarized by the following hypotheses:

- Moisture enters the system as net infiltration principally as liquid-water flow (derived from snowmelt and high rainfall events) into and within the fractures of the surficial tuff unit with subsequent uptake under capillary forces into the rock matrix. It is expected that during sufficiently low rates of net infiltration, nearly all of the water entering the surficial unit will be drawn into the matrix at very shallow depths. In the past, during the applications of large volumes of wastes the fractures probably were the predominant avenue for flow and transport. However, deep unsaturated flow will approach steady state if the transient moisture pulses have been dampened out.

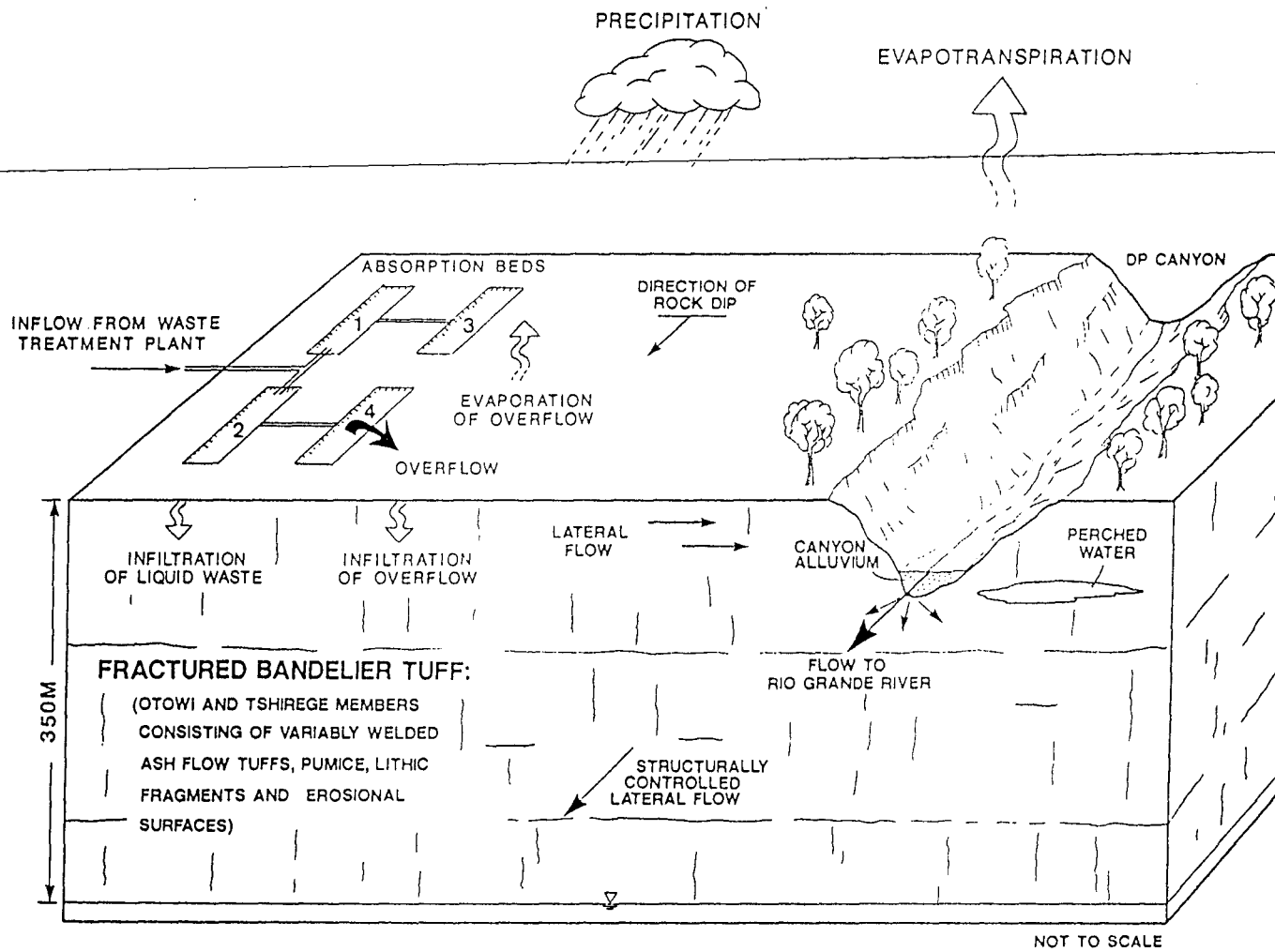


Figure 7.1. Site conceptual model.

- 
- The eastwardly dip may induce lateral flow and transport either under saturated (perched) or unsaturated conditions at the contact between units of contrasting hydraulic conductivities. This could be a consequence of (1) efficient fracture-dominated flow because of high infiltration rates or (2) capillary barrier effects. Capillary barriers may inhibit water movement between contrasting strata and thus favor lateral movement.
  - Both vertical and lateral flow and transport may occur in the surficial units at times of increased recharge. This lateral flow and transport may occur if the surficial units exhibit intrinsic anisotropy and if lower matrix conductivities in deeper units impede the vertical movement of water. However, ambient recharge on mesa tops does not appear to be great enough to transport the radionuclides over significant distances.
  - Flow in the surficial unit is expected to be essentially vertical and under steady-state conditions with the exception of areas influenced by the waste additions. Flow is expected to be dominated by the matrix until some critical value of flux is reached, related to the saturated matrix hydraulic conductivity. At that point, fracture flow will become more dominant.
  - The finer grained rocks have greater moisture retention and radionuclide adsorption properties than the coarser grained rocks.
  - Waste water appears to have moved to greater depths than the upper 100 feet. However, there is no evidence to suggest that radionuclides have also moved to greater depths or have moved laterally.

In general, the conceptual model describes a heterogeneous system where the addition of liquid wastes provided a contaminant source and a driving force for at least limited migration of radionuclides. The rate and depth of radionuclide migration is largely controlled by the rate of water movement and retardation due to adsorption of dissolved radionuclides onto the solid rock matrix. It appears that the volume of waste water discharged to the absorption beds in the period 1945-1967, in conjunction with the rock hydraulic properties requires that the majority of the waste-water has already moved to depths greater than 100 ft. However, the relatively high adsorption capacity of the Bandelier tuff, as reflected in the assumed distribution coefficient values would probably have severely retarded the migration of radionuclides through the rock matrix. At the same time fractures may have provided a conduit for fairly rapid transport of radionuclides during the disposal of waste water into the absorption beds. Even in the case of fracture-dominated flow, matrix diffusion effects would act to significantly retard the movement of dissolved constituents.

---

When waste water additions to the beds were discontinued in 1967, ambient recharge became the primary force driving the migration of radionuclides. Its magnitude does not appear to be sufficient to induce measurable fracture or matrix transport of the radionuclides over significant distances within time periods of a few thousand years. However, other processes such as lateral migration, canyon alluvial recharge, or groundwater movement may have contributed to contaminant migration.

---

## 8.0 RECOMMENDED CHARACTERIZATION ACTIVITIES AND DATA REQUIREMENTS

The relationship of the characterization program to the overall program objectives is outlined in Figure 8.1. The following recommendations have evolved from the results of the pathway analysis, review of the available information pertaining to the site and from previous involvement with programs designed to characterize the unsaturated zone.

The design of the characterization program should have the flexibility to accommodate long-term monitoring, and allow for evaluation of the effectiveness of remedial measures. A comprehensive characterization program that has the potential to be cost effective and satisfies these requirements is outlined below. The approach is divided into four distinct phases: (1) background research; (2) bench-scale studies; (3) field investigation; and (4) confirmatory modeling.

### 8.1 Background Research

The background research should be initiated during the planning stages and continued throughout the characterization program. The primary objectives of this research should include: (1) collection of information that is currently available and pertains to the other three phases of the characterization program; (2) identification of pertinent information that still needs to be obtained; (3) review of analogous programs that may have been designed elsewhere to address similar concerns; and (4) development of a characterization/remediation logic diagram.

One objective of the background research should be to produce a characterization program plan outline. This should include a strategy diagram in the form of a decision-tree. This diagram would have each aspect of the characterization program well outlined with major decision points and options eventually leading to one of several potential remedial alternatives. One strength of a logic diagram is that the rationale of the program may be clearly presented to the technical community as well as regulatory agencies. The following are topics that may be useful for developing the characterization program plans and the associated logic diagram.

Key background information needs are summarized in Table 8.1 and include:

- Information pertaining to the site history that describes the mixing of radioactive waste as a concrete slurry and the subsequent emplacement into approximately sixty subsurface containers on site. Review of any research discussing the potential for radionuclides leaching from similar concrete slurry mixes.

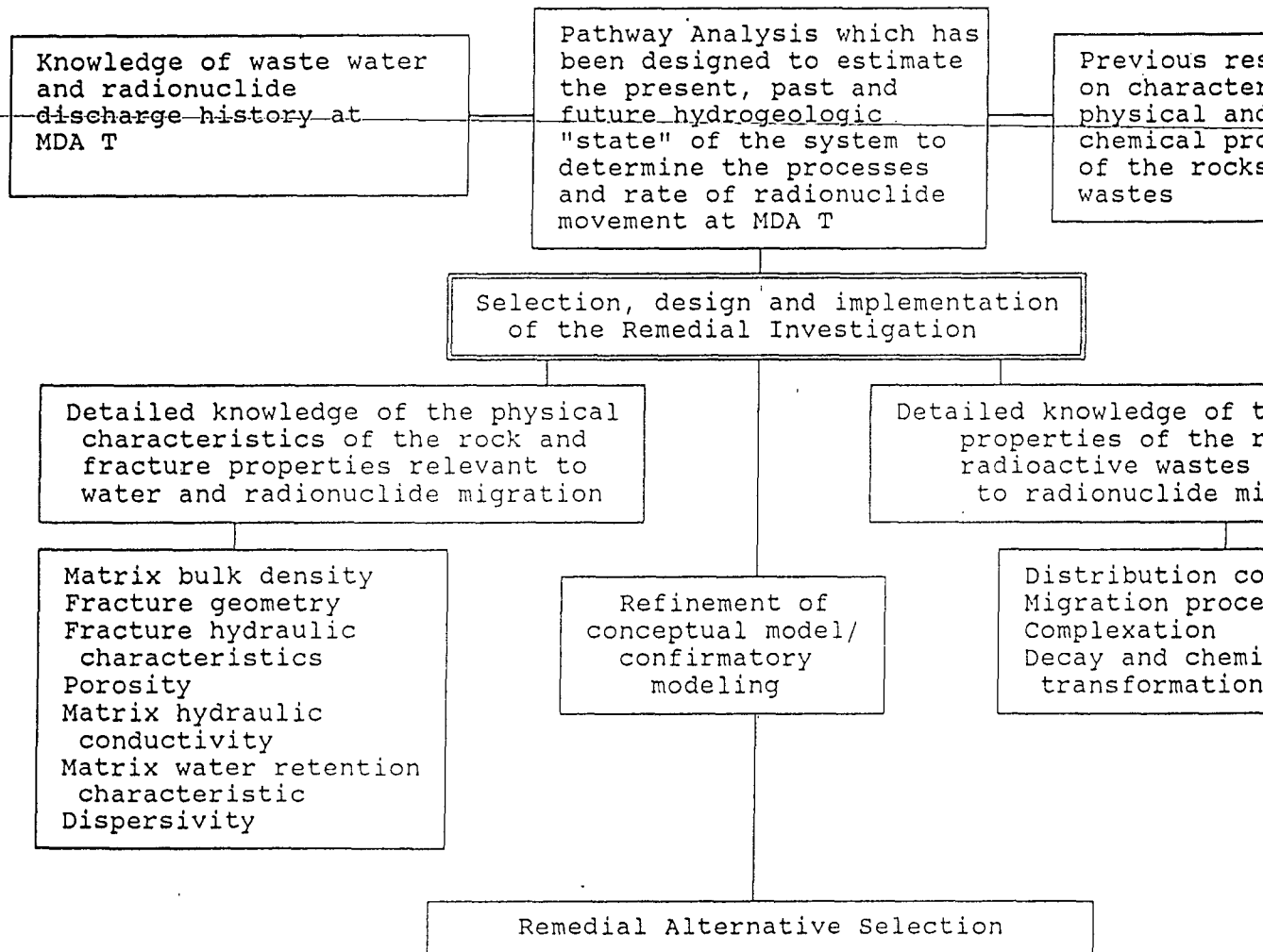


Figure 8.1. Site Characterization Process.

Table 8.1. Fulfillment of information needs.

<u>Information Needs</u>	<u>Data Requirements</u>	<u>Proposed Activities</u>	<u>Technical</u>
Knowledge of water and radionuclide discharge history	Information pertaining to past volumes of fluid introduced into the absorption beds	Literature review (completed)	The volume concentration of radioactive material disposed of in the absorption beds has not been used in the past, present, or future hydrologic "state" of the system.
	Information pertaining to past concentrations of various radionuclide species introduced into the absorption beds	Literature review (completed)	
Detailed knowledge of the physical characteristics of the rock and fractures relevant to water and radionuclide migration	Bulk density Fracture geometry and density Fracture hydraulic characteristics Matrix water retention characteristics Porosity Matrix hydraulic conductivity	Laboratory and field experiments	The movement of radionuclides is influenced by the unsaturated zone, which is strongly influenced by the rate and volume of water movement. In turn, the hydraulic conductivity of the layer and the fracture geometry and hydraulic characteristics of the Bandel...

83

Table 8.1. Continued.

<u>Information Needs</u>	<u>Data Requirements</u>	<u>Proposed Activities</u>	<u>Technic</u>
Detailed knowledge of the chemical characteristics controlling radionuclide movement	Solid-liquid phase distribution coefficients Radioactive decay and chemical transformation rates Formation of colloidal complexes	Laboratory and field experiments	The rate by which nuclides reported to system will be dependent rate and the water through but also chemical of the water. colloidal complexa port of can mobile nuclide otherwise adsorbed

- 
- Information pertaining to the on site Retrievable Waste Storage Area, which was decommissioned in April 1983; in particular, information pertaining to the storage history and procedures, should be reviewed.
  - Information on the ratios of Pu-241 to Pu-239 in discharge waste streams. In addition to americium being directly released to the beds, it may be produced by plutonium decay. Pu-241 has a half-life of 13.2 years and decays to Am-241. Although the weight fraction of Pu-241 to Pu-239 is normally expected to be in the range of about .05 percent, the ratio may have varied considerably in waste streams. Any information that can be obtained on concentrations of Pu-241 discharged to the disposal pits may be useful in resolving the accuracy of estimated distribution coefficients.
  - Additional information on the chemical composition and characteristics of the liquid wastes would be useful in conducting laboratory complexing and distribution coefficient studies. This should include a review of complexing behavior of Pu and Am and resultant effects on mobility.
  - Additional data on tritium concentrations in MDA T waste streams. Rogers (1977) presents concentrations of tritium that were measured in 1974. Tritium present at the site will be free to move through fractures in both vapor and liquid phases and potentially could be released at the surface.
  - Any information available pertaining to the distribution coefficients of Pu, Am, and other waste products in contact with the Bandelier tuff.
  - Results of water analyses which have been performed on many of the municipal wells in the vicinity of Los Alamos (Purtymun, 1984). This information could provide a data base from which to evaluate spatial and temporal trends in water quality.
  - Geologic logs and any other pertinent information from test holes TW-2 and TW-3 which are in relatively close proximity to the site, plus similar data from any other holes that have been placed in the area. Information that could potentially be useful includes stratigraphic and lithologic information, the depth at which water was encountered while drilling, the static water level in the well after well completion and whether any perched water was encountered.
  - Results of other programs which are currently researching and improving instrumentation methods for use in the unsaturated zone. Information should be obtained on instrumentation methods that have

---

been successful in similar environments. Section 8.3.4 provides a discussion on suggested instrumentation.

- Updated information pertaining to "state of the art" drilling and coring technology in unsaturated tuffs and similar rocks.
- Data and experience pertaining to worker and public exposure risks, relative to the potential excavation and removal of the wastes.
- Information pertaining to sampling techniques for collecting and preserving intact core samples for laboratory testing.
- Potential methods for closing any excavations and boreholes after the completion of the site characterization/remediation.
- Additional data and information pertaining to hydraulic testing of Bandelier tuff.
- Potential remedial measures that may be successfully employed at site.
- Potential costs analyses for characterization and remedial alternatives.

## 8.2 Bench-Scale Laboratory Studies

The specific details of the recommended laboratory investigation should be developed from information obtained during the background research. The following are several key chemical and physical characteristics that may affect flow and transport, and therefore warrant additional investigation.

### 8.2.1 Chemical Characteristics

- The pathway analysis results indicate that the most critical parameters influencing the rate of movement of the radionuclides are their distribution coefficients. Distribution coefficients are affected by the physical/chemical properties of solutions as well as the geochemical properties of materials in which the radionuclides are migrating. Therefore, it would be very useful to perform a series of column and batch studies to investigate the effect of the solution on the  $K_d$ 's of plutonium and americium. Specifically, solutions with very low pH, and high concentrations of ammonium citrate, silica, fluoride and bicarbonate should be investigated.

- 
- Several of the previous investigators reported significant chemical alteration of materials in the Bandelier tuff underlying the disposal beds, as Nyhan and others (1984) observed;

"...this layer, previously described as Bed B (Rogers, 1977), would be less permeable than the rest of the surrounding tuff and probably resulted from the severe chemical and hydrologic tuff-weathering processes brought about by the acidic liquid wastes added to this absorption bed."

The implications of the tuff alteration is that more clay material will be available for adsorbing plutonium and americium. Some of the clay particles with adsorbed nuclides could also act as vehicles to transport plutonium and americium in groundwater in colloidal suspension. This possibility should be evaluated in laboratory studies.

- Researchers have noted that waste and aqueous solutions of plutonium and americium exhibited anomalous migration behavior (Nyhan and others, 1984). This research demonstrated that plutonium appeared to exist in two forms, one of which (probably a hydrolyzed or complexed form) migrated much more rapidly than the "ionic" form. The experimental results suggested a predicted rate of the more mobile plutonium form of about 200 cm/yr when accompanied by unsaturated water flow in the tuff (Fried and others, 1975; Nyhan and others, 1984). Additional laboratory testing is needed to identify the various oxidation states and chemical forms of dissolved (or suspended) Pu and Am which are likely to be present in the subsurface.
- Other chemical processes that may affect the transport rates of americium and plutonium include complexation with other constituents that may be present in the wastes. These processes also warrant laboratory characterization.
- The termination of the characterization and/or remediation program may require the filling of trenches and boreholes. Consequently, it may be useful to investigate suitable grout and fill materials, i.e., materials that are compatible with site geology and which retard radionuclide migration (have high  $K_d$ 's).
- Some useful experiments would be leaching tests on samples of tuffs containing sorbed Pu/Am, extracted or cored from beneath the disposal sites. These tests would help determine desorption and mobility characteristics of the sorbed Pu/Am beneath the disposal beds.

### 8.2.2 Physical Characteristics

- Some information is currently available on the hydraulic properties of the Bandelier tuff (Abee, 1984). However, very little hydraulic property data are available specific to the site. It would be useful to obtain information on the rock properties which are important to the movement of water and solutes. These properties are water content, grain density, porosity, bulk density, matric potential, moisture retention curves, saturated water and gas permeability and relative permeabilities.
- Movement of water and radionuclides through fractures, coupled with matrix diffusion may have had an important role in the transport of americium and plutonium and should also be evaluated, e.g., through laboratory diffusion studies.

### 8.3 Field Investigation

The field investigation should be an integrated program comprised of drilling, sampling, instrumentation and testing. These facets of the field investigation should be directed towards the following objectives:

- (1) Determine the present rate of movement and three-dimensional extent of water and radionuclides in the unsaturated zone;
- (2) Obtain data needed to determine likely ranges in future rates of water and radionuclide movement in the unsaturated and saturated zones, under various assumed conditions;
- (3) Provide adequate monitoring to enable early detection of migrating radionuclides in the unsaturated and saturated zones;
- (4) Provide additional information to support or revise the current conceptual model;
- (5) Provide information from which to plan and implement remedial actions;
- (6) Provide data from which to evaluate the potential effectiveness of remedial actions.

---

### 8.3.1 Location of Proposed Boreholes

The placement and orientation of the proposed boreholes have been selected based on current knowledge of the site. The exact placement and depths of the proposed boreholes will be dependent on the information obtained from holes drilled while the site characterization program is underway.

Four separate areas have been selected for specific investigation during the characterization program and should be examined in the sequential order that they are discussed. Special techniques for drilling and coring should be investigated. Optimally, the techniques should reduce the possibilities for cross contamination, worker exposures, and should enhance core and sample recovery and integrity. Available techniques might include the ODEX methods (proposed for the Yucca Mountain Nevada site); air and air-mist drilling; drilling method developed and employed by EG&G at the Idaho National Engineering Laboratory.

#### 8.3.1.1 Proposed Borehole Investigation Area 1

The first proposed borehole would be placed on the canyon rim immediately to the north of the site and drilled vertically to approximately 50 feet below the canyon floor (Figure 8.2). The objectives of this borehole would be similar to those of the LANL Pajarito Canyon study (Devaurs and Purtymun, 1984). Specifically, this borehole would provide information on the lateral extent of radionuclide movement, the existence of perched water and the potential for radionuclide releases to the canyon. If feasible, this hole should be drilled at the end of the highest recharge season of highest precipitation due to the often ephemeral nature of perched water. The information on proposed testing, instrumentation and sampling are discussed in Section 8.3.3.

#### 8.3.1.2 Proposed Borehole Investigation Area 2

The second area of interest is in the immediate vicinity of Material Disposal Bed 1. Previous field information suggests that rocks in this area contain the highest concentrations of radionuclides at the greatest depths. Therefore, to obtain "worst case" information, data from this area are very important. Furthermore, this area has been more extensively studied than any other area on the site and additional information will allow comparisons with past to be made from which the conceptual model may be tested.

A minimum of three holes are proposed for this area all of which would be drilled at an angle. These slanted holes would be started at the periphery of the source area and drilled to depth, toward the center of source area, similar to the holes placed by Christenson (1962). The advantages of slanted holes are vertical fracture frequencies may be mapped, drilling directly through the contaminated source area is avoided thus

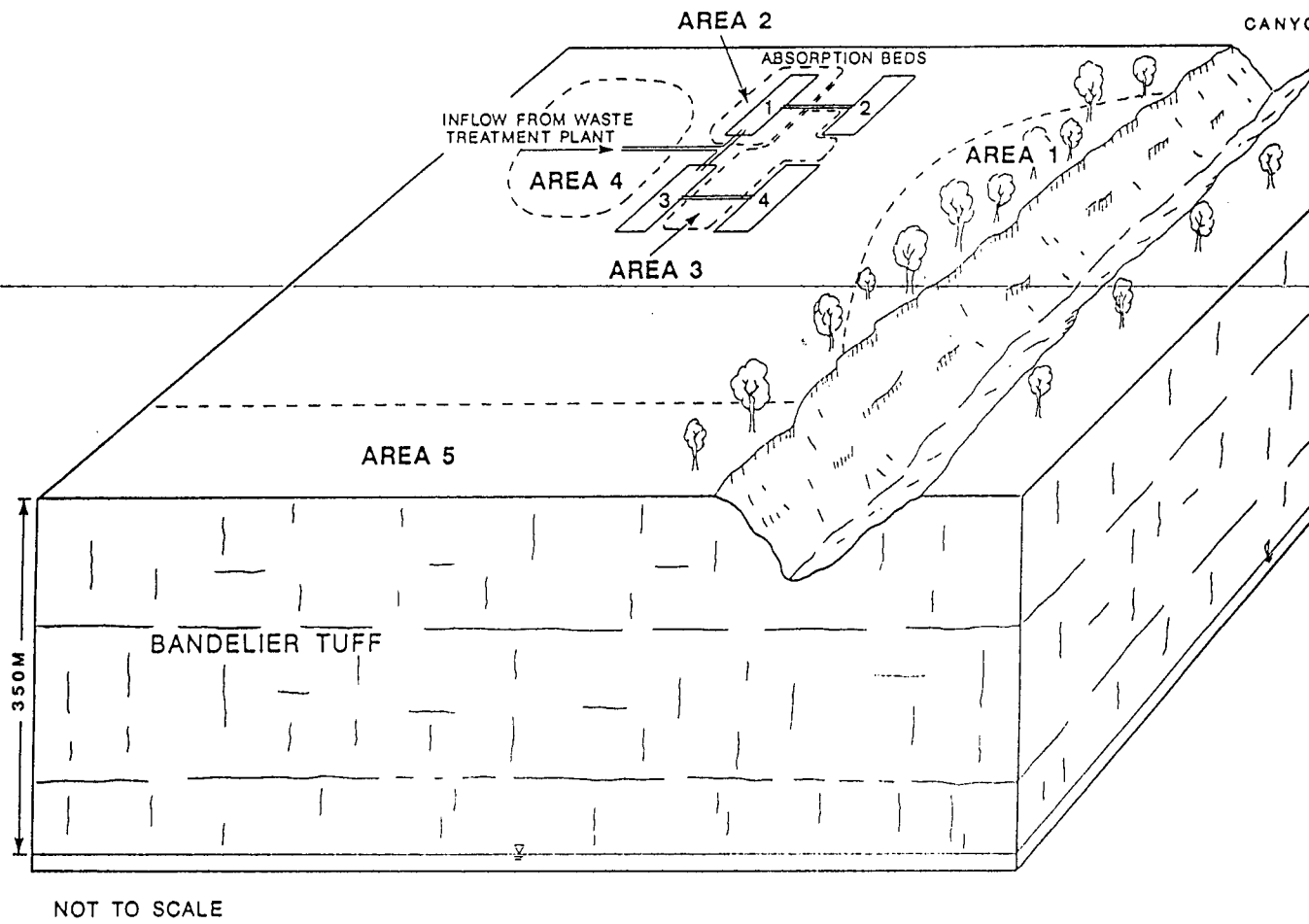


Figure 8.2. Map of proposed boreholes.

---

reducing the potential problems of down-hole contamination and future downhole migration of source area contaminants, and vertical cross-hole testing may be performed, if desired. Disadvantages of angularly drilled holes are that holes are more difficult to drill and to run geophysical logging equipment.

The recommended depth for the first hole is approximately 50 feet (vertical depth). Data from this hole would be used: to compare with previously collected data from the same area, to estimate maximum concentrations that may need to be removed, as confirmatory information for the conceptual model and future monitoring, and to establish any site-specific procedures that may be required for the angular drilling method.

The second hole should be placed to a depth of approximately 150 feet (vertical depth). This hole is necessary to obtain radionuclide concentration data to a depth that has not been previously sampled.

The placement of the third hole will be dependent on the sampling results obtained from the previous hole drilled to about 150 ft. If radionuclides are encountered at that depth, the third hole should be drilled to an even greater depth, based on the concentrations found at 150 ft. However, if no radionuclides are discovered at 150 ft the third hole should be drilled at an intermediate depth, possibly around 100 ft (vertical depth).

#### 8.3.1.3 Proposed Borehole Investigation Area 3

The third area of concern is the zone underlying the concrete monoliths that have been buried on site. A single slanted hole is proposed to sample and monitor any radionuclide migration that may have originated from the concrete/radionuclide filled shafts. The depth to which this hole should be drilled will be dependent on the feasibility of drilling a relatively steep angled hole perhaps 45° or more from vertical). Ideally the depth of the hole should be fairly shallow (in the range of 30 feet). If contamination were found at this depth, it would become important to drill additional deeper holes (Figure 8.2).

#### 8.3.1.4 Proposed Borehole Investigation Area 4

The fourth area that is important to examine is in the vicinity of the pipe that had been leaking for a number of years. The estimated rate of leakage is fairly high (1 - 2 gpm) and water could have moved laterally towards the absorption beds and induced radionuclide transport. A single slanted hole is recommended and should be placed between the absorptions beds and the pipe (Figure 8.2). The depth to which this hole should be drilled would be dependent upon the results of radionuclide concentrations

---

and water content measured in the other exploratory holes. However, an initial recommended depth is 200 feet.

#### 8.3.1.5 Proposed Borehole Investigation Area 5

The fifth area of interest is the area to the east of the site, down the water table potentiometric gradient. The estimated groundwater velocities are relatively fast in this area (Figure 8.2). These rapid velocities make it important to ensure that the monitoring program detects migrating radionuclides as early as possible. A monitoring well, drilled to the water table, in this area may be optimally placed based on the information collected after the boreholes have been placed in the other investigative areas. In general, this borehole should be placed far enough away from the source areas to preclude the vertical migration of radionuclides down the borehole, yet close enough to provide timely information on radionuclide movement in the saturated zone.

#### 8.3.2 Sampling

Extensive sampling may enable the three-dimensional delineation of radionuclide concentrations and extent of movement. These results will have a direct impact on the selection and implementation of the testing, monitoring and remediation programs.

If radionuclides are found to be relatively limited in vertical extent and there is a high confidence that source removal can effectively eliminate future contaminant releases, then the testing and monitoring program may be appropriately reduced. However, if during the sampling program it is discovered that the radionuclides have moved considerably greater distances or at significantly higher concentrations than originally believed, complete or partial source removal may be less feasible than alternative remedial measures. If other remedial measures are considered, greater emphasis should be placed on the testing and monitoring program to accommodate the added responsibility of determining future migration rates and evaluating the long term effectiveness of the chosen remedial action.

Specific guidance for sampling in each of the Investigative Areas will depend on the sampling results obtained from the previous boreholes. However, some general guidelines that may be followed are presented:

- Rock samples - rock samples and oriented cores obtained to determine hydrologic characteristics and radionuclide concentrations should be collected at a frequency that is consistent with the degree of interest in the particular area. Areas of heightened interest include lithologic contacts, fracture surfaces, weathered zones and areas where high concentrations of americium and plutonium have been found in the past.

- 
- Perched water - any perched water zones that are encountered during drilling should be sampled for silica and aluminum, all major cations and anions in addition to ammonium citrate, fluoride, tritium, americium, uranium and plutonium. Silica and aluminum concentrations may provide some information as to the degree of chemical weathering that the clays have experienced. Cations and anions may be used to verify flow paths and to indicate the extent of water rock interactions.
  - Samples of high-clay zones - previous investigations in the site area have not found substantial amounts of clay at depth. However, zones high in clay content (or in other finer grained minerals) are expected to have higher absorption capacities and therefore potentially higher concentrations of americium and plutonium. Therefore, samples of higher clay content zones should be collected when encountered and analyzed for americium and plutonium. Furthermore, x-ray diffraction studies on clay samples may be useful in delineating the degree of chemical alteration and hence the extent and pathways of waste movement even if no radionuclides are found in the sample.
  - Gas sampling - interstitial gas samples of tritium and chloro-fluorocarbons would be useful as a tracer in conjunction with fluorocarbons to estimate air permeabilities and ultimately water permeabilities.
  - Seeps and springs - at the end of the season of greatest precipitation and runoff, most likely in April, the canyon to the north should be studied for signs of discharge by seeps and springs. If seeps or springs are present they should be mapped and sampled.

### 8.3.3 Testing

The following discussion is an outline of what tests appear, at this time, to be the most feasible to perform in order to address the technical concerns at the site. The actual scope of the testing program should be based largely on the conclusions reached at this stage in the characterization program.

The focusing of potential remedial measures will have a major impact on the design of the testing program. If the radionuclides have migrated over such a limited extent that removal is practical and feasible, only a limited testing program should be implemented. On the other hand, if site characterization activities indicate widespread radionuclide movement, a more comprehensive testing program should be implemented.

- Borehole Logs - In addition to the geologic logs constructed by the site geologist there are a number of relatively straight forward logging

---

techniques that provide considerable information and do not require a fluid-filled borehole. These are natural gamma, neutron density, gamma-gamma, thermal and caliper logs.

Other methods useful in delineating fracture properties are radial-(side scan viewing) and axial-(forward viewing) oriented television video camera logs.

- Air Permeability Tests - To determine bulk pneumatic permeabilities of the combined fracture and rock matrix system, single and/or dual hole packer nitrogen-injection tests could be performed. Furthermore, down hole barometric fluctuations may be monitored to obtain similar information.
- Tracer tests - Passive tracer tests may be performed by determining tritium and fluorocarbon distributions to estimate fluid travel times and diffusion properties through the unsaturated zone. Active tracer tests may be performed by injecting fluid or gas into a borehole and determining breakthrough curves for other boreholes.
- Geophysical testing - Several other geophysical techniques are available which may provide pertinent information on fracture relationships. Two such methods are vertical seismic profiling (VSP) and down-hole tomography.
- In-situ tension measurements - There are many problems involved with obtaining reliable in-situ water tension measurements especially at depths greater than a few feet. The problems associated with collecting in-situ measurements make an evaluation necessary to estimate the importance of the in-situ tension measurements to the characterization program.

The high matrix saturations obtained during the pathway analysis suggest that the bulk of the previous fluid movement and hence radionuclide transport was through the fractures and not through the matrix. Therefore, transport in the past probably has been controlled predominantly by fracture properties rather than matrix properties. However, future long-term migration of water and radionuclides will more likely be controlled by properties of the rock matrix. Therefore, it is important to gain a better understanding of those properties to predict long-term migration patterns of radionuclides which may not be removed during remediation. In that case it would be desirable to determine subsurface tension, water content, permeability, and porosity profiles.

---

#### 8.3.4 Permanent Instrumentation

Moisture flux in the unsaturated zone cannot be measured directly and must be calculated from measured values of hydraulic conductivity, water content, and total potential gradient along the path of flow. Fluid potentials that govern variably saturated two-phase (liquid and gas) flow are as follows: (1) matric potential for the liquid phase; (2) gravitational potential; (3) gas-phase pressure, or pneumatic potential; (4) osmotic potential; and (5) thermal potential. Although a permanently instrumented borehole could provide a more sensitive means of monitoring moisture changes than neutron moisture logs, the length of time required to establish data trends may make such an approach impractical. The following text is a brief description of some of the more popular instrumentation available and their limitations:

- Thermocouple psychrometers - (Pressure range -4.5 to -75. bars)  
Thermocouple psychrometers infer the water potential (matric and osmotic potentials combined) of the liquid phase of the surrounding rocks from measurements within the equilibrated vapor phase.

Thermocouple psychrometers placed in the borehole would normally be packed in silica flour, the silica flour will eventually equilibrate with the nearby rocks. However, this equilibration time may take as long as several years before meaningful data may be obtained. It has been observed that gas sampling from access tubes in the vicinity of the thermocouple psychrometers tends to bring the system into equilibrium at a faster rate. Furthermore, to speed up the equilibration process the silica flour may be moistened to the approximate saturation of the surrounding rocks. Computer modeling could be used to estimate saturations that the silica flour should be moistened to. Water potential measurements are made by passing an electrical current between electrodes evaporating any water that may have condensed on the electrodes. Eventually this condensation-evaporation process encrusts the electrodes to where measurements can no longer be made. Furthermore, some uncertainty exists in the reliable determination of matric potential if the osmotic potential is relatively high.

- Heat dissipation probes - (Pressure range -0.1 to -5.0 bars) Thermal conductivity of a porous material is a complicated function of water content, pore size distribution, and makeup of the porous material. Heat dissipation is determined by applying a heat pulse to a heater within the ceramic probe and monitoring the temperature at the center of the probe before and after heating. The temperature difference is a function of the thermal diffusivity, and therefore of water content. There may be some errors accompanying the determination of the matric potential indirectly by measuring thermal diffusivity. In addition, heat dissipation probes have been plagued by high frequency of failures

---

when installed at depth and the heat dissipation probes may not have particularly good resolution in the range between -5 and 0.0 bars.

- Tensiometers - (Pressure range -.8 to 0.0 bars) Tensiometers use porous ceramic cups connected to vacuum gauges or manometers to measure the capillary potential of the water in a soil or rock. They are generally reliable but difficult to use at great depths and are limited to a very narrow pressure range.
- Pressure transducers - Pressure transducers are designed to measure pore-gas pressure from which estimates of bulk permeabilities may be made. An inherent problem with the pressure transducers is that they tend to drift over time.

#### 8.4 Confirmatory Modeling

As more data become available, the additional use of modeling throughout the site characterization and remediation process would be useful for the following tasks:

- Refinement of the site conceptual model. The site conceptual model presented in this report was developed from limited field data and largely one dimensional modeling. As more data become available the conceptual model will be refined to better approximate the physical system.
- Additional detailed sensitivity analysis on field parameters. As more data become available it would be very useful to continue the sensitivity analysis, particularly in two dimensions. This analysis would provide additional guidance for the selection of instrumentation methods.
- Historical Matching. All of the historical matching was performed in one dimension. To fully understand the two and three dimensional effects on the radionuclide and water distribution it would be beneficial to perform this analysis in these dimensions.
- Identification of data gaps. Currently, very little data are available for MDA T. Additional modeling exercises would identify what additional data would be most useful, where this data should be collected and at what sensitivity and frequency the data should be measured.
- Technical support for laboratory column and batch experiments. A series of laboratory experiments have been recommended to identify physical and chemical properties of the Bandelier tuff. One

---

dimensional modeling could support these studies and facilitate their interpretation.

- Selection and design of borehole instrumentation methods. The selection of instrumentation for the monitoring at MDA T will be dependent on what objectives need to be met. Additional modeling could aid in defining realistic objectives.
- Design and implementation of potential field testing methods. The field testing methods that may be implemented at MDA T should be evaluated through numerical simulations prior to the actual field tests. Numerical simulations could help to determine the optimal duration of the tests, and placement and frequency of the measuring points.
- Two and three dimensional modeling. The scarcity of data does not presently justify detailed two or three dimensional analyses. However, as more data become available it would be advantageous to perform more detailed two-dimensional and possibly three dimensional modeling. The two and three dimensional nature of flow and transport at MDA T are not well understood. The geometry of fractures is of particular interest. The potential influence of fractures on flow and transport warrants further study. Through additional modeling the two and three dimensional nature of the site and the influence of fractures may be better defined.
- Site remediation. After the remedial investigation is completed, some form of site remediation will be selected. Numerical modeling should be an integral part of the selection, design, implementation and evaluation of the effectiveness of the selected remedial measure(s).

---

## 9.0 POTENTIAL REMEDIAL ALTERNATIVES

The majority of the waste at the MDA T was disposed of in shallow land burial trenches for economic reasons. The isolation of these wastes in a safe and environmentally acceptable manner requires technologies that focus on fluid controls at and below the surface of the waste. A major concern with waste disposal at MDA T is that moisture in the unsaturated zone or infiltrating surface water will mobilize or has mobilized potential hazardous radionuclides. The rate of radionuclide movement depends on the amount of precipitation, rate of infiltration, chemical form of the waste, permeability and chemistry of the geological formation, and the chemistry of the water in the unsaturated zone. The amount of precipitation available to drive the migration of radionuclides is relatively low at MDA T. However, the specific situation for the MDA T, in which most precipitation accumulates as snowfall, dictates the need for specific design features, that will accommodate melting snow in a rapid time period.

Several potential remediation possibilities have been summarized from proceedings of an engineering workshop held by EG&G Idaho, Inc. in September of 1987 (Interoffice Correspondence on Waste Isolation Techniques Value Engineering Workshop, dated September 30, 1987) and from a Site Reconnaissance Plan for LANL (1988) are discussed below. The following list is not all inclusive. For example, notably absent is a discussion of long-term monitoring and institutional controls. Also, specific applicability and/or development of techniques mentioned herein at LANL is not inclusively discussed. Applicable remedial action technologies for MDA T will be chosen as part of the remedial alternative development process required in the RCRA/CERCLA cleanup process.

### 9.1 No Action Alternative

To undertake no action is to refrain from intervening in the fate and transport of contaminants at MDA T. No action does not necessarily perpetuate the status quo because natural processes may be transforming the site. However, such processes as natural biodegradation, volatilization, photolysis, leaching, and adsorption may have beneficial effects. The no action alternative serves as a basis for comparison with other alternatives.

### 9.2 Waste Disposal

This alternative involves removing wastes present at MDA T and transferring them to either an onsite or offsite disposal area, as required by the nature of the waste.

---

### 9.3 Capping

Engineered improvements encompass all corrective measures designed to reduce infiltration, biointrusion, runoff, and erosion at MDA T. Several authors have reported the success of selected configurations of soil and rock materials in preventing the intrusion of plant roots and burrowing animals using waste site trench caps. Erosion control methods and biointrusion barriers may be an effective method of limiting radionuclide migration at MDA T. These technologies are being investigated at Los Alamos.

### 9.4 Vapor Extraction

This technique can be used to immobilize or isolate plutonium and other non-volatile contaminants by removing the water, which serves as the transporting agent within the unsaturated zone. It also has the additional major advantage of removing volatile organic contaminants simultaneously with the removal of moist air.

#### 9.4.1 Description of Technique

##### 9.4.1.1 General Principle

This technique is based on the assumption that the plutonium (as well as other contaminants) is migrating (or has migrated) as a dissolved or suspended substance in downward percolating liquid water in the unsaturated zone. Removal of water, therefore, can remove the transporting medium and might also precipitate or deposit the plutonium and other contaminants on mineral surfaces in a more immobile state. The unsaturated-zone fluid in both the basalts and sediments would be removed by one of several methods:

1. Pump relatively dry atmospheric air through simple wells and allow the pumped air to evaporate water in the formations and exit diffusely through the land surface, carrying the additional water vapor with it (Figure 9.1).
2. Using air pumps, suck moisture-saturated formation air out through simple extraction wells completed into the unsaturated zone. The removed moist air is replaced by dryer atmospheric air entering through ground surface or through open wells (Figure 9.2).
3. Use a combination of injection wells for dry air and extraction wells for moist air (Figure 9.3).

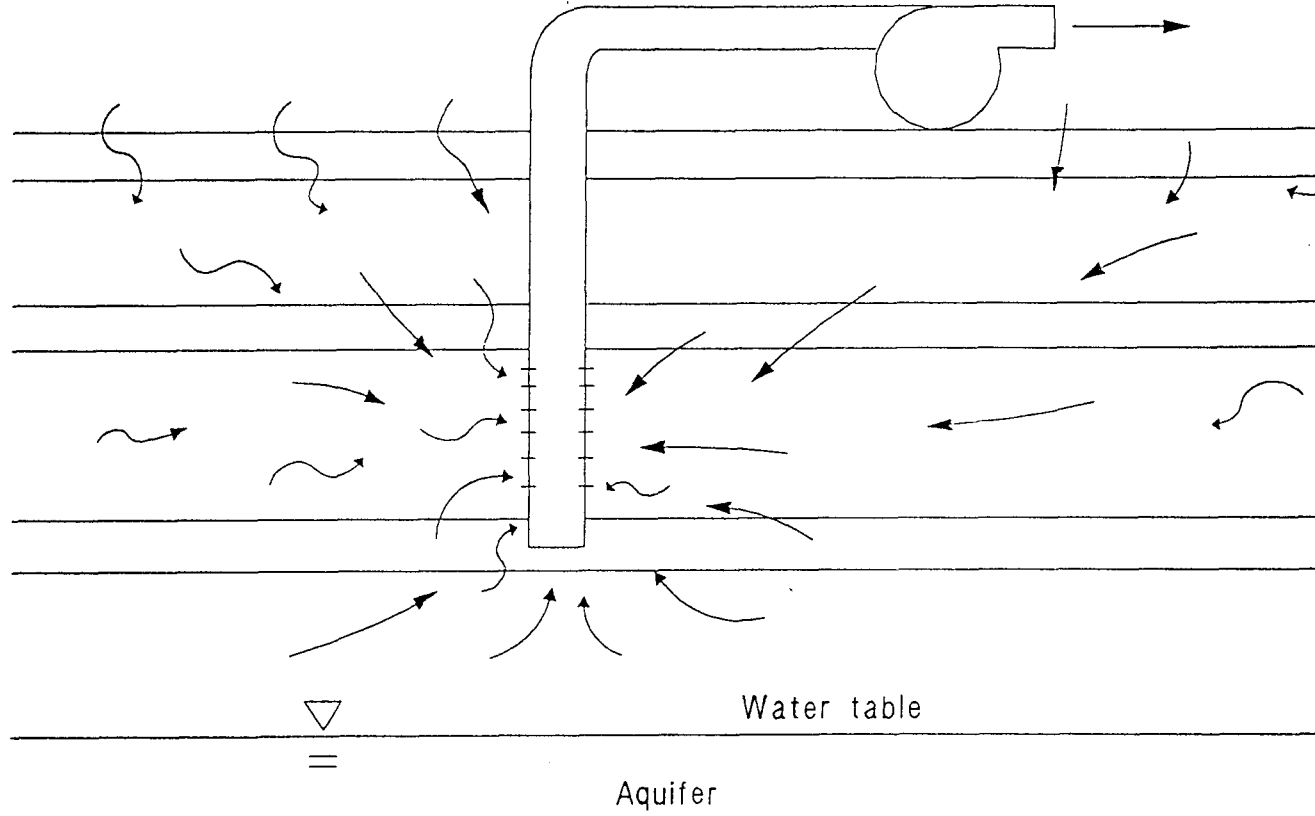


Figure 9.1. Simple vapor extraction system.

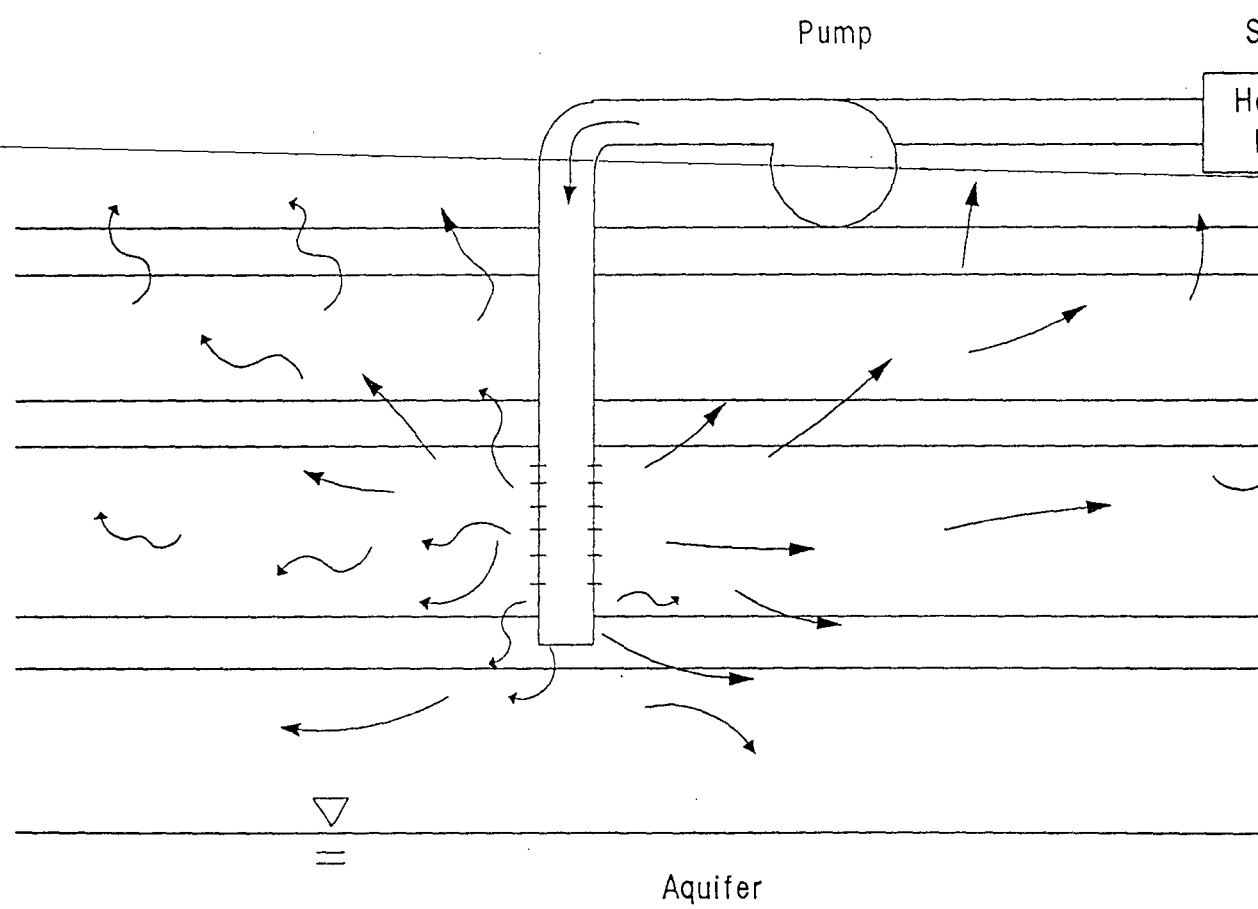


Figure 9.2. Air pump activated vapor extraction system.

9-5

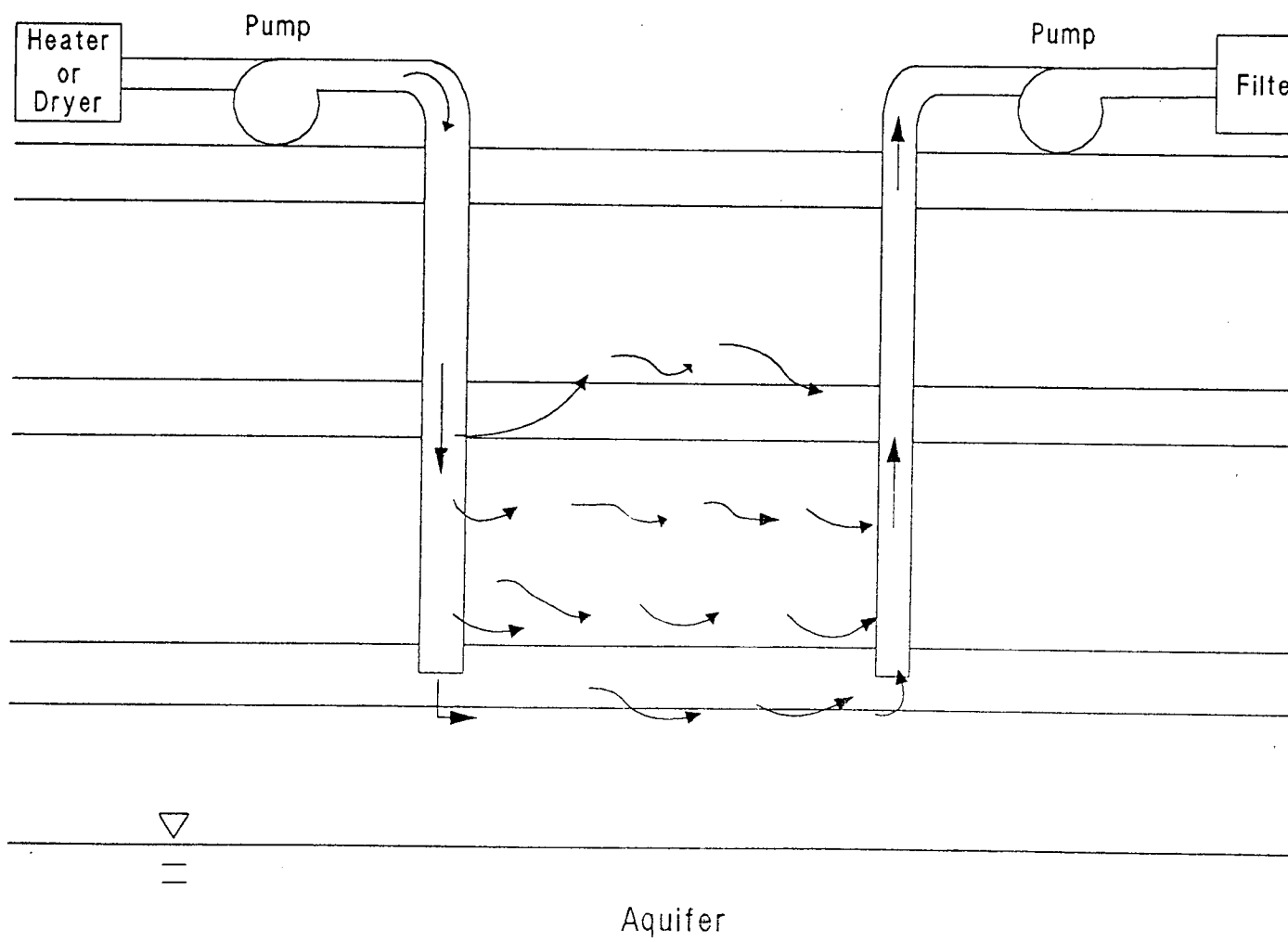


Figure 9.3. Dual well vapor extraction system.

- 
4. Construct specially designed and controlled wells that allow barometric pressure changes to automatically cause dry air to enter the formations during rising barometer and moist air to exhaust from the formation during falling barometer (Figure 9.4).

The basic objective of the method is to remove a sufficient quantity of water so that any remaining water is immobilized by capillary forces in the sediments and tuffs.

#### 9.4.1.2 Theory and Operating Principles

This method is based on the principle that liquid water in contact with air tends to maintain an equilibrium partitioning dependent on its vapor pressure (which is temperature controlled). Air that is unsaturated with water vapor (less than 100% humidity) will evaporate water from liquid it comes in contact with it. The theory behind this method involves passing air unsaturated with water through the wet formation and allowing the air to evaporate some of the formation water. The wetter air and its acquired water are then removed, treated if necessary and discharged to the atmosphere, causing the formation to become drier.

If no infiltration or recharge of new water is entering the unsaturated zone, this method can be used as a one-time drying operation, which could be repeated again later, if needed. If periodic or continued recharge is occurring, the method might require continual or period applications for an indefinite period of time to maintain the desired state of dryness in the subsurface.

To enhance the method, injected air can be heated or dried prior to injection. The method also removes volatile organic compounds, in accordance with their individual Henry's Law constants.

The method can probably best be used in combination with other remedial measures to reduce infiltration of water, thus constructing an effect cap and water diversion system over the site.

#### 9.4.1.3 Design Parameters

The following parameters are needed for designing an appropriate system:

1. Dimensions of the unsaturated zone to be dried, (area, depth, thickness of basalt and sediment layers).
2. Liquid water content (degree of saturation) of all major geologic zones.
3. Temperature range of subsurface unsaturated zone.

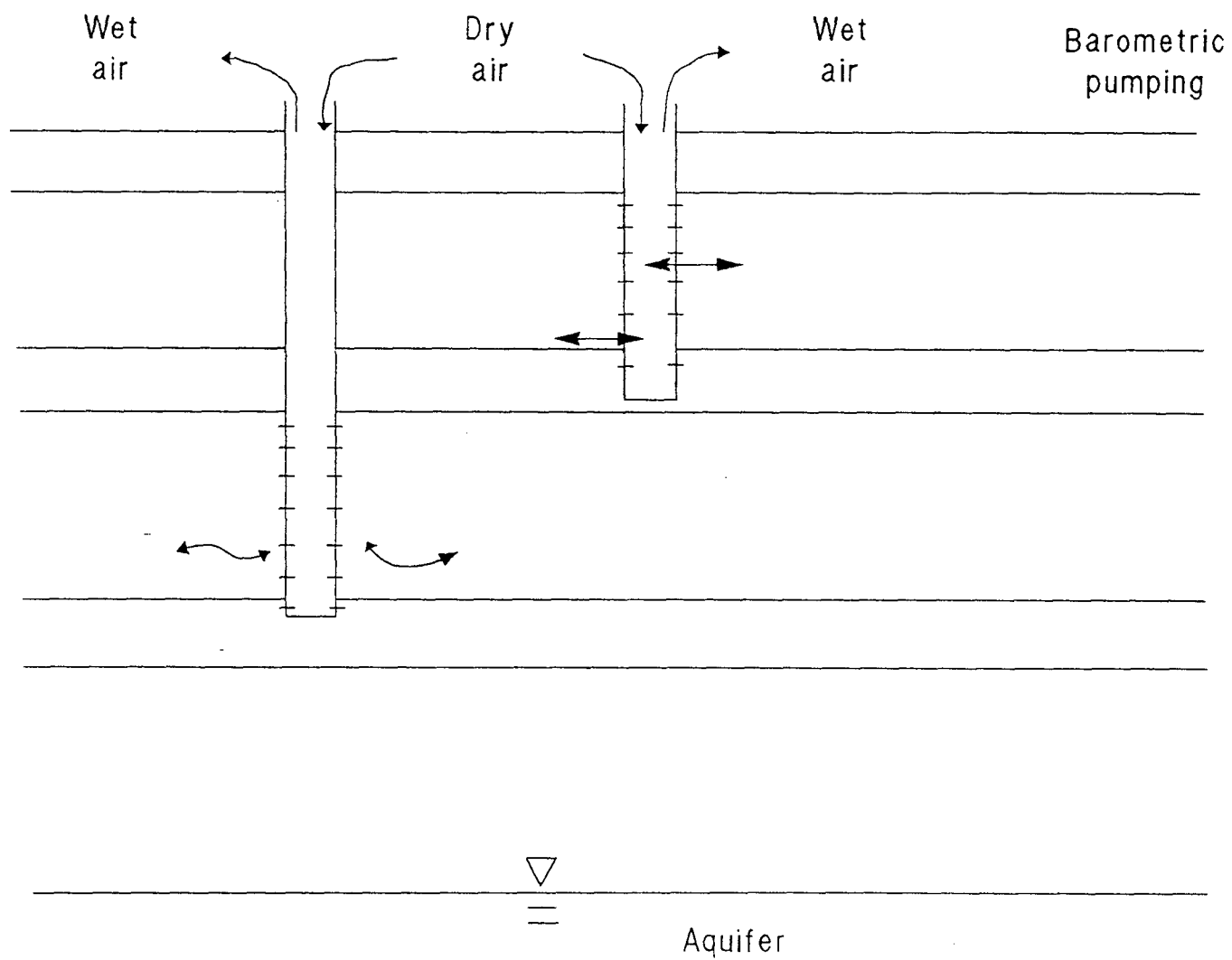


Figure 9.4. Barometrically driven dual well vapor extraction system.

- 
4. Air-permeability of unsaturated strata.
  5. Temperature and relative humidity ranges of near-surface atmospheric air.
  6. Number, size, depth, spacing, and criteria for injection/withdrawal wells.
  7. Air pumping rates needed to achieve the desired degree of water removal.
  8. Atmospheric pressure variations diurnally and longer-term.
  9. Unsaturated hydraulic properties of subsurface formations.
  10. Infiltration and recharge rates over the area of concern.
  11. A numerical modeling analysis of the air-flow, moisture-transfer system would be required for efficient design.

Materials and Equipment Needs:

1. Injection and withdrawal wells perhaps 5 to 30, depending on permeability and desired rates of removal and specific method used.
2. Air injection or suction pumps (unless natural barometric pumping is used); output rating of pumps depends on desired removal rate, number of wells, and permeability.
3. Air humidity, temperature, and flow rate monitoring instruments for injected and/or withdrawn air.
4. Filters and traps to remove any potential contaminated particulate or gases.
5. Valving and piping systems to handle pumped air and/or control barometric pumping.
6. Heating devices or systems (perhaps solar) for heating injected air, if desired.

This method relies on readily available, relatively simple, equipment and materials. No major R&D is needed except on a site-specific pilot scale.

---

#### 9.4.2 Stage of Development

This method probably has not been used for the specific application proposed here. However, the concept has recently received increasing use as a method for removing volatile organic contaminants from unsaturated formations.

The equipment, materials, and general methods are standard and well developed. The method has proven to be very successful in removing volatile organics such as gasoline and chlorinated solvents. In one application, more than 1500 liters of gasoline were removed using three relatively small-capacity vapor extraction wells in a period of three months (EPRI, 1987). In another application, more than 1600 lbs of TCE were removed from soil in a pilot vapor extraction project (EPRI, 1987). The U.S. Army Toxic and Hazardous Materials Agency (USATHMA) has been developing and testing this method for the past three years.

#### Development Needed:

Relatively minor development and demonstrations work is needed on the following aspects:

1. Literature review of research and applications of this concept.
2. Scoping feasibility and modeling analysis for numerous ranges of possible conditions.
3. Field tests of potential air pumping and water removal rates under site conditions.
4. Field tests of barometric pumping efficiencies for water removal rates at various depths, under site conditions.
5. Numerical model development to simulate air and moisture transfer through the subsurface system in 2- and 3-dimensions.
6. Relationships between heating or drying air and increased water removal efficiencies (perhaps using solar heat).
7. Assessment of moisture recharge or influx rates during or after drying cycle.

---

### 9.4.3 Background

This method probably has not been used before for removing water from the unsaturated zone. However, it has proven to be effective at several sites for removing volatile chlorinated and non-chlorinated compounds from unsaturated soils. USATHMA is currently using this method successfully to clean up an extensive chlorinated solvent problem (TCE and other compounds) at the Twin cities ammunition plant at Minneapolis, MN. EPA and some state environmental protection agencies have approved of the method for cleaning up several other industrial contamination sites involving chlorinated solvents. The U.S. Air Force is also applying the method to some of its contaminated soil problems. The method has been used successfully to remove spilled gasoline from soil at several sites.

### 9.4.4 Benefits

The air-drying method has several potential benefits and advantages for immobilizing plutonium in the unsaturated zone, including:

1. Based on very simple, proven principles.
2. Uses relatively simple, readily available materials, equipment and technology.
3. Can be quickly designed, tested, demonstrated, and implemented.
4. Is relatively inexpensive to implement and operate.
5. Immobilizes all other dissolved solid contaminants that might be present, in addition to plutonium.
6. Will remove volatile contaminants such as carbon tetrachloride, TCE, etc., from the unsaturated zone. These substances can then be captured and disposed of or treated in an appropriate manner.
7. Has considerable flexibility in its design and application. For instance, it could be operated continuously or periodically on a weekly, monthly, or seasonal basis.
8. Can readily be combined with other methods to provide a greater degree of remediation and protection. For instance, it probably should be combined with methods to reduce infiltrations at the surface such as impermeable caps and runoff diversion.

- 
9. Involves no additional objectional materials that might cause environmental concerns.
  10. Its effectiveness can be verified relatively easily and repeatedly.
  11. Does not preclude the use of other or additional methods, if, for some reason, it proves ineffective.
  12. Can be used effectively in combination with other methods such as surface capping.

#### 9.4.5 Constraints

##### 9.4.5.1 Environmental/Climate

Effectiveness is dependent on relatively low moisture content of atmospheric or injected air. At times when atmospheric air moisture is too high, method might be temporarily stopped or the air must be artificially dried. Neither of these constraints is a significant problem to overcome; otherwise, the method can be used under nearly all weather and climatic conditions.

##### 9.4.5.2 Accessibility

The only accessibility constraint is the ability to place wells in the approximate locations and patterns needed. The number of wells, locations, and patterns has considerable flexibility so that it does not appear to be a significant constraint.

##### 9.4.5.3 By-Products

The method does not use or create any by-products. However, it could possibly blow a small amount of dust contaminated with plutonium, hazardous gases, or other substances to the ground surface. Any dust could easily be trapped on a filter. Gases can be trapped by various techniques. This method will carry volatile organic contaminants to the surface, which must be properly managed. However, that is an intended benefit of the method.

##### 9.4.5.4 Schedule/Duration

This method could be designed, tested, and implemented within approximately two or three years. A significant disadvantage is that it might require periodic operation for an indefinite period of many decades. This would depend partly upon what other methods

---

---

might be employed to reduce water infiltration or to reduce plutonium mobility. Some potential options of this method involve a total passive mechanism naturally driven by barometric pressure changes. If that option can be demonstrated to be feasible, the system could be self-sustaining indefinitely with periodic check-up visits.

#### 9.4.5.5 Support Systems

Initial implementation would require only routine support, including access for drilling rigs, electric power for air pumps, and instrumentation. Over long-term operation, minimal support systems may be required for the passive barometric-driven option. No other unusual support systems are needed, except those that may be needed to trap contaminants or treat volatile organics removed with the exhaust air.

#### 9.4.5.6 Equipment Size

Air wells: 5 to 30 (depending on several factors).  
4 to 12-in. in diameter, 50 to 400 ft deep.

Air pumps: 2 to 30 off-the-shelf designs with 100 to 1000 CFM capacity (depending on several factors).

Air heaters For injection pumps. Optional, probably not needed; could be solar or driers: heaters.

Filters: For exhaust wells; small, simple design.

Equipment such as charcoal canisters or combustors to trap or treat volatile organics in exhaust air and to extract any other contaminants in exhaust air.

Instrumentation/control trailer or building.

#### 9.4.5.7 Operational Factors

Simple to operate on continuous or periodic basis. Occasional break downs or stoppage will not cause problems (continuous operation not required). Continuous presence of personnel is not required.

---

#### 9.4.5.8 Safety

This method has some potential safety problems that would be easy to handle. If exhaust air has high concentrations of toxics, it must be managed accordingly. Once system is operational, no personnel would be needed most of the time.

#### 9.4.5.9 Regulatory Issues

Immobilizing plutonium in the ground at depths of 110 ft or greater is a new environmental issue that probably has never been dealt with by EPA or other regulatory agencies; therefore, it may be difficult to obtain their concurrence on any proposed remedial method. The simplicity of this method might make it more readily acceptable to a regulatory agency.

#### 9.4.5.10 Efficiencies

The potential efficiency of this method for drying the subsurface environment sufficiently to halt downward water migration (and the migration of plutonium and other dissolved or suspended contaminants) appears to be promising. However, an analysis would be needed using fairly simple numerical modeling techniques and pilot tests to more accurately assess efficiencies. The method has proven to be highly effective for removing volatile organics from the unsaturated zone.

### 9.5 Alteration of Recharge Flow Paths

#### 9.5.1 Application

Isolation of migrated/migrating plutonium in unsaturated zone by diverting the downward flow of water which might be transporting the plutonium.

#### 9.5.2 Description of Technique

##### 9.5.2.1 General Principle

This technique is based on the assumption that plutonium was/is carried downward in dissolved or suspended form by percolating water in the unsaturated zone. If the flow of percolating water can be diverted in such a way that it no longer contacts or transports the subsurface plutonium, then further downward migration will be prevented. Changing the moisture flow path and rates can be accomplished by changing the physical conditions that control unsaturated moisture flow, including:

1. Unsaturated zone matric potential (suction) distribution.
2. Unsaturated relative permeability distribution.
3. Liquid water content.

Alteration of these properties can be accomplished by inserting materials such as grout to change permeability, removing or adding water, imposing different pressures (suctions) in the subsurface, changing temperature of water and/or formation, changing capillary pressure properties of subsurface materials.

One possible method would be to decrease the water retention potential of the plutonium-contaminated zones and/or increasing the water retention capacity of materials immediately surrounding the contaminated zone (Figure 9.5). In this manner, percolating water would naturally migrate to and through the zone with higher capillary suction and thereby avoid the zone containing the plutonium.

Another method would be to slightly pressurize the contaminated zone by continually injecting dry air while retaining lower pressures in the zone surrounding the contamination zone (Figure 9.5). Percolating water would migrate from the higher pressure zone to the lower pressure zone, thus avoiding contact with the plutonium.

This technique relies on the fundamental principles describing movement of water through unsaturated porous/fractured materials, which are reasonably well established.

The design parameters would include determination of moisture content distribution in the subsurface basalts and sediments, infiltration and recharge rates, unsaturated hydraulic properties of basalts and sediments (moisture retention curves, relative permeabilities, etc.).

Another possible technique to enhance the potential of water to move toward the surrounding media is the application of fracturing. This technique produces cracks by the application of pressure and, by controlling the conditions, can produce vertical fractures in unconsolidated sediments. The vertical fractures then could be filled with the appropriate blend of particles that induces both moisture flow towards the fracture and eventual downward migration of the water. This type of application is related to the secondary recovery of oil in many localities of the United States.

### Change Ground Water Flow Path

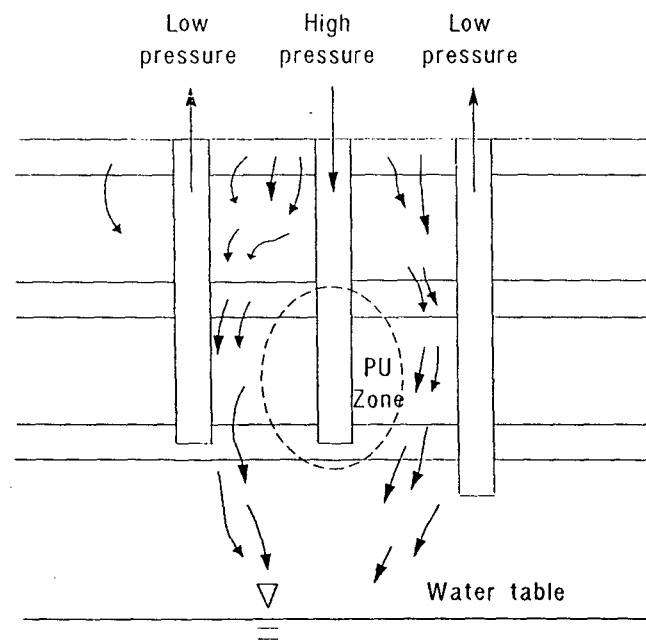
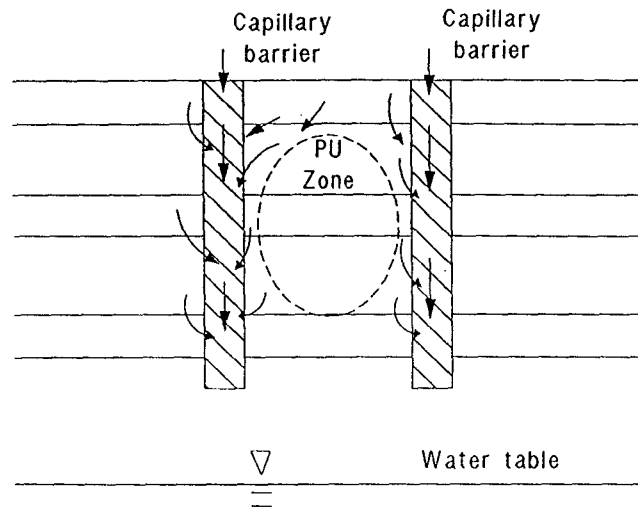


Figure 9.5. Water flow path changed through pressurization.

---

### 9.5.3 State of Development

This method has been proposed and pilot tested for isolation of low-level buried nuclear wastes and toxic wastes. However, most of these test evaluations involved shallow excavated and engineered construction techniques. The concept is also being considered for the design of a potential high-level nuclear waste repository at Yucca Mountain, Nevada.

The methods are still in the theoretical stage for the application proposed here; however, some of the potential methods to implement this are relatively simple and based on well-developed technology, equipment and materials. A considerable amount of lab and field development, testing, and demonstrations would be needed.

#### Initial Recommended LANL Actions

1. Literature review of potential applicability.
2. Numerical modeling scoping analysis to determine conditions under which various hypothetical approaches could be effective.
3. Laboratory tests on unsaturated hydraulic properties of tuffs and sediments at the MDA T.
4. Small scale pilot field test of promising approaches.

### 9.5.4 Background

This principle has probably never been used for this specific type of application. It has been used, at least on a pilot scale, to divert water in the unsaturated zone around buried waste, using engineered capillary barriers.

It would probably be extremely difficult or unfeasible to excavate and construct capillary barrier walls down to depths of 110 feet or 240 feet. The pressure control method, using injected air, appears to be very feasible. Mechanical alterations of hydraulic properties, such as hydrofracturing and injecting capillary barrier material into basalts and sediments might be feasible but would have major potential problems and complexities to overcome.

### 9.5.5 Benefits

Depending on the type of method used for controlling fluid flow paths, the concept has the following potential benefits:

---

#### 9.5.5.1 Pressure Control by Air Injection/Withdrawal

1. Simple technology, easy to implement.
2. Relatively inexpensive.
3. Injecting air would also remove organic contaminants and water.
4. No additional hazardous materials used.
5. Would not preclude application of other methods.
6. Could be used effectively in combination with other methods such as forced-air drying and infiltration control.
7. Easy to operate and relatively safe.

#### 9.5.5.2 Mechanical Alteration of Permeability Capillary/Fracturing

1. Permanent solution, with no continued maintenance required.
2. No additional contaminants introduced.
3. Relatively safe.

#### 9.5.6 Constraints

##### 9.5.6.1 Pressure Control by Air Injection/Withdrawal

1. Unproven technology; considerable development demonstration needs.
2. Requires continued maintenance and monitoring (non-passive).
3. May be difficult to get EPA/State approval.
4. May be difficult to demonstrate effectiveness.

##### 9.5.6.2 Mechanical Alteration of Permeability by Capillary, by Hydrofracturing, or by Construction of Capillary Barrier

1. May be technically infeasible in fractured basalt.

2. Probably very expensive.
3. Difficult to demonstrate effectiveness.
4. Could damage hydraulic properties rather than improve them.
5. Might require injection of water in the unsaturated zone.
6. May be difficult to obtain EPA/State approval.
7. Considerable, potentially expensive, R & D needed; might require several years.

## 9.6 Freezing of the Unsaturated Zone

### 9.6.1 Application

The process of bringing the unsaturated zone beneath the MDA T to a subfreezing temperature is a potential method to immobilize all water within the desired zone, thereby immobilizing any dissolved or suspended contaminants such as plutonium which could be carried downward by water percolating water. The method has application to all contaminants except the more volatile substances which could move in the vapor phase after the water is frozen.

### 9.6.2 Description of Technique

#### 9.6.2.1 General Principle

This method is based on the concept of immobilizing the presumed transporting fluid, water, by freezing it in place. Although at first glance, the method might seem a little far-fetched to some, it merits further consideration. The principle is quite simple, extract a sufficient quantity of heat from the desired subsurface unsaturated zone to bring the rock/sediment/water temperature below 0°C. This can be achieved by very simple, readily available technology, merely by injecting sub-freezing air into the appropriate strata. The air may not even require artificial refrigeration if used only in sub-freezing winter conditions.

The method has been used before to isolate contaminants in the saturated zone and would be even easier to use in the unsaturated zone. A properly designed system might be able to operate on a virtually self-sustaining basis for hundreds of years.

Once a sufficient volume of the unsaturated zone is brought below freezing, all the liquid water held in the intergranular pores and cracks is frozen and thus immobile.

---

The process could probably be controlled so as to freeze the desired intervals. Once frozen, relatively little energy would have to be removed to maintain the frozen state because the frozen zone would be well insulated by more than 100 ft of geologic material above and below it.

The initial freezing would readily be accomplished by blowing subfreezing air into the desired permeable basalt strata. Sufficient quantities of subfreezing air are available during lengthy periods of winter. The air could be blown in through simple wells which are relatively easy to construct.

The extent of freezing in the subsurface could be readily determined through temperature monitoring in wells. Once the desired extent of freezing is obtained, the low temperature can be sustained by periodically introducing more cold air each winter. This can probably be accomplished without mechanical pumping, using only natural barometric breathing mechanisms and appropriate simple valving.

Any recharging water which enters the frozen zone will freeze and stop. At some places, the upper frozen zone might become completely saturated with ice and essentially impermeable.

#### 9.6.2.2 Design Parameters

To implement this system, some of the design data that would be needed are:

1. Temperature, density, heat capacity, thermal conductivity, and water content of tuffs and sediments in the unsaturated zone. (Most of this is already known fairly well.)
2. Air permeability of tuffs and sediments in the unsaturated zone.
3. Effects of freezing water on air permeability of basalts and sediments.
4. Long-term seasonal distributions of density, moisture content, and temperature ranges of atmospheric air at Los Alamos.
5. Geothermal gradient and heat flux at the MDA T.
6. Ranges of expected recharge rates at the MDA T.
7. Numerical model analysis of subsurface air-fluid-heat-transfer system in three dimensions.
8. Quantity and rates of heat extraction needed to achieve desired degree of freezing.

- 
9. Barometric pressure fluctuation on daily and seasonal basis and resultant potential air transfer rates between atmosphere and subsurface geologic strata.
  10. Refrigeration and air pumping requirements (if any) to achieve desired freezing.

#### 9.6.2.3 Design, Procure, Construct, Fabricate Information

All anticipated equipment, material, and technology is readily available to design, test, and implement this process. Air injection can be accomplished by off-the-shelf high-capacity ventilation-type air pumps. Cold air can be obtained from Mother Nature or from (at a much higher cost) commercially available refrigeration systems. The injection and monitoring wells would be very basic designs and readily installed with standard methods. Determining the appropriate number and location of wells would require a numerical modeling analysis of the subsurface air-water-heat transport system.

#### 9.6.3 Stage of Development

Ground freezing technology has been well developed and applied to construction/excavation techniques on numerous construction sites. This method has also been applied successfully on a pilot scale basis for isolating contaminants in the saturated zone (several references available). It probably has not been applied to the unsaturated zone, but would be much easier to implement in a permeable unsaturated media, such as that beneath the MDA T, than saturated media. This is because it is easier to extract heat by circulating cold air than by refrigerating an aquifer.

The ability to pump large quantities of air into unsaturated permeable basalts has been previously demonstrated in field experiments at INEL (Robertson, 1969). The natural capacity of atmospheric pressure changes to pump large quantities of air through wells has also been demonstrated at INEL (Annual Reports of INEL-USGS Project Office, 1966, 1967, 1968). The natural capability of natural processes to maintain perpetually frozen geologic media in the subsurface environment, is clearly demonstrated at Crystal Ice Caves, Idaho, and other subsurface frozen environments caused by a combination of atmospheric and geologic phenomena that generates self-perpetuating local subsurface frozen conditions.

---

### 9.6.3.1 Initial LANL Action and Subsequent Actions

To test, evaluate, and develop this method, the following actions would be recommended:

1. Literature search to collect and review pertinent literature relating to the application of this technique.
2. Feasibility scoping calculations to determine more quantitatively the potential feasibility.
3. Numerical modeling formulation and analysis to evaluate potential effectiveness and design criteria.
4. Laboratory measurements (if needed) of physical properties of basalts and sediments.
5. Small-scale field pilot tests of barometric pumping vs. mechanical pumping techniques.
6. Large-scale demonstration tests with cold-air injection wells and monitoring wells to prove and refine technology.

### 9.6.4 Benefits

This technique offers numerous potential benefits, including:

1. May be able to use the earth's natural heat-pumping capability.
2. Very simple technology, requiring no new developments.
3. Can be developed, tested, and implemented relatively quickly and easily.
4. Can be used in combination or sequentially with other remedial schemes, such as infiltration reduction, in-situ stripping of volatile organics, etc.
5. Easily monitored for effectiveness.
6. Once implemented, might be maintained indefinitely with very low-cost reliable technology.
7. No undesirable environmental impacts and no undesirable substances introduced.

8. Few, if any, significant safety concerns.
9. No potential negative or irreversible effects; if the method proves to be ineffective, other measures can be readily substituted with no lost ground.

#### 9.6.5 Constraints

The major potential constraints of this method might include the following:

1. Limitations in the ability of naturally available cold air to achieve required heat extraction.
2. Limitations in the ability to refrigerate air to achieve required results.
3. Uncertainties in maintaining required frozen conditions over a long-term period of decades or centuries.
4. Might be less efficient than other potential methods, such as air-drying.
5. Accessibility for needed locations of air-injection wells could be a constraint based on unknown locations of buried waste.
6. Because this is an innovative, albeit simple, method, regulatory agencies might be reluctant to endorse it.

#### 9.7 Microbial Products Utilized as a Grout

##### 9.7.1 Application

The utilization of microorganisms or their exocellular products for the purpose of blocking or filling small subsurface fissures.

##### 9.7.2 Description of Technique

Many microorganisms under environmental stressed conditions produce copious amounts of exopolymeric materials. These materials commonly called slimes have been shown to reduce fluid flow and cause a reduced thermo transfer from the interface of one surface to another. There are also organisms that produce exopolymeric material under nonstressed conditions, e.g., filamentous cells.

---

These biofilms or slimes have been shown to adsorb on wall materials of metal, rock, concrete, plastic and many others. Adsorption occurs as a result of chemical bonding between the abiotic wall material and the biotic cell material. As these films are being deposited or developed, fluid frictional resistance increases dramatically within the flow system. It has been shown that flow reduction occurred as a result of reduced cross sectional area, increased roughness of the surface, and an increase in the drag of the fluid by virtue of their visco-elastic properties.

Since microbial cells are very small, 0.5 micron by 1.0 micron, and many are motile, they can easily get into fissures that are normally difficult to reach and fill. Once the organism is in the fissure, it has the ability to multiply at great rates producing daughter cells and exocellular polymeric material which fills the fissure and adsorbs to it, thus causing a block.

The process would involve growing desired organisms in a tank on location and pumping the solution into the subsurface permeable area. A nutrient solution would be pumped in a series arrangement at intervals between microbial injection. A monitoring system to determine the extent of penetration and/or percolation testing to check the flow reduction may be desired.

### 9.7.3 Stage of Development

Although an extensive history of biofilms exist within the environment that demonstrate their ability to inhibit and prevent liquid flow, very little has been done on a planned and designed closure using biofilms. Therefore, this method should be considered in a developmental stage. Research has shown how and what produces biofilms. Industrial situations have shown the effectiveness of biofilms. The effort would have to be in developing an organism or mixed population to the subsurface conditions at the location.

### 9.7.4 Background

The history of biofilms causing severe industrial problems is extensive and broad in scope. The petroleum industry has been plagued with flow restrictions and reduced oil recovery due to the presence of organisms. The industries that require raw water or treat raw water have experienced biofilm problems, e.g., nuclear power plants (heat exchange units plugged), service water supply lines (pipe lines plugged); water treatment plants, sludge dewatering; pulp and paper plants, the screens that collect the fibers, etc. Iron crown gall is another biofilm and inorganic matrix which forms on pipes in fresh water systems as in residential well systems.

Biofilms have been used to seal pond bottoms. Alga mats are allowed to develop on the surface of ponds. The ponds are allowed to dry and the biomass is left at the pond's bottom. This interface seal has been shown to be much less permeable than the

---

soil matrix itself. Biofilms are also developed in many biocorrosion situations. The film is often a mixture of inorganic mineral and bioorganic polymers in the form of a scale. These scales have prevented leakage in pipes and tanks until they were physically removed.

### 9.7.5 Advantages/Disadvantages

Since microorganisms can multiply at a very fast rate and produce copious amounts of biofilm material, with very little energy or food input, this technique could be very cost effective. In addition, the microbe is very small, motile, elastic and only slightly electrostatically charged. Therefore, microbial growth could be superior to other materials or could be effectively used in conjunction with other materials in sealing small fissures. Cells also have the ability to regenerate and in doing so maintain the integrity of the grout. Many of the exocellular polymers have the ability to bind, adsorb, dissolve inorganic ions and compounds. This could be a benefit in not only blocking the path of particulate plutonium but also in preventing further migration of dissolved plutonium.

The only two factors worth mentioning as a potential disadvantage would be seasonal conditions and time. In order to grow microorganisms in batch operation at the location, the temperature should be above freezing and the warmer the ambient temperature the quicker cells will multiply under field conditions.

Although the scale of size does not preclude using this method, time to achieve desired plugging may be extended beyond the "normal" technique of pumping cement to seal the strata.

Operational factors would not be greatly different than handling a liquid solution and injecting it into the subsurface.

## 9.8 In-Situ Coating With Inorganics/Clay

### 9.8.1 Application

The objective of this technique is to produce "nonradioactive" particles originating from plutonium contaminated soil minerals and possible plutonium oxide particles now present in the environs outside the immediate confines of the buried source term. In addition, the treatment will result in several smaller particles to bind together, thus forming a larger, potentially less mobile and less hazardous particle. It may also produce a system whose pores are less interconnected and thus reduce permeability to any intruding water.

---

### 9.8.2 Description of Technique

The method to be employed includes introduction of a solution or suspension which, when it encounters the contaminated zone, would result in formation of new precipitates that would "coat" the existing contaminants. The "coating" could also be a clay introduced as a suspension.

The percolating solution (and/or suspension) would be allowed to enter the contaminated zone several times in order to ensure better coverage of the particles; after each addition, the zone would be allowed to dry (become unsaturated) to foster better adhesion to the contaminants.

This approach will take advantage of known pedologic reactions occurring in this semi-arid area, as well as to attenuate alpha ( $\alpha$ ) radiation emanating from plutonium isotopes by the shielding offered by the coating. The pedologic reaction is one encountered in desert environments. This is the commonly observed formation of caliche layers in these soils. The caliche represents reforming or forming new compounds at a deeper depth of dissolved minerals when the percolating water stops; and as drying occurs, the dissolved components revert back to a solid phase. In addition to forming a new solid phase, these phases such as iron oxides/manganese oxides tend to coat existing particles. It is well known that accurate plutonium analysis depends on removing such impurities as iron and manganese prior to electro deposition for radioanalytic assay; otherwise, the alpha ( $\alpha$ ) spectrum is poorly defined due to attenuation by the coated oxides. Hence, the reverse phenomenon of keeping the "impurities" on the contaminated particles would greatly reduce the potential radiologic hazard. In addition to forming a coating on particles, these precipitates and clays can serve as intergranular cementing agents between particles. The cementitious condition will "glue" the particles and reduce any further downward migration.

In designing the operating principles, it should be noted that the plutonium existing in the formation beneath the source was transported by water that passed through the tuff. Hence, introduction of precipitating solutions and/or clay should be made to follow the same pathway as closely as possible. An important consideration is the saturating capacity of the interbeds so that appropriate volumes of the solution can be introduced per injection. In addition to the stated objective of stabilizing and detoxifying by attenuation of the radiation, the application of the chemicals can additionally serve as a "tracer" in the distribution of the percolating water.

### 9.8.3 Stage of Development/Background

Presently, very little information has been developed for the particular coating application intended. Surface sprays of solutions were applied at the Nevada Test Site (NTS) but the objective was to reduce resuspension (induce agglomeration or gluing of particles).

---

Clays are commonly used in agricultural systems to impede flow of water into or out of a system. In these systems, the clay forms a barrier by swelling (clay layer) and thus plugging pores. A possible modification for this application would be to use these same clays that have been heat treated prior to forming the suspension so that they will swell only after a fixed period of time, thus allowing much deeper penetration. Selected heating times and temperatures have been done (not for this application) and have shown the delayed swelling phenomenon.

#### 9.8.4 Action Plan

Obtain representative samples from the basalt and interbed zones for initial characterization studies. These studies would set the reference conditions for later tests and measurements. Samples, if possible, should include undisturbed cores (~4 in. diameter) in order to obtain properties including but not limited to:

1. Bulk density;
2. Pore volume/pore size;
3. Hydraulic conductivity;
4. Moisture holding capacity.

Disturbed samples would be used to determine the following properties (but not limited to):

1. Particle size analysis;
2. Mineralogical analysis;
3. Free oxide analysis;
4. Ion exchange capacity;
5. Exchangeable ion content;
6. Organic carbon content;
7. pH/buffer capacity.

The core samples will be used later for more critical laboratory tests after column testing is complete. Columns containing materials of different properties (clay, sand, silty clay, basalt, etc.) and whose properties have been determined will be set up and different solutions added to induce coating of insoluble phases. The variables could include

---

different dissolved ions and/or clays, different concentrations, different rate of application, different contact times, and different drying cycles, etc.

After the tests are complete, the columns will be disassembled, segmented, and the amount of surface adsorption determined. From these results, modifications and changes for further tests would be conducted. A possible pre-test condition may be to pre-adsorb a dye or artificially pre-coat the particles so that the evaluation of the test could be based in part on the pre-adsorbed material's fate. For example, a fluorosium dye may be precoated on the material. After the test, the amount of dye desirable can be measured, including the amount of iron oxide coating.

If field tests are to be pursued, technologists must consider the mode of application including equipment, logistics, staging, etc.

#### 9.8.5 Benefits

In addition to the benefit of inactivating the contaminated zone in-situ with off-the-shelf equipment, this approach may be regarded as a technique to study the flow path of the percolating water. If laboratory and field trials show limited achievement of the inactivation goal, the definition of the water pathway (the precipitates and clays may serve as "tracers") will better define the zones that must be treated with other more drastic and costly techniques.

The demonstration of inactivating the radiologic hazard by attenuation, the increased adhesion of the contaminated particles to the substrate (less migration), and the reduced permeability of the contaminated zone should prove particularly valuable. In addition, no new hazardous materials are introduced, so the method is relatively safe.

#### 9.8.6 Constraints

Field activities would be limited to the non-frigid season. Prior to embarking on a field scale demonstration, tests of water permeability, pore volumes, solution, and suspension permeabilities should be measured on representative cores obtained from the site area. These results would guide the decisions of when in the formation to introduce the solution, any pressures to be used to hasten distribution of solutions, injection rates, volumes, etc., in the field test.

In generating hydroxy precipitates of elements such as iron or manganese, the residual liquids should be devoid of soluble constituents by engineered control of the volumes. Several applications of solutions/suspensions may be required; it may be necessary to blow dry the zone in order that each application will not produce excess liquids percolating downward.

---

## 9.9 Grout Fissures and Pores

### 9.9.1 Application

The major transporting agent of plutonium downward from the disposal pits is water; and the pathway downward may be through fissures and pores. If the pathway can be blocked by the placement of an impermeable grout, further leaching of plutonium from the source downward would be prevented. The existing plutonium below the source would thus remain in their present location.

In contrast to the coating of different contaminated zones, submitted separately, the grouts would occupy the void spaces as fully as possible and thus eliminate any further penetration of water.

### 9.9.2 Description of Technique

Grouting involves preparing a suitable slurry and injecting the grout to the desired locations to achieve the goal of immobilizing and isolating the contaminated zone. The type of grout depends on the desired goal--generally categorized as chemical (solution) grout or particulate grout. Chemical grouts have the advantage of being able to penetrate much smaller pores than particulate grouts. Chemical grouts almost without exception require a wet environment after setting; on the other hand, particulate grouts such as cements do not. It is conceivable that the grout application be repeated so as to sufficiently reduce the sizes of the voids and fissures to hinder penetration.

The lower the viscosity (consistency) of a grout, the more likely will be the path that of the original water. Chemical grouts whose viscosity approaches that of water are available; additives to control the set time are used depending on the conditions. Chief criticisms against chemical grouts have been their unknown long term durability.

Organic grouts meet objections usually due to unknown long-term biodegradability. This might be countered with appropriate studies of the MDA T water quality including micro biologic conditions. Research on appropriate additions of biocides might be performed to obviate this argument.

It may be possible to develop inorganic grouts that may possess the low initial viscosities of organic grouts, but not the biodegradability. These may include a grout consisting of sodium aluminate-sodium silicate with set control additive to form an alumina silicate solid. A modified system may be a two-stage injection of sodium phosphate followed by calcium chloride to form insoluble calcium phosphate. These latter two types of grout would require more research but would exhibit longer term durability compared to sodium silicate alone.

---

Injection techniques vary with the application. If fracturing (creation of new fissures and cracks) is to be avoided, lower pressures are used. Note that these new fissures and cracks formed will be filled with grout using this technique (in contrast, if water is used to fracture, the fissures will be filled with water and new pathways are formed). However if too low pressures are used, the lateral spread is limited and only a limited zone is grouted. Grouting to stop water flow is a widely used technique--notably, this technique is used to stop leakage of water in dam systems.

### 9.9.3 Stage of Development/Background

Grouting has been used to seal shallow land burial trenches. Both chemical and particulate grouts have been used. If the grout is to be injected at fairly shallow depths, then mobile equipment is available. To access greater depths, equipment is available but would be less mobile and require pre-drilled injection wells.

If grouting is to be pursued, appropriate LANL personnel (those to be involved in procuring equipment) should contact companies such as: GKN Woodbine Corp. of Fort Worth, TX; Dowell Company, Tulsa, OK; and GKN Hayward-Baker, Odenton, MD, to name three companies for their engineering experience.

LANL personnel should also perform grout formulations and biostability testing. It should be noted that private grouting companies all have their "pet" formulations and approaches; at the minimum, LANL staff must work with them closely since the problem and solution remain LANL's.

#### 9.9.3.1 Action Plan

LANL personnel familiar with grouting should contact oil well servicing companies. These companies tend to be more objective about the process than commercial grouting companies. Through contact, one learns about grouts as well as equipment that can inject the grout. Laboratory development would include: (a) alumina silicate, calcium phosphate, and possibly other combinations of inorganic salts, and (b) biostable organic grouts such as acrylimides, acrylate, and other non-degradable combinations including addition of biocides.

Another test that may be useful and valuable to LANL would be a grouting demonstration using existing grouts. First, one of the low viscosity organic grouts may be tested. In Figure 9.6a, the introduction is at low pressure, allowing the low viscosity grout to flow downward through fractures down to the interbed. In Figure 9.6b, the injection is conducted at the top of the interbed. Most of the grout will be in the interbed. In Figure 9.6c, the injection is conducted under higher pressure and the grout is squeezed into the fractures of tuff, as well as in interbed. Additional fracturing could occur with pressure. In Figure 9.6d the pressure injection is at the bottom of the interbed. Depending on pressures, fracturing could occur and form pancakes at

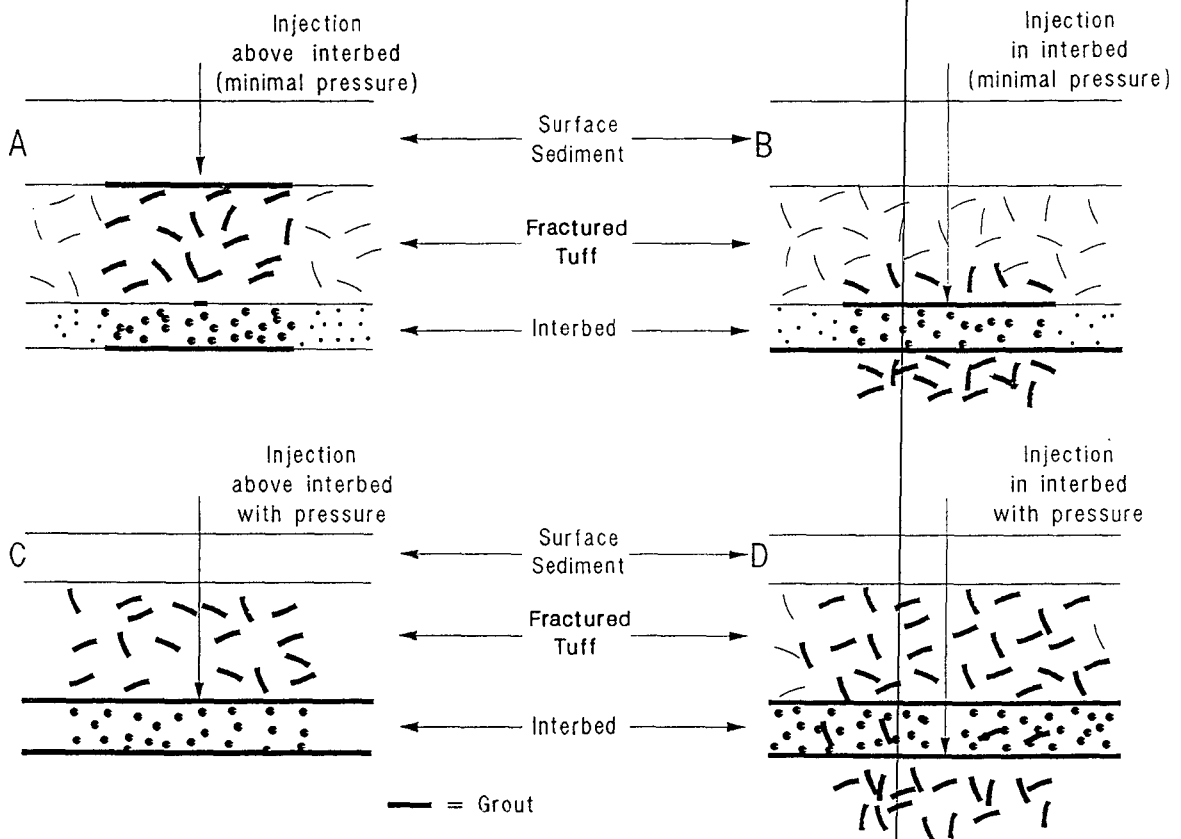


Figure 9.6. Potential grouting methods for remediation.

---

formation interfaces. Before and after these simple tests, water would be added and the degree of water barrier formation established. These tests should to far in determining the potential of this grouting approach.

#### 9.9.4 Benefits

The major objective of this application is to prevent water from contacting the contaminated materials that have migrated below the burial site and thus eliminate further downward migration. The application of grouting is a well known and widely accepted technique that would enhance acceptability.

#### 9.9.5 Constraints

The major constraint would be the regulatory issue of toxicity if certain organic chemicals are used. Reliable formulations and application of the grout should reduce objections. If injection is to be in the deeper strata directly with pre-emplaced injection wells, several large mounted equipments are used such as a pumper, blender/mixer, and water tanks. It may require several applications to obtain the desired results and increase the cost.

### 9.10 In-Situ Treatment

#### 9.10.1 Application

Immobilization of Plutonium (Pu) in partially saturated zone below disposal beds.

#### 9.10.2 Description of Technique

##### 9.10.2.1 General Principle

In-situ thermal treatment is a general category of in situ waste treatment operations used or potentially used to significantly reduce or eliminate Pu transport.

In-situ thermal treatment herein is limited to basalt and basalt interbed material contaminated or potentially contaminated with Pu. Furthermore, treatment is limited to the partially saturated hydrogeologic system.

---

### 9.10.2.2 Theory/Operating Principles

This general technology involves producing sufficient energy (heat) within the zone of contamination to melt or partially melt (phase change) minerals and associated materials, and subsequent solidification of materials into a wholly or partially amorphous media. This media is very resistant to physical, chemical, or biologic degradation and as such may produce a durable treated waste form, capable of waste confinement for millennia.

In-situ Thermal Treatment can conveniently be divided into two subcategories, in situ sintering and in situ vitrification.

#### 9.10.2.2.1 In-Situ Sintering

This is a process presently being investigated (preconceptual engineering phase) by Westinghouse Hanford Company. It involves partial melting and solidification of contaminants and melt into a stable and resistant porous media. Only partial melt of geologic media and incorporation of contaminants is necessary.

This process operates by combustion of gases injected through boreholes penetrating the media to be treated. Boreholes are drilled, cased, and perforated using high temperature oil patch well completion methods and materials. A plan matrix of wells are used alternatively for gas injection, and/or withdrawal. Injection wells are pressurized, whereas withdrawal wells are held at less than atmospheric pressure. As a result, the direction and magnitude of the treated contaminated zone can be controlled. Combustible gases and additives are stored and pumped using surface storage tanks, gas pumps, and compressors connected to injection well manifolds. Off-gas treatment of collected gases and particulates is done in surface scrubber and entrainment modules.

As injected gas is continually introduced into the formation through injector well perforations, a partial melt of porous media occurs. However, the media remains porous permitting continuous flux of injected gases and offgases. The treated zone radiates outwardly over time due to control by negative pressure induced by withdrawal wells. Injection wells may or may not (as the treatment process continues) be used as withdrawal wells, and the inverse. Continual or intermittent treatment progresses until the porous media containing the contaminant is fully treated over depth and aerial extent of the contamination. Bore holes are subsequently filled and sealed on completion of operations.

#### 9.10.2.2.2 Design Parameters (Examples)

- morphology of contaminant zone(s);
- general category of contaminant physical form;

- 
- degree of saturation;
  - porosity, pore size distribution;
  - fracture; aperture, length, extent;
  - mineralogy of porous media;
  - concentration and form of contaminant and associated materials;
  - intrinsic conductivity;
  - thermal conductivity/diffusivity.

#### 9.10.2.2.3 Design/Procure/Construct/Fabricate

This technique has not been used to immobilize contaminants in hydrogeologic systems. Scientific and engineering activities required to develop, test, and demonstrate this technique are needed. However, several areas of related waste treatment processes are applicable i.e., incineration and combustion waste materials treatment. Other areas related to this technology include: in situ retort, and compressed air reservoir storage.

#### 9.10.2.2.4 Stage of Development

A moderate development activity (field task) will be required in order to utilize this technique for contaminant immobilization. Existing DOE laboratory equipment and expertise may be used to reduce cost impacts and provide immediate access to experienced senior personnel.

This technique will need to be tested and evaluated under simulated conditions as a precursor to application to actual partially saturated contaminated porous media treatment.

Contacts - Steve Phillips Westinghouse Hanford Company (WHC)

#### 9.10.2.2.5 Background

- history - none;
- past use application - none;
- results - NA.

---

#### 9.10.2.2.6 Benefits

##### 9.10.2.2.6.1 Advantages (examples)

- nominal or no dose;
- moderate cost;
- high degree of long term immobilization.

##### 9.10.2.2.6.2 Disadvantages (examples)

- testing in simulated and actual conditions needed;
- complex technology requiring experience and expertise.

##### 9.10.2.2.7 Constraints

- Environmental/climate - none;
- Accessibility - subsequent to testing and demonstration the equipment and methodologies will be publicly available for procurement, fabrication, and use;
- By-products - liquids and sludges from scrubbers and intrainers will be produced in addition to equipment contaminated during operations which will require decontamination and/or decommissioning;
- Schedule - approximately one week per  $1 \times 10^2 \text{m}^3$  of media treated;
- Support systems - none;
- Equipment size - large mobile equipment required;
- Operational factors - none;
- Considerations - explosives, pyrophorics, etc., may cause loss of confinement if encountered;
- Regulatory issues of factors - unknown;
- Efficiencies - unknown.

---

### 9.10.3 Description of Technique

#### 9.10.3.1 In-Situ Vitrification

This is a process presently under final development and demonstration by Pacific Northwest Laboratories. It involves total melting and solidification of contaminants into a vitrified (glass) monolith or matrix of monoliths. This waste form is very stable and resistant.

This process operates by resistance heating between electrodes placed within the media to be treated. Electrodes are typically implaced from grade to depth using coaxial casing driving, placement, and subsequent casing removal. A electro conducting media is typically placed at the ground surface between electrodes in order to initiate current flow. An off-gas hood is placed over the area to be treated in order to collect and treat vapor and particulate contaminants. These (except for tritium, mobile gases, etc.) are collected and treated in mobile structures containing scrubber, and disentrainment-entrainment modules. Power and system control are provided through a central mobile operations structure. Other support structures and modules are used for equipment decontamination, contaminated solution and sludge storage, and auxiliary power.

As current is applied between electrodes, a melt of geological media and contaminants occurs near grade. This melt progresses vertically downward over time until the melt zone extends below the implaced electrodes (zone of contamination). Current is then interrupted and the treated mass is permitted to cool and solidify. This process including electrode installation is then repeated over a plan matrix of points to depth until the contaminated zone volume has been treated in its entirety.

##### 9.10.3.1.1 Design Parameters (Examples)

- morphology of contaminant zone;
- physical form of contaminant;
- thermal conductivity/diffusivity.

##### 9.10.3.1.2 Design/Procure/Construct/Fabricate

This technique has been developed and demonstrated for contaminated materials at or near grade. Design, procurement information, and costs, construction and fabrication experience and operational experience for this technique is available from Pacific Northwest Laboratory and Westinghouse Hanford Company staff members.

---

Application of this in situ treatment process to intermediate depths (100 m) will require additional effort especially for electrode placement and initiation of melting.

Contacts - Jim Buelt, Vince Fitzpatric  
Pacific Northwest Laboratory (PML)

Steve Phillips - WHC

Brian Spalding  
Oak Ridge National Laboratory (ORNL)

#### 9.10.3.2 Stage of Development

The surface and subsurface support equipment and experience is adequate for simple treatment of contaminated soils. Subsurface treatment of contaminants (100 m) requires well development and geotechnical engineering development activities.

Idaho National Engineering Laboratory (INEL) is currently involved in testing in situ vitrification in surface or near surface materials at the INEL Radioactive Waste Management Complex (RWMC).

#### 9.10.3.3 Background

##### 9.10.3.3.1 History

This technology has a well documented history from laboratory production of borosilicate glass, through bench scale vitrification of simulated soil and actual field demonstration of in-situ vitrification of contaminated soil materials.

##### 9.10.3.3.2 Past Use/Applications

This technology has been applied to one liquid waste disposal structure at the Hanford site. This application was conducted on a demonstration basis. Ongoing demonstration activities are in progress at ORNL.

---

#### 9.10.3.4 Benefits

##### 9.10.3.4.1 Advantages (examples)

###### (1) Demonstrated to 10 m

- minimal or no dose due to removal of coaxial casing electrode method used;
- large scale demonstrations completed and in progress on two types of waste materials;
- high degree of long term immobilization.

##### 9.10.3.4.2 Disadvantages (examples)

###### (1) Complex technology requiring experience and expertise

- cost.

#### 9.10.3.5 Constraints

- Environmental/climate - None;
- Accessibility - Equipment for dedicated site application will have to be procured, fabricated, etc.;
- By-products - Scrubber liquids, sludges, decontamination/decommissioning of equipment;
- Schedule - Approximately one week per 10 m<sup>3</sup> of media treated;
- Support systems - Electrical power (grid or diesel generator) required;
- Equipment size - Large mobile equipment and off-gas hood required;
- Operational factors - None;
- Safety considerations/factors - Explosive, pyrophorics, etc., may cause loss of confinement and high industrial risk;

- Regulatory issues/factors - Unknown;
- Efficiencies - Unknown.

## 9.11 Bioaccumulation of Pu

### 9.11.1 Application

Removal of Pu and other radionuclides from aqueous solution of suspension by accumulation and concentration into microorganisms.

### 9.11.2 Description of Technique

Some microorganisms have long been known to accumulate and concentrate (a) metal ions or complexes from solution as well as metals found as (b) insoluble suspensions of microparticulate metal oxides, sulfides, etc. In addition some suspended microparticulates also adsorb metal ions (and other chemicals) from solution and in turn can be biosorbed with the microparticulates. The same physical-chemical forces responsible for the above biosorption phenomenon are also responsible for adsorption of microorganisms to surfaces; i.e., the conceptualization of whether a microparticle adsorbs to a microorganism (another microparticle) or whether microorganisms adsorb to a surface depends upon the relative size of adsorbing material relative to the microbe (Dugan, 1975; Dugan, 1986; Friedman and Dugan, 1968).

#### 9.11.2.1 Surface Treatment of Contaminated Aquifer or Interbed Sediments Brought to the Surface

Microbes can be a solid surface (e.g., a rotating biocontactor) and used as a biosorbent for Pu and other radioactive metals found in the water, then the complex of organisms and with the concentrated metals can be removed and treated as a more concentrated waste via conventional waste management techniques. Conversely, the microbes can be held in suspension and used as biosorbents then subsequently removed from suspension by known flocculation techniques.

#### 9.11.2.2 In-Situ Biosorption of Pu from Aquifer

The same principle will be used as for the biological surface treatment discussed above except that microorganisms will be added to the aquifer enclosed in a semipermeable membrane which will not allow the microbes to escape into the aquifer but will allow soluble transuranides to pass into the membrane container. The membrane container

---

will be periodically removed to the surface and analyzed and/or disposed via conventional waste management techniques.

### 9.11.3 State of Development

The techniques of biosorption to microbes are well known. These technologies are being investigated at Los Alamos. However, they have never been applied to the removal of subsurface Pu.

#### 9.11.3.1 Action Plan

The selection of specific microorganisms relative to functional activity in the type of waste environment found at MDA T will require laboratory and site experimentation. It will also require more extensive laboratory experimentation to determine the optimum membrane/organism combination and the membrane configuration, pore size, etc., for use in in-situ experiments.

### 9.11.4 Background

<sup>241</sup>Am was biosorbed by both the green alga Scenedesmus obliquus and the bacterium Aeromonas hydrophila. For both long (24 h to 96 h) and short term (4 h) studies the concentration (picocuries/cch) of <sup>241</sup>Am increased in cells with increasing Am concentrations. Naturally occurring organics extracted from surface water near Savannah River, Georgia and separated into various fractions, influenced uptake of <sup>241</sup>Am by both organisms [of 4 organic fractions, one stimulated uptake, two had essentially no effect, and one decreased uptake by the algal cell] (Giesy and Paine, 1977).

Strandberg and others, showed that the yeast Saccharomyces cerevisiae slowly (hours) concentrated uranium and to a less extent radium and cesium on its cell surface and the bacterium Pseudomonas aeruginosa accumulated uranium rapidly (minutes) into the cell where it remained. Uptake of the metal did not require active metabolism by either organism (Standberg and others, 1981).

Leachates from shallow-land, low-level waste disposal sites at Maxey Flats, KY and at West Valley, NY contained <sup>14</sup>C, <sup>3</sup>H, <sup>60</sup>Co, <sup>90</sup>Sr, <sup>134</sup>, <sup>135</sup>Cs, <sup>241</sup>Am and <sup>238</sup>, <sup>239</sup>, <sup>240</sup>Pu as well as several organic contaminants. These leachates contained active microorganisms; predominantly species of Bacillus, Citrobacter, Pseudomonas (all aerobes) and Clostridium (anaerobic). The bacterial isolates were reintroduced into sterilized leachates from the sites to which isotopes (<sup>60</sup>Co, <sup>85</sup>Sr, and <sup>134</sup>, <sup>137</sup>Cs) were added. Mixed cultures of the isolates (both aerobes and anaerobes) were able to grow in the presence of 2.7 x 10<sup>4</sup> pCi/ml but were inhibited by 2.7 x 10<sup>4</sup> pCi/ml which indicates that the

---

radionuclides and organic constituents present were not toxic to the organisms (Francis and others, 1980).

Soil fungal isolates have been shown to produce metabolites that form complexes with Pu which are thought to mobilize Pu by reducing their sorption to soil and sediments (Wildung and others, 1979). Wildung and Garland (1980, 1982) studied the effects of Pu on normal soil microorganisms and reported that both aerobic spore forming (bacillus) and anaerobic bacteria were inhibited by soil Pu levels as low as 1  $\mu\text{g/g}$  when Pu was added as  $^{239}\text{Pu}(\text{NO}_3)_4$ . Other organisms (except fungi) were significantly affected at Pu levels of 10  $\mu\text{g/g}$  and fungi were affected only at the 180  $\mu\text{g/g}$  level. The effect of Pu on fungal colony-forming units was a function of Pu solubility in the soil and specific activity of Pu toxicity to the organisms was primarily due to radiation effects rather than to chemical effects.

#### 9.11.5 Benefits

The technique has potential for concentration and removal of Pu and other radionuclides from both low level mixed waste and from higher activity mixed waste and from contaminated processing water. With variation, the technique has potential for removal of Pu from water, without the need for addition of chemicals into the subsurface environment. None of the organisms being considered are hazardous or pathogenic.

#### 9.11.6 Constraints

Removal of transuranides in-situ will require flow of water or diffusion past the biosorbent and may require pumping of aquifer water or other means of creating a flow. The stability of membranes under the environmental conditions has not been tested. Information on the bioaccumulation of Pu is limited and it is assumed that it will biosorb in a manner similar to other metals.

### 9.12 Leach and Collect

#### 9.12.1 Application

To remove plutonium from the tuffs.

#### 9.12.2 Description of Technique

A leachant solution capable of dissolving or suspending the plutonium is pumped into the interbed. After a suitable residence time, preferably with agitation, the solution is pumped to the surface and the plutonium removed by standard techniques, such as ultra

---

filtration to remove particulates, followed by carrier precipitation solvent extraction or ion exchange to take out dissolved Pu. The theoretical bases of the technique are straightforward, involving chemical (leaching and subsequent recovery of the Pu) and hydrologic (water injection and removal) principles.

Dissolution/suspension of the plutonium would probably require more than one type of leachant. The least-aggressive agent for dissolution would be a solution of a complexing agent, such as citrate or EDTA, and a detergent to suspend Pu-containing particulates. A follow-up treatment with a strong acid such as  $\text{HNO}_3$  would probably leach additional Pu, but complete dissolution of the Pu might require such severe and impractical measures as dissolution of the entire interbed in HF.

In practice, successful application of the technique would require sufficient wells to ensure that the injected leachants would penetrate all the Pu contaminated areas of the interbed and subsequently be removable by pumping. A further requirement is that escape of the Pu containing leachant into adjacent areas be minimized, either by some preliminary grouting technique, or by limiting residence time in the interbed. The wells would be the only construction requirement; the only equipment needed would be pumps and containers for the Pu-containing leachant (the latter designed to be critically-safe). Undoubtedly, facilities already exist at the site for recovery of the Pu from the leachant.

### 9.12.3 Stage of Development

This technique has never been applied to the removal of subsurface Pu.

### 9.12.4 Background

This technique is an adaptation of a process known as solution mining that has been used for a number of years in the mining industry. A typical example is the mining of uranium by pumping a carbonate solution through a uranium ore body; the uranium is dissolved by carbonate complexation, and the U-containing solution is pumped to the surface. The present application differs from the uranium example in that it would probably require more aggressive leachants than carbonate solutions, and it involves plutonium, a much more toxic element.

### 9.12.5 Benefits

The technique is simple and requires a minimum investment in equipment. Hence, it would be relatively easy to implement in a timely manner.

### 9.12.6 Constraints

Potential environmental hazards are associated with application of this technique.

Plutonium, which may well be fixed in the interbed, is mobilized for the purpose of removing it by pumping. There is no assurance that some of this plutonium would not diffuse into surrounding strata and ultimately move to the water table, particularly when the Pu is dissolved in a strong acid. Even if the Pu were confined, the presence of complexing agents, detergents, and strong acids would cause undesirable changes in groundwater composition. These effects would probably be unacceptable to EPA.

Accessibility of the leaching solutions to the contaminated interbeds would require drilling of additional wells after the location of the plutonium has been accurately defined. Perhaps the sampling wells could be used as access wells for the leachant. In any case, extensive well drilling might be required. Implementation of the technique would require electric power and an adequate supply of water.

Other than any residual leachant entrained in the interbed, the only other by-product would be the solution remaining after the Pu has been chemically removed; this is easily disposed of.

---

## REFERENCES

- Abeele, W.V., 1979. Determination of Hydraulic Conductivity in Crushed Bandelier Tuff, Los Alamos Scientific Lab., LA-8147-MS, Informal Report, UC-70.
- Abeele, W.V., 1979. Determination of Relative Hydraulic Conductivity from Moisture Retention Data Obtained in the Bandelier Tuff, Los Alamos, LA-7625-MS Informal Report, UC-11.
- Abeele, W.V., M.L. Wheeler, and B.W. Borton, 1981. Geohydrology of Bandelier Tuff, Los Alamos, pp. 1-50, LA-8962-MS-UC-11.
- Abeele, W.V., 1984. Hydraulic Testing of Crushed Bandelier Tuff, Los Alamos Scientific Laboratory Report, LA-10037-MS-VC-11.
- Abeele, W.V., 1984. Geotechnical Characteristics of Bentonite/Sandy Silt Mixes for Use in Waste Disposal Sites, Los Alamos, LA-0101-MS-VC-70.
- Abeele, W.V., H.R. Fuentes, J. Hosch, and J. Hosch, 1986. Characterization of Soil Moisture Characteristic Curves in 30 to 1000 kPa Tension Range For Bandelier Tuff in Waste Disposal Areas G and L, Technical Area 54, Los Alamos National Lab.
- Abeele, W.V., J. Nyhan, T. Hakonson, B.J. Drennon, E.A Lopez, W.J. Herrera, G. Langhorst, J.L. Martinez, and G. Trujillo, 1986. Low Level Integrated System Test, Los Alamos, LA-10572-MS, VC-70B.
- Abrahams Jr., J.H., 1963. Physical properties of and Movement of Water in Bandelier Tuff, Los Alamos and Santa Fe, United States Department of the Interior Geological Survey.
- Anastros, G.C., et al., 1985. Task II: In Situ Stripping of Soils: Pilot Study, prepared for USATHAM, Aberdeen Proving Ground, MD, Report No. AMXTH-TE-85026 by Roy F. Weston, Inc., West Chester, PA.
- Annual Reports of INEL-USGS Project Office for 1966, 1967, and 1968.
- Christenson, C.W., 1973. Memorandum to H. Jordan, Nuclide Inventory Data, H7-CWC-437.
- Christenson, C.W., E.B. Fowler, G.L. Johnson, E.H. Rex, and F.A. Virgil, 1958. Soil adsorption of radioactive wastes at Los Alamos, Sewage and Industrial Wastes 30, pp. 1478-1489.
-

---

Christenson, C.W., and R.G. Thomas, 1961. Movement of Plutonium Through Los Alamos Tuff, Los Alamos Scientific Lab. Report, pp. 248-281.

Domenico, P.A., 1983. Determination of Bulk Rock Properties from Ground Water Level Fluctuation, Bulletin of The Association of Engineering Geologists, pp. 283-287, Vol. xx, No. 3.

Dugan, P.R., 1975. Bioflocculation and the accumulation of chemicals by floc forming organisms. Report EPA-600/2-75-02. US EPA, Cincinnati, Ohio.

Dugan, P.R., 1986. The function of microbial polysacchapidies in bioflocculation and biosorption of mineral ions. (In) Y. Attia (ed.) Proceed. Symposium on Flocculation in Biotechnology and Separation Systems, pp. 337-350.

EG&G Idaho, Inc., 1987. Interoffice Correspondence Memorandum from D.M. Martinson to S.P. Fogdall on Waste Isolation Techniques Value Engineering Workshop - DMM-13-87, September 30.

Electric Power Research Institute, 1987. Remedial technologies for linking underground storage tanks, EPRI Report CS-5261.

Environmental Surveillance Group, 1984. Environmental Surveillance at Los Alamos during 1983, LA-10100-ENV.

Environmental Surveillance Group, 1986. Los Alamos, Group LA-10990-ENV.

Environmental Surveillance Group, 1987. Environmental Surveillance at Los Alamos during 1986, LA-10992-ENV.

ER Program Project Group, 1988. Site reconnaissance plan, Los Alamos National Laboratory, Task 8, Technical Area 21, Synopsis.

Essington, E.H., D.M. Nelson, K.A. Orlandine, W.R. Penrose, and W.L. Polzer, Speciation and Mobility of Actinides in a Shallow Aquifer at Mortandad Canyon, New Mexico, Los Alamos National Lab., Eng-36.

Essington, E.H., E.B. Fowler, and W.L. Polzer, 1981. The Interactions of Low-Level Radioactive Wastes With Soils: 2 Differences in Radionuclide Distribution Among Four Surface Soils, Los Alamos National Lab., Vol. 132, No. 1, pp. 13-18.

Essington, E.H., E.B. Fowler, and W.L. Polzer, 1981. The Interactions of Low-Level Radioactive Waste With Soils: 3 Interaction of Waste Radionuclides With Soil From Horizons of Two Soil Series, Los Alamos National Lab., Vol. 132, No. 1, pp. 19-24.

---

---

Fowler, E.B., E.H. Essington, and W.L. Polzer, 1981. The Interactions of Low-Level Liquid Radioactive Wastes With Soils: 1 Behavior of Radionuclides in Soil Waste Systems.", Los Alamos National Lab., pp. 2-12.

Francis, A.J., S. Dobbs, and B.J. Nine, 1980. Microbial activity of trench leachates from shallow-land, low-level radioactive waste disposal sites. Applied and Environmental Microbiology 40, pp. 108-113.

Fried, S.M., A.M. Friedman, J.J. Hines, and L.A. Quarterman, 1975. Annual report on DWMT Project AN0115A, FY 1975, Argonne National Laboratory Report ANL-75-64.

Fried, S.M., A.M. Friedman, J.J. Hines, R.W. Atcher, L.A. Quarterman, and A. Volesky, 1976. Annual report for FY 1976 on Project AN0115A: The migration of plutonium and americium in the lithosphere, Argonne National Laboratory report ANL-76-127.

Fried, A.M., A.M. Friedman, J.J. Hines, G. Schmitz, and M. Wheeler, 1977. Distribution of plutonium and americium at a former Los Alamos waste disposal site, in Transuranics in Natural Environments, M.G. White and P.B. Dunaway (Eds.), Nevada Applied Ecology Group report NVO-178, pp. 115-126.

Fried, S.S., A.M. Friedman, D. Cohen, J.J. Hines, and R.G. Strickert, 1978. The migration of long-lived radioactive processing wastes in selected rocks, Argonne National Laboratory Report ANL-78-46.

Friedman, B.A., and P.R. Dugan, 1968. Concentration and accumulation of metallic ions by the bacterium Zoogloea. Developments in Industrial Microbiology 9, pp. 381-388.

Gelhar, L.W., A. Mantoglou, C. Welty, and K.R. Rehfeldt, 1985. A review of field-scale physical solute transport processes in saturated and unsaturated porous media, Tech. Report prepared for Electric Power Research Institute, Palo Alto, CA 94304.

Giesy, J.P. and D. Paine, 1977. Efforts of naturally occurring aquatic organic fractions on <sup>241</sup>Am uptake by Senedesmus obliquus and Aeromonas hydrophila, Applied and Environmental Microbiology 33, pp. 89-96.

Grouting in Geotechnical Engineering, Proceeds of Conference at New Orleans, LA, February 10-12, 1982, Sponsored by ASCE.

Huyakorn, P.S., and G.F. Pinder, 1983. Computational Methods in Subsurface Flow. Academic Press.

---

---

Huyakorn, P.S., J.B. Kool, and J.B. Robertson, 1989. VAM2D - Variably Saturated Analysis Model in Two Dimensions, NUREG/CR-5352, HGL/89-01.

IT Corporation, 1987. Hydrogeologic Assessment of Technical Area 54, Areas G&L", Los Alamos National Lab., Docket Number: NMHWA 001007.

Martinson, D.M., 1987. INTEROFFICE CORRESPONDENCE, Waste Isolation Techniques Value Engineering Workshop-DMM-13-87.

McCord J.T., D.B. Stephens, and J.L. Wilson, 1988. Field Experiments and Numerical Simulations of Unsaturated Flow and Transport: The Roles of Hysteresis and State-Dependent Anisotropy, NATO Advanced Study Institute on Recent Advances in Modeling Hydrologic Systems, Sintra, Portugal.

Milly, P.C.D., 1985. A mass-conservative procedure for time stepping in models of unsaturated flow, *Advances Water Resources* 8, pp. 32-36.

Nyan J.W., B.J. Drennon, W.V. Abeele, G. Trujillo, W.J. Herrera, M.L. Wheeler, J.W. Booth, and W.D. Purtymun, 1984. Distribution of Radionuclides and Water in Bandelier Tuff Beneath a Former Los Alamos Liquid Waste Disposal Site After 33 Years, Los Alamos, pp. 1-51, LA-10159-LL WM-VC-70B.

Polzer, E.P., 1988. Perched Water Identification with Nuclear Logs, Ground Water, Vol. 26, No. 1.

Purtymun, W.D., 1984. Hydrologic Characteristics of the Main Aquifer in Los Alamos Area: Development of Ground Water Supplies, Los Alamos, LA-9957-MS, VC-11.

Robertson, J.B., 1968. Injection of Xenon 133 gas into the unsaturated zone, National Reactor Testing Station; USGS Open-File Report (available from INEL USGS Project Office).

Robertson, J.B., 1969. Behavior of Xenon-133 gas after injection underground: Molecular diffusion, materials balance, barometric pressure effects, USGS Open File Report, issued by US Atomic Energy Commission, Report #IDO-22051, 37 p.

Rogers, M.A., 1977. History and Environmental Setting of LASL Near Surface Land Disposal Facilities for Radioactive Wastes (AREAS: A,B,C,D,E,F,Q, and T), Los Alamos Scientific Lab. Report, LA-6848-MS, Vol. I.

Sinnock, S., Y.T. Lin, and J.P. Branner, 1984. Preliminary Bounds on the Expected Postclosure Performance of the Yucca Mountain Repository Site, Southern Nevada, prepared by Sandia National Lab.

---

---

Springer, E.P., and H.R. Fuentes, 1987. Manuscript: Modeling Study of Solute Transport in the Unsaturated Zone, NUREG/CR-4615 LA-10730-MS, Vol. 2.

Standberg, G.W., S.E. Shumate, J.R. Parrott, and S.E. North, 1981. Microbial accumulation of uranium, radium and cesium. (In) F.E. Brinkman and R.H. Fish (eds.). Speciation and Monitoring Needs for Trace-Metal Containing Substances from Energy Related Processes, pp. 274-283. US NBS Publ. No. 618.

Sullivan, J.M., D.R. Lynch, and K.I. Iskandar, 1984. The economics of ground freezing for management of uncontrolled hazardous waste sites, in Management of Uncontrolled Hazardous Waste Sites, 1984, Fifth National Conference, Hazardous Materials Control Research Institute, Silver Spring, Maryland.

Thomas, J.M., 1987. Literature review of forced air venting to remove subsurface organic vapors from aquifers and soil, Report prepared for HQ, AFESCK/RDV, Tyndall AFB, FL, by Dynamac Corp., Rockville, MD.

Travis, B.J., and H.E. Nuttall, 1984. A Transport Code For Radiocolloid Migration: With an Assessment of an Actual Low-Level Waste Site, In: Materials Research Society Symposia Proceedings, Scientific Basis of Nuclear Waste Management, Volume 44.

USGS Annual Reports for 1966, 1967, and 1968, NRTS/INEL Project.

van Genuchten, M. Th., 1978. Numerical Solutions of The One-Dimensional Saturated-Unsaturated Flow Equation, Research Report 78-Wr-09 Water Resources Program, Department of Civil Engineering, Princeton University.

van Genuchten, M. Th., 1987. A numerical model for water and solute movement in and below the root zone, Research Report No. 121, US Department of Agriculture, Agricultural Research Service, US Salinity Laboratory, Riverside, California.

Wildung, R.E., T.R. Garland, and D.A. Cataldo, 1979. Environmental processes leading to the presence of organically bound plutonium in plant tissues consumed by animals. p. 319-334. (In) Proceedings of International Atomic Energy Agency Intern. Symp. on Biological Implications of Radionuclides Released from Nuclear Industries. Internat. Atomic Energy Agency, Vienna.

Wildung, R.E., and T.R. Garland, 1980. The relationship of microbial processes to the fate and behavior of transuranic elements in soils, plants, and animals. (In) W.C. Hansen (ed.) Transuranic Elements in the Environment. DOE/TIC 22800. NTIS.

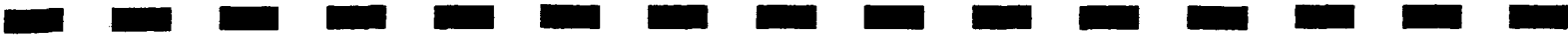
Wildung, R.E., and T.R. Garland, 1982. Effects of plutonium in soil microorganisms, Applied and Environmental Microbiology 43, pp. 418-423.

---

APPENDICES



APPENDIX A



### METRIC-ENGLISH UNIT CONVERSION TABLE

[Read as follows: Dimension—metric unit (symbol) equals English equivalent].

#### Length—

1 meter (m) = 39.37 inches = 3.28 feet = 1.09 yards.  
 1 kilometer (km) = 0.62 miles.  
 1 millimeter (mm) = 0.03937 inches.  
 1 centimeter (cm) = 0.3937 inches.  
 1 micrometer ( $\mu\text{m}$ ) =  $3.937 \times 10^{-5} = 10^{-4}$  A.

#### Area—

1 square meter ( $\text{m}^2$ ) = 10.764 square feet = 1.196 square yards.  
 1 square kilometer ( $\text{km}^2$ ) = .386 square miles = 247 acres.  
 1 square centimeter ( $\text{cm}^2$ ) = 0.155 square inches.  
 1 square millimeter ( $\text{mm}^2$ ) = 0.00155 square inches.  
 1 hectare (ha) = 2.471 acres.

#### Volume—

1 cubic meter ( $\text{m}^3$ ) = 35.314 cubic feet = 1.3079 cubic yards.  
 1 cubic centimeter ( $\text{cm}^3$ ) = 0.061 cubic inches.  
 1 liter (l) = 1.057 quarts = 0.264 gallons =  $0.81 \times 10^{-6}$  acre-feet.

#### Mass—

1 kilogram (kg) = 2.205 pounds.  
 1 gram (g) = 0.035 ounces = 15.43 grains.  
 1 milligram (mg) = 0.01543 grains.  
 1 tonne (t) = 0.984 ton (long) = 1.1023 ton (short).

#### Time—

second day (s day). year (yr or a).

#### Force—

1 newton (N) = 0.22481 pounds (weight) = 7.5 poundals.

#### Velocity, linear—

1 meter per second (m/s) = 3.28 feet per second.  
 1 millimeter per second (mm/s) = 0.00328 feet per second.  
 1 kilometer per second (km/s) = 2,237 miles per hour.  
 1 meter per second (m/s) = 2.237 miles per hour.

#### Velocity, angular—

radians per second (rad/s).

#### Flow Rate (volumetric)—

1 cubic meter per second ( $\text{m}^3/\text{s}$ ) = 15,850 gallons per minute = 2,119 cubic feet per minute.  
 1 liter per second (l/s) = 15.85 gallons per minute.  
 1 cubic meter per day ( $\text{m}^3/\text{d}$ ) = 0.183 gallons per minute.  
 1 cubic hectometer per day ( $\text{hm}^3/\text{d}$ ) = 264.2 million gallons per day.  
 1 quinaria (Ancient Rome) = 0.47-0.48 liter per second.  
 1 U.S. gallon per minute (gpm) = 0.0631 liter per second =  $5.45 \text{ m}^3/\text{day}$ .  
 1 million U.S. gallons per day (mgd) = 43.8 liters per second =  $3,785 \text{ m}^3/\text{day}$ .  
 1 million Imperial gallons per day = 52.62 liters per second.  
 1 billion U.S. gallons per day (bgd) =  $3,785 \text{ hm}^3/\text{day}$ .  
 1 cubic foot per second (cfs) = 449 gallons per minute (gpm) = 28.3 liters per second (l/s).  
 1 acre-foot per day = 14.3 liters per second (l/s).

#### Transmissivity—

1 square meter per day = 80.5 gallons per day per foot.

#### Viscosity—

poise =  $1.45 \times 10^{-5}$  pounds (weight) seconds/square inch.

#### Pressure—

1 newton per square meter ( $\text{N}/\text{m}^2$ ) = 0.00014 pounds per square inch.  
 1 kilonewton per square meter ( $\text{kN}/\text{m}^2$ ) = 0.145 pounds per square inch.  
 1 kilogram (force) per square centimeter = 14.223 pounds per square inch.

#### Temperature—

degrees Celsius (C) = (5F)/9 - 17.77.  
 degrees K = degrees C + 273.16.

#### Work, energy, quantity of heat—

1 joule (J) =  $2.778 \times 10^{-7}$  kilowatt-hours =  $3.725 \times 10^{-7}$  horsepower-hours =  $0.73756$  foot-pounds =  $9.48 \times 10^{-4}$  British thermal units.  
 1 kilojoule (kJ) =  $2.778 \times 10^{-4}$  kilowatt-hours.

#### Power—

watt (W). kilowatt (kW).  
 joule per second (J/s).

(Unless otherwise noted, all gallons are U.S. gallons.)

APPENDIX B

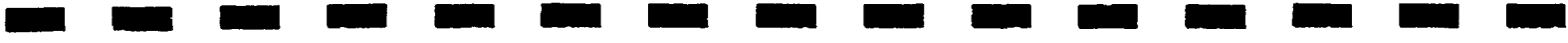


TABLE ~~IV~~ 1

## PLUTONIUM CONCENTRATIONS IN SAMPLES FROM 1953 TEST HOLES

(Table modified from Hermann 1953<sup>264</sup>)

Date	Depth Below Surface	Description	Plutonium dpm/cry α	Notes
<u>DPW-1</u>				
August 25-27, 1953	Surface	Very fine sandy soil	70	
	1'	Very fine sandy soil	8	
	2'	Very sandy soil	4	
	3'	Sandy soil	8	
	4'	Coarse sand and clay	4	
	5'	Sand	4	
	6'	Sand	4	
	6' - 10'	Sand	2	
	10' - 14'	Sand	2	
	15'	Sand	4	
<u>DPW-2</u>				
August 25-27, 1953	Surface	Very fine sandy soil	9	
	1'	Very fine sandy soil	4	
	2'	Sandy soil	3	
	3'	Sandy soil	1	
	4'	Sand	2	
	5'	Sand	3	
	6'	Sand	2	
	7'	Sand and clay soil	4	
	8'	Sand	1	
	9'	Sand	3	
	10'	Very coarse sand	4	
	11'	Fine sand, some gravel	4	
	12'	Fine sand	3	
	13'	Fine sand	3	
	14'	Sand	3	
	15'	Sand	2	
	16'	Sand	4	
	17'	Sand	3	
	18'	Sand	2	
	19'	Sand	3	
20'	Sand	3		
<u>DPW-3</u>				
August 28, 1953	Surface	Very fine sandy soil	32	Hole drilled on a 45° slant extending under adjacent absorption bed. Depths given are slant depths.
	1'	Very fine sandy soil	5	
	2'	Very fine sandy soil	9	
	3'	Very fine sandy soil	7	
	4'	Sandy soil	8	
	5'	Sand	6	
	6'	Very sandy soil	4	
	7'	Very sandy soil	7	
	8'	Very sandy soil	3	
	9'	Sand and clay	3	
	10'	Fine sand	2	
	11'	Sand	2	
	12'	Loose tufaceous sand	450*	
12.5'	Loose tufaceous sand	1510		
13'	Loose tufaceous sand	1330		

TABLE T-V (continued)  
 PLUTONIUM CONCENTRATIONS IN SAMPLES FROM 1953 TEST HOLES  
 (Table modified from Hermann 1953<sup>264</sup>)

Date	Depth Below Surface	Description	Plutonium dpm/dry g	Notes
<u>DPW-4</u>				
September 21, 24, 25, 30 and October 1, 1953	Surface	Sandy soil	8	
	1'	Sand and gravel, some clay	400	
	2'	Sand and gravel, some clay	36,100	
	3'	Sand and gravel, some clay	45,600	
	12'	Very fine loose tuff	1,400	
	15'	Fine sand	5,000	
	16'	Fine sand	5,100	
	17'	Loose tuff	720	
	18'	Sandy loose tuff	24	
	19'	Loose tuff	12	
	20'	Broken tuff core	12	
<u>DPW-5</u>				
September 21, 24, 25, 30 and October 1, 1953	Surface	Sand and clay soil	410	
	1'	Sand and clay soil	600	
	2'	Sand and clay soil	16	
	3'	Sand and gravel	80	
	4'	Sand and gravel	3,400	
	5'	Solid tuff core from a boulder	530	
	6'	Solid tuff core from a boulder	80	
	7'	Friable tuff core	1,800	
	8'	Fine sand and clay	40	
	9'	Fine sand and clay	360	
	15'	Fine sand	2,400	

The 1961 study was reported by both the USGS and LASL. The USGS report<sup>160</sup> stated

*"[1] ...that waste water movement may have changed some of the physical properties of the tuff, such as pore and particles sizes. [2] Some of the wastes discharged in the east end of the disposal pit may have moved laterally through the sand material [Bed A on Sketch C and D, Fig. T-10] along the sloping top of the tuff and then vertically into the tuff. [3] The lower moisture values... seem to coincide with areas of tuff in which the greatest amount of staining had occurred. The stained areas may indicate a different stage of weathering than that at the clay layer due to alternate wetting and drying cycles... [4] The tuff is extensively jointed [Fig. T-10], and the tendency for a liquid to move through the joints is indicated by higher gross alpha count of a 1000 per minute per dry gram at the 20' depth... [5] [There were] several open joints... below a depth of 25 ft. Waste water had penetrated the fineline joints to depth of at least 22 feet and subsequently altered the tuff adjacent to the joint as much as one-quarter inch. Clays developed locally and impeded drainage so that the joints retained water to the extent that the moisture content of the tuff was locally as much as 35%... [6] ...Water in the low moisture range apparently moved to depths greater than 90 feet. Water in unknown quantities moves through open joints or joints enlarged by solvents in the waste. [7] ...Below a depth of about 15-20 feet the alpha activity was low, except for local areas of high alpha activity where water carried the activity along the joints. Rapid movement of water through joints was substantiated during infiltration studies..."<sup>160</sup>*

Average Gross  $\alpha$ , Total Solids,  
Total Hardness While Feeding Waste

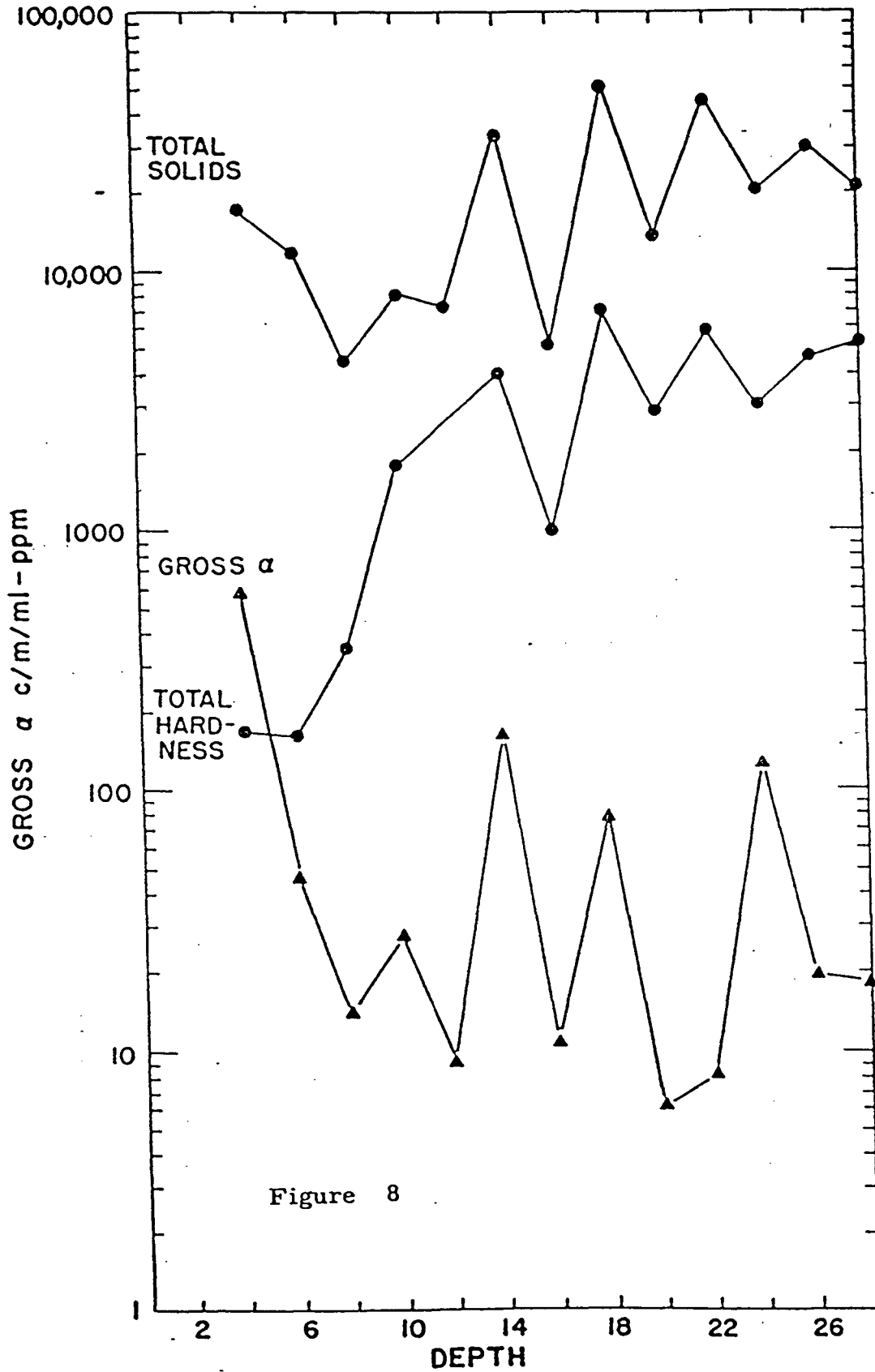


Figure 8

Average Gross  $\alpha$ , Total Solids,  
Total Hardness While Washing with Water

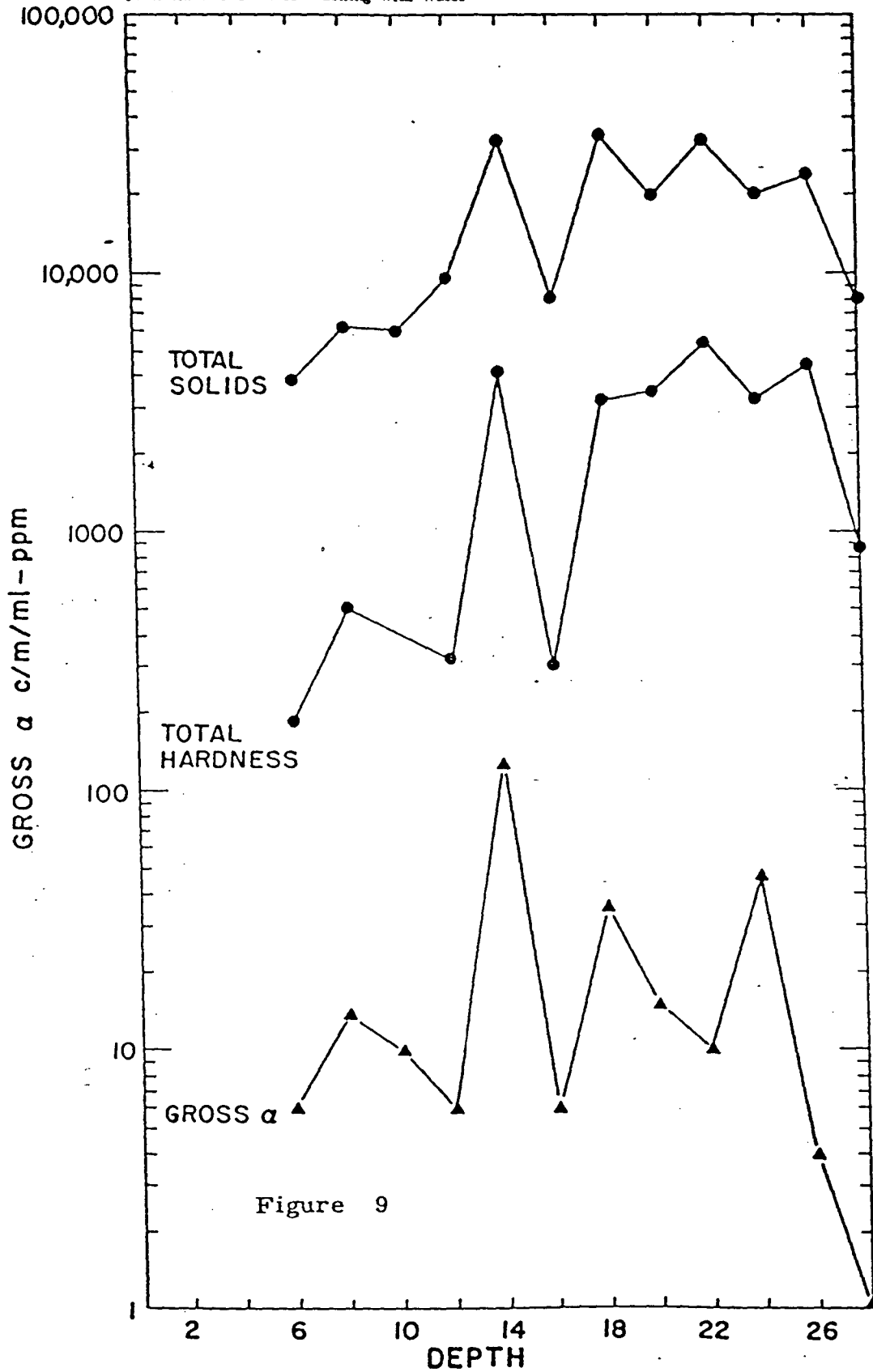


Figure 9

Average Gross  $\alpha$ , Total Solids,  
Total Hardness (All 9 Samples)

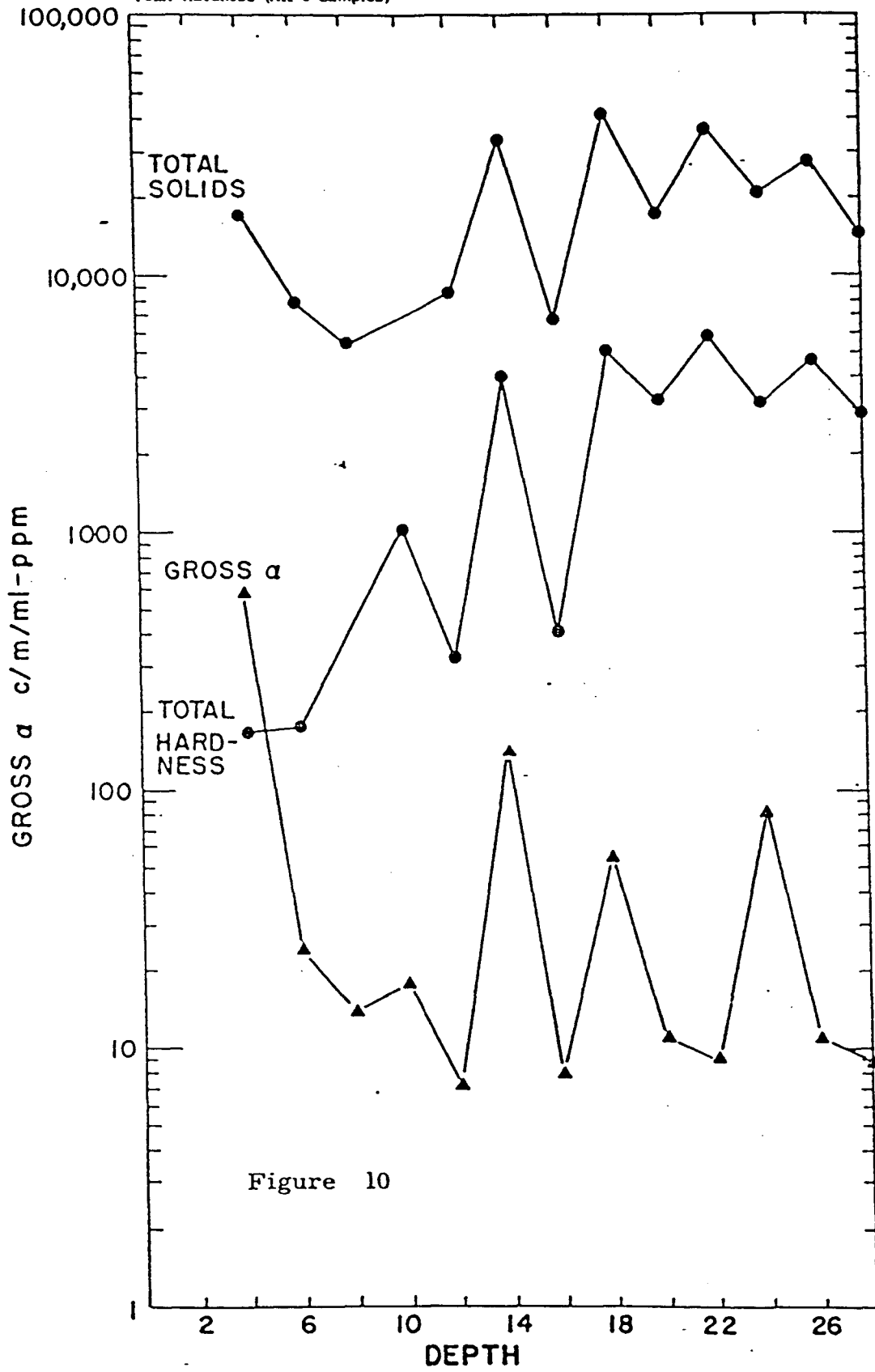


Figure 10

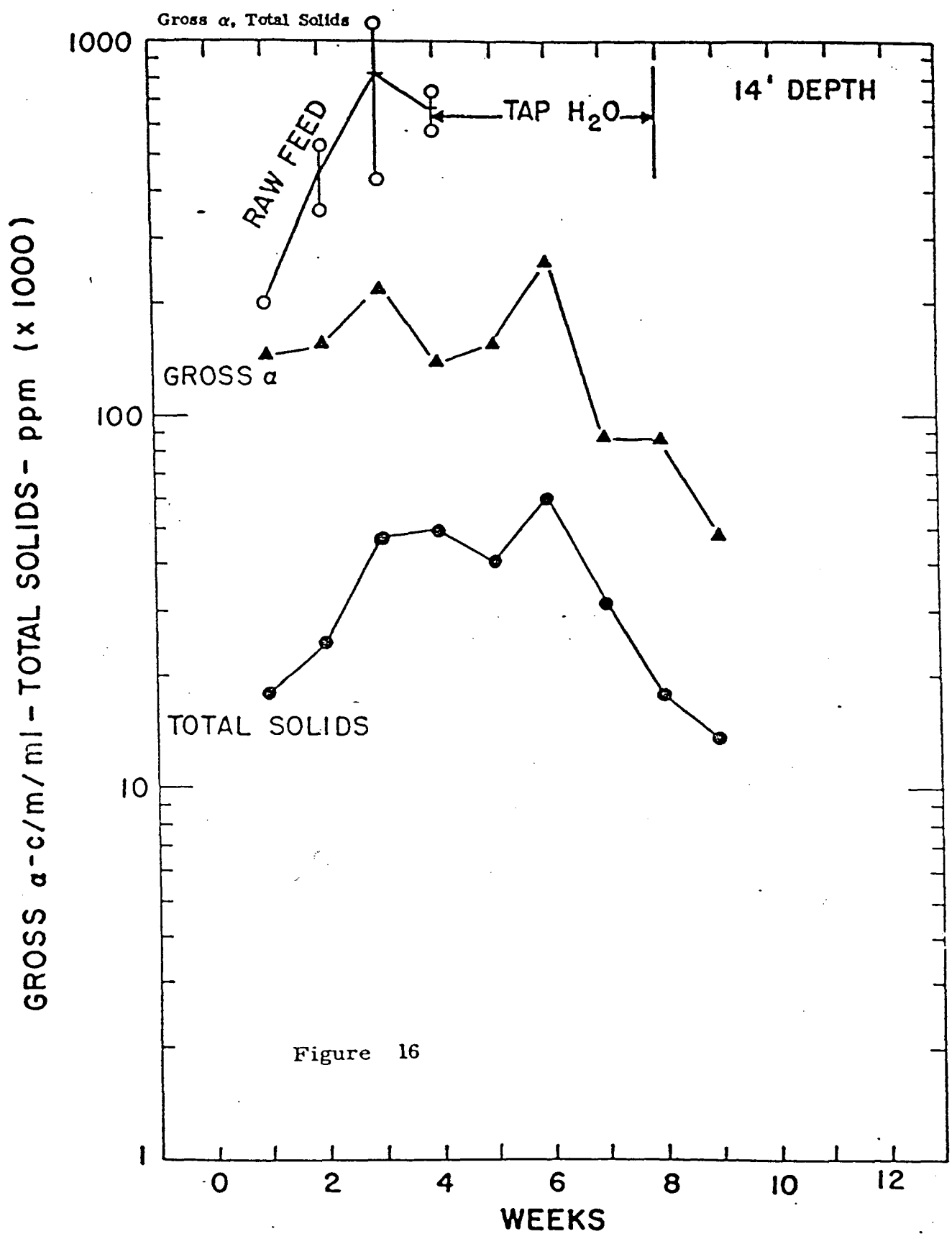


Figure 16

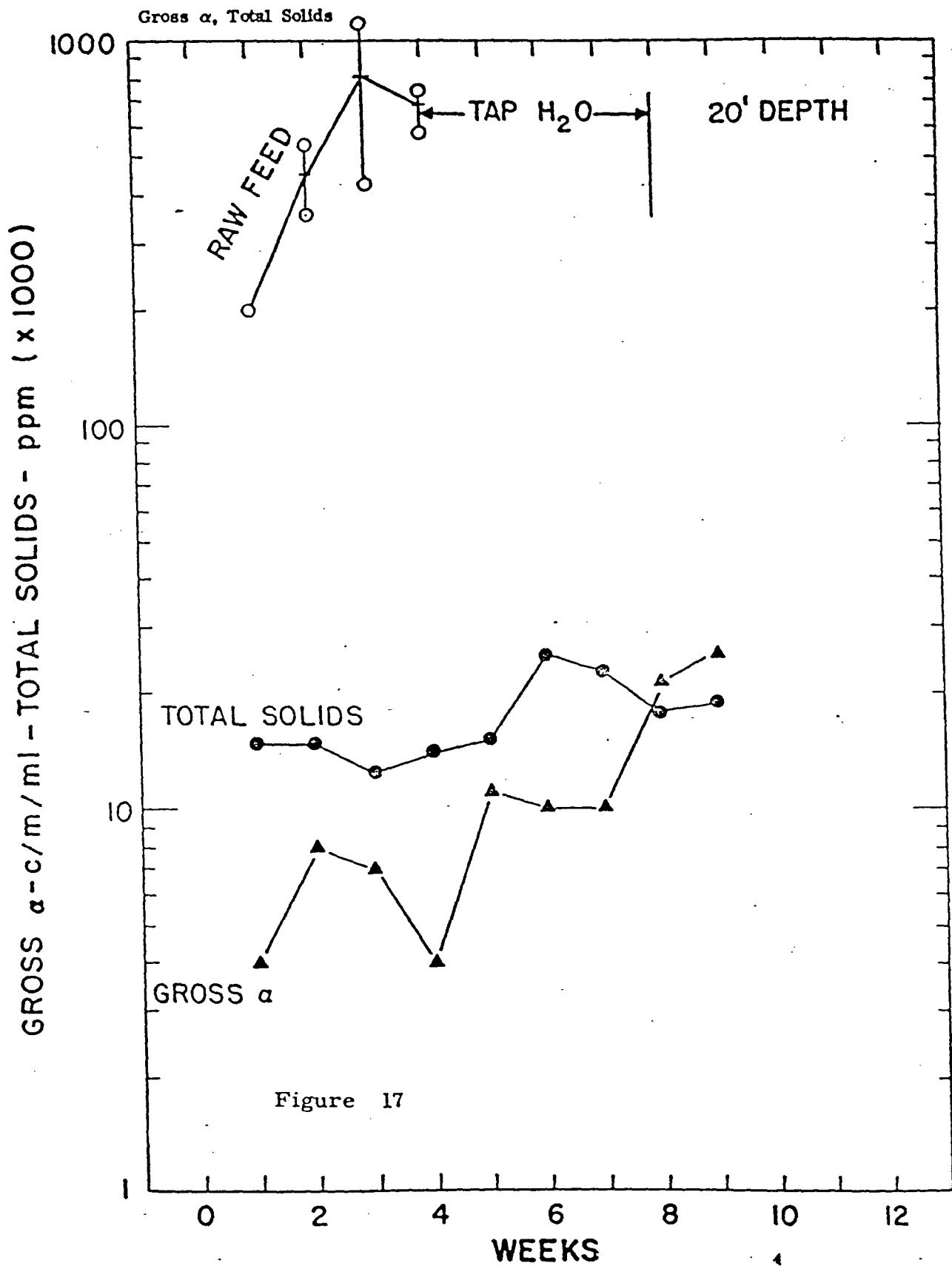


Figure 17

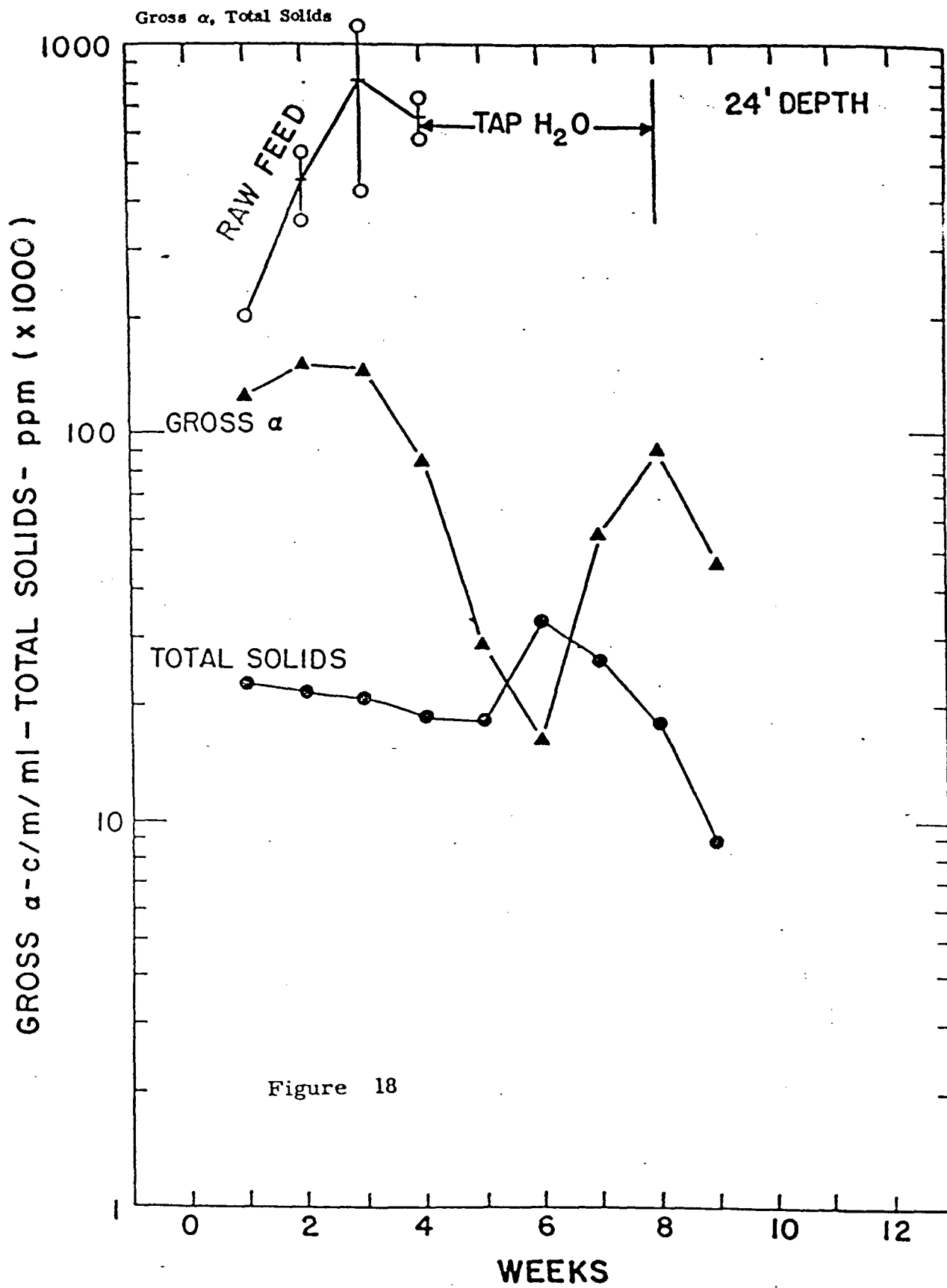


Figure 18

APPENDIX C

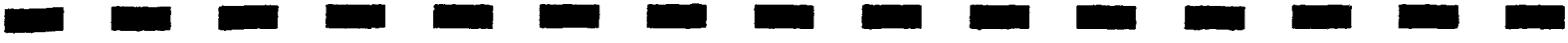
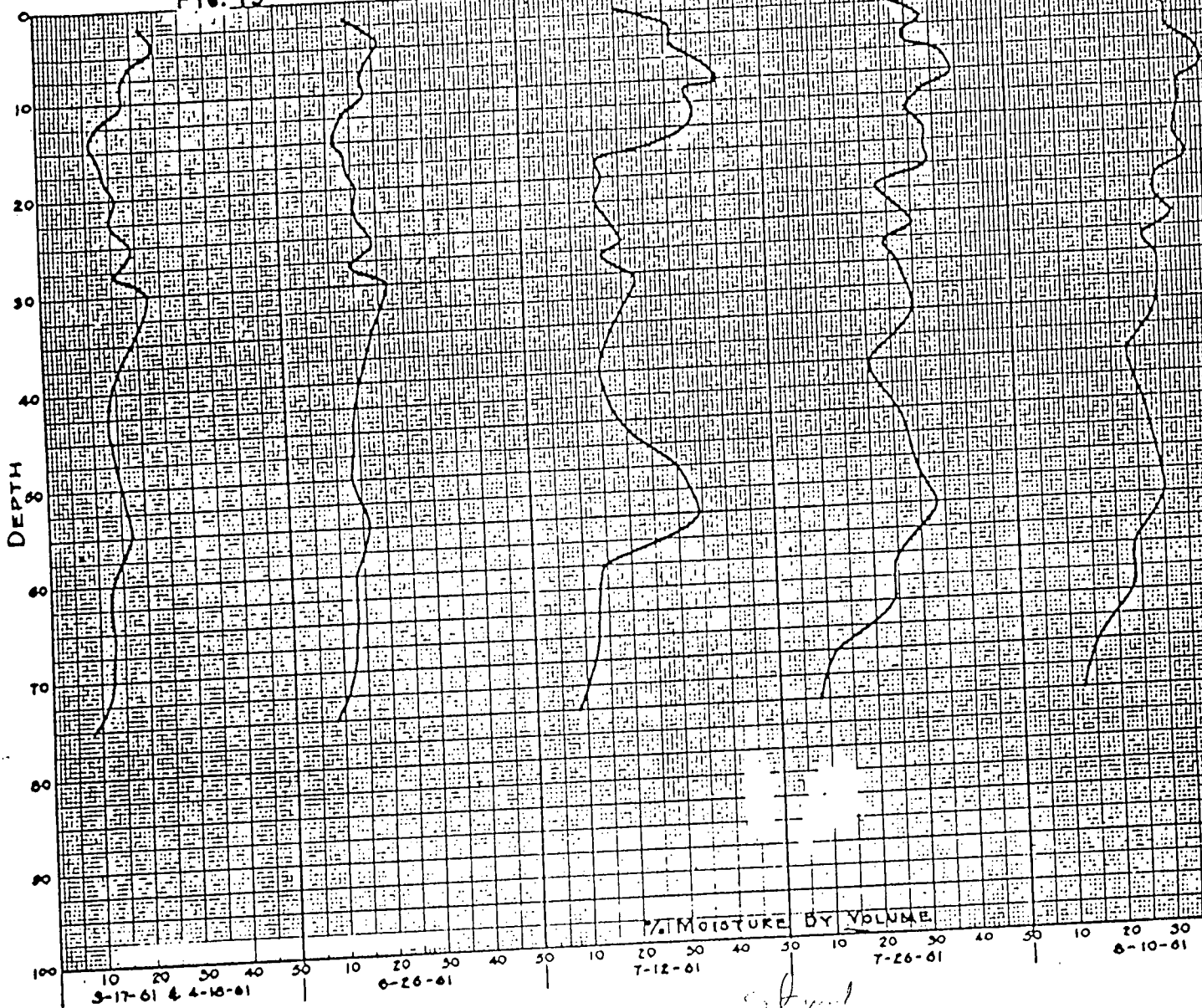


FIG. 19

DP WEST

TEST HOLE #1

MOISTURE DATA



- 275 -

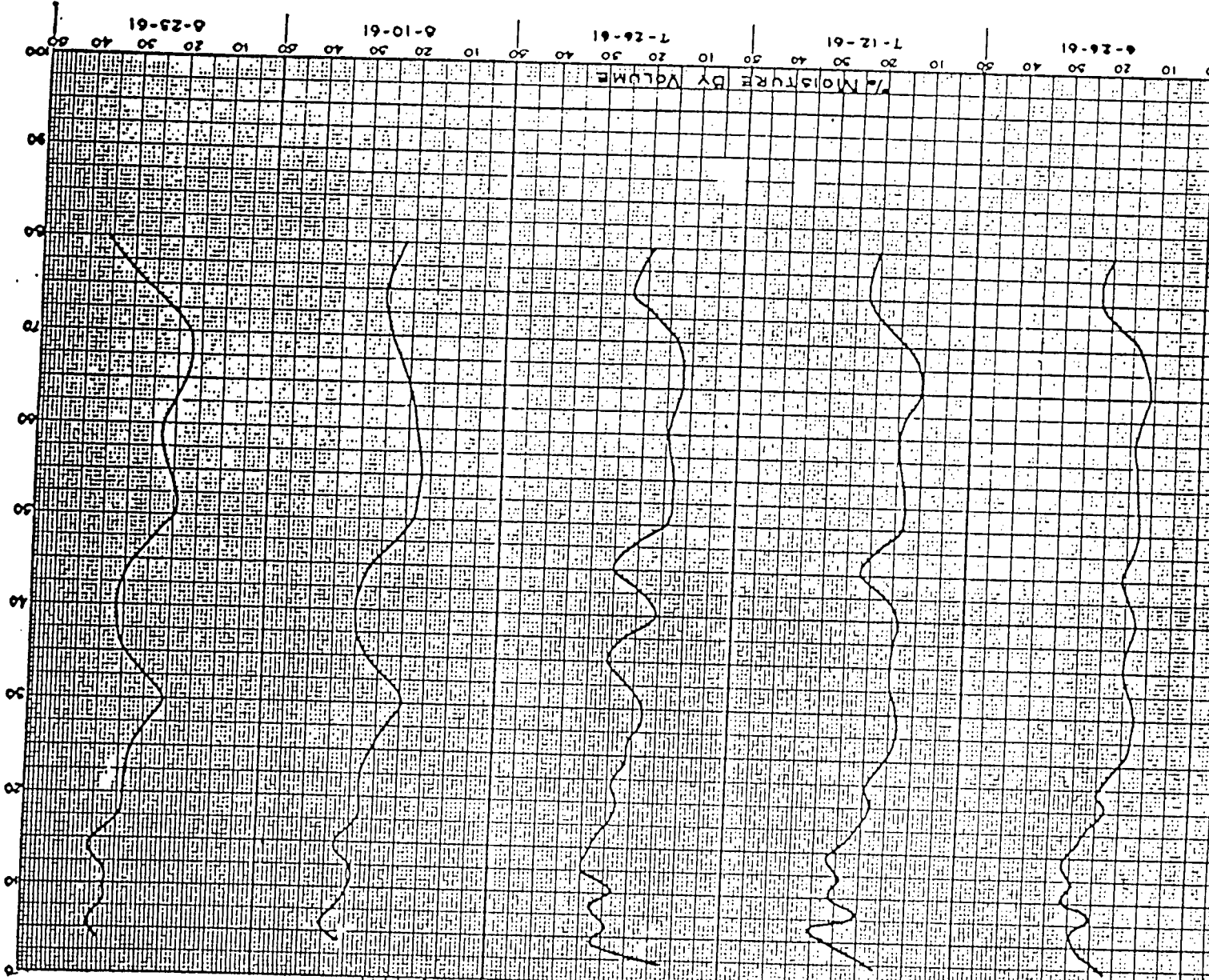


FIG. 21

DP WEST

TEST HOLE #2

MOISTURE DATA

-277-

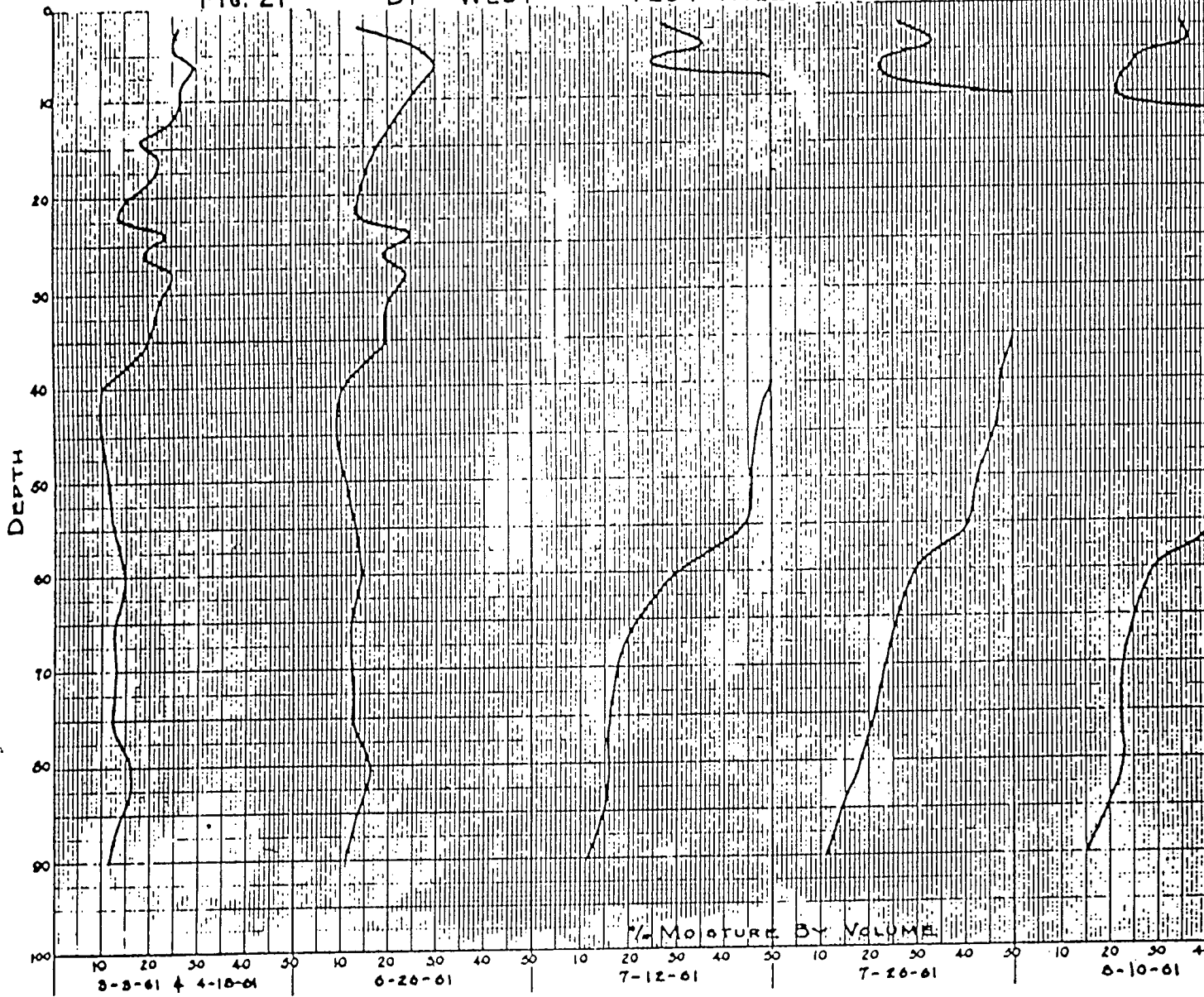
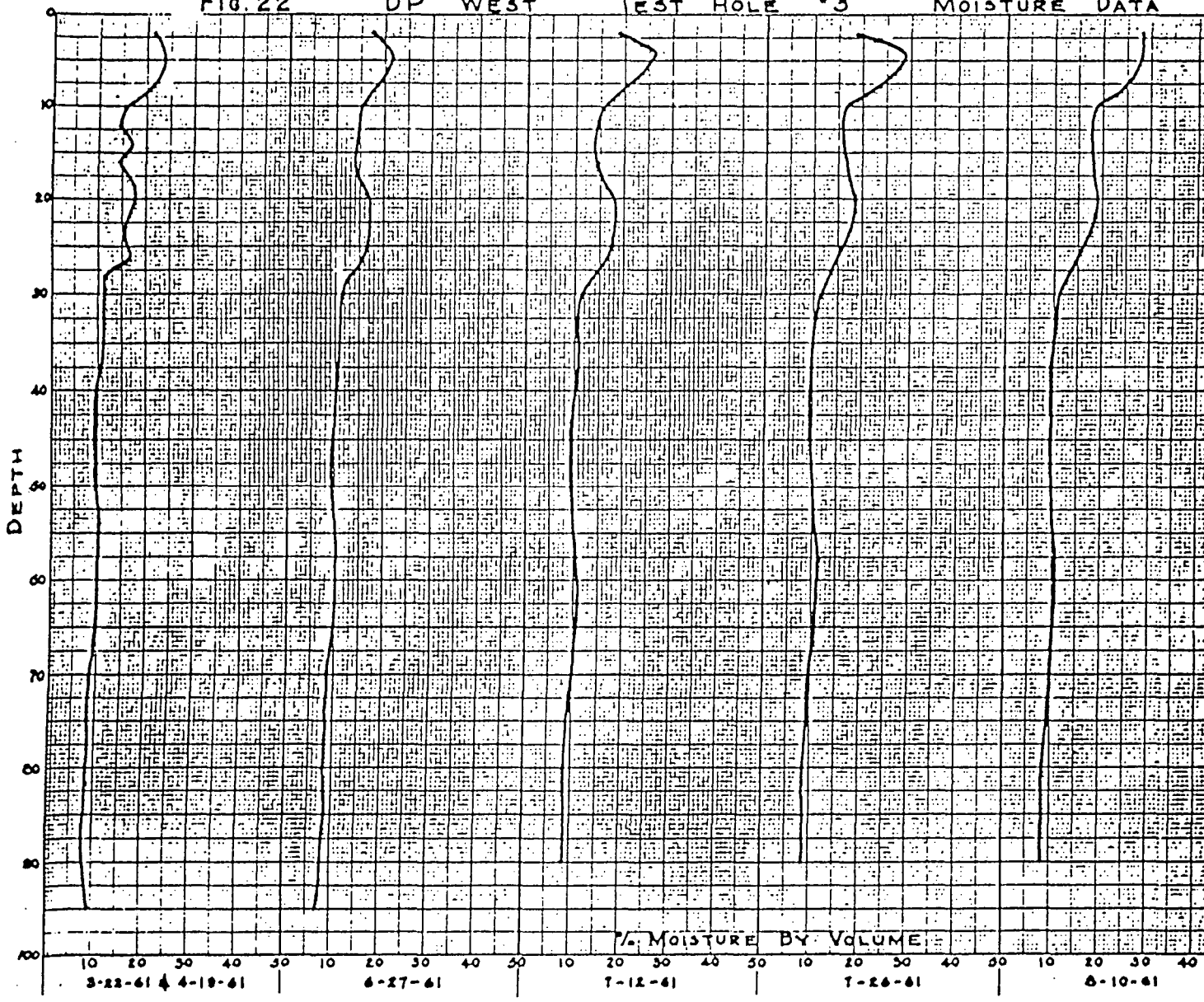


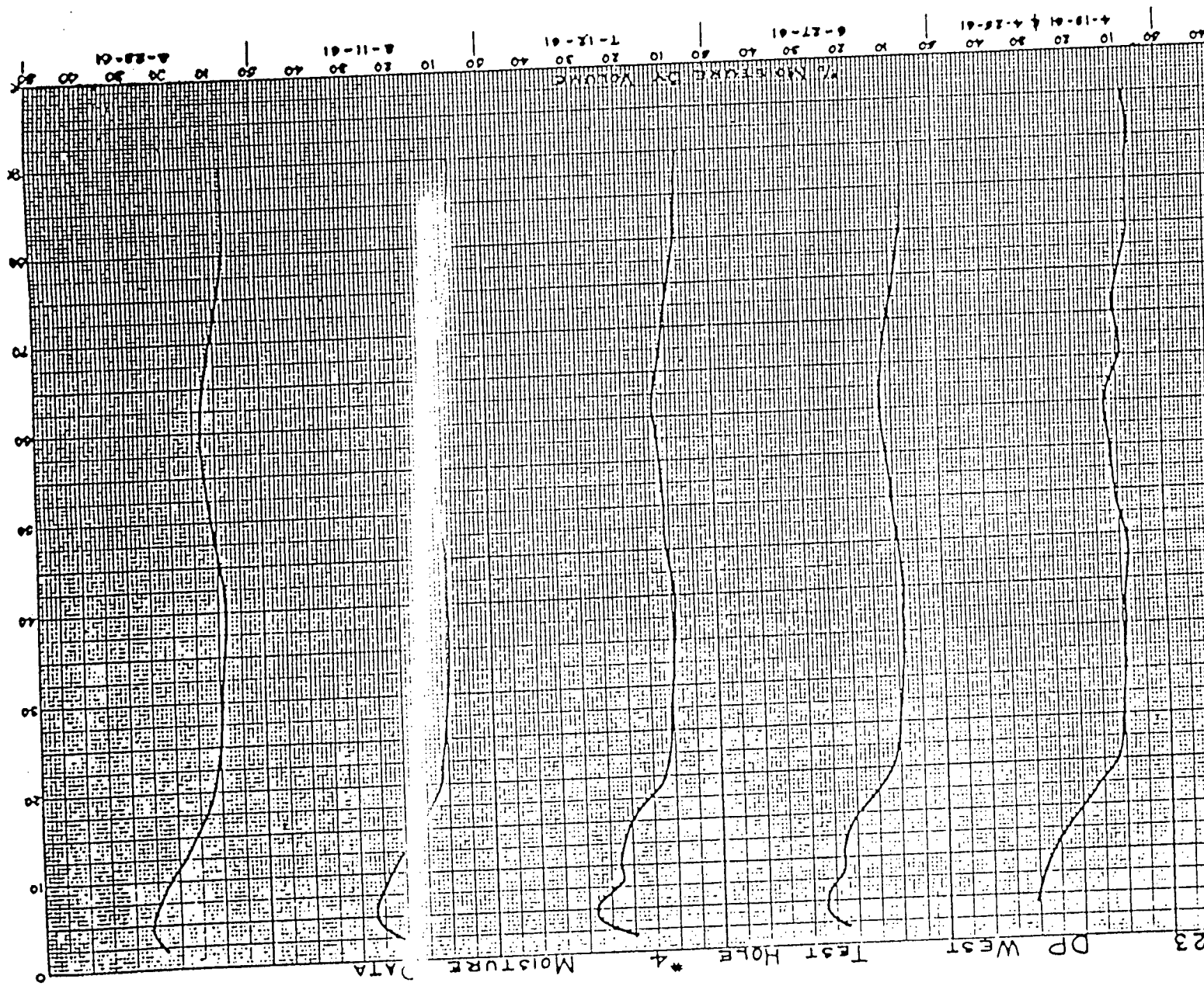
FIG. 22

DP WEST

TEST HOLE #3

MOISTURE DATA





APPENDIX D

\*\*\*\*\*  
 \*  
 \* NON-LINEAR LEAST SQUARES ANALYSIS  
 \*  
 \* Bandelier Tuff (VAN, GENUCHTEN, 1978)  
 \*  
 \*\*\*\*\*

INPUT PARAMETERS  
 =====

MODEL NUMBER..... 2  
 NUMBER OF OBSERVATIONS..... 14  
 SATURATED MOISTURE CONTENT..... 1.0000  
 SATURATED HYDRAULIC CONDUCTIVITY..... 25.4670

OBSERVED DATA  
 =====

OBS. NO.	PRESSURE (MPa)	Saturation	
		MOISTURE CONTENT	WEIGHT
1	79.54	0.0170	1.00
2	20.39	0.0830	1.00
3	11.73	0.1500	1.00
4	8.36	0.2170	1.00
5	6.12	0.2830	1.00
6	4.89	0.3500	1.00
7	4.18	0.4170	1.00
8	3.67	0.4830	1.00
9	3.36	0.5500	1.00
10	2.96	0.6170	1.00
11	2.55	0.6830	1.00
12	2.04	0.7500	1.00
13	1.33	0.9170	1.00
14	0.10	0.9830	1.00

PSI 2. 155

$\psi$   $\Sigma \omega$

$k_{rw}$   
REL K

PR. HEAD	WE	REL K	ABS K	DIFFUS
0.000E+00	1.0000	0.100E+01	0.254E+02	
0.141E+01	0.8592	0.271E+00	0.688E+01	0.385E+02
0.168E+01	0.8104	0.195E+00	0.496E+01	0.265E+02
0.200E+01	0.7512	0.131E+00	0.333E+01	0.179E+02
0.237E+01	0.6831	0.818E-01	0.208E+01	0.119E+02
0.282E+01	0.6089	0.475E-01	0.121E+01	0.773E+01
0.335E+01	0.5326	0.257E-01	0.653E+00	0.496E+01
0.396E+01	0.4580	0.131E-01	0.333E+00	0.315E+01
0.473E+01	0.3882	0.635E-02	0.161E+00	0.198E+01
0.562E+01	0.3254	0.296E-02	0.751E-01	0.124E+01
0.668E+01	0.2705	0.134E-02	0.339E-01	0.768E+00
0.794E+01	0.2234	0.590E-03	0.150E-01	0.475E+00
0.944E+01	0.1838	0.256E-03	0.651E-02	0.294E+00
0.112E+02	0.1508	0.110E-03	0.280E-02	0.151E+00
0.133E+02	0.1236	0.469E-04	0.119E-02	0.111E+00
0.158E+02	0.1013	0.199E-04	0.505E-03	0.695E-01
0.188E+02	0.0830	0.839E-05	0.213E-03	0.421E-01
0.224E+02	0.0681	0.353E-05	0.897E-04	0.238E-01
0.266E+02	0.0560	0.148E-05	0.376E-04	0.139E-01
0.316E+02	0.0462	0.622E-06	0.153E-04	0.974E-02
0.376E+02	0.0382	0.261E-06	0.663E-05	0.598E-02
0.447E+02	0.0317	0.109E-06	0.278E-05	0.367E-02
0.531E+02	0.0264	0.458E-07	0.116E-05	0.226E-02
0.631E+02	0.0221	0.192E-07	0.488E-06	0.139E-02
0.750E+02	0.0187	0.804E-08	0.204E-06	0.851E-03
0.891E+02	0.0159	0.337E-08	0.855E-07	0.522E-03
0.106E+03	0.0136	0.141E-08	0.358E-07	0.321E-03
0.126E+03	0.0118	0.590E-09	0.150E-07	0.197E-03
0.150E+03	0.0103	0.247E-09	0.628E-08	0.121E-03
0.178E+03	0.0091	0.103E-09	0.263E-08	0.742E-04
0.211E+03	0.0081	0.433E-10	0.110E-08	0.455E-04
0.251E+03	0.0073	0.181E-10	0.460E-09	0.279E-04
0.299E+03	0.0066	0.759E-11	0.193E-09	0.172E-04
0.355E+03	0.0061	0.318E-11	0.807E-10	0.105E-04
0.422E+03	0.0057	0.133E-11	0.338E-10	0.646E-05
0.501E+03	0.0054	0.556E-12	0.141E-10	0.397E-05
0.596E+03	0.0051	0.233E-12	0.592E-11	0.244E-05
0.708E+03	0.0049	0.975E-13	0.248E-11	0.150E-05
0.841E+03	0.0047	0.408E-13	0.104E-11	0.918E-06
0.100E+04	0.0045	0.171E-13	0.434E-12	0.563E-06
0.119E+04	0.0044	0.715E-14	0.182E-12	0.346E-06
0.141E+04	0.0043	0.299E-14	0.760E-13	0.212E-06
0.168E+04	0.0042	0.125E-14	0.318E-13	0.130E-06
0.200E+04	0.0042	0.524E-15	0.133E-13	0.800E-07
0.237E+04	0.0041	0.219E-15	0.557E-14	0.491E-07
0.282E+04	0.0041	0.919E-16	0.233E-14	0.301E-07
0.335E+04	0.0040	0.385E-16	0.977E-15	0.185E-07
0.398E+04	0.0040	0.161E-16	0.409E-15	0.114E-07
0.473E+04	0.0040	0.674E-17	0.171E-15	0.697E-08
0.562E+04	0.0040	0.282E-17	0.716E-16	0.428E-08
0.668E+04	0.0040	0.118E-17	0.300E-16	0.263E-08
0.794E+04	0.0039	0.494E-18	0.125E-16	0.161E-08

ITERATION NO	SSQ	RWC	PHA	BETA
0	0.2377693	0.2000	1.0000	2.0000
1	0.1498743	0.0882	0.4963	1.8383
2	0.0248870	0.0032	0.4259	2.1152
3	0.0205523	0.0040	0.4249	2.2071
4	0.0205365	0.0038	0.4236	2.2163
5	0.0205365	0.0037	0.4234	2.2166
6	0.0205365	0.0038	0.4234	2.2168
7	0.0205365	0.0039	0.4234	2.2173
8	0.0205365	0.0039	0.4234	2.2173
9	0.0205365	0.0039	0.4234	2.2173
10	0.0205365	0.0039	0.4234	2.2173
11	0.0205365	0.0039	0.4234	2.2173

CORRELATION MATRIX

	1	2	3
1	1.0000		
2	-0.1873	1.0000	
3	0.7571	-0.6956	1.0000

NON-LINEAR LEAST-SQUARES ANALYSIS: FINAL RESULTS

VARIABLE	VALUE	S.E. COEFF.	T-VALUE	95% CONFIDENCE LOWER
RWC	0.00389	0.0417	0.09	-0.0379
ALPHA	0.42340	0.0307	13.81	0.3589
BETA	2.21721	0.1940	11.43	1.7902

OBSERVED AND FITTED WATER CONTENT

NO	PR. HEAD	OBS	FITTED	RESI-DUAL
1	79.540	0.017	0.018	-0.001
2	20.390	0.083	0.076	0.007
3	11.730	0.150	0.143	0.007
4	8.360	0.217	0.211	0.006
5	6.120	0.283	0.297	-0.014
6	4.890	0.350	0.376	-0.026
7	4.180	0.417	0.438	-0.021
8	3.670	0.483	0.493	-0.010
9	3.360	0.550	0.531	0.019
10	2.960	0.617	0.587	0.030
11	2.550	0.683	0.652	0.031
12	2.040	0.750	0.743	0.007
13	1.330	0.817	0.874	-0.057
14	0.102	0.883	0.999	-0.116

SSQ  
↓

0.944E+04	0.0039	0.207E-18	0.525E-17	0.990E-09
0.112E+05	0.0039	0.866E-19	0.220E-17	0.608E-09
0.133E+05	0.0039	0.362E-19	0.920E-18	0.373E-09
0.158E+05	0.0039	0.152E-19	0.385E-18	0.229E-09
0.188E+05	0.0039	0.635E-20	0.161E-18	0.141E-09
0.224E+05	0.0039	0.266E-20	0.675E-19	0.663E-10
0.266E+05	0.0039	0.111E-20	0.263E-19	0.530E-10
0.316E+05	0.0039	0.466E-21	0.118E-19	0.325E-10
0.376E+05	0.0039	0.195E-21	0.495E-20	0.200E-10
0.447E+05	0.0039	0.816E-22	0.207E-20	0.123E-10
0.531E+05	0.0039	0.341E-22	0.867E-21	0.752E-11
0.631E+05	0.0039	0.143E-22	0.363E-21	0.462E-11
0.750E+05	0.0039	0.598E-23	0.152E-21	0.283E-11
0.891E+05	0.0039	0.290E-23	0.639E-22	0.176E-11
0.106E+06	0.0039	0.105E-23	0.247E-22	0.107E-11
0.128E+06	0.0039	0.449E-24	0.117E-22	0.414E-12
0.150E+06	0.0039	0.184E-24	0.467E-23	0.403E-12
0.178E+06	0.0039	0.769E-25	0.186E-23	0.247E-12
0.211E+06	0.0039	0.322E-25	0.817E-24	0.102E-12
0.251E+06	0.0039	0.133E-25	0.342E-24	0.931E-13
0.298E+06	0.0039	0.564E-25	0.143E-24	0.872E-13
0.353E+06	0.0039	0.236E-25	0.643E-24	0.572E-13
0.422E+06	0.0039	0.988E-27	0.251E-25	0.215E-13
0.501E+06	0.0039	0.413E-27	0.105E-25	0.132E-13

APPENDIX E

```
C*****
C PROGRAM TRAPEZ.FOR CALCULATES THE AREA UNDER A CURVE USING THE
C TRAPEZOIDAL METHOD. DEVELOPED BY GGA FOR LOS ALAMOS PROJECT
C 07/05/89
C NOTE: INPUT IS ANTILOG/LINEAR FORMAT (X,Y)
C*****
```

```
DIMENSION POINTS(50,50)
CHARACTER*11 CHAR, FILE1, FILE2
ITRAP=1
IOUT=2
```

```
C...
WRITE(*,*) ' ENTER INPUT FILENAME : '
READ(*,1) FILE1
WRITE(*,*) ' ENTER OUTPUT FILENAME : '
READ(*,1) FILE2
```

```
C... OPEN FILES
OPEN(UNIT=ITRAP, FILE=FILE1, STATUS='UNKNOWN')
OPEN(UNIT=IOUT, FILE=FILE2, STATUS='UNKNOWN')
```

```
C... READ FILE INTO ARRAY
READ(ITRAP, '(I5)') NUMPT
WRITE(IOUT,8) FILE1
WRITE(IOUT,9)
```

```
8 FORMAT('FILENAME = ',A11)
9 FORMAT(/1X, ' CONC. PL ',4X, ' DEPTH ')
DO 10 I=1, NUMPT
```

```
READ(ITRAP, '(2F10.2)') XPOINT, YPOINT
XPOINT=10**XPOINT
POINTS(I,1)=XPOINT
POINTS(I,2)=YPOINT
WRITE(*,11) POINTS(I,1), POINTS(I,2)
WRITE(IOUT,11) POINTS(I,1), POINTS(I,2)
11 FORMAT(/1X, F12.2, 2X, F10.2)
```

```
10 CONTINUE
SUM=0.0
```

```
DO 20 I=1, NUMPT-1
X1=POINTS(I,1)
Y1=POINTS(I,2)
X2=POINTS(I+1,1)
Y2=POINTS(I+1,2)
DELTA=(X2-X1)*((Y1+Y2)/2)
SUM=SUM+DELTA
```

```
20 CONTINUE
AREA=ABS(SUM)
WRITE(*,21) AREA
WRITE(IOUT,21) AREA
```

```
1 FORMAT(A11)
21 FORMAT(/1X, 'THE AREA UNDER THE CURVE IS',E12.4)
CLOSE(UNIT=ITRAP)
CLOSE(UNIT=IOUT)
END
```

FILENAME = PLUTH1.DAT

CONC. PL	DEPTH
10.23	2.68
6456.54	2.90
38904.53	3.12
8912.51	3.29
6309.57	3.48
1949.84	3.50
2511.89	3.78
1288.25	3.89
870.96	4.35
645.65	4.40
1621.81	4.60
2691.54	4.74
5888.44	4.83
2041.74	4.98
660.69	5.39
1000.00	5.56
851.14	5.77
9120.11	5.87
426.58	5.99
2187.76	6.39
331.13	6.56
275.42	6.93
245.47	6.96
371.54	7.19
144.54	7.38
138.04	7.53
251.19	7.72
263.03	7.90

151.36	8.19
912.01	8.42
2454.71	8.55
1819.70	8.81
5888.44	9.15
20892.97	9.22
31622.78	9.46
10715.20	9.64
8709.64	9.82
2089.30	9.96
2511.89	10.39
1318.26	10.38
1258.93	10.65
562.34	10.80
977.24	10.87
812.83	11.20
501.19	11.29
524.81	11.39
794.33	11.54
660.69	11.74
645.65	11.87
1071.52	12.00
741.31	12.11
275.42	12.14
302.00	12.25
309.03	12.38
288.40	12.77
154.88	12.93
141.25	13.13
165.96	13.21

177.83	13.31
181.97	13.60
257.04	13.67
302.00	13.86
144.54	14.00
151.36	14.34
125.89	14.64
109.65	14.78
112.20	14.98
58.88	15.25
64.57	15.44
100.00	15.60
34.67	15.74
109.65	15.88
51.29	16.15
69.18	16.32
52.48	16.58
338.84	16.67
52.48	16.74
74.13	16.99
72.44	17.19
19.05	17.48
95.50	17.59
165.96	17.89
616.59	18.07
162.18	18.20
120.23	18.37
173.78	18.64
61.66	19.04
120.23	19.20

89.13	19.31
173.78	19.45
19.50	19.78
19.05	19.97
81.28	20.23
19.50	20.39
19.50	20.55
407.38	20.83
549.54	21.01
1778.28	21.12
281.84	21.27
446.68	21.46
74.13	21.65
63.10	21.85
173.78	22.07
104.71	22.25
85.11	22.31
109.65	22.91
64.57	23.24
61.66	23.39
134.90	23.47
134.90	23.61
97.72	23.83
95.50	24.05
46.77	24.31
107.15	24.41
83.18	24.59
131.83	25.02
85.11	25.21
123.03	25.60

89.13	26.33
109.65	26.39
53.70	26.69
43.65	27.05
41.69	27.16
69.18	27.32
28.18	27.49
44.67	27.64
19.50	27.95
18.62	28.22
42.66	28.40
19.05	28.62
19.50	29.92

THE AREA UNDER THE CURVE IS 0.7139E+07

FILENAME = PLUTH2.DAT

CONC. PL	DEPTH
10.00	0.05
18.62	0.07
18.62	1.36
512.86	1.60
426.58	3.02
18.20	3.40
30.20	3.55
18.62	3.71
18.62	5.89
33.88	6.05
19.05	6.16
19.05	7.64
75.86	7.78
19.05	7.94
19.05	8.22
77.62	8.59
16.22	8.71
3467.37	9.18
275.42	9.27
223.87	9.36
54.95	9.63
37.15	9.82
66.07	10.20
19.50	10.48
19.50	11.23
151.36	11.63
28.18	11.91
45.71	12.07

18.62	12.21
39.81	12.35
41.69	12.50
38.02	12.65
51.29	12.76
35.48	12.90
38.02	13.08
19.05	13.25
19.50	13.54
34.67	13.77
19.05	13.90
31.62	14.06
19.05	14.27
19.05	14.43
9.33	14.41

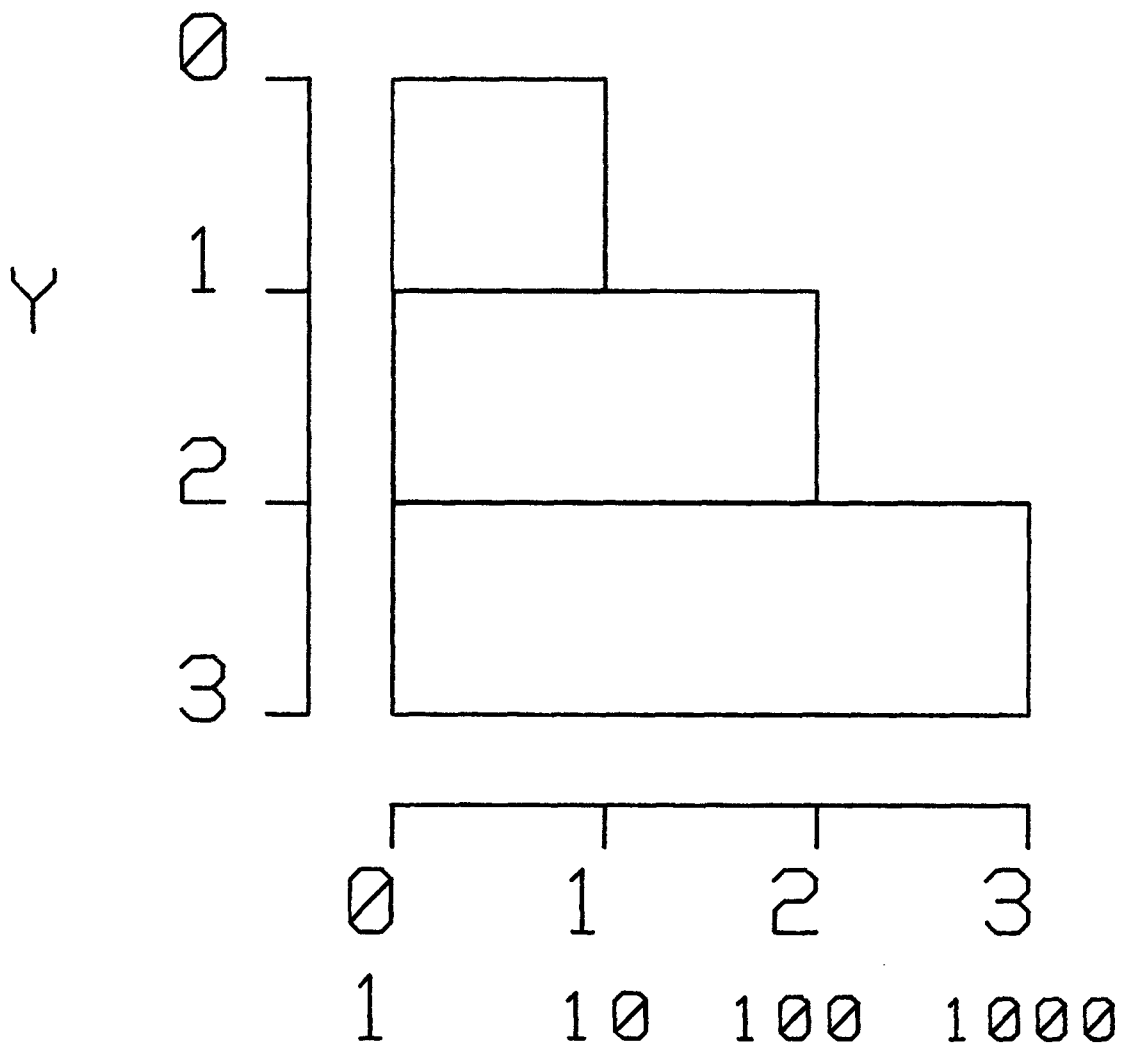
THE AREA UNDER THE CURVE IS 0.2070E+04

FILENAME = TEST.DAT

CONC. PL	DEPTH
1.00	0.00
10.00	0.00
10.00	-1.00
100.00	-1.00
100.00	-2.00
1000.00	-2.00
1000.00	-3.00
1.00	-3.00

THE AREA UNDER THE CURVE IS 0.1107E+04

# TEST PROBLEM



APPENDIX F



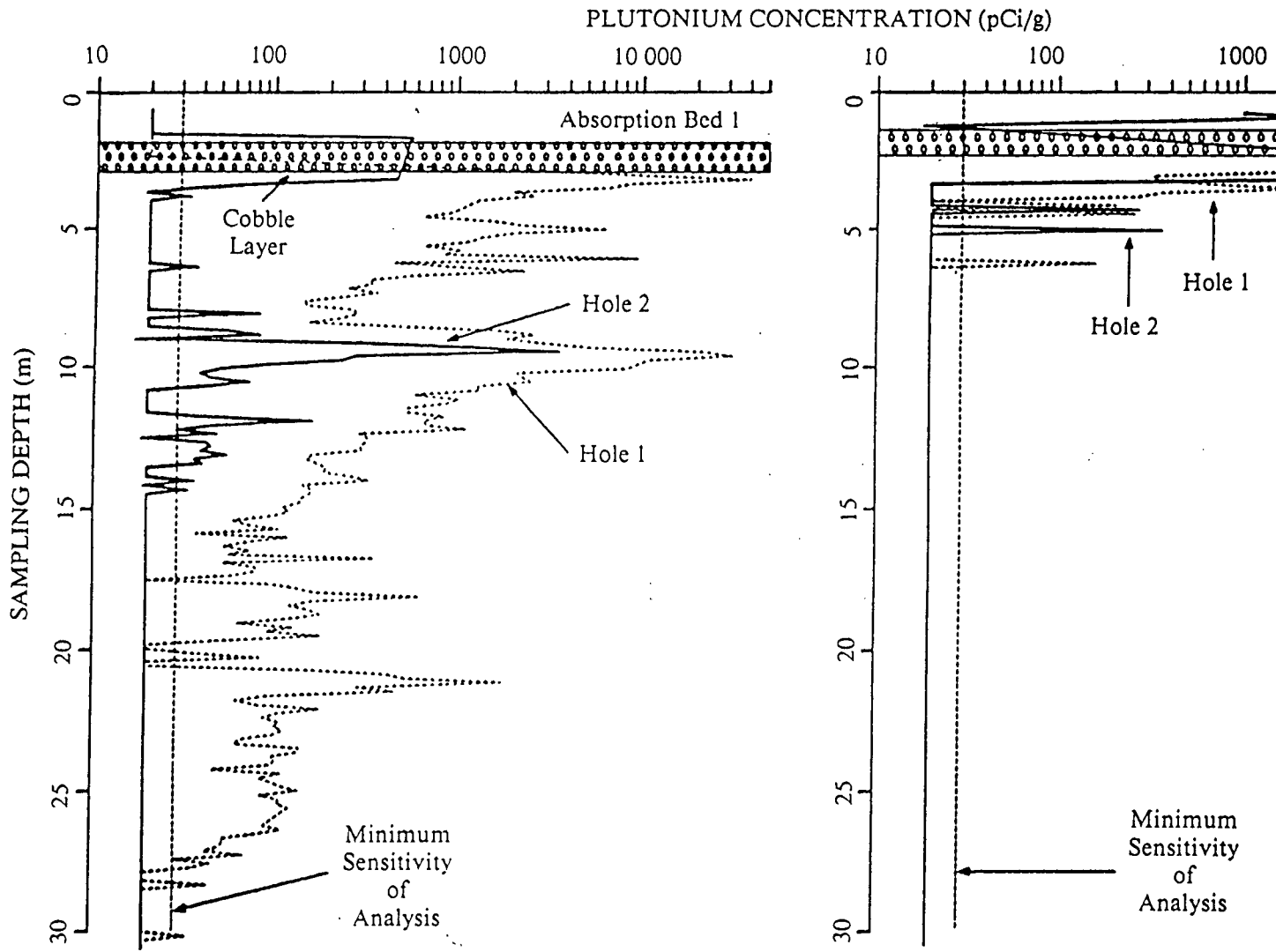


Fig. 3. Concentration of plutonium as a function of sampling depth for absorption beds 1 and 2 in 1978.

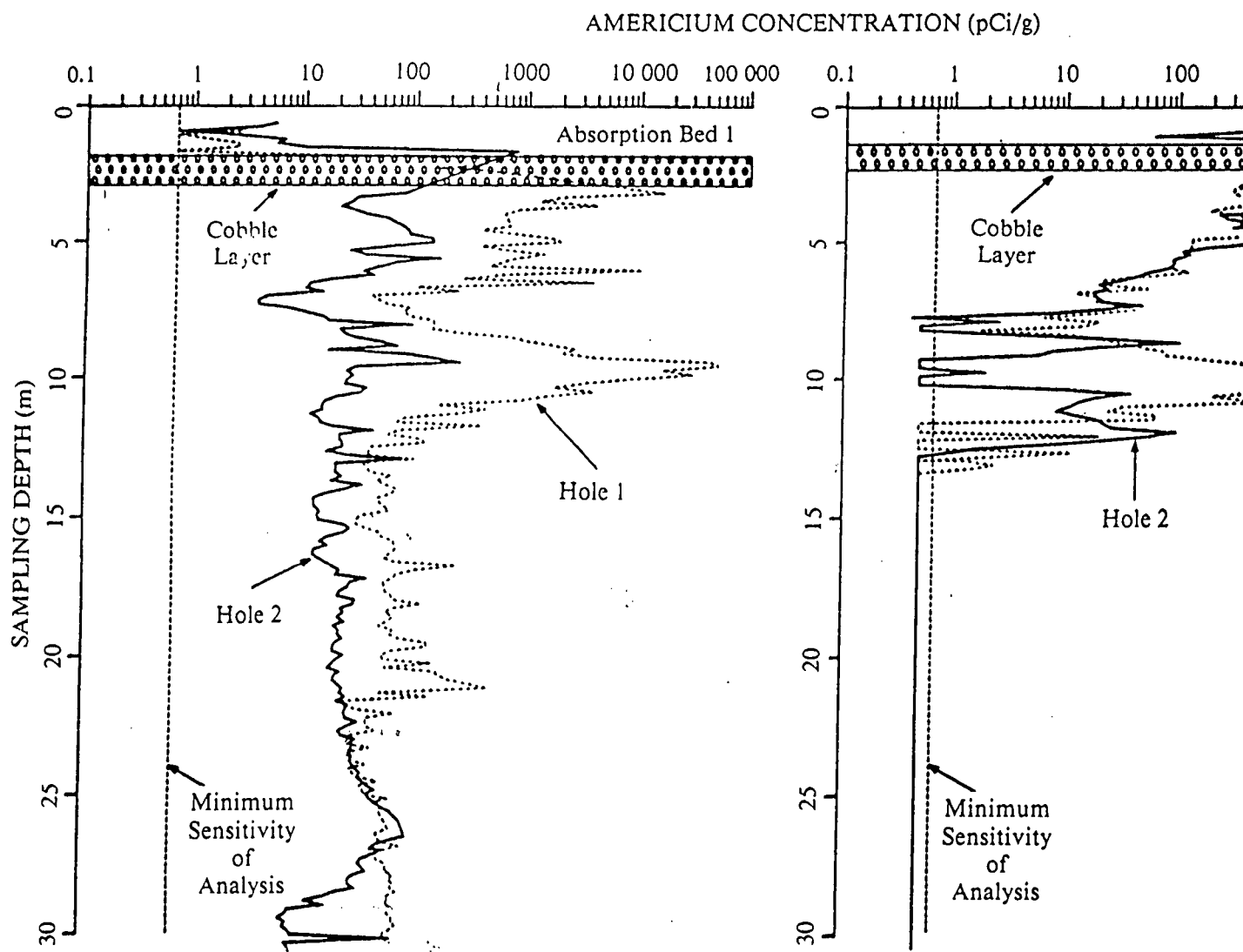


Fig. 4. Concentration of  $^{241}\text{Am}$  as a function of sampling depth for absorption beds 1 and 2 in 1978.

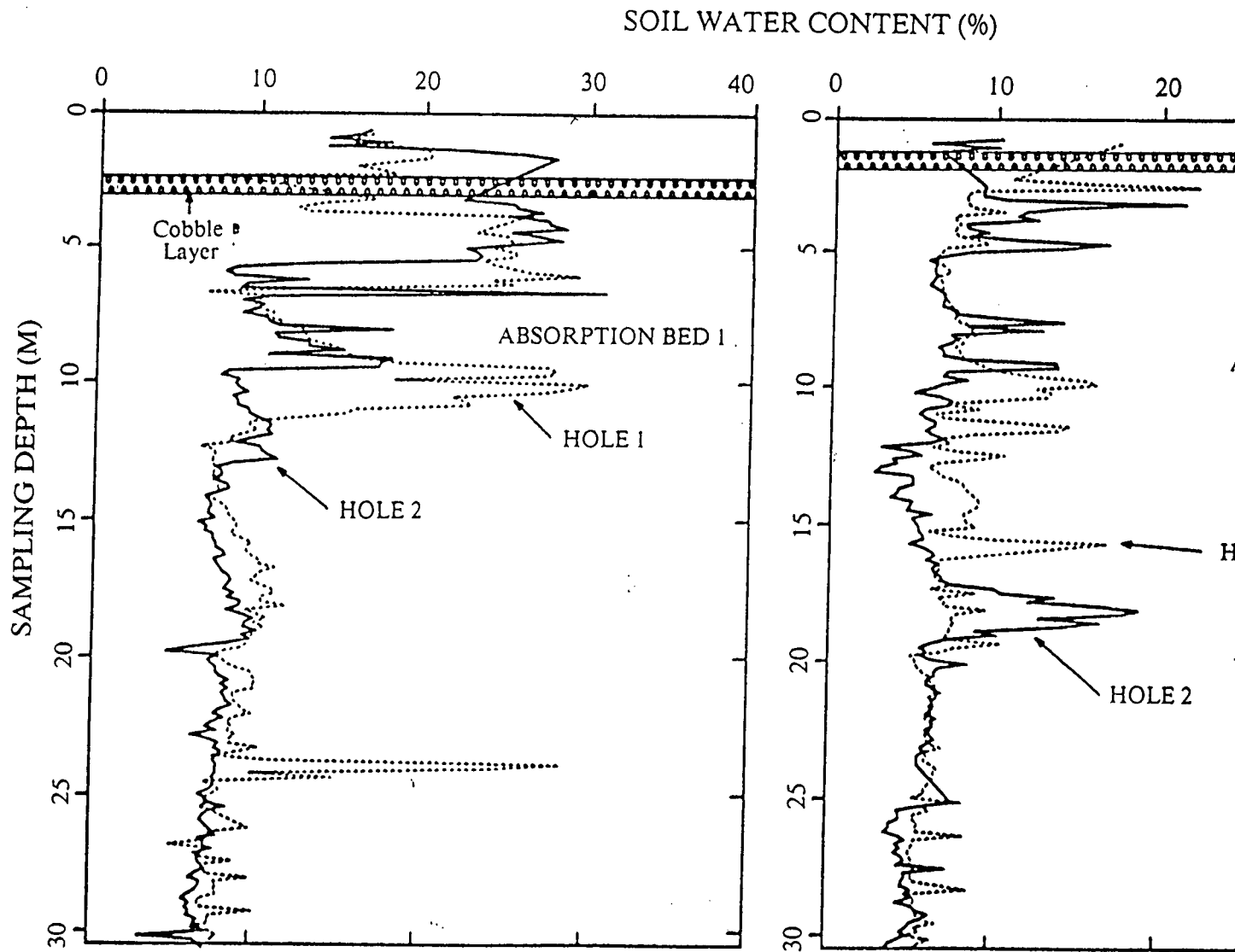


Fig. 5. Gravimetric soil water content as a function of sampling depth for absorption beds 1 and 2 in 1978.

*Gravimetric > 1.55 = volumetric*

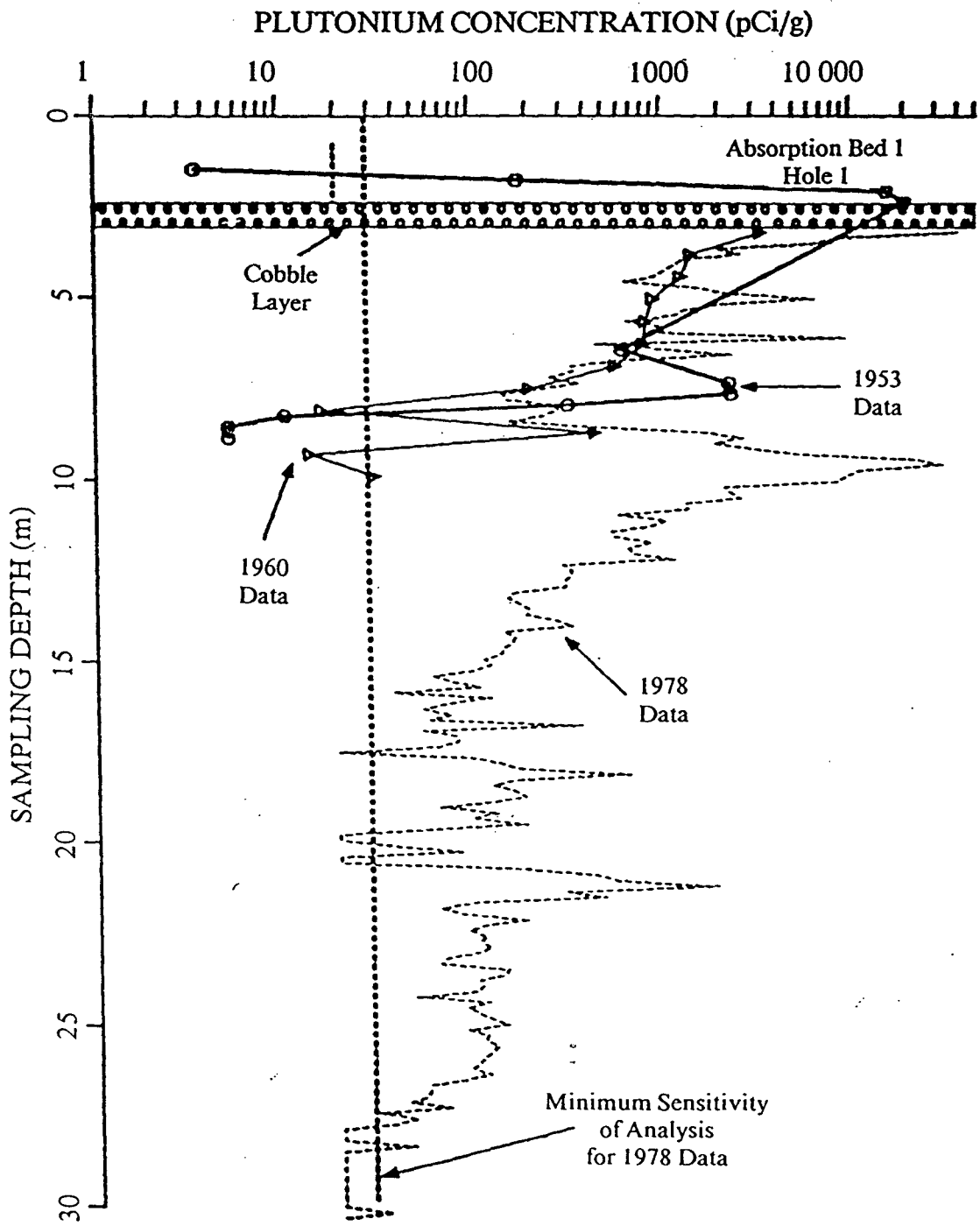


Fig. 6. Concentration of plutonium as a function of sampling depth in absorption bed 1 found in 1953 (Herman 1954), 1960 (Christenson and Thomas 1962), and in our study in 1978.

APPENDIX G



This data corresponds with figure 5.2.

DEPTH (meters)	CONCENTRATION			
	1949	1961	1978	1990
0.0050	0.0130	0.0470	0.0540	0.0540
3.5000	0.0000	0.0010	0.0010	0.0010

This data corresponds with figure 5.3.

DEPTH (meters)	CONCENTRATION			
	1949	1961	1978	1990
0.0000	0.0060	0.0200	0.0230	0.0230
3.5000	0.0000	0.0000	0.0000	0.0000

This data corresponds with figure 5.4.

DEPTH (meters)	CONCENTRATION			
	1949	1961	1978	1990
0.0000	0.0040	0.0130	0.0150	0.0150
3.5000	0.0000	0.0000	0.0000	0.0000

This data corresponds with figure 5.5.

DEPTH (meters)	CONCENTRATION			
	1949	1961	1978	1990
0.000	74.987	52.937	31.815	31.799
1.000	31.421	78.883	60.710	60.688
2.000	9.636	66.239	64.543	64.534
3.000	2.305	43.356	50.881	50.888
4.000	0.450	24.390	33.221	33.237
5.000	0.074	12.188	18.941	18.957
6.000	0.011	5.478	9.683	9.695
7.000	0.001	2.230	4.500	4.508
8.000	0.000	0.827	1.917	1.922
9.000	0.000	0.281	0.753	0.756
10.000	0.000	0.088	0.274	0.275
11.000	0.000	0.026	0.093	0.093
12.000	0.000	0.007	0.029	0.030
13.000	0.000	0.002	0.009	0.009
14.000	0.000	0.000	0.002	0.002
15.000	0.000	0.000	0.001	0.001
16.000	0.000	0.000	0.000	0.000
17.000	0.000	0.000	0.000	0.000
18.000	0.000	0.000	0.000	0.000
19.000	0.000	0.000	0.000	0.000
20.000	0.000	0.000	0.000	0.000

This data corresponds with figure 5.6.

DEPTH (meters)	CONCENTRATION			
	1949	1961	1978	1990
0.000	47.831	60.121	42.276	42.260
1.000	9.879	49.356	47.690	47.685
2.000	1.407	22.724	27.573	27.579
3.000	0.152	7.967	11.543	11.549
4.000	0.013	2.312	3.915	3.919
5.000	0.001	0.574	1.131	1.132
6.000	0.000	0.125	0.286	0.286
7.000	0.000	0.024	0.064	0.064
8.000	0.000	0.004	0.013	0.013
9.000	0.000	0.001	0.002	0.002
10.000	0.000	0.000	0.000	0.000

This data corresponds with figure 5.7.

DEPTH (meters)	CONCENTRATION			
	1949	1961	1978	1990
0.000	17.884	40.435	35.323	35.316
3.500	1.109	10.389	12.154	12.156
7.000	0.046	1.531	2.233	2.235
10.500	0.001	0.168	0.297	0.298
14.000	0.000	0.015	0.032	0.032
17.500	0.000	0.001	0.003	0.003

This data corresponds with figure 5.8.

DEPTH (meters)	CONCENTRATION			
	1949	1961	1978	1990
0.000	12.832	32.016	29.067	29.063
3.500	0.553	5.711	6.883	6.884
7.000	0.016	0.588	0.881	0.882
10.500	0.000	0.045	0.082	0.082
14.000	0.000	0.003	0.006	0.006
17.500	0.000	0.000	0.000	0.000

This data corresponds with figure 5.9.

DEPTH (meters)	CONCENTRATION			
	1949	1961	1978	1990
0.000	96.311	36.695	19.188	19.176
1.000	65.130	76.486	44.572	44.543
2.000	36.063	96.237	68.446	68.407
3.000	16.569	94.685	82.061	82.029
4.000	6.437	81.196	83.156	83.143
5.000	2.154	63.846	74.770	74.780
6.000	0.631	47.024	61.529	61.557
7.000	0.164	32.665	47.227	47.266
8.000	0.038	21.428	34.177	34.219
9.000	0.008	13.270	23.448	23.488
10.000	0.002	7.758	15.292	15.327
11.000	0.000	4.284	9.493	9.521
12.000	0.000	2.237	5.615	5.635
13.000	0.000	1.106	3.166	3.181
14.000	0.000	0.518	1.705	1.714
15.000	0.000	0.231	0.877	0.883
16.000	0.000	0.098	0.432	0.435
17.000	0.000	0.040	0.204	0.205
18.000	0.000	0.015	0.092	0.093
19.000	0.000	0.006	0.040	0.041
20.000	0.000	0.002	0.017	0.017
21.000	0.000	0.001	0.007	0.007
22.000	0.000	0.000	0.003	0.003
23.000	0.000	0.000	0.001	0.001
24.000	0.000	0.000	0.000	0.000
25.000	0.000	0.000	0.000	0.000

This data corresponds with figure 5.10.

DEPTH (meters)	CONCENTRATION			
	1949	1961	1978	1990
0.000	105.079	27.056	12.312	12.301
1.000	83.692	61.797	29.899	29.875
2.000	58.351	91.385	51.980	51.946
3.000	35.446	106.413	73.130	73.093
4.000	18.825	107.370	88.257	88.228
5.000	8.809	99.182	94.938	94.922
6.000	3.666	86.495	93.600	93.597
7.000	1.369	72.288	86.330	86.339
8.000	0.463	58.217	75.573	75.588
9.000	0.143	45.213	63.378	63.396
10.000	0.041	33.822	51.190	51.209
11.000	0.011	24.334	39.924	39.942
12.000	0.003	16.821	30.093	30.110
13.000	0.001	11.164	21.924	21.938
14.000	0.000	7.114	15.435	15.447
15.000	0.000	4.354	10.500	10.508
16.000	0.000	2.560	6.900	6.907
17.000	0.000	1.448	4.382	4.387
18.000	0.000	0.788	2.690	2.693
19.000	0.000	0.413	1.597	1.599
20.000	0.000	0.209	0.918	0.919
21.000	0.000	0.102	0.511	0.511
22.000	0.000	0.048	0.275	0.276
23.000	0.000	0.022	0.144	0.144
24.000	0.000	0.010	0.073	0.073
25.000	0.000	0.004	0.036	0.036
26.000	0.000	0.002	0.017	0.017
27.000	0.000	0.001	0.008	0.008
28.000	0.000	0.000	0.004	0.004
29.000	0.000	0.000	0.002	0.002
30.000	0.000	0.000	0.001	0.001
31.000	0.000	0.000	0.000	0.000
32.000	0.000	0.000	0.000	0.000
33.000	0.000	0.000	0.000	0.000
34.000	0.000	0.000	0.000	0.000
35.000	0.000	0.000	0.000	0.000
36.000	0.000	0.000	0.000	0.000
37.000	0.000	0.000	0.000	0.000
38.000	0.000	0.000	0.000	0.000
39.000	0.000	0.000	0.000	0.000
40.000	0.000	0.000	0.000	0.000
41.000	0.000	0.000	0.000	0.000
42.000	0.000	0.000	0.000	0.000
43.000	0.000	0.000	0.000	0.000
44.000	0.000	0.000	0.000	0.000
45.000	0.000	0.000	0.000	0.000
46.000	0.000	0.000	0.000	0.000
47.000	0.000	0.000	0.000	0.000
48.000	0.000	0.000	0.000	0.000
49.000	0.000	0.000	0.000	0.000
50.000	0.000	0.000	0.000	0.000
51.000	0.000	0.000	0.000	0.000

52.000	0.000	0.000	0.000	0.000
53.000	0.000	0.000	0.000	0.000
54.000	0.000	0.000	0.000	0.000
55.000	0.000	0.000	0.000	0.000
56.000	0.000	0.000	0.000	0.000
57.000	0.000	0.000	0.000	0.000
58.000	0.000	0.000	0.000	0.000
59.000	0.000	0.000	0.000	0.000
60.000	0.000	0.000	0.000	0.000
61.000	0.000	0.000	0.000	0.000
62.000	0.000	0.000	0.000	0.000
63.000	0.000	0.000	0.000	0.000
64.000	0.000	0.000	0.000	0.000
65.000	0.000	0.000	0.000	0.000
66.000	0.000	0.000	0.000	0.000
67.000	0.000	0.000	0.000	0.000
68.000	0.000	0.000	0.000	0.000
69.000	0.000	0.000	0.000	0.000
70.000	0.000	0.000	0.000	0.000
71.000	0.000	0.000	0.000	0.000
72.000	0.000	0.000	0.000	0.000
73.000	0.000	0.000	0.000	0.000
74.000	0.000	0.000	0.000	0.000
75.000	0.000	0.000	0.000	0.000
76.000	0.000	0.000	0.000	0.000
77.000	0.000	0.000	0.000	0.000
78.000	0.000	0.000	0.000	0.000
79.000	0.000	0.000	0.000	0.000
80.000	0.000	0.000	0.000	0.000
81.000	0.000	0.000	0.000	0.000
82.000	0.000	0.000	0.000	0.000
83.000	0.000	0.000	0.000	0.000
84.000	0.000	0.000	0.000	0.000
85.000	0.000	0.000	0.000	0.000
86.000	0.000	0.000	0.000	0.000
87.000	0.000	0.000	0.000	0.000
88.000	0.000	0.000	0.000	0.000
89.000	0.000	0.000	0.000	0.000
90.000	0.000	0.000	0.000	0.000
91.000	0.000	0.000	0.000	0.000
92.000	0.000	0.000	0.000	0.000
93.000	0.000	0.000	0.000	0.000
94.000	0.000	0.000	0.000	0.000
95.000	0.000	0.000	0.000	0.000
96.000	0.000	0.000	0.000	0.000
97.000	0.000	0.000	0.000	0.000
98.000	0.000	0.000	0.000	0.000
99.000	0.000	0.000	0.000	0.000
100.000	0.000	0.000	0.000	0.000

This data corresponds with figure 5.11.

DEPTH (meters)	CONCENTRATION			
	1949	1961	1978	1990
0.000	47.831	60.120	42.275	42.259
1.000	9.879	49.356	47.690	47.685
2.000	1.407	22.724	27.574	27.579
3.000	0.152	7.967	11.543	11.549
4.000	0.013	2.312	3.915	3.919
5.000	0.001	0.574	1.131	1.132
6.000	0.000	0.125	0.286	0.286
7.000	0.000	0.024	0.064	0.064
8.000	0.000	0.004	0.013	0.013
9.000	0.000	0.001	0.002	0.002
10.000	0.000	0.000	0.000	0.000

This data corresponds with figure 5.12.

DEPTH (meters)	CONCENTRATION			
	1949	1961	1978	1990
0.000	25.512	49.687	40.965	40.954
3.500	2.373	19.111	21.348	21.350
7.000	0.148	4.182	5.848	5.852
10.500	0.007	0.685	1.160	1.162
14.000	0.000	0.091	0.185	0.186
17.500	0.000	0.010	0.025	0.025
21.000	0.000	0.001	0.003	0.003
24.500	0.000	0.000	0.000	0.000

This data corresponds with figure 5.13.

DEPTH (meters)	SATURATION			
	1949	1961	1978	1990
0.000	0.797	0.712	0.120	0.107
1.000	0.797	0.712	0.124	0.109
2.000	0.797	0.712	0.128	0.111
3.000	0.797	0.712	0.132	0.113
4.000	0.797	0.712	0.136	0.115
5.000	0.797	0.712	0.139	0.117
6.000	0.797	0.712	0.143	0.119
7.000	0.797	0.712	0.146	0.121
8.000	0.797	0.712	0.150	0.123
9.000	0.797	0.712	0.153	0.125
10.000	0.797	0.712	0.156	0.127
11.000	0.796	0.712	0.159	0.129
12.000	0.796	0.712	0.162	0.131
13.000	0.796	0.712	0.164	0.133
14.000	0.795	0.712	0.167	0.135
15.000	0.795	0.712	0.170	0.136
16.000	0.795	0.712	0.172	0.138
17.000	0.795	0.712	0.175	0.140
18.000	0.795	0.712	0.177	0.141
19.000	0.796	0.712	0.180	0.143
20.000	0.797	0.712	0.182	0.145
21.000	0.798	0.712	0.184	0.146
22.000	0.800	0.712	0.186	0.148
23.000	0.801	0.712	0.189	0.149
24.000	0.802	0.712	0.191	0.151
25.000	0.803	0.712	0.193	0.152
26.000	0.803	0.712	0.195	0.154
27.000	0.803	0.712	0.197	0.155
28.000	0.802	0.712	0.199	0.156
29.000	0.800	0.712	0.201	0.158
30.000	0.798	0.712	0.203	0.159
31.000	0.795	0.712	0.205	0.161
32.000	0.793	0.712	0.206	0.162
33.000	0.791	0.712	0.208	0.163
34.000	0.789	0.712	0.210	0.164
35.000	0.789	0.712	0.212	0.166
36.000	0.789	0.712	0.213	0.167
37.000	0.790	0.712	0.215	0.168
38.000	0.792	0.712	0.217	0.169
39.000	0.794	0.712	0.218	0.171
40.000	0.797	0.712	0.220	0.172
41.000	0.799	0.712	0.222	0.173
42.000	0.801	0.712	0.223	0.174
43.000	0.803	0.712	0.225	0.175
44.000	0.804	0.712	0.226	0.176
45.000	0.804	0.712	0.228	0.178
46.000	0.803	0.712	0.229	0.179
47.000	0.802	0.712	0.231	0.180
48.000	0.801	0.712	0.232	0.181
49.000	0.799	0.712	0.234	0.182
50.000	0.797	0.712	0.235	0.183
51.000	0.795	0.712	0.237	0.184

0.185	0.238	0.712	0.794	52.000
0.186	0.239	0.712	0.793	53.000
0.187	0.241	0.712	0.793	54.000
0.188	0.242	0.712	0.793	55.000
0.189	0.244	0.712	0.793	56.000
0.190	0.245	0.712	0.794	57.000
0.191	0.246	0.712	0.795	58.000
0.192	0.248	0.712	0.796	59.000
0.193	0.249	0.712	0.798	60.000
0.194	0.250	0.713	0.799	61.000
0.195	0.251	0.713	0.799	62.000
0.196	0.253	0.713	0.800	63.000
0.197	0.254	0.713	0.800	64.000
0.198	0.255	0.713	0.800	65.000
0.198	0.256	0.712	0.799	66.000
0.199	0.258	0.711	0.799	67.000
0.200	0.259	0.709	0.798	68.000
0.201	0.260	0.706	0.797	69.000
0.202	0.261	0.702	0.796	70.000
0.203	0.262	0.696	0.795	71.000
0.204	0.263	0.687	0.795	72.000
0.205	0.265	0.675	0.795	73.000
0.205	0.266	0.661	0.795	74.000
0.206	0.267	0.642	0.795	75.000
0.207	0.268	0.621	0.795	76.000
0.208	0.269	0.597	0.795	77.000
0.209	0.270	0.572	0.796	78.000
0.210	0.271	0.547	0.796	79.000
0.210	0.272	0.525	0.797	80.000
0.211	0.273	0.506	0.797	81.000
0.212	0.274	0.492	0.798	82.000
0.213	0.276	0.481	0.798	83.000
0.214	0.277	0.473	0.799	84.000
0.214	0.278	0.468	0.799	85.000
0.215	0.279	0.465	0.799	86.000
0.216	0.280	0.462	0.799	87.000
0.217	0.281	0.461	0.798	88.000
0.217	0.282	0.460	0.798	89.000
0.218	0.283	0.460	0.798	90.000
0.219	0.284	0.460	0.797	91.000
0.220	0.285	0.460	0.797	92.000
0.220	0.286	0.460	0.797	93.000
0.221	0.287	0.460	0.797	94.000
0.222	0.288	0.461	0.796	95.000
0.222	0.289	0.461	0.796	96.000
0.223	0.289	0.461	0.796	97.000
0.223	0.290	0.462	0.796	98.000
0.223	0.290	0.462	0.796	99.000
0.223	0.290	0.462	0.796	100.000

This data corresponds with figure 5.14.

DEPTH (meters)	SATURATION			
	1949	1961	1978	1990
0.000	0.797	0.712	0.124	0.11
3.500	0.797	0.712	0.139	0.117
7.000	0.797	0.712	0.151	0.125
10.500	0.797	0.712	0.162	0.131
14.000	0.797	0.712	0.172	0.138
17.500	0.797	0.712	0.180	0.144
21.000	0.797	0.712	0.188	0.149
24.500	0.797	0.712	0.196	0.155
28.000	0.797	0.712	0.203	0.159
31.500	0.797	0.712	0.209	0.164
35.000	0.797	0.712	0.215	0.168
38.500	0.797	0.712	0.221	0.173
42.000	0.797	0.712	0.226	0.177
45.500	0.797	0.712	0.232	0.181
49.000	0.797	0.712	0.237	0.184
52.500	0.797	0.712	0.242	0.188
56.000	0.797	0.711	0.246	0.191
59.500	0.797	0.709	0.251	0.195
63.000	0.797	0.704	0.255	0.198
66.500	0.797	0.692	0.259	0.201
70.000	0.797	0.670	0.263	0.204
73.500	0.797	0.637	0.267	0.207
77.000	0.797	0.594	0.271	0.210
80.500	0.797	0.549	0.275	0.213
84.000	0.797	0.511	0.279	0.216
87.500	0.797	0.488	0.282	0.218
91.000	0.797	0.476	0.286	0.221
94.500	0.797	0.471	0.289	0.223
98.000	0.797	0.470	0.293	0.226
101.500	0.797	0.471	0.296	0.228
105.000	0.797	0.473	0.299	0.231
108.500	0.796	0.475	0.302	0.233
112.000	0.796	0.477	0.305	0.235
115.500	0.796	0.480	0.308	0.238
119.000	0.796	0.483	0.311	0.240
122.500	0.795	0.486	0.314	0.242
126.000	0.794	0.489	0.317	0.244
129.500	0.794	0.492	0.320	0.246
133.000	0.793	0.495	0.323	0.249
136.500	0.792	0.498	0.325	0.251
140.000	0.790	0.501	0.328	0.253
143.500	0.787	0.504	0.331	0.255
147.000	0.780	0.507	0.333	0.257
150.500	0.764	0.509	0.336	0.259
154.000	0.720	0.512	0.338	0.260
157.500	0.598	0.515	0.341	0.262
161.000	0.340	0.518	0.343	0.264
164.500	0.121	0.521	0.346	0.266
168.000	0.098	0.523	0.348	0.268
171.500	0.098	0.526	0.350	0.270
175.000	0.098	0.528	0.353	0.271
178.500	0.098	0.531	0.355	0.273



This data corresponds with figure 5.15.

DEPTH (meters)	CONCENTRATION			
	1949	1961	1978	1990
0.000	105.079	27.056	12.312	12.301
1.000	83.692	61.797	29.899	29.875
2.000	58.351	91.385	51.980	51.946
3.000	35.446	106.413	73.130	73.093
4.000	18.825	107.370	88.257	88.228
5.000	8.809	99.182	94.938	94.922
6.000	3.666	86.495	93.600	93.597
7.000	1.369	72.288	86.330	86.339
8.000	0.463	58.217	75.573	75.588
9.000	0.143	45.213	63.378	63.396
10.000	0.041	33.822	51.190	51.209
11.000	0.011	24.334	39.924	39.942
12.000	0.003	16.821	30.093	30.110
13.000	0.001	11.164	21.924	21.938
14.000	0.000	7.114	15.435	15.447
15.000	0.000	4.354	10.500	10.508
16.000	0.000	2.560	6.900	6.907
17.000	0.000	1.448	4.382	4.387
18.000	0.000	0.788	2.690	2.693
19.000	0.000	0.413	1.597	1.599
20.000	0.000	0.209	0.918	0.919
21.000	0.000	0.102	0.511	0.511
22.000	0.000	0.048	0.275	0.276
23.000	0.000	0.022	0.144	0.144
24.000	0.000	0.010	0.073	0.073
25.000	0.000	0.004	0.036	0.036
26.000	0.000	0.002	0.017	0.017
27.000	0.000	0.001	0.008	0.008
28.000	0.000	0.000	0.004	0.004
29.000	0.000	0.000	0.002	0.002
30.000	0.000	0.000	0.001	0.001
31.000	0.000	0.000	0.000	0.000
32.000	0.000	0.000	0.000	0.000
33.000	0.000	0.000	0.000	0.000
34.000	0.000	0.000	0.000	0.000
35.000	0.000	0.000	0.000	0.000
36.000	0.000	0.000	0.000	0.000
37.000	0.000	0.000	0.000	0.000
38.000	0.000	0.000	0.000	0.000
39.000	0.000	0.000	0.000	0.000
40.000	0.000	0.000	0.000	0.000
41.000	0.000	0.000	0.000	0.000
42.000	0.000	0.000	0.000	0.000
43.000	0.000	0.000	0.000	0.000
44.000	0.000	0.000	0.000	0.000
45.000	0.000	0.000	0.000	0.000
46.000	0.000	0.000	0.000	0.000
47.000	0.000	0.000	0.000	0.000
48.000	0.000	0.000	0.000	0.000
49.000	0.000	0.000	0.000	0.000
50.000	0.000	0.000	0.000	0.000
51.000	0.000	0.000	0.000	0.000

0.000	0.000	0.000	0.000	52.000
0.000	0.000	0.000	0.000	53.000
0.000	0.000	0.000	0.000	54.000
0.000	0.000	0.000	0.000	55.000
0.000	0.000	0.000	0.000	56.000
0.000	0.000	0.000	0.000	57.000
0.000	0.000	0.000	0.000	58.000
0.000	0.000	0.000	0.000	59.000
0.000	0.000	0.000	0.000	60.000
0.000	0.000	0.000	0.000	61.000
0.000	0.000	0.000	0.000	62.000
0.000	0.000	0.000	0.000	63.000
0.000	0.000	0.000	0.000	64.000
0.000	0.000	0.000	0.000	65.000
0.000	0.000	0.000	0.000	66.000
0.000	0.000	0.000	0.000	67.000
0.000	0.000	0.000	0.000	68.000
0.000	0.000	0.000	0.000	69.000
0.000	0.000	0.000	0.000	70.000
0.000	0.000	0.000	0.000	71.000
0.000	0.000	0.000	0.000	72.000
0.000	0.000	0.000	0.000	73.000
0.000	0.000	0.000	0.000	74.000
0.000	0.000	0.000	0.000	75.000
0.000	0.000	0.000	0.000	76.000
0.000	0.000	0.000	0.000	77.000
0.000	0.000	0.000	0.000	78.000
0.000	0.000	0.000	0.000	79.000
0.000	0.000	0.000	0.000	80.000
0.000	0.000	0.000	0.000	81.000
0.000	0.000	0.000	0.000	82.000
0.000	0.000	0.000	0.000	83.000
0.000	0.000	0.000	0.000	84.000
0.000	0.000	0.000	0.000	85.000
0.000	0.000	0.000	0.000	86.000
0.000	0.000	0.000	0.000	87.000
0.000	0.000	0.000	0.000	88.000
0.000	0.000	0.000	0.000	89.000
0.000	0.000	0.000	0.000	90.000
0.000	0.000	0.000	0.000	91.000
0.000	0.000	0.000	0.000	92.000
0.000	0.000	0.000	0.000	93.000
0.000	0.000	0.000	0.000	94.000
0.000	0.000	0.000	0.000	95.000
0.000	0.000	0.000	0.000	96.000
0.000	0.000	0.000	0.000	97.000
0.000	0.000	0.000	0.000	98.000
0.000	0.000	0.000	0.000	99.000
0.000	0.000	0.000	0.000	100.000

This data corresponds with figure 5.16.

DEPTH (meters)	CONCENTRATION			
	1949	1961	1978	1990
0.000	74.931	52.385	37.156	37.143
1.000	61.777	66.094	47.389	47.371
2.000	48.939	75.649	56.219	56.195
3.000	37.157	80.160	62.955	62.924
4.000	26.987	79.948	67.112	67.079
5.000	18.722	76.102	68.564	68.533
6.000	12.394	69.925	67.513	67.488
7.000	7.825	62.556	64.393	64.380
8.000	4.711	54.821	59.757	59.755
9.000	2.704	47.250	54.163	54.174
10.000	1.481	40.148	48.106	48.129
11.000	0.774	33.671	41.981	42.012
12.000	0.386	27.889	36.070	36.109
13.000	0.184	22.815	30.560	30.603
14.000	0.084	18.431	25.559	25.605
15.000	0.037	14.698	21.116	21.163
16.000	0.015	11.568	17.240	17.286
17.000	0.006	8.982	13.912	13.955
18.000	0.002	6.878	11.096	11.137
19.000	0.001	5.194	8.747	8.785
20.000	0.000	3.867	6.815	6.849
21.000	0.000	2.839	5.247	5.277
22.000	0.000	2.054	3.992	4.018
23.000	0.000	1.465	3.001	3.023
24.000	0.000	1.030	2.228	2.247
25.000	0.000	0.714	1.635	1.650
26.000	0.000	0.488	1.185	1.198
27.000	0.000	0.329	0.848	0.859
28.000	0.000	0.218	0.600	0.608
29.000	0.000	0.143	0.419	0.426
30.000	0.000	0.092	0.289	0.294
31.000	0.000	0.059	0.197	0.201
32.000	0.000	0.037	0.133	0.136
33.000	0.000	0.023	0.089	0.091
34.000	0.000	0.014	0.058	0.060
35.000	0.000	0.008	0.038	0.039
36.000	0.000	0.005	0.024	0.025
37.000	0.000	0.003	0.015	0.016
38.000	0.000	0.002	0.010	0.010
39.000	0.000	0.001	0.006	0.006
40.000	0.000	0.001	0.004	0.004
41.000	0.000	0.000	0.002	0.002
42.000	0.000	0.000	0.001	0.001
43.000	0.000	0.000	0.001	0.001
44.000	0.000	0.000	0.000	0.000
45.000	0.000	0.000	0.000	0.000

This data corresponds with figure 5.17.

DEPTH (meters)	CONCENTRATION			
	1949	1961	1978	1990
0.000	104.864	27.299	12.521	12.511
1.000	83.338	62.271	30.303	30.278
2.000	57.971	91.792	52.354	52.310
3.000	35.106	106.537	73.294	73.238
4.000	18.579	107.161	88.156	88.103
5.000	8.662	98.685	94.634	94.599
6.000	3.590	85.781	93.197	93.189
7.000	1.335	71.432	85.911	85.930
8.000	0.449	57.295	75.181	75.223
9.000	0.138	44.295	63.032	63.090
10.000	0.039	32.966	50.899	50.968
11.000	0.010	23.581	39.692	39.764
12.000	0.002	16.193	29.920	29.990
13.000	0.001	10.668	21.804	21.869
14.000	0.000	6.741	15.358	15.416
15.000	0.000	4.088	10.455	10.503
16.000	0.000	2.379	6.878	6.917
17.000	0.000	1.331	4.374	4.403
18.000	0.000	0.716	2.689	2.711
19.000	0.000	0.370	1.600	1.614
20.000	0.000	0.185	0.921	0.931
21.000	0.000	0.089	0.513	0.520
22.000	0.000	0.041	0.277	0.281
23.000	0.000	0.019	0.145	0.148
24.000	0.000	0.008	0.074	0.075
25.000	0.000	0.003	0.037	0.037
26.000	0.000	0.001	0.018	0.018
27.000	0.000	0.001	0.008	0.008
28.000	0.000	0.000	0.004	0.004
29.000	0.000	0.000	0.002	0.002
30.000	0.000	0.000	0.001	0.001
31.000	0.000	0.000	0.000	0.000
32.000	0.000	0.000	0.000	0.000
33.000	0.000	0.000	0.000	0.000
34.000	0.000	0.000	0.000	0.000
35.000	0.000	0.000	0.000	0.000

This data corresponds with figure 5.18.

DEPTH (meters)	CONCENTRATION			
	1949	1961	1978	1990
0.000	104.837	27.328	12.535	12.525
1.000	83.299	62.322	30.334	30.309
2.000	57.935	91.827	52.399	52.354
3.000	35.079	106.542	73.342	73.283
4.000	18.558	107.135	88.188	88.130
5.000	8.646	98.631	94.636	94.597
6.000	3.580	85.703	93.163	93.154
7.000	1.330	71.335	85.842	85.863
8.000	0.447	57.188	75.083	75.132
9.000	0.137	44.190	62.915	62.983
10.000	0.039	32.872	50.775	50.854
11.000	0.010	23.503	39.569	39.653
12.000	0.002	16.131	29.806	29.888
13.000	0.001	10.621	21.704	21.780
14.000	0.000	6.707	15.275	15.342
15.000	0.000	4.064	10.388	10.444
16.000	0.000	2.364	6.827	6.871
17.000	0.000	1.321	4.336	4.370
18.000	0.000	0.710	2.662	2.687
19.000	0.000	0.367	1.581	1.598
20.000	0.000	0.183	0.909	0.920
21.000	0.000	0.088	0.506	0.513
22.000	0.000	0.041	0.273	0.277
23.000	0.000	0.018	0.143	0.146
24.000	0.000	0.008	0.073	0.074
25.000	0.000	0.003	0.036	0.037
26.000	0.000	0.001	0.017	0.018
27.000	0.000	0.001	0.008	0.008
28.000	0.000	0.000	0.004	0.004
29.000	0.000	0.000	0.002	0.002
30.000	0.000	0.000	0.001	0.001
31.000	0.000	0.000	0.000	0.000
32.000	0.000	0.000	0.000	0.000
33.000	0.000	0.000	0.000	0.000
34.000	0.000	0.000	0.000	0.000
35.000	0.000	0.000	0.000	0.000
36.000	0.000	0.000	0.000	0.000
37.000	0.000	0.000	0.000	0.000
38.000	0.000	0.000	0.000	0.000
39.000	0.000	0.000	0.000	0.000
40.000	0.000	0.000	0.000	0.000
41.000	0.000	0.000	0.000	0.000
42.000	0.000	0.000	0.000	0.000
43.000	0.000	0.000	0.000	0.000
44.000	0.000	0.000	0.000	0.000
45.000	0.000	0.000	0.000	0.000
46.000	0.000	0.000	0.000	0.000
47.000	0.000	0.000	0.000	0.000
48.000	0.000	0.000	0.000	0.000
49.000	0.000	0.000	0.000	0.000
50.000	0.000	0.000	0.000	0.000
51.000	0.000	0.000	0.000	0.000

52.000	0.000	0.000	0.000	0.000
53.000	0.000	0.000	0.000	0.000
54.000	0.000	0.000	0.000	0.000
55.000	0.000	0.000	0.000	0.000
56.000	0.000	0.000	0.000	0.000
57.000	0.000	0.000	0.000	0.000
58.000	0.000	0.000	0.000	0.000
59.000	0.000	0.000	0.000	0.000
60.000	0.000	0.000	0.000	0.000
61.000	0.000	0.000	0.000	0.000
62.000	0.000	0.000	0.000	0.000
63.000	0.000	0.000	0.000	0.000
64.000	0.000	0.000	0.000	0.000
65.000	0.000	0.000	0.000	0.000
66.000	0.000	0.000	0.000	0.000
67.000	0.000	0.000	0.000	0.000
68.000	0.000	0.000	0.000	0.000
69.000	0.000	0.000	0.000	0.000
70.000	0.000	0.000	0.000	0.000
71.000	0.000	0.000	0.000	0.000
72.000	0.000	0.000	0.000	0.000
73.000	0.000	0.000	0.000	0.000
74.000	0.000	0.000	0.000	0.000
75.000	0.000	0.000	0.000	0.000
76.000	0.000	0.000	0.000	0.000
77.000	0.000	0.000	0.000	0.000
78.000	0.000	0.000	0.000	0.000
79.000	0.000	0.000	0.000	0.000
80.000	0.000	0.000	0.000	0.000
81.000	0.000	0.000	0.000	0.000
82.000	0.000	0.000	0.000	0.000
83.000	0.000	0.000	0.000	0.000
84.000	0.000	0.000	0.000	0.000
85.000	0.000	0.000	0.000	0.000
86.000	0.000	0.000	0.000	0.000
87.000	0.000	0.000	0.000	0.000
88.000	0.000	0.000	0.000	0.000
89.000	0.000	0.000	0.000	0.000
90.000	0.000	0.000	0.000	0.000
91.000	0.000	0.000	0.000	0.000
92.000	0.000	0.000	0.000	0.000
93.000	0.000	0.000	0.000	0.000
94.000	0.000	0.000	0.000	0.000
95.000	0.000	0.000	0.000	0.000
96.000	0.000	0.000	0.000	0.000
97.000	0.000	0.000	0.000	0.000
98.000	0.000	0.000	0.000	0.000
99.000	0.000	0.000	0.000	0.000

This data corresponds with figure 5.19.

DEPTH (meters)	CONCENTRATION			
	1949	1961	1978	1990
0.000	104.807	27.305	12.522	12.513
1.000	83.289	62.284	30.318	30.295
2.000	57.946	91.818	52.403	52.355
3.000	35.084	106.565	73.362	73.297
4.000	18.560	107.183	88.217	88.154
5.000	8.649	98.704	94.669	94.626
6.000	3.584	85.801	93.198	93.188
7.000	1.333	71.449	85.882	85.906
8.000	0.449	57.299	75.130	75.182
9.000	0.138	44.277	62.963	63.036
10.000	0.039	32.927	50.817	50.901
11.000	0.010	23.530	39.599	39.687
12.000	0.002	16.139	29.822	29.907
13.000	0.001	10.620	21.707	21.785
14.000	0.000	6.703	15.270	15.338
15.000	0.000	4.060	10.380	10.437
16.000	0.000	2.361	6.819	6.863
17.000	0.000	1.320	4.329	4.363
18.000	0.000	0.709	2.658	2.682
19.000	0.000	0.367	1.578	1.595
20.000	0.000	0.183	0.907	0.918
21.000	0.000	0.088	0.505	0.512
22.000	0.000	0.041	0.273	0.277
23.000	0.000	0.018	0.143	0.145
24.000	0.000	0.008	0.072	0.074
25.000	0.000	0.003	0.036	0.037
26.000	0.000	0.001	0.017	0.018
27.000	0.000	0.001	0.008	0.008
28.000	0.000	0.000	0.004	0.004
29.000	0.000	0.000	0.002	0.002
30.000	0.000	0.000	0.001	0.001
31.000	0.000	0.000	0.000	0.000
32.000	0.000	0.000	0.000	0.000
33.000	0.000	0.000	0.000	0.000
34.000	0.000	0.000	0.000	0.000
35.000	0.000	0.000	0.000	0.000
36.000	0.000	0.000	0.000	0.000
37.000	0.000	0.000	0.000	0.000
38.000	0.000	0.000	0.000	0.000
39.000	0.000	0.000	0.000	0.000
40.000	0.000	0.000	0.000	0.000
41.000	0.000	0.000	0.000	0.000
42.000	0.000	0.000	0.000	0.000
43.000	0.000	0.000	0.000	0.000
44.000	0.000	0.000	0.000	0.000
45.000	0.000	0.000	0.000	0.000
46.000	0.000	0.000	0.000	0.000
47.000	0.000	0.000	0.000	0.000
48.000	0.000	0.000	0.000	0.000
49.000	0.000	0.000	0.000	0.000
50.000	0.000	0.000	0.000	0.000
51.000	0.000	0.000	0.000	0.000

52.000	0.000	0.000	0.000	0.000
53.000	0.000	0.000	0.000	0.000
54.000	0.000	0.000	0.000	0.000
55.000	0.000	0.000	0.000	0.000
56.000	0.000	0.000	0.000	0.000
57.000	0.000	0.000	0.000	0.000
58.000	0.000	0.000	0.000	0.000
59.000	0.000	0.000	0.000	0.000
60.000	0.000	0.000	0.000	0.000
61.000	0.000	0.000	0.000	0.000
62.000	0.000	0.000	0.000	0.000
63.000	0.000	0.000	0.000	0.000
64.000	0.000	0.000	0.000	0.000
65.000	0.000	0.000	0.000	0.000
66.000	0.000	0.000	0.000	0.000
67.000	0.000	0.000	0.000	0.000
68.000	0.000	0.000	0.000	0.000
69.000	0.000	0.000	0.000	0.000
70.000	0.000	0.000	0.000	0.000
71.000	0.000	0.000	0.000	0.000
72.000	0.000	0.000	0.000	0.000
73.000	0.000	0.000	0.000	0.000
74.000	0.000	0.000	0.000	0.000
75.000	0.000	0.000	0.000	0.000
76.000	0.000	0.000	0.000	0.000
77.000	0.000	0.000	0.000	0.000
78.000	0.000	0.000	0.000	0.000
79.000	0.000	0.000	0.000	0.000
80.000	0.000	0.000	0.000	0.000
81.000	0.000	0.000	0.000	0.000
82.000	0.000	0.000	0.000	0.000
83.000	0.000	0.000	0.000	0.000
84.000	0.000	0.000	0.000	0.000
85.000	0.000	0.000	0.000	0.000
86.000	0.000	0.000	0.000	0.000
87.000	0.000	0.000	0.000	0.000
88.000	0.000	0.000	0.000	0.000
89.000	0.000	0.000	0.000	0.000
90.000	0.000	0.000	0.000	0.000
91.000	0.000	0.000	0.000	0.000
92.000	0.000	0.000	0.000	0.000
93.000	0.000	0.000	0.000	0.000
94.000	0.000	0.000	0.000	0.000
95.000	0.000	0.000	0.000	0.000
96.000	0.000	0.000	0.000	0.000
97.000	0.000	0.000	0.000	0.000
98.000	0.000	0.000	0.000	0.000
99.000	0.000	0.000	0.000	0.000
100.000	0.000	0.000	0.000	0.000

This data corresponds with figure 5.20.

DEPTH (meters)	CONCENTRATION			
	1949	1961	1978	1990
0.000	104.743	27.296	12.508	12.497
1.000	83.098	62.264	30.274	30.249
2.000	57.711	91.801	52.325	52.283
3.000	34.902	106.603	73.289	73.237
4.000	18.445	107.299	88.202	88.153
5.000	8.584	98.874	94.745	94.712
6.000	3.551	85.980	93.362	93.354
7.000	1.318	71.600	86.101	86.118
8.000	0.443	57.398	75.362	75.401
9.000	0.136	44.324	63.176	63.231
10.000	0.038	32.940	50.993	51.058
11.000	0.010	23.528	39.736	39.804
12.000	0.002	16.131	29.922	29.989
13.000	0.001	10.608	21.778	21.840
14.000	0.000	6.689	15.318	15.373
15.000	0.000	4.046	10.410	10.456
16.000	0.000	2.349	6.836	6.872
17.000	0.000	1.310	4.338	4.366
18.000	0.000	0.703	2.662	2.682
19.000	0.000	0.363	1.580	1.594
20.000	0.000	0.181	0.908	0.917
21.000	0.000	0.087	0.505	0.511
22.000	0.000	0.040	0.273	0.276
23.000	0.000	0.018	0.143	0.145
24.000	0.000	0.008	0.072	0.074
25.000	0.000	0.003	0.036	0.036
26.000	0.000	0.001	0.017	0.018
27.000	0.000	0.001	0.008	0.008
28.000	0.000	0.000	0.004	0.004
29.000	0.000	0.000	0.002	0.002
30.000	0.000	0.000	0.001	0.001
31.000	0.000	0.000	0.000	0.000
32.000	0.000	0.000	0.000	0.000
33.000	0.000	0.000	0.000	0.000
34.000	0.000	0.000	0.000	0.000
35.000	0.000	0.000	0.000	0.000
36.000	0.000	0.000	0.000	0.000
37.000	0.000	0.000	0.000	0.000
38.000	0.000	0.000	0.000	0.000
39.000	0.000	0.000	0.000	0.000
40.000	0.000	0.000	0.000	0.000
41.000	0.000	0.000	0.000	0.000
42.000	0.000	0.000	0.000	0.000
43.000	0.000	0.000	0.000	0.000
44.000	0.000	0.000	0.000	0.000
45.000	0.000	0.000	0.000	0.000
46.000	0.000	0.000	0.000	0.000
47.000	0.000	0.000	0.000	0.000
48.000	0.000	0.000	0.000	0.000
49.000	0.000	0.000	0.000	0.000
50.000	0.000	0.000	0.000	0.000
51.000	0.000	0.000	0.000	0.000

52.000	0.000	0.000	0.000	0.000
53.000	0.000	0.000	0.000	0.000
54.000	0.000	0.000	0.000	0.000
55.000	0.000	0.000	0.000	0.000
56.000	0.000	0.000	0.000	0.000
57.000	0.000	0.000	0.000	0.000
58.000	0.000	0.000	0.000	0.000
59.000	0.000	0.000	0.000	0.000
60.000	0.000	0.000	0.000	0.000
61.000	0.000	0.000	0.000	0.000
62.000	0.000	0.000	0.000	0.000
63.000	0.000	0.000	0.000	0.000
64.000	0.000	0.000	0.000	0.000
65.000	0.000	0.000	0.000	0.000
66.000	0.000	0.000	0.000	0.000
67.000	0.000	0.000	0.000	0.000
68.000	0.000	0.000	0.000	0.000
69.000	0.000	0.000	0.000	0.000
70.000	0.000	0.000	0.000	0.000
71.000	0.000	0.000	0.000	0.000
72.000	0.000	0.000	0.000	0.000
73.000	0.000	0.000	0.000	0.000
74.000	0.000	0.000	0.000	0.000
75.000	0.000	0.000	0.000	0.000
76.000	0.000	0.000	0.000	0.000
77.000	0.000	0.000	0.000	0.000
78.000	0.000	0.000	0.000	0.000
79.000	0.000	0.000	0.000	0.000
80.000	0.000	0.000	0.000	0.000
81.000	0.000	0.000	0.000	0.000
82.000	0.000	0.000	0.000	0.000
83.000	0.000	0.000	0.000	0.000
84.000	0.000	0.000	0.000	0.000
85.000	0.000	0.000	0.000	0.000
86.000	0.000	0.000	0.000	0.000
87.000	0.000	0.000	0.000	0.000
88.000	0.000	0.000	0.000	0.000
89.000	0.000	0.000	0.000	0.000
90.000	0.000	0.000	0.000	0.000
91.000	0.000	0.000	0.000	0.000
92.000	0.000	0.000	0.000	0.000
93.000	0.000	0.000	0.000	0.000
94.000	0.000	0.000	0.000	0.000
95.000	0.000	0.000	0.000	0.000
96.000	0.000	0.000	0.000	0.000
97.000	0.000	0.000	0.000	0.000
98.000	0.000	0.000	0.000	0.000
99.000	0.000	0.000	0.000	0.000
100.000	0.000	0.000	0.000	0.000

This data corresponds with figure 5.21.

DEPTH (meters)	CONCENTRATION			
	1949	1961	1978	1990
0.000	104.796	27.289	12.508	12.500
1.000	83.257	62.249	30.295	30.272
2.000	57.938	91.758	52.387	52.340
3.000	35.099	106.492	73.353	73.288
4.000	18.575	107.112	88.203	88.139
5.000	8.658	98.636	94.633	94.590
6.000	3.588	85.738	93.133	93.123
7.000	1.335	71.399	85.791	85.816
8.000	0.449	57.276	75.026	75.080
9.000	0.138	44.291	62.864	62.937
10.000	0.039	32.975	50.735	50.820
11.000	0.010	23.600	39.542	39.630
12.000	0.002	16.217	29.789	29.874
13.000	0.001	10.691	21.695	21.773
14.000	0.000	6.761	15.271	15.339
15.000	0.000	4.103	10.388	10.444
16.000	0.000	2.390	6.828	6.872
17.000	0.000	1.338	4.338	4.371
18.000	0.000	0.720	2.664	2.688
19.000	0.000	0.373	1.583	1.599
20.000	0.000	0.186	0.910	0.921
21.000	0.000	0.090	0.507	0.514
22.000	0.000	0.042	0.273	0.278
23.000	0.000	0.019	0.143	0.146
24.000	0.000	0.008	0.073	0.074
25.000	0.000	0.003	0.036	0.037
26.000	0.000	0.001	0.017	0.018
27.000	0.000	0.001	0.008	0.008
28.000	0.000	0.000	0.004	0.004
29.000	0.000	0.000	0.002	0.002
30.000	0.000	0.000	0.001	0.001
31.000	0.000	0.000	0.000	0.000
32.000	0.000	0.000	0.000	0.000
33.000	0.000	0.000	0.000	0.000
34.000	0.000	0.000	0.000	0.000
35.000	0.000	0.000	0.000	0.000
36.000	0.000	0.000	0.000	0.000
37.000	0.000	0.000	0.000	0.000
38.000	0.000	0.000	0.000	0.000
39.000	0.000	0.000	0.000	0.000
40.000	0.000	0.000	0.000	0.000
41.000	0.000	0.000	0.000	0.000
42.000	0.000	0.000	0.000	0.000
43.000	0.000	0.000	0.000	0.000
44.000	0.000	0.000	0.000	0.000
45.000	0.000	0.000	0.000	0.000
46.000	0.000	0.000	0.000	0.000
47.000	0.000	0.000	0.000	0.000
48.000	0.000	0.000	0.000	0.000
49.000	0.000	0.000	0.000	0.000
50.000	0.000	0.000	0.000	0.000
51.000	0.000	0.000	0.000	0.000

0.000	0.000	0.000	0.000	52.000
0.000	0.000	0.000	0.000	53.000
0.000	0.000	0.000	0.000	54.000
0.000	0.000	0.000	0.000	55.000
0.000	0.000	0.000	0.000	56.000
0.000	0.000	0.000	0.000	57.000
0.000	0.000	0.000	0.000	58.000
0.000	0.000	0.000	0.000	59.000
0.000	0.000	0.000	0.000	60.000
0.000	0.000	0.000	0.000	61.000
0.000	0.000	0.000	0.000	62.000
0.000	0.000	0.000	0.000	63.000
0.000	0.000	0.000	0.000	64.000
0.000	0.000	0.000	0.000	65.000
0.000	0.000	0.000	0.000	66.000
0.000	0.000	0.000	0.000	67.000
0.000	0.000	0.000	0.000	68.000
0.000	0.000	0.000	0.000	69.000
0.000	0.000	0.000	0.000	70.000
0.000	0.000	0.000	0.000	71.000
0.000	0.000	0.000	0.000	72.000
0.000	0.000	0.000	0.000	73.000
0.000	0.000	0.000	0.000	74.000
0.000	0.000	0.000	0.000	75.000
0.000	0.000	0.000	0.000	76.000
0.000	0.000	0.000	0.000	77.000
0.000	0.000	0.000	0.000	78.000
0.000	0.000	0.000	0.000	79.000
0.000	0.000	0.000	0.000	80.000
0.000	0.000	0.000	0.000	81.000
0.000	0.000	0.000	0.000	82.000
0.000	0.000	0.000	0.000	83.000
0.000	0.000	0.000	0.000	84.000
0.000	0.000	0.000	0.000	85.000
0.000	0.000	0.000	0.000	86.000
0.000	0.000	0.000	0.000	87.000
0.000	0.000	0.000	0.000	88.000
0.000	0.000	0.000	0.000	89.000
0.000	0.000	0.000	0.000	90.000
0.000	0.000	0.000	0.000	91.000
0.000	0.000	0.000	0.000	92.000
0.000	0.000	0.000	0.000	93.000
0.000	0.000	0.000	0.000	94.000
0.000	0.000	0.000	0.000	95.000
0.000	0.000	0.000	0.000	96.000
0.000	0.000	0.000	0.000	97.000
0.000	0.000	0.000	0.000	98.000
0.000	0.000	0.000	0.000	99.000
0.000	0.000	0.000	0.000	100.000

This data corresponds with figure 5.22.

DEPTH (meters)	CONCENTRATION			
	1949	1961	1978	1990
0.000	104.882	27.289	12.495	12.484
1.000	83.354	62.251	30.243	30.218
2.000	57.973	91.788	52.282	52.243
3.000	35.103	106.577	73.243	73.195
4.000	18.577	107.239	88.144	88.099
5.000	8.662	98.785	94.680	94.650
6.000	3.592	85.891	93.305	93.297
7.000	1.337	71.524	86.049	86.064
8.000	0.450	57.333	75.315	75.350
9.000	0.138	44.275	63.142	63.192
10.000	0.039	32.909	50.975	51.035
11.000	0.010	23.512	39.732	39.796
12.000	0.002	16.127	29.927	29.991
13.000	0.001	10.611	21.786	21.845
14.000	0.000	6.696	15.325	15.377
15.000	0.000	4.054	10.416	10.461
16.000	0.000	2.356	6.843	6.879
17.000	0.000	1.316	4.347	4.374
18.000	0.000	0.707	2.671	2.691
19.000	0.000	0.366	1.588	1.602
20.000	0.000	0.182	0.914	0.923
21.000	0.000	0.088	0.509	0.515
22.000	0.000	0.041	0.275	0.279
23.000	0.000	0.018	0.144	0.146
24.000	0.000	0.008	0.073	0.075
25.000	0.000	0.003	0.036	0.037
26.000	0.000	0.001	0.017	0.018
27.000	0.000	0.001	0.008	0.008
28.000	0.000	0.000	0.004	0.004
29.000	0.000	0.000	0.002	0.002
30.000	0.000	0.000	0.001	0.001
31.000	0.000	0.000	0.000	0.000
32.000	0.000	0.000	0.000	0.000
33.000	0.000	0.000	0.000	0.000
34.000	0.000	0.000	0.000	0.000
35.000	0.000	0.000	0.000	0.000
36.000	0.000	0.000	0.000	0.000
37.000	0.000	0.000	0.000	0.000
38.000	0.000	0.000	0.000	0.000
39.000	0.000	0.000	0.000	0.000
40.000	0.000	0.000	0.000	0.000
41.000	0.000	0.000	0.000	0.000
42.000	0.000	0.000	0.000	0.000
43.000	0.000	0.000	0.000	0.000
44.000	0.000	0.000	0.000	0.000
45.000	0.000	0.000	0.000	0.000
46.000	0.000	0.000	0.000	0.000
47.000	0.000	0.000	0.000	0.000
48.000	0.000	0.000	0.000	0.000
49.000	0.000	0.000	0.000	0.000
50.000	0.000	0.000	0.000	0.000
51.000	0.000	0.000	0.000	0.000



This data corresponds with figure 5.23.

DEPTH (meters)	SATURATION			
	1949	1961	1978	1990
0.000	0.438	0.393	0.074	0.068
1.000	0.438	0.393	0.075	0.068
2.000	0.438	0.393	0.076	0.069
3.000	0.438	0.393	0.077	0.070
4.000	0.438	0.393	0.079	0.070
5.000	0.438	0.393	0.080	0.071
6.000	0.438	0.393	0.081	0.071
7.000	0.438	0.393	0.082	0.072
8.000	0.438	0.393	0.083	0.072
9.000	0.438	0.393	0.084	0.073
10.000	0.438	0.393	0.085	0.074
11.000	0.438	0.393	0.086	0.074
12.000	0.438	0.393	0.087	0.075
13.000	0.438	0.393	0.088	0.075
14.000	0.438	0.393	0.089	0.076
15.000	0.438	0.393	0.090	0.076
16.000	0.438	0.393	0.091	0.077
17.000	0.438	0.393	0.092	0.078
18.000	0.438	0.393	0.093	0.078
19.000	0.438	0.393	0.094	0.079
20.000	0.438	0.393	0.095	0.079
21.000	0.438	0.393	0.096	0.080
22.000	0.438	0.393	0.096	0.080
23.000	0.438	0.393	0.097	0.081
24.000	0.438	0.393	0.098	0.081
25.000	0.438	0.393	0.099	0.082
26.000	0.438	0.393	0.100	0.082
27.000	0.438	0.393	0.100	0.083
28.000	0.438	0.393	0.101	0.083
29.000	0.438	0.393	0.102	0.084
30.000	0.438	0.393	0.103	0.084
31.000	0.439	0.393	0.103	0.085
32.000	0.439	0.393	0.104	0.085
33.000	0.439	0.393	0.105	0.086
34.000	0.439	0.393	0.106	0.086
35.000	0.439	0.393	0.106	0.087
36.000	0.439	0.393	0.107	0.087
37.000	0.439	0.393	0.108	0.088
38.000	0.439	0.393	0.108	0.088
39.000	0.439	0.393	0.109	0.089
40.000	0.439	0.393	0.110	0.089
41.000	0.438	0.393	0.110	0.090
42.000	0.438	0.393	0.111	0.090
43.000	0.438	0.393	0.111	0.091
44.000	0.438	0.393	0.112	0.091
45.000	0.438	0.393	0.113	0.091
46.000	0.437	0.393	0.113	0.092
47.000	0.437	0.393	0.114	0.092
48.000	0.437	0.393	0.115	0.093
49.000	0.437	0.393	0.115	0.093
50.000	0.437	0.393	0.116	0.094
51.000	0.437	0.393	0.116	0.094

52.000	0.438	0.393	0.117	0.094
53.000	0.438	0.393	0.117	0.095
54.000	0.438	0.393	0.118	0.095
55.000	0.438	0.393	0.119	0.096
56.000	0.439	0.393	0.119	0.096
57.000	0.439	0.393	0.120	0.096
58.000	0.440	0.393	0.120	0.097
59.000	0.440	0.393	0.121	0.097
60.000	0.440	0.393	0.121	0.097
61.000	0.440	0.393	0.122	0.098
62.000	0.440	0.393	0.122	0.098
63.000	0.440	0.393	0.123	0.099
64.000	0.440	0.393	0.123	0.099
65.000	0.439	0.393	0.124	0.099
66.000	0.439	0.393	0.124	0.100
67.000	0.439	0.393	0.125	0.100
68.000	0.438	0.393	0.125	0.100
69.000	0.438	0.393	0.126	0.101
70.000	0.437	0.393	0.126	0.101
71.000	0.437	0.393	0.127	0.102
72.000	0.436	0.393	0.127	0.102
73.000	0.436	0.393	0.128	0.102
74.000	0.436	0.393	0.128	0.103
75.000	0.436	0.393	0.129	0.103
76.000	0.437	0.393	0.129	0.103
77.000	0.437	0.393	0.130	0.104
78.000	0.437	0.393	0.130	0.104
79.000	0.438	0.393	0.131	0.104
80.000	0.438	0.394	0.131	0.105
81.000	0.439	0.394	0.131	0.105
82.000	0.439	0.394	0.132	0.105
83.000	0.440	0.394	0.132	0.106
84.000	0.440	0.394	0.133	0.106
85.000	0.440	0.394	0.133	0.106
86.000	0.440	0.394	0.134	0.106
87.000	0.440	0.394	0.134	0.107
88.000	0.440	0.394	0.134	0.107
89.000	0.440	0.394	0.135	0.107
90.000	0.440	0.393	0.135	0.108
91.000	0.440	0.393	0.136	0.108
92.000	0.439	0.392	0.136	0.108
93.000	0.439	0.392	0.136	0.108
94.000	0.438	0.391	0.137	0.109
95.000	0.438	0.391	0.137	0.109
96.000	0.438	0.391	0.137	0.109
97.000	0.438	0.390	0.138	0.109
98.000	0.438	0.390	0.138	0.109
99.000	0.438	0.390	0.138	0.109
100.000	0.438	0.390	0.138	0.109

This data corresponds with figure 5.24.

DEPTH (meters)	SATURATION			
	1949	1961	1978	1990
0.000	0.692	0.619	0.106	0.096
1.000	0.692	0.619	0.109	0.097
2.000	0.692	0.619	0.112	0.099
3.000	0.692	0.619	0.115	0.100
4.000	0.692	0.619	0.118	0.102
5.000	0.692	0.619	0.121	0.103
6.000	0.692	0.619	0.124	0.105
7.000	0.692	0.619	0.126	0.106
8.000	0.692	0.619	0.129	0.108
9.000	0.692	0.619	0.131	0.109
10.000	0.692	0.619	0.134	0.111
11.000	0.692	0.619	0.136	0.112
12.000	0.692	0.619	0.138	0.113
13.000	0.693	0.619	0.141	0.115
14.000	0.693	0.619	0.143	0.116
15.000	0.693	0.619	0.145	0.118
16.000	0.693	0.619	0.147	0.119
17.000	0.693	0.619	0.149	0.120
18.000	0.693	0.619	0.151	0.122
19.000	0.692	0.619	0.153	0.123
20.000	0.692	0.619	0.154	0.124
21.000	0.692	0.619	0.156	0.125
22.000	0.691	0.619	0.158	0.127
23.000	0.691	0.619	0.160	0.128
24.000	0.691	0.619	0.162	0.129
25.000	0.690	0.619	0.163	0.130
26.000	0.690	0.619	0.165	0.131
27.000	0.691	0.619	0.166	0.132
28.000	0.691	0.619	0.168	0.133
29.000	0.692	0.619	0.170	0.135
30.000	0.692	0.619	0.171	0.136
31.000	0.693	0.619	0.173	0.137
32.000	0.694	0.619	0.174	0.138
33.000	0.694	0.619	0.176	0.139
34.000	0.695	0.619	0.177	0.140
35.000	0.695	0.619	0.178	0.141
36.000	0.694	0.619	0.180	0.142
37.000	0.694	0.619	0.181	0.143
38.000	0.693	0.619	0.183	0.144
39.000	0.691	0.619	0.184	0.145
40.000	0.690	0.619	0.185	0.146
41.000	0.689	0.619	0.187	0.147
42.000	0.688	0.619	0.188	0.148
43.000	0.687	0.619	0.189	0.149
44.000	0.687	0.619	0.190	0.149
45.000	0.687	0.619	0.192	0.150
46.000	0.689	0.619	0.193	0.151
47.000	0.690	0.619	0.194	0.152
48.000	0.692	0.619	0.195	0.153
49.000	0.694	0.619	0.196	0.154
50.000	0.696	0.619	0.198	0.155
51.000	0.697	0.619	0.199	0.156

52.000	0.698	0.619	0.200	0.156
53.000	0.699	0.619	0.201	0.157
54.000	0.699	0.619	0.202	0.158
55.000	0.698	0.619	0.203	0.159
56.000	0.696	0.619	0.204	0.160
57.000	0.694	0.619	0.205	0.160
58.000	0.692	0.619	0.206	0.161
59.000	0.690	0.619	0.208	0.162
60.000	0.688	0.618	0.209	0.163
61.000	0.687	0.618	0.210	0.164
62.000	0.686	0.618	0.211	0.164
63.000	0.686	0.618	0.212	0.165
64.000	0.686	0.618	0.213	0.166
65.000	0.687	0.618	0.214	0.167
66.000	0.688	0.618	0.215	0.167
67.000	0.689	0.618	0.216	0.168
68.000	0.691	0.618	0.217	0.169
69.000	0.693	0.619	0.218	0.169
70.000	0.695	0.619	0.219	0.170
71.000	0.696	0.619	0.220	0.171
72.000	0.697	0.619	0.220	0.172
73.000	0.698	0.620	0.221	0.172
74.000	0.698	0.620	0.222	0.173
75.000	0.698	0.620	0.223	0.174
76.000	0.697	0.621	0.224	0.174
77.000	0.696	0.621	0.225	0.175
78.000	0.695	0.621	0.226	0.176
79.000	0.693	0.621	0.227	0.176
80.000	0.692	0.619	0.228	0.177
81.000	0.691	0.617	0.229	0.178
82.000	0.690	0.613	0.230	0.178
83.000	0.689	0.607	0.231	0.179
84.000	0.688	0.599	0.231	0.180
85.000	0.688	0.587	0.232	0.180
86.000	0.688	0.573	0.233	0.181
87.000	0.688	0.556	0.234	0.181
88.000	0.689	0.536	0.235	0.182
89.000	0.689	0.515	0.235	0.183
90.000	0.690	0.494	0.236	0.183
91.000	0.690	0.474	0.237	0.184
92.000	0.691	0.456	0.238	0.184
93.000	0.691	0.441	0.238	0.185
94.000	0.692	0.429	0.239	0.186
95.000	0.692	0.420	0.240	0.186
96.000	0.692	0.413	0.241	0.187
97.000	0.692	0.409	0.241	0.187
98.000	0.692	0.405	0.242	0.187
99.000	0.692	0.404	0.242	0.187
100.000	0.692	0.404	0.242	0.187

This data corresponds with figure 5.25.

DEPTH (meters)	CONCENTRATION			
	1949	1961	1978	1990
0.000	104.987	27.207	12.414	12.404
1.000	83.617	62.099	30.123	30.100
2.000	58.364	91.686	52.272	52.234
3.000	35.508	106.641	73.416	73.371
4.000	18.899	107.512	88.488	88.448
5.000	8.869	99.234	95.095	95.071
6.000	3.702	86.451	93.683	93.678
7.000	1.387	72.149	86.341	86.354
8.000	0.471	57.995	75.511	75.538
9.000	0.146	44.928	63.246	63.282
10.000	0.041	33.501	51.000	51.040
11.000	0.011	24.007	39.691	39.732
12.000	0.003	16.514	29.839	29.878
13.000	0.001	10.897	21.670	21.705
14.000	0.000	6.897	15.199	15.230
15.000	0.000	4.189	10.295	10.319
16.000	0.000	2.442	6.733	6.752
17.000	0.000	1.368	4.253	4.267
18.000	0.000	0.737	2.595	2.606
19.000	0.000	0.382	1.531	1.538
20.000	0.000	0.191	0.873	0.878
21.000	0.000	0.092	0.482	0.485
22.000	0.000	0.043	0.258	0.259
23.000	0.000	0.019	0.133	0.135
24.000	0.000	0.008	0.067	0.068
25.000	0.000	0.003	0.033	0.033
26.000	0.000	0.001	0.015	0.016
27.000	0.000	0.001	0.007	0.007
28.000	0.000	0.000	0.003	0.003
29.000	0.000	0.000	0.001	0.001
30.000	0.000	0.000	0.001	0.001
31.000	0.000	0.000	0.000	0.000
32.000	0.000	0.000	0.000	0.000
33.000	0.000	0.000	0.000	0.000
34.000	0.000	0.000	0.000	0.000
35.000	0.000	0.000	0.000	0.000

This data corresponds with figure 5.26.

DEPTH (meters)	CONCENTRATION			
	1949	1961	1978	1990
0.000	104.910	27.300	12.499	12.489
1.000	83.422	62.279	30.273	30.249
2.000	58.080	91.831	52.364	52.323
3.000	35.221	106.635	73.373	73.320
4.000	18.672	107.326	88.301	88.252
5.000	8.722	98.905	94.819	94.788
6.000	3.623	86.030	93.390	93.383
7.000	1.350	71.676	86.083	86.101
8.000	0.456	57.503	75.314	75.352
9.000	0.140	44.449	63.115	63.166
10.000	0.040	33.065	50.927	50.987
11.000	0.010	23.635	39.669	39.731
12.000	0.002	16.217	29.856	29.917
13.000	0.001	10.674	21.715	21.771
14.000	0.000	6.739	15.261	15.310
15.000	0.000	4.083	10.361	10.402
16.000	0.000	2.375	6.797	6.829
17.000	0.000	1.327	4.308	4.333
18.000	0.000	0.713	2.640	2.658
19.000	0.000	0.369	1.565	1.577
20.000	0.000	0.184	0.897	0.906
21.000	0.000	0.088	0.498	0.504
22.000	0.000	0.041	0.268	0.271
23.000	0.000	0.018	0.140	0.142
24.000	0.000	0.008	0.071	0.072
25.000	0.000	0.003	0.035	0.035
26.000	0.000	0.001	0.017	0.017
27.000	0.000	0.001	0.008	0.008
28.000	0.000	0.000	0.004	0.004
29.000	0.000	0.000	0.002	0.002
30.000	0.000	0.000	0.001	0.001
31.000	0.000	0.000	0.000	0.000
32.000	0.000	0.000	0.000	0.000
33.000	0.000	0.000	0.000	0.000
34.000	0.000	0.000	0.000	0.000
35.000	0.000	0.000	0.000	0.000

This data corresponds with figure 5.27.

DEPTH (meters)	CONCENTRATION			
	1949	1961	1978	1990
0.000	74.983	45.166	30.513	30.504
1.000	61.838	57.463	39.136	39.123
2.000	49.003	67.219	47.115	47.098
3.000	37.225	73.394	53.904	53.881
4.000	27.054	75.663	59.016	58.990
5.000	18.784	74.374	62.152	62.125
6.000	12.448	70.314	63.227	63.203
7.000	7.869	64.415	62.360	62.341
8.000	4.744	57.532	59.823	59.812
9.000	2.728	50.334	55.984	55.982
10.000	1.497	43.282	51.243	51.251
11.000	0.784	36.664	45.983	46.000
12.000	0.392	30.636	40.537	40.562
13.000	0.188	25.268	35.166	35.198
14.000	0.086	20.577	30.065	30.100
15.000	0.038	16.545	25.358	25.397
16.000	0.016	13.132	21.119	21.159
17.000	0.006	10.286	17.379	17.418
18.000	0.003	7.950	14.135	14.173
19.000	0.001	6.060	11.366	11.402
20.000	0.000	4.556	9.038	9.071
21.000	0.000	3.377	7.106	7.136
22.000	0.000	2.468	5.525	5.552
23.000	0.000	1.778	4.248	4.272
24.000	0.000	1.263	3.230	3.250
25.000	0.000	0.884	2.428	2.445
26.000	0.000	0.610	1.805	1.819
27.000	0.000	0.415	1.326	1.338
28.000	0.000	0.278	0.963	0.973
29.000	0.000	0.184	0.692	0.699
30.000	0.000	0.120	0.491	0.497
31.000	0.000	0.077	0.345	0.349
32.000	0.000	0.049	0.239	0.243
33.000	0.000	0.030	0.164	0.167
34.000	0.000	0.019	0.111	0.113
35.000	0.000	0.011	0.075	0.076
36.000	0.000	0.007	0.049	0.051
37.000	0.000	0.004	0.032	0.033
38.000	0.000	0.002	0.021	0.022
39.000	0.000	0.001	0.013	0.014
40.000	0.000	0.001	0.009	0.009
41.000	0.000	0.000	0.005	0.006
42.000	0.000	0.000	0.003	0.003
43.000	0.000	0.000	0.002	0.002
44.000	0.000	0.000	0.001	0.001
45.000	0.000	0.000	0.001	0.001
46.000	0.000	0.000	0.000	0.000
47.000	0.000	0.000	0.000	0.000
48.000	0.000	0.000	0.000	0.000
49.000	0.000	0.000	0.000	0.000
50.000	0.000	0.000	0.000	0.000

This data corresponds with figure 5.28.

DEPTH (meters)	SATURATION			
	1949	1961	1978	1990
0.000	0.655	0.584	0.119	0.107
1.000	0.655	0.584	0.123	0.109
2.000	0.655	0.584	0.127	0.111
3.000	0.655	0.584	0.131	0.113
4.000	0.655	0.584	0.135	0.115
5.000	0.655	0.584	0.139	0.117
6.000	0.655	0.584	0.142	0.119
7.000	0.655	0.584	0.145	0.121
8.000	0.655	0.584	0.149	0.123
9.000	0.655	0.584	0.152	0.125
10.000	0.655	0.584	0.155	0.127
11.000	0.655	0.584	0.158	0.129
12.000	0.655	0.584	0.161	0.131
13.000	0.655	0.584	0.163	0.132
14.000	0.655	0.584	0.166	0.134
15.000	0.655	0.584	0.169	0.136
16.000	0.655	0.584	0.171	0.138
17.000	0.655	0.584	0.174	0.139
18.000	0.655	0.584	0.176	0.141
19.000	0.655	0.584	0.178	0.143
20.000	0.655	0.584	0.181	0.144
21.000	0.655	0.584	0.183	0.146
22.000	0.655	0.584	0.185	0.147
23.000	0.655	0.584	0.187	0.149
24.000	0.655	0.584	0.189	0.150
25.000	0.655	0.584	0.191	0.152
26.000	0.655	0.584	0.193	0.153
27.000	0.655	0.584	0.195	0.155
28.000	0.655	0.584	0.197	0.156
29.000	0.655	0.584	0.199	0.157
30.000	0.655	0.583	0.201	0.159
31.000	0.655	0.582	0.203	0.160
32.000	0.655	0.580	0.205	0.161
33.000	0.655	0.577	0.207	0.163
34.000	0.655	0.572	0.208	0.164
35.000	0.655	0.564	0.210	0.165
36.000	0.655	0.554	0.212	0.166
37.000	0.655	0.540	0.213	0.168
38.000	0.655	0.522	0.215	0.169
39.000	0.655	0.500	0.217	0.170
40.000	0.655	0.475	0.218	0.171
41.000	0.655	0.450	0.220	0.172
42.000	0.655	0.426	0.221	0.174
43.000	0.655	0.405	0.223	0.175
44.000	0.655	0.389	0.225	0.176
45.000	0.655	0.378	0.226	0.177
46.000	0.655	0.371	0.228	0.178
47.000	0.655	0.367	0.229	0.179
48.000	0.655	0.364	0.230	0.180
49.000	0.655	0.363	0.232	0.181
50.000	0.655	0.363	0.233	0.182
51.000	0.655	0.364	0.235	0.183

52.000	0.655	0.365	0.236	0.184
53.000	0.655	0.366	0.237	0.185
54.000	0.655	0.367	0.239	0.186
55.000	0.655	0.368	0.240	0.187
56.000	0.655	0.370	0.241	0.188
57.000	0.655	0.371	0.243	0.189
58.000	0.655	0.372	0.244	0.190
59.000	0.655	0.374	0.245	0.191
60.000	0.655	0.375	0.247	0.192
61.000	0.655	0.377	0.248	0.193
62.000	0.655	0.378	0.249	0.194
63.000	0.655	0.380	0.250	0.195
64.000	0.655	0.381	0.252	0.196
65.000	0.655	0.382	0.253	0.197
66.000	0.655	0.384	0.254	0.198
67.000	0.654	0.385	0.255	0.199
68.000	0.654	0.387	0.256	0.200
69.000	0.654	0.388	0.257	0.200
70.000	0.654	0.389	0.259	0.201
71.000	0.654	0.391	0.260	0.202
72.000	0.654	0.392	0.261	0.203
73.000	0.654	0.394	0.262	0.204
74.000	0.653	0.395	0.263	0.205
75.000	0.653	0.396	0.264	0.206
76.000	0.653	0.398	0.265	0.206
77.000	0.653	0.399	0.266	0.207
78.000	0.652	0.400	0.267	0.208
79.000	0.652	0.401	0.269	0.209
80.000	0.652	0.403	0.270	0.210
81.000	0.651	0.404	0.271	0.210
82.000	0.651	0.405	0.272	0.211
83.000	0.650	0.406	0.273	0.212
84.000	0.649	0.408	0.274	0.213
85.000	0.648	0.409	0.275	0.214
86.000	0.646	0.410	0.276	0.214
87.000	0.643	0.411	0.277	0.215
88.000	0.639	0.412	0.278	0.216
89.000	0.633	0.413	0.279	0.217
90.000	0.623	0.414	0.280	0.217
91.000	0.607	0.416	0.281	0.218
92.000	0.581	0.417	0.282	0.219
93.000	0.538	0.418	0.283	0.220
94.000	0.470	0.419	0.283	0.220
95.000	0.367	0.420	0.284	0.221
96.000	0.236	0.421	0.285	0.221
97.000	0.125	0.421	0.286	0.222
98.000	0.099	0.422	0.286	0.222
99.000	0.098	0.423	0.286	0.223
100.000	0.098	0.423	0.286	0.223

This data corresponds with figure 5.29.

DEPTH (meters)	SATURATION			
	1949	1961	1978	1990
0.000	0.758	0.676	0.136	0.122
1.000	0.758	0.676	0.141	0.124
2.000	0.758	0.676	0.147	0.127
3.000	0.758	0.676	0.152	0.129
4.000	0.758	0.676	0.157	0.132
5.000	0.758	0.676	0.162	0.135
6.000	0.758	0.676	0.166	0.138
7.000	0.758	0.676	0.170	0.140
8.000	0.758	0.676	0.175	0.143
9.000	0.758	0.676	0.179	0.145
10.000	0.758	0.676	0.183	0.148
11.000	0.758	0.676	0.186	0.150
12.000	0.758	0.676	0.190	0.153
13.000	0.758	0.676	0.193	0.155
14.000	0.758	0.676	0.197	0.157
15.000	0.758	0.676	0.200	0.160
16.000	0.758	0.676	0.203	0.162
17.000	0.758	0.675	0.206	0.164
18.000	0.758	0.675	0.209	0.166
19.000	0.758	0.675	0.212	0.168
20.000	0.758	0.675	0.215	0.170
21.000	0.758	0.675	0.218	0.172
22.000	0.758	0.675	0.221	0.174
23.000	0.758	0.675	0.223	0.176
24.000	0.758	0.674	0.226	0.178
25.000	0.758	0.673	0.229	0.180
26.000	0.758	0.671	0.231	0.182
27.000	0.758	0.669	0.234	0.183
28.000	0.758	0.664	0.236	0.185
29.000	0.758	0.658	0.238	0.187
30.000	0.758	0.648	0.241	0.189
31.000	0.758	0.635	0.243	0.190
32.000	0.758	0.616	0.245	0.192
33.000	0.758	0.593	0.248	0.194
34.000	0.758	0.564	0.250	0.195
35.000	0.758	0.533	0.252	0.197
36.000	0.758	0.502	0.254	0.198
37.000	0.758	0.475	0.256	0.200
38.000	0.758	0.454	0.258	0.201
39.000	0.758	0.440	0.260	0.203
40.000	0.758	0.430	0.262	0.204
41.000	0.758	0.425	0.264	0.206
42.000	0.758	0.422	0.266	0.207
43.000	0.758	0.421	0.268	0.209
44.000	0.758	0.421	0.270	0.210
45.000	0.758	0.422	0.272	0.211
46.000	0.758	0.423	0.273	0.213
47.000	0.758	0.425	0.275	0.214
48.000	0.758	0.427	0.277	0.215
49.000	0.758	0.428	0.279	0.217
50.000	0.758	0.430	0.281	0.218
51.000	0.758	0.432	0.282	0.219

52.000	0.758	0.434	0.284	0.221
53.000	0.758	0.436	0.286	0.222
54.000	0.758	0.438	0.287	0.223
55.000	0.758	0.440	0.289	0.224
56.000	0.758	0.442	0.291	0.226
57.000	0.757	0.444	0.292	0.227
58.000	0.757	0.445	0.294	0.228
59.000	0.757	0.447	0.295	0.229
60.000	0.757	0.449	0.297	0.230
61.000	0.757	0.451	0.299	0.232
62.000	0.756	0.453	0.300	0.233
63.000	0.756	0.455	0.302	0.234
64.000	0.756	0.456	0.303	0.235
65.000	0.755	0.458	0.305	0.236
66.000	0.755	0.460	0.306	0.237
67.000	0.754	0.462	0.308	0.238
68.000	0.753	0.463	0.309	0.239
69.000	0.752	0.465	0.310	0.241
70.000	0.751	0.467	0.312	0.242
71.000	0.749	0.468	0.313	0.243
72.000	0.746	0.470	0.315	0.244
73.000	0.742	0.471	0.316	0.245
74.000	0.736	0.473	0.317	0.246
75.000	0.726	0.475	0.319	0.247
76.000	0.710	0.476	0.320	0.248
77.000	0.683	0.478	0.321	0.249
78.000	0.639	0.479	0.323	0.250
79.000	0.567	0.481	0.324	0.251
80.000	0.451	0.482	0.325	0.252
81.000	0.293	0.483	0.327	0.253
82.000	0.143	0.485	0.328	0.254
83.000	0.099	0.486	0.329	0.255
84.000	0.098	0.487	0.331	0.256
85.000	0.098	0.489	0.332	0.257
86.000	0.098	0.490	0.333	0.258
87.000	0.098	0.491	0.335	0.259
88.000	0.098	0.492	0.336	0.260
89.000	0.098	0.494	0.337	0.261
90.000	0.098	0.495	0.338	0.262
91.000	0.098	0.496	0.339	0.262
92.000	0.098	0.497	0.340	0.263
93.000	0.098	0.498	0.340	0.264
94.000	0.098	0.499	0.341	0.265
95.000	0.098	0.500	0.342	0.266
96.000	0.098	0.501	0.343	0.267
97.000	0.098	0.502	0.344	0.267
98.000	0.098	0.503	0.345	0.268
99.000	0.098	0.503	0.345	0.268
100.000	0.098	0.503	0.345	0.268

This data corresponds with figure 5.32.

CONCENTRATION (year 1978)	DEPTH (meters)
144.0	0.000
186.0	1.000
9260.0	2.000
9030.0	3.000
815.0	4.000
709.0	5.000
582.0	6.000
427.0	7.000
7230.0	8.000
2080.0	9.000
442.0	10.000
79.1	11.000
12.0	12.000
.9	13.000
.9	14.000
.9	15.000
.9	16.000
.9	17.000
.9	18.000
.9	19.000
.9	20.000
.9	21.000
.9	22.000

This data corresponds with figure 5.33.

CONCENTRATION (year 1978)	DEPTH (meters)
0.900	0.000
0.900	1.000
11600.000	2.000
10100.000	3.000
0.900	4.000
0.900	5.000
0.900	6.000
0.900	7.000
7390.000	8.000
1860.000	9.000
327.000	10.000
48.100	11.000
5.730	12.000
0.900	13.000
0.900	14.000
0.900	15.000
0.900	16.000
0.900	17.000
0.900	18.000
0.900	19.000
0.900	20.000
0.900	21.000
0.900	22.000

This data corresponds with figure 5.34.

CONCENTRATION (year 1978)	DEPTH (meters)
0.900	0.000
0.900	1.000
9560.000	2.000
9640.000	3.000
0.900	4.000
0.900	5.000
0.900	6.000
0.900	7.000
15400.000	8.000
3080.000	9.000
404.000	10.000
43.000	11.000
3.440	12.000
0.900	21.000
0.900	22.000
0.900	13.000
0.900	14.000
0.900	15.000
0.900	16.000
0.900	17.000
0.900	18.000
0.900	19.000
0.900	20.000
0.900	21.000
0.900	22.000

This data corresponds with figure 5.35.

CONCENTRATION (year 1978)	DEPTH (meters)
0.900	0.000
0.900	1.000
11600.000	2.000
10100.000	3.000
0.900	4.000
0.900	5.000
0.900	6.000
0.900	7.000
10400.000	8.000
1560.000	9.000
155.000	10.000
12.900	11.000
0.900	12.000
0.900	13.000
0.900	14.000
0.900	15.000
0.900	16.000
0.900	17.000
0.900	18.000
0.900	19.000
0.900	20.000
0.900	21.000
0.900	22.000

This data corresponds with figure 5.36.

CONCENTRATION (year 1978)	DEPTH (meters)
0.900	0.000
0.900	1.000
6410.000	2.000
7120.000	3.000
0.900	4.000
0.900	6.000
0.900	7.000
10900.000	8.000
6190.000	9.000
2680.000	10.000
989.000	11.000
326.000	12.000
0.900	13.000
0.900	14.000
0.900	15.000
0.900	16.000
0.900	17.000
0.900	18.000
0.900	19.000
0.900	20.000
0.900	21.000
0.900	22.000

This data corresponds with figure 5.37.

CONCENTRATION (year 1978)	DEPTH (meters)
20.070	0.000
26.042	1.000
32.329	2.000
31.521	3.000
28.446	4.000
24.767	5.000
20.319	6.000
14.918	7.000
8.408	8.000
2.426	9.000
0.514	10.000
0.092	11.000
0.014	12.000
0.002	13.000
0.001	14.000
0.000	15.000
0.000	16.000
0.000	17.000
0.000	18.000
0.000	19.000
0.000	20.000
0.000	21.000
0.000	22.000

This data corresponds with figure 5.38.

CONCENTRATION (year 1978)	DEPTH (meters)
17.376	0.000
22.099	1.000
27.005	2.000
23.541	3.000
21.082	4.000
18.006	5.000
14.622	6.000
10.819	7.000
6.447	8.000
1.620	9.000
0.285	10.000
0.042	11.000
0.005	12.000
0.001	13.000
0.0	14.000
0.0	15.000
0.0	16.000
0.0	17.000
0.0	18.000
0.0	19.000
0.0	20.000
0.0	21.000
0.0	22.000

This data corresponds with figure 5.39.

CONCENTRATION (year 1978)	DEPTH (meters)
20.855	0.000
26.524	1.000
33.367	2.000
33.669	3.000
31.098	4.000
26.453	5.000
21.338	6.000
15.588	7.000
8.9765	8.000
1.7949	9.000
0.235	10.000
0.025	11.000
0.002	12.000
0.000	13.000
0.000	14.000
0.000	15.000
0.000	16.000
0.000	17.000
0.000	18.000
0.000	19.000
0.000	20.000
0.000	21.000
0.000	22.000

This data corresponds with figure 5.40.

CONCENTRATION (year 1978)	DEPTH (meters)
17.366	0.000
22.086	1.000
26.983	2.000
23.473	3.000
20.868	4.000
17.509	5.000
13.808	6.000
9.645	7.000
4.856	8.000
0.726	9.000
0.072	10.000
0.006	11.000
0.000	12.000
0.000	13.000
0.000	14.000
0.000	15.000
0.000	16.000
0.000	17.000
0.000	18.000
0.000	19.000
0.000	20.000
0.000	21.000
0.000	22.000

This data corresponds with figure 5.41.

CONCENTRATION (year 1978)	DEPTH (meters)
27.613	0.000
35.123	1.000
44.740	2.000
49.720	3.000
47.891	4.000
43.103	5.000
37.860	6.000
31.992	7.000
25.265	8.000
14.399	9.000
6.231	10.000
2.302	11.000
0.758	12.000
0.272	13.000
0.202	14.000
0.201	15.000
0.201	16.000
0.200	17.000
0.199	18.000
0.198	19.000
0.198	20.000
0.197	21.000
0.197	22.000

This data corresponds with figure 5.42.

DEPTH (meters)	SATURATION	
	1951	1978
0.000	0.693	0.106
1.000	0.753	0.111
2.000	0.847	0.116
3.000	0.788	0.117
4.000	0.658	0.118
5.000	0.689	0.124
6.000	0.746	0.130
7.000	0.838	0.137
8.000	1.000	0.146
9.000	1.000	0.156
10.000	1.000	0.155
11.000	1.000	0.152
12.000	1.000	0.146
13.000	0.849	0.135
14.000	0.623	0.118
15.000	0.623	0.119
16.000	0.623	0.120
17.000	0.623	0.121
18.000	0.623	0.123
19.000	0.623	0.124
20.000	0.623	0.125
21.000	0.623	0.126
22.000	0.623	0.127
23.000	0.623	0.128
24.000	0.623	0.129
25.000	0.623	0.130
26.000	0.623	0.131
27.000	0.623	0.132
28.000	0.622	0.133
29.000	0.622	0.134
30.000	0.622	0.135
31.000	0.621	0.136
32.000	0.621	0.137
33.000	0.621	0.138
34.000	0.621	0.139
35.000	0.622	0.140
36.000	0.622	0.141
37.000	0.623	0.142
38.000	0.624	0.143
39.000	0.624	0.143
40.000	0.625	0.144
41.000	0.625	0.145
42.000	0.625	0.146
43.000	0.625	0.147
44.000	0.625	0.148
45.000	0.624	0.148
46.000	0.623	0.149
47.000	0.622	0.150
48.000	0.621	0.151
49.000	0.620	0.152
50.000	0.620	0.152
51.000	0.619	0.153
52.000	0.619	0.154
53.000	0.619	0.155

55.000	0.620	0.156
56.000	0.622	0.157
57.000	0.623	0.158
58.000	0.624	0.158
59.000	0.626	0.159
60.000	0.627	0.160
61.000	0.627	0.160
62.000	0.628	0.161
63.000	0.628	0.162
64.000	0.627	0.163
65.000	0.626	0.163
66.000	0.625	0.164
67.000	0.623	0.165
68.000	0.621	0.165
69.000	0.620	0.166
70.000	0.619	0.166
71.000	0.618	0.167
72.000	0.617	0.168
73.000	0.617	0.168
74.000	0.618	0.169
75.000	0.619	0.170
76.000	0.620	0.170
77.000	0.621	0.171
78.000	0.623	0.172
79.000	0.624	0.172
80.000	0.626	0.173
81.000	0.627	0.173
82.000	0.628	0.174
83.000	0.628	0.175
84.000	0.628	0.175
85.000	0.627	0.176
86.000	0.626	0.176
87.000	0.625	0.177
88.000	0.624	0.177
89.000	0.622	0.178
90.000	0.621	0.178
91.000	0.620	0.179
92.000	0.620	0.180
93.000	0.619	0.180
94.000	0.619	0.181
95.000	0.620	0.181
96.000	0.620	0.181
97.000	0.621	0.182
98.000	0.621	0.182
99.000	0.621	0.182
100.000	0.621	0.182

This data corresponds with figure 5.43.

DEPTH (meters)	SATURATION	
	1951	1978
0.000	0.693	0.106
1.000	0.753	0.111
2.000	0.847	0.116
3.000	0.788	0.117
4.000	0.658	0.118
5.000	0.689	0.124
6.000	0.746	0.130
7.000	0.838	0.137
8.000	1.000	0.146
9.000	1.000	0.156
10.000	1.000	0.155
11.000	1.000	0.152
12.000	1.000	0.146
13.000	0.849	0.135
14.000	0.623	0.118
15.000	0.623	0.119
16.000	0.623	0.120
17.000	0.623	0.121
18.000	0.623	0.123
19.000	0.623	0.124
20.000	0.623	0.125
21.000	0.623	0.126
22.000	0.623	0.127
23.000	0.623	0.128
24.000	0.623	0.129
25.000	0.623	0.130
26.000	0.623	0.131
27.000	0.623	0.132
28.000	0.622	0.133
29.000	0.622	0.134
30.000	0.622	0.135
31.000	0.621	0.136
32.000	0.621	0.137
33.000	0.621	0.138
34.000	0.621	0.139
35.000	0.622	0.140
36.000	0.622	0.141
37.000	0.623	0.142
38.000	0.624	0.143
39.000	0.624	0.143
40.000	0.625	0.144
41.000	0.625	0.145
42.000	0.625	0.146
43.000	0.625	0.147
44.000	0.625	0.148
45.000	0.624	0.148
46.000	0.623	0.149
47.000	0.622	0.150
48.000	0.621	0.151
49.000	0.620	0.152
50.000	0.620	0.152
51.000	0.619	0.153
52.000	0.619	0.154
53.000	0.619	0.155

0.156	0.620	55.000
0.157	0.622	56.000
0.158	0.623	57.000
0.158	0.624	58.000
0.159	0.626	59.000
0.160	0.627	60.000
0.160	0.627	61.000
0.161	0.628	62.000
0.162	0.628	63.000
0.163	0.627	64.000
0.163	0.626	65.000
0.164	0.625	66.000
0.165	0.623	67.000
0.165	0.621	68.000
0.166	0.620	69.000
0.166	0.619	70.000
0.167	0.618	71.000
0.168	0.617	72.000
0.168	0.617	73.000
0.169	0.618	74.000
0.170	0.619	75.000
0.170	0.620	76.000
0.171	0.621	77.000
0.172	0.623	78.000
0.172	0.624	79.000
0.173	0.626	80.000
0.173	0.627	81.000
0.174	0.628	82.000
0.175	0.628	83.000
0.175	0.628	84.000
0.176	0.627	85.000
0.176	0.626	86.000
0.177	0.625	87.000
0.177	0.624	88.000
0.178	0.622	89.000
0.178	0.621	90.000
0.179	0.620	91.000
0.180	0.620	92.000
0.180	0.619	93.000
0.181	0.619	94.000
0.181	0.620	95.000
0.181	0.620	96.000
0.182	0.621	97.000
0.182	0.621	98.000
0.182	0.621	99.000
0.182	0.621	100.000

This data corresponds with figure 5.44.

DEPTH (meters)	SATURATION	
	1951	1978
0.000	1.000	0.120
1.000	1.000	0.127
2.000	1.000	0.135
3.000	1.000	0.130
4.000	0.658	0.120
5.000	0.689	0.126
6.000	0.747	0.133
7.000	0.838	0.140
8.000	1.000	0.149
9.000	1.000	0.159
10.000	1.000	0.158
11.000	1.000	0.155
12.000	1.000	0.148
13.000	0.849	0.137
14.000	0.623	0.119
15.000	0.623	0.121
16.000	0.623	0.122
17.000	0.623	0.123
18.000	0.623	0.124
19.000	0.622	0.125
20.000	0.622	0.126
21.000	0.622	0.128
22.000	0.622	0.129
23.000	0.622	0.130
24.000	0.622	0.131
25.000	0.622	0.132
26.000	0.623	0.133
27.000	0.623	0.134
28.000	0.623	0.135
29.000	0.624	0.136
30.000	0.624	0.137
31.000	0.624	0.138
32.000	0.624	0.138
33.000	0.624	0.139
34.000	0.624	0.140
35.000	0.624	0.141
36.000	0.623	0.142
37.000	0.622	0.143
38.000	0.622	0.144
39.000	0.621	0.145
40.000	0.620	0.146
41.000	0.620	0.146
42.000	0.620	0.147
43.000	0.620	0.148
44.000	0.620	0.149
45.000	0.621	0.150
46.000	0.622	0.150
47.000	0.623	0.151
48.000	0.624	0.152
49.000	0.626	0.153
50.000	0.627	0.153
51.000	0.627	0.154
52.000	0.627	0.155
53.000	0.627	0.156

0.157	0.626	55.000
0.158	0.624	56.000
0.159	0.623	57.000
0.159	0.621	58.000
0.160	0.619	59.000
0.161	0.618	60.000
0.161	0.617	61.000
0.162	0.617	62.000
0.163	0.617	63.000
0.163	0.617	64.000
0.164	0.619	65.000
0.165	0.620	66.000
0.165	0.622	67.000
0.166	0.624	68.000
0.167	0.626	69.000
0.167	0.627	70.000
0.168	0.629	71.000
0.169	0.629	72.000
0.169	0.630	73.000
0.170	0.629	74.000
0.171	0.628	75.000
0.171	0.627	76.000
0.172	0.625	77.000
0.172	0.623	78.000
0.173	0.621	79.000
0.174	0.619	80.000
0.174	0.618	81.000
0.175	0.617	82.000
0.175	0.617	83.000
0.176	0.617	84.000
0.177	0.617	85.000
0.177	0.618	86.000
0.178	0.620	87.000
0.178	0.621	88.000
0.179	0.623	89.000
0.179	0.624	90.000
0.180	0.625	91.000
0.180	0.626	92.000
0.181	0.627	93.000
0.181	0.627	94.000
0.182	0.627	95.000
0.182	0.626	96.000
0.182	0.626	97.000
0.183	0.625	98.000
0.183	0.625	99.000
0.183	0.625	100.000

This data corresponds with figure 5.45.

DEPTH (meters)	SATURATION	
	1951	1978
0.000	0.794	0.114
1.000	0.900	0.120
2.000	1.000	0.127
3.000	0.905	0.125
4.000	0.658	0.119
5.000	0.689	0.125
6.000	0.747	0.132
7.000	0.838	0.139
8.000	1.000	0.148
9.000	1.000	0.158
10.000	1.000	0.157
11.000	1.000	0.154
12.000	1.000	0.147
13.000	0.849	0.136
14.000	0.623	0.119
15.000	0.623	0.120
16.000	0.623	0.121
17.000	0.623	0.122
18.000	0.623	0.124
19.000	0.623	0.125
20.000	0.623	0.126
21.000	0.623	0.127
22.000	0.623	0.128
23.000	0.623	0.129
24.000	0.623	0.130
25.000	0.623	0.131
26.000	0.623	0.132
27.000	0.623	0.133
28.000	0.622	0.134
29.000	0.622	0.135
30.000	0.622	0.136
31.000	0.621	0.137
32.000	0.621	0.138
33.000	0.621	0.139
34.000	0.621	0.140
35.000	0.622	0.141
36.000	0.622	0.142
37.000	0.623	0.142
38.000	0.624	0.143
39.000	0.624	0.144
40.000	0.625	0.145
41.000	0.625	0.146
42.000	0.625	0.147
43.000	0.625	0.148
44.000	0.625	0.148
45.000	0.624	0.149
46.000	0.623	0.150
47.000	0.622	0.151
48.000	0.621	0.152
49.000	0.620	0.152
50.000	0.620	0.153
51.000	0.619	0.154
52.000	0.619	0.155
53.000	0.619	0.155

55.000	0.620	0.157
56.000	0.622	0.158
57.000	0.623	0.158
58.000	0.624	0.159
59.000	0.626	0.160
60.000	0.627	0.160
61.000	0.627	0.161
62.000	0.628	0.162
63.000	0.628	0.162
64.000	0.627	0.163
65.000	0.626	0.164
66.000	0.625	0.164
67.000	0.623	0.165
68.000	0.622	0.166
69.000	0.620	0.166
70.000	0.619	0.167
71.000	0.618	0.168
72.000	0.617	0.168
73.000	0.617	0.169
74.000	0.618	0.170
75.000	0.619	0.170
76.000	0.620	0.171
77.000	0.621	0.171
78.000	0.623	0.172
79.000	0.624	0.173
80.000	0.626	0.173
81.000	0.627	0.174
82.000	0.628	0.174
83.000	0.628	0.175
84.000	0.628	0.176
85.000	0.627	0.176
86.000	0.626	0.177
87.000	0.625	0.177
88.000	0.624	0.178
89.000	0.623	0.179
90.000	0.621	0.179
91.000	0.620	0.180
92.000	0.620	0.180
93.000	0.619	0.181
94.000	0.619	0.181
95.000	0.620	0.181
96.000	0.620	0.182
97.000	0.621	0.182
98.000	0.621	0.182
99.000	0.621	0.183
100.000	0.621	0.183

This data corresponds with figure 5.46.

CONCENTRATION 1978	DEPTH (meters)
837.000	0.000
1080.000	1.000
1270.000	2.000
1350.000	3.000
1520.000	4.000
1680.000	5.000
1730.000	6.000
1780.000	7.000
1860.000	8.000
1780.000	9.000
1540.000	10.000
1380.000	11.000
1180.000	12.000
918.000	13.000
840.000	14.000
793.000	15.000
655.000	16.000
540.000	17.000
440.000	18.000
355.000	19.000
283.000	20.000
223.000	21.000
174.000	22.000
135.000	23.000
103.000	24.000
77.600	25.000
57.900	26.000
42.700	27.000
31.200	28.000
22.500	29.000
16.000	30.000
11.300	31.000
7.850	32.000
5.390	33.000
3.670	34.000
2.460	35.000
1.630	36.000
1.060	37.000
0.687	38.000
0.458	39.000
0.286	40.000
0.172	41.000
0.115	42.000
0.573	43.000
0.0286	44.000
0.0286	45.000
0.0286	46.000

This data corresponds with figure 5.47.

CONCENTRATION 1978	DEPTH (meters)
1120.000	0.000
1430.000	1.000
1650.000	2.000
1700.000	3.000
1850.000	4.000
1990.000	5.000
1970.000	6.000
1950.000	7.000
1960.000	8.000
1790.000	9.000
1460.000	10.000
1250.000	11.000
1020.000	12.000
741.000	13.000
642.000	14.000
577.000	15.000
448.000	16.000
347.000	17.000
265.000	18.000
200.000	19.000
148.000	20.000
109.000	21.000
78.800	22.000
56.300	23.000
39.600	24.000
27.500	25.000
18.800	26.000
12.000	27.000
8.450	28.000
5.550	29.000
3.580	30.000
2.290	31.000
0.895	32.000
0.537	33.000
0.322	34.000
0.179	35.000
0.107	36.000
0.0716	37.000
0.0358	38.000
0.0358	39.000

This data corresponds with figure 5.48.

CONCENTRATION 1978	DEPTH (meters)
1090.000	0.000
1400.000	1.000
1620.000	2.000
1580.000	3.000
1780.000	4.000
1990.000	5.000
1970.000	6.000
1950.000	7.000
1970.000	8.000
1810.000	9.000
1490.000	10.000
1270.000	11.000
1040.000	12.000
764.000	13.000
665.000	14.000
600.000	15.000
468.000	16.000
363.000	17.000
278.000	18.000
210.000	19.000
157.000	20.000
115.000	21.000
83.400	22.000
59.600	23.000
42.000	24.000
29.200	25.000
20.000	26.000
13.500	27.000
8.9900	28.000
5.9100	29.000
3.8300	30.000
2.4300	31.000
1.5400	32.000
0.9670	33.000
0.5730	34.000
0.3580	35.000
0.2150	36.000
0.1070	37.000
0.0716	38.000
0.0358	39.000
0.0358	40.000

This data corresponds with figure 5.49.

CONCENTRATION 1978	DEPTH (meters)
1110.000	0.000
1420.000	1.000
1640.000	2.000
1620.000	3.000
1800.000	4.000
1990.000	5.000
1970.000	6.000
1950.000	7.000
1960.000	8.000
1800.000	9.000
1480.000	10.000
1260.000	11.000
1030.000	12.000
754.000	13.000
654.000	14.000
589.000	15.000
459.000	16.000
356.000	17.000
272.000	18.000
206.000	19.000
153.000	20.000
112.000	21.000
81.400	22.000
58.200	23.000
41.000	24.000
28.500	25.000
19.600	26.000
13.200	27.000
8.810	28.000
5.760	29.000
3.720	30.000
2.400	31.000
1.500	32.000
0.931	33.000
0.573	34.000
0.358	35.000
0.215	36.000
0.107	37.000
0.0716	38.000
0.0358	39.000
0.0358	40.000

This data corresponds with figure 5.50.

CONCENTRATION 1978 -----	DEPTH (meters) -----
29.218	0.000
37.564	1.000
44.290	2.000
47.204	3.000
52.961	4.000
58.565	5.000
60.428	6.000
62.241	7.000
64.899	8.000
61.982	9.000
53.642	10.000
48.077	11.000
41.263	12.000
32.051	13.000
29.329	14.000
27.687	15.000
22.871	16.000
18.842	17.000
15.368	18.000
12.396	19.000
9.888	20.000
7.800	21.000
6.087	22.000
4.698	23.000
3.587	24.000
2.708	25.000
2.021	26.000
1.492	27.000
1.088	28.000
0.785	29.000
0.559	30.000
0.394	31.000
0.274	32.000
0.188	33.000
0.128	34.000
0.086	35.000
0.057	36.000
0.037	37.000
0.024	38.000
0.016	39.000
0.010	40.000
0.006	41.000
0.004	42.000
0.002	43.000
0.001	44.000
0.001	45.000
0.001	46.000
0.000	47.000

This data corresponds with figure 5.51.

CONCENTRATION 1978	DEPTH (meters)
31.144	0.000
39.843	1.000
46.198	2.000
47.560	3.000
51.783	4.000
55.541	5.000
55.019	6.000
54.371	7.000
54.644	8.000
49.984	9.000
40.901	10.000
34.869	11.000
28.399	12.000
20.697	13.000
17.923	14.000
16.104	15.000
12.511	16.000
9.678	17.000
7.395	18.000
5.574	19.000
4.144	20.000
3.040	21.000
2.200	22.000
1.571	23.000
1.106	24.000
0.768	25.000
0.526	26.000
0.335	27.000
0.236	28.000
0.155	29.000
0.100	30.000
0.064	31.000
0.025	32.000
0.015	33.000
0.009	34.000
0.005	35.000
0.003	36.000
0.002	37.000
0.001	38.000
0.001	39.000
0.000	40.000
0.000	41.000
0.000	42.000
0.000	43.000
0.000	44.000
0.000	45.000
0.000	46.000
0.000	47.000

This data corresponds with figure 5.52.

CONCENTRATION 1978	DEPTH (meters)
30.480	0.000
39.134	1.000
45.336	2.000
44.064	3.000
49.645	4.000
55.511	5.000
54.961	6.000
54.523	7.000
54.988	8.000
50.511	9.000
41.548	10.000
35.590	11.000
29.125	12.000
21.324	13.000
18.562	14.000
16.744	15.000
13.061	16.000
10.139	17.000
7.770	18.000
5.871	19.000
4.374	20.000
3.214	21.000
2.329	22.000
1.665	23.000
1.173	24.000
0.816	25.000
0.559	26.000
0.378	27.000
0.251	28.000
0.165	29.000
0.107	30.000
0.068	31.000
0.043	32.000
0.027	33.000
0.016	34.000
0.010	35.000
0.006	36.000
0.003	37.000
0.002	38.000
0.001	39.000
0.001	40.000
0.000	41.000
0.000	42.000
0.000	43.000
0.000	44.000
0.000	45.000
0.000	46.000
0.000	47.000

This data corresponds with figure 5.53.

CONCENTRATION 1978	DEPTH (meters)
30.873	0.000
39.591	1.000
45.825	2.000
45.270	3.000
50.405	4.000
55.625	5.000
55.046	6.000
54.502	7.000
54.872	8.000
50.298	9.000
41.265	10.000
35.265	11.000
28.793	12.000
21.045	13.000
18.269	14.000
16.452	15.000
12.811	16.000
9.931	17.000
7.602	18.000
5.740	19.000
4.274	20.000
3.139	21.000
2.274	22.000
1.625	23.000
1.146	24.000
0.796	25.000
0.546	26.000
0.369	27.000
0.246	28.000
0.161	29.000
0.104	30.000
0.067	31.000
0.042	32.000
0.026	33.000
0.016	34.000
0.010	35.000
0.006	36.000
0.003	37.000
0.002	38.000
0.001	39.000
0.001	40.000
0.000	41.000
0.000	42.000
0.000	43.000
0.000	44.000
0.000	45.000
0.000	46.000
0.000	47.000

This data corresponds with figure 5.54.

DEPTH (meters)	SATURATION
0.000	0.098
3.500	0.098
7.000	0.098
10.500	0.098
14.000	0.098
17.500	0.098
21.000	0.098
24.500	0.098
28.000	0.098
31.500	0.098
35.000	0.098
38.500	0.098
42.000	0.098
45.500	0.098
49.000	0.098
52.500	0.098
56.000	0.098
59.500	0.098
63.000	0.098
66.500	0.098
70.000	0.098
73.500	0.098
77.000	0.098
80.500	0.098
84.000	0.098
87.500	0.098
91.000	0.098
94.500	0.098
98.000	0.098
101.500	0.098
105.000	0.098
108.500	0.098
112.000	0.098
115.500	0.098
119.000	0.098
122.500	0.098
126.000	0.098
129.500	0.098
133.000	0.098
136.500	0.098
140.000	0.098
143.500	0.098
147.000	0.098
150.500	0.098
154.000	0.098
157.500	0.098
161.000	0.098
164.500	0.098
168.000	0.098
171.500	0.098
175.000	0.098
178.500	0.098
182.000	0.098
185.500	0.098

192.500	0.098	0.540	0.364	0.280
196.000	0.098	0.542	0.366	0.282
199.500	0.098	0.544	0.368	0.283
203.000	0.098	0.546	0.370	0.285
206.500	0.098	0.548	0.372	0.286
210.000	0.098	0.550	0.374	0.288
213.500	0.098	0.552	0.376	0.289
217.000	0.098	0.554	0.378	0.291
220.500	0.098	0.555	0.380	0.293
224.000	0.098	0.557	0.382	0.294
227.500	0.098	0.558	0.384	0.296
231.000	0.098	0.560	0.386	0.297
234.500	0.098	0.561	0.388	0.299
238.000	0.098	0.563	0.390	0.300
241.500	0.098	0.564	0.392	0.301
245.000	0.098	0.565	0.394	0.303
248.500	0.098	0.565	0.396	0.304
252.000	0.098	0.565	0.397	0.306
255.500	0.098	0.565	0.399	0.307
259.000	0.098	0.565	0.401	0.309
262.500	0.098	0.565	0.403	0.310
266.000	0.098	0.565	0.405	0.311
269.500	0.098	0.564	0.406	0.313
273.000	0.098	0.561	0.408	0.314
276.500	0.098	0.555	0.410	0.315
280.000	0.098	0.548	0.411	0.317
283.500	0.098	0.541	0.413	0.318
287.000	0.098	0.534	0.415	0.319
290.500	0.098	0.528	0.416	0.321
294.000	0.098	0.520	0.418	0.322
297.500	0.098	0.512	0.419	0.323
301.000	0.098	0.504	0.421	0.325
304.500	0.098	0.497	0.423	0.326
308.000	0.098	0.492	0.424	0.327
311.500	0.098	0.489	0.425	0.327
315.000	0.098	0.487	0.427	0.328
318.500	0.098	0.486	0.429	0.329
322.000	0.098	0.486	0.431	0.330
325.500	0.098	0.486	0.434	0.332
329.000	0.099	0.487	0.435	0.336
332.500	0.106	0.489	0.436	0.339
336.000	0.132	0.492	0.438	0.345
339.500	0.179	0.501	0.448	0.357
343.000	0.272	0.534	0.486	0.401
346.500	0.524	0.675	0.641	0.581
350.000	1.000	1.000	1.000	1.000

This data corresponds with figure 5.55.

DEPTH (meters)	SATURATION			
	1949	1961	1978	1990
0.000	0.797	0.464	0.124	0.110
3.500	0.797	0.464	0.139	0.117
7.000	0.797	0.464	0.151	0.125
10.500	0.797	0.464	0.162	0.131
14.000	0.797	0.464	0.172	0.138
17.500	0.797	0.464	0.180	0.144
21.000	0.797	0.464	0.188	0.149
24.500	0.797	0.464	0.196	0.154
28.000	0.797	0.463	0.203	0.159
31.500	0.797	0.463	0.209	0.164
35.000	0.797	0.463	0.215	0.168
38.500	0.797	0.462	0.221	0.173
42.000	0.797	0.462	0.226	0.177
45.500	0.797	0.461	0.232	0.181
49.000	0.797	0.461	0.237	0.184
52.500	0.797	0.460	0.242	0.188
56.000	0.797	0.460	0.246	0.191
59.500	0.797	0.459	0.251	0.195
63.000	0.797	0.459	0.255	0.198
66.500	0.797	0.459	0.259	0.201
70.000	0.797	0.459	0.263	0.204
73.500	0.797	0.459	0.267	0.207
77.000	0.797	0.459	0.271	0.210
80.500	0.797	0.460	0.275	0.213
84.000	0.797	0.461	0.279	0.215
87.500	0.797	0.462	0.282	0.218
91.000	0.797	0.464	0.286	0.221
94.500	0.797	0.466	0.289	0.223
98.000	0.797	0.468	0.293	0.226
101.500	0.797	0.470	0.296	0.228
105.000	0.797	0.472	0.299	0.231
108.500	0.796	0.475	0.302	0.233
112.000	0.796	0.477	0.305	0.235
115.500	0.796	0.480	0.308	0.238
119.000	0.796	0.483	0.311	0.240
122.500	0.795	0.486	0.314	0.242
126.000	0.794	0.489	0.317	0.244
129.500	0.794	0.492	0.320	0.246
133.000	0.793	0.495	0.323	0.248
136.500	0.792	0.498	0.325	0.251
140.000	0.790	0.501	0.328	0.253
143.500	0.787	0.504	0.331	0.255
147.000	0.780	0.507	0.333	0.257
150.500	0.764	0.509	0.336	0.258
154.000	0.720	0.512	0.338	0.260
157.500	0.598	0.515	0.341	0.262
161.000	0.340	0.518	0.343	0.264
164.500	0.121	0.521	0.346	0.266
168.000	0.098	0.523	0.348	0.268
171.500	0.098	0.526	0.350	0.270
175.000	0.098	0.528	0.353	0.271
178.500	0.098	0.531	0.355	0.273
182.000	0.098	0.533	0.357	0.275
185.500	0.098	0.535	0.360	0.276

192.500	0.098
196.000	0.098
199.500	0.098
203.000	0.098
206.500	0.098
210.000	0.098
213.500	0.098
217.000	0.098
220.500	0.098
224.000	0.098
227.500	0.098
231.000	0.098
234.500	0.098
238.000	0.098
241.500	0.098
245.000	0.098
248.500	0.098
252.000	0.098
255.500	0.098
259.000	0.098
262.500	0.098
266.000	0.098
269.500	0.098
273.000	0.098
276.500	0.098
280.000	0.098
283.500	0.098
287.000	0.098
290.500	0.098
294.000	0.098
297.500	0.098
301.000	0.098
304.500	0.098
308.000	0.098
311.500	0.098
315.000	0.098
318.500	0.098
322.000	0.098
325.500	0.098
329.000	0.098
332.500	0.099
336.000	0.108
339.500	0.165
343.000	0.270
346.500	0.523
350.000	1.000

This data corresponds with figure 5.56.

DEPTH (meters)	SATURATION			
	1949	1961	1978	1990
0.000	0.7970	0.4640	0.1200	0.1070
1.000	0.7970	0.4640	0.1240	0.1090
2.000	0.7970	0.4640	0.1280	0.1110
3.000	0.7970	0.4640	0.1320	0.1130
4.000	0.7970	0.4640	0.1360	0.1150
5.000	0.7970	0.4640	0.1390	0.1170
6.000	0.7970	0.4640	0.1430	0.1190
7.000	0.7970	0.4640	0.1460	0.1210
8.000	0.7970	0.4640	0.1500	0.1230
9.000	0.7970	0.4640	0.1530	0.1250
10.000	0.7970	0.4640	0.1560	0.1270
11.000	0.7960	0.4640	0.1590	0.1290
12.000	0.7960	0.4640	0.1620	0.1310
13.000	0.7960	0.4640	0.1640	0.1330
14.000	0.7950	0.4640	0.1670	0.1350
15.000	0.7950	0.4640	0.1700	0.1360
16.000	0.7950	0.4640	0.1720	0.1380
17.000	0.7950	0.4640	0.1750	0.1400
18.000	0.7950	0.4640	0.1770	0.1410
19.000	0.7960	0.4640	0.1800	0.1430
20.000	0.7970	0.4640	0.1820	0.1450
21.000	0.7980	0.4640	0.1840	0.1460
22.000	0.8000	0.4630	0.1860	0.1480
23.000	0.8010	0.4630	0.1890	0.1490
24.000	0.8020	0.4630	0.1910	0.1510
25.000	0.8030	0.4630	0.1930	0.1520
26.000	0.8030	0.4630	0.1950	0.1540
27.000	0.8030	0.4630	0.1970	0.1550
28.000	0.8020	0.4630	0.1990	0.1560
29.000	0.8000	0.4640	0.2010	0.1580
30.000	0.7980	0.4640	0.2030	0.1590
31.000	0.7950	0.4640	0.2050	0.1610
32.000	0.7930	0.4640	0.2060	0.1620
33.000	0.7910	0.4640	0.2080	0.1630
34.000	0.7890	0.4640	0.2100	0.1640
35.000	0.7890	0.4640	0.2120	0.1660
36.000	0.7890	0.4630	0.2130	0.1670
37.000	0.7900	0.4630	0.2150	0.1680
38.000	0.7920	0.4630	0.2170	0.1690
39.000	0.7940	0.4620	0.2180	0.1710
40.000	0.7970	0.4620	0.2200	0.1720
41.000	0.7990	0.4620	0.2220	0.1730
42.000	0.8010	0.4610	0.2230	0.1740
43.000	0.8030	0.4610	0.2250	0.1750
44.000	0.8040	0.4610	0.2260	0.1760
45.000	0.8040	0.4610	0.2280	0.1780
46.000	0.8030	0.4610	0.2290	0.1790
47.000	0.8020	0.4610	0.2310	0.1800
48.000	0.8010	0.4610	0.2320	0.1810
49.000	0.7990	0.4610	0.2340	0.1820
50.000	0.7970	0.4610	0.2350	0.1830
51.000	0.7950	0.4610	0.2370	0.1840
52.000	0.7940	0.4610	0.2380	0.1850
53.000	0.7930	0.4610	0.2390	0.1860

0.000	0.000	0.000	0.000	55.000
0.000	0.000	0.000	0.000	56.000
0.000	0.000	0.000	0.000	57.000
0.000	0.000	0.000	0.000	58.000
0.000	0.000	0.000	0.000	59.000
0.000	0.000	0.000	0.000	60.000
0.000	0.000	0.000	0.000	61.000
0.000	0.000	0.000	0.000	62.000
0.000	0.000	0.000	0.000	63.000
0.000	0.000	0.000	0.000	64.000
0.000	0.000	0.000	0.000	65.000
0.000	0.000	0.000	0.000	66.000
0.000	0.000	0.000	0.000	67.000
0.000	0.000	0.000	0.000	68.000
0.000	0.000	0.000	0.000	69.000
0.000	0.000	0.000	0.000	70.000
0.000	0.000	0.000	0.000	71.000
0.000	0.000	0.000	0.000	72.000
0.000	0.000	0.000	0.000	73.000
0.000	0.000	0.000	0.000	74.000
0.000	0.000	0.000	0.000	75.000
0.000	0.000	0.000	0.000	76.000
0.000	0.000	0.000	0.000	77.000
0.000	0.000	0.000	0.000	78.000
0.000	0.000	0.000	0.000	79.000
0.000	0.000	0.000	0.000	80.000
0.000	0.000	0.000	0.000	81.000
0.000	0.000	0.000	0.000	82.000
0.000	0.000	0.000	0.000	83.000
0.000	0.000	0.000	0.000	84.000
0.000	0.000	0.000	0.000	85.000
0.000	0.000	0.000	0.000	86.000
0.000	0.000	0.000	0.000	87.000
0.000	0.000	0.000	0.000	88.000
0.000	0.000	0.000	0.000	89.000
0.000	0.000	0.000	0.000	90.000
0.000	0.000	0.000	0.000	91.000
0.000	0.000	0.000	0.000	92.000
0.000	0.000	0.000	0.000	93.000
0.000	0.000	0.000	0.000	94.000
0.000	0.000	0.000	0.000	95.000
0.000	0.000	0.000	0.000	96.000
0.000	0.000	0.000	0.000	97.000
0.000	0.000	0.000	0.000	98.000
0.000	0.000	0.000	0.000	99.000
0.000	0.000	0.000	0.000	100.000

This data corresponds with figure 5.64.

DEPTH (meters)	CONCENTRATION			
	1949	1961	1978	1990
0.000	74.931	52.385	37.156	37.143
1.000	61.777	66.094	47.389	47.371
2.000	48.939	75.649	56.219	56.195
3.000	37.157	80.160	62.955	62.924
4.000	26.987	79.948	67.112	67.079
5.000	18.722	76.102	68.564	68.533
6.000	12.394	69.925	67.513	67.488
7.000	7.825	62.556	64.393	64.380
8.000	4.711	54.821	59.757	59.755
9.000	2.704	47.250	54.163	54.174
10.000	1.481	40.148	48.106	48.129
11.000	0.774	33.671	41.981	42.012
12.000	0.386	27.889	36.070	36.109
13.000	0.184	22.815	30.560	30.603
14.000	0.084	18.431	25.559	25.605
15.000	0.037	14.698	21.116	21.163
16.000	0.015	11.568	17.240	17.286
17.000	0.006	8.982	13.912	13.955
18.000	0.002	6.878	11.096	11.137
19.000	0.001	5.194	8.747	8.785
20.000	0.000	3.867	6.815	6.849
21.000	0.000	2.839	5.247	5.277
22.000	0.000	2.054	3.992	4.018
23.000	0.000	1.465	3.001	3.023
24.000	0.000	1.030	2.228	2.247
25.000	0.000	0.714	1.635	1.650
26.000	0.000	0.488	1.185	1.198
27.000	0.000	0.329	0.848	0.859
28.000	0.000	0.218	0.600	0.608
29.000	0.000	0.143	0.419	0.426
30.000	0.000	0.092	0.289	0.294
31.000	0.000	0.059	0.197	0.201
32.000	0.000	0.037	0.133	0.136
33.000	0.000	0.023	0.089	0.091
34.000	0.000	0.014	0.058	0.060
35.000	0.000	0.008	0.038	0.039
36.000	0.000	0.005	0.024	0.025
37.000	0.000	0.003	0.015	0.016
38.000	0.000	0.002	0.010	0.010
39.000	0.000	0.001	0.006	0.006
40.000	0.000	0.001	0.004	0.004
41.000	0.000	0.000	0.002	0.002
42.000	0.000	0.000	0.001	0.001
43.000	0.000	0.000	0.001	0.001
44.000	0.000	0.000	0.000	0.000
45.000	0.000	0.000	0.000	0.000
46.000	0.000	0.000	0.000	0.000
47.000	0.000	0.000	0.000	0.000
48.000	0.000	0.000	0.000	0.000
49.000	0.000	0.000	0.000	0.000
50.000	0.000	0.000	0.000	0.000
51.000	0.000	0.000	0.000	0.000
52.000	0.000	0.000	0.000	0.000
53.000	0.000	0.000	0.000	0.000

55.000	0.7930	0.4600	0.2420	0.1880
56.000	0.7930	0.4600	0.2440	0.1890
57.000	0.7940	0.4590	0.2450	0.1900
58.000	0.7950	0.4590	0.2460	0.1910
59.000	0.7960	0.4580	0.2480	0.1920
60.000	0.7980	0.4580	0.2490	0.1930
61.000	0.7990	0.4580	0.2500	0.1940
62.000	0.7990	0.4580	0.2510	0.1950
63.000	0.8000	0.4580	0.2530	0.1960
64.000	0.8000	0.4580	0.2540	0.1970
65.000	0.8000	0.4580	0.2550	0.1980
66.000	0.7990	0.4580	0.2560	0.1980
67.000	0.7990	0.4580	0.2580	0.1990
68.000	0.7980	0.4580	0.2590	0.2000
69.000	0.7970	0.4590	0.2600	0.2010
70.000	0.7960	0.4590	0.2610	0.2020
71.000	0.7950	0.4590	0.2620	0.2030
72.000	0.7950	0.4590	0.2630	0.2040
73.000	0.7950	0.4590	0.2650	0.2050
74.000	0.7950	0.4580	0.2660	0.2050
75.000	0.7950	0.4580	0.2670	0.2060
76.000	0.7950	0.4580	0.2680	0.2070
77.000	0.7950	0.4580	0.2690	0.2080
78.000	0.7960	0.4580	0.2700	0.2090
79.000	0.7960	0.4570	0.2710	0.2100
80.000	0.7970	0.4570	0.2720	0.2100
81.000	0.7970	0.4570	0.2730	0.2110
82.000	0.7980	0.4570	0.2740	0.2120
83.000	0.7980	0.4570	0.2760	0.2130
84.000	0.7990	0.4570	0.2770	0.2140
85.000	0.7990	0.4570	0.2780	0.2140
86.000	0.7990	0.4570	0.2790	0.2150
87.000	0.7990	0.4570	0.2800	0.2160
88.000	0.7980	0.4580	0.2810	0.2170
89.000	0.7980	0.4580	0.2820	0.2170
90.000	0.7980	0.4580	0.2830	0.2180
91.000	0.7970	0.4590	0.2840	0.2190
92.000	0.7970	0.4590	0.2850	0.2200
93.000	0.7970	0.4590	0.2860	0.2200
94.000	0.7970	0.4600	0.2870	0.2210
95.000	0.7960	0.4600	0.2880	0.2220
96.000	0.7960	0.4610	0.2890	0.2220
97.000	0.7960	0.4610	0.2890	0.2230
98.000	0.7960	0.4620	0.2900	0.2230
99.000	0.7960	0.4620	0.2900	0.2230
100.000	0.7960	0.4620	0.2900	0.2230

This data corresponds with figure 5.65.

DEPTH (meters)	CONCENTRATION			
	1949	1961	1978	1990
0.000	74.931	52.373	37.155	37.142
1.000	61.777	66.092	47.387	47.369
2.000	48.939	75.649	56.217	56.193
3.000	37.157	80.160	62.953	62.922
4.000	26.987	79.948	67.111	67.077
5.000	18.722	76.102	68.563	68.532
6.000	12.394	69.925	67.512	67.488
7.000	7.825	62.556	64.393	64.379
8.000	4.711	54.821	59.757	59.755
9.000	2.704	47.250	54.163	54.174
10.000	1.481	40.148	48.106	48.129
11.000	0.774	33.671	41.981	42.012
12.000	0.386	27.889	36.070	36.109
13.000	0.184	22.815	30.560	30.603
14.000	0.084	18.431	25.559	25.605
15.000	0.037	14.698	21.116	21.163
16.000	0.015	11.568	17.240	17.286
17.000	0.006	8.982	13.912	13.955
18.000	0.002	6.878	11.096	11.137
19.000	0.001	5.194	8.747	8.785
20.000	0.000	3.867	6.815	6.849
21.000	0.000	2.839	5.247	5.277
22.000	0.000	2.054	3.992	4.018
23.000	0.000	1.465	3.001	3.023
24.000	0.000	1.030	2.228	2.247
25.000	0.000	0.714	1.635	1.650
26.000	0.000	0.488	1.185	1.198
27.000	0.000	0.329	0.848	0.859
28.000	0.000	0.218	0.600	0.608
29.000	0.000	0.143	0.419	0.426
30.000	0.000	0.092	0.289	0.294
31.000	0.000	0.059	0.197	0.201
32.000	0.000	0.037	0.133	0.136
33.000	0.000	0.023	0.089	0.091
34.000	0.000	0.014	0.058	0.060
35.000	0.000	0.008	0.038	0.039
36.000	0.000	0.005	0.024	0.025
37.000	0.000	0.003	0.015	0.016
38.000	0.000	0.002	0.010	0.010
39.000	0.000	0.001	0.006	0.006
40.000	0.000	0.001	0.004	0.004
41.000	0.000	0.000	0.002	0.002
42.000	0.000	0.000	0.001	0.001
43.000	0.000	0.000	0.001	0.001
44.000	0.000	0.000	0.000	0.000
45.000	0.000	0.000	0.000	0.000
46.000	0.000	0.000	0.000	0.000
47.000	0.000	0.000	0.000	0.000
48.000	0.000	0.000	0.000	0.000
49.000	0.000	0.000	0.000	0.000
50.000	0.000	0.000	0.000	0.000
51.000	0.000	0.000	0.000	0.000
52.000	0.000	0.000	0.000	0.000
53.000	0.000	0.000	0.000	0.000